ENHANCING THE PERFORMANCE OF DISTANCE PROTECTION RELAYS UNDER PRACTICAL OPERATING CONDITIONS

by

Kerrylynn Rochelle Pillay

Submitted in fulfilment of the academic requirements for the Master of Science in Electrical Engineering degree, in the School of Electrical, Electronic and Computer Engineering, University of KwaZulu-Natal, Durban, South Africa.

November 2013

Supervisor: Dr BS Rigby

EXAMINERS COPY

DECLARATION

I, Kerrylynn Rochelle Pillay, declare that:

(i) The research reported in this thesis, except where otherwise indicated, is my original research.

(ii) This thesis has not been submitted for any degree or examination at any other university.

(iii) This thesis does not contain other persons' data, pictures, graphs or other information, unless specifically acknowledged as being sourced from other persons.

(iv) This thesis does not contain other persons' writing, unless specifically acknowledged as being sourced from other researchers. Where other written sources have been quoted, then:

a) Their words have been re-written but the general information attributed to them has been referenced;

b) Where their exact words have been used, their writing has been placed inside quotation marks, and referenced.

(v) Where I have reproduced a publication of which I am an author, co-author or editor, I have indicated in detail which part of the publication was actually written by myself alone and have fully referenced such publications.

(vi) This thesis does not contain text, graphics or tables copied and pasted from the Internet, unless specifically acknowledged, and the source being detailed in the thesis and in the References sections.

Kerrylynn Rochelle Pillay …….. ……..
(BScEng) Signature Date

As the candidate's Supervisor I agree to the submission of this thesis.

Supervisor: Bruce Rigby …….. ……..
(BScEng, MScEng, PhD (Natal), MIEEE) Signature Date

This thesis is dedicated to my parents

ABSTRACT

This thesis examines the use of real time digital simulation as a tool for enhancing the performance of modern numerical distance protection relays under complex, practical fault scenarios and operating conditions, in particular those associated with distance protection of closely-coupled parallel lines. Double-circuit and parallel transmission lines, in various topologies, are widely used in South African electrical networks due to servitude and cost constraints. The particular topology and separation of adjacent transmission lines affects the individual lines' electrical characteristics and dynamics, and hence, in-turn, affects the performance of the protection schemes designed to protect the lines against short circuit faults. The design of protection schemes to accommodate the effects of this environment presents a number of challenges. The particular challenges that are considered in this thesis are: the effect of mutual coupling between double-circuit and parallel transmission lines on distance protection relays; the effect of untransposed transmission lines on distance protection relays; the effects of cross country faults on distance protection relays.

The effects of each of these practical operating conditions on the performance of distance protection relays can be complex and interacting, and therefore detailed analysis is required in order to avoid the occurrence of a protection mal-operation. However, with the emergence of powerful simulation tools, like the Real Time Digital Simulator (RTDS), it is possible to model the characteristics of untransposed and closely-coupled transmission lines in detail for the purposes of such analysis. A Real Time Digital Simulator also allows one to connect actual protection relay hardware in closed-loop with the real time model of the protected transmission lines in order to be able to analyse the performance of actual distance protection relays in response to complex fault scenarios and operating environments that may occur on the power system.

The thesis begins by presenting a review of the fundamental theory and prior research into distance protection in complex line topologies, including mutual coupling and non-transposition. The thesis then presents a detailed, first-principles analysis of the mathematical models of transmission lines and the theoretical impedance seen by a distance protection relay for faults, firstly on mutually-coupled lines, and then on untransposed lines, in order to establish the validity of the mathematical models and hardware-in-loop test procedures used. The findings of the hardware-in-loop studies confirm the true extent of the impact of mutual coupling and non-transposition of lines and show that these issues need to be taken into account when designing a protection scheme.

Finally, the thesis considers the practical issue of cross country faults, in which simultaneous, or near-simultaneous, occurrences of ground faults on nearby lines may result in incorrect performance of distance protection relays. Techniques used to minimise the impact of cross-country faults in modern protection relays are reviewed, and a detailed real time simulation study is presented to assess the performance of such schemes under practical conditions in a utility environment in which the nearby lines are both mutually coupled and untransposed.

ACKNOWLEDGEMENTS

My sincere gratitude goes to my supervisor Dr Bruce Rigby for the opportunity to do my MSc under his supervision. The immense guidance and assistance I received during my study is greatly appreciated.

I would like to thank eThekwini Electricity for affording me the opportunity to pursue this degree.

A special thank you goes to my husband and family for bearing with me during my research work and during the preparation of this document.

All glory and honour goes to God, for giving me the ability to complete this degree.

TABLE OF CONTENTS

CHAPTER 1
INTRODUCTION

CHAPTER 2
BACKGROUND THEORY AND LITERATURE REVIEW

CHAPTER 3
CALCULATION OF IMPEDANCES OF MUTUALLY COUPLED TRANSMISSION LINES

CHAPTER 4
INVESTIGATING THE IMPACT OF MUTUAL COUPLING ON DISTANCE PROTECTION RELAYS USING A REAL TIME DIGITAL SIMULATOR

CHAPTER 5
THE IMPACT OF UNTRANSPOSED TRANSMISSION LINES ON THE DISTANCE PROTECTION SCHEME

CHAPTER 6
INVESTIGATING THE COMBINED EFFECTS OF MUTUAL COUPLING AND UNTRANSPOSED TRANSMISSION LINES ON THE DISTANCE PROTECTION RELAY, USING A REAL TIME DIGITAL SIMULATOR

CHAPTER 7
INVESTIGATING THE EFFECTS OF A CROSS COUNTRY FAULT ON THE DISTANCE PROTECTION RELAY USING A REAL TIME DIGITAL SIMULATOR

CHAPTER 8
CONCLUSION

LIST OF SYMBOLS AND ABBREVIATIONS USED

RTPSS	Real Time Power System Simulation Centre
RTDS	Real Time Digital Simulator
SEL	Schweitzer Engineering Laboratories
DUT	Durban University of Technology
UKZN	University of Kwa-Zulu Natal
CT	Current Transformer
VT	Voltage Transformer
EMF	Electro-Magnetic Field
GMR	Geometric Mean Radius
GMD	Geometric Mean Distance
POTT	Permissive Over-reaching Transfer Trip
DUTT	Direct under-reaching transfer trip
PUTT	Permissive under-reaching transfer trip

E	electric field
H	magnetic field
R	resistance
L	inductance
C	capacitance
D	distance between the centres of two conductors
a	radius of a conductor
μ	permeability in henrys/meter
μ_0	permeability of free space in henrys/meter
μ_r	relative permeability
ε	permittivity in farads/meter
ε_0	permittivity of free space in farads/meter
ε_r	relative permittivity
Z	impedance
V	voltage/volts
I	current
Ω	ohm
A	amperes
V_1	positive sequence voltage
V_2	negative sequence voltage
V_0	zero sequence voltage

I_1	positive sequence current
I_2	negative sequence current
I_0	zero sequence current
Z_{L1}	positive sequence impedance of the line
Z_{L2}	negative sequence impedance of the line
Z_{L0}	zero sequence impedance of the line
Z_{S1}	positive sequence impedance of the source
Z_{S2}	negative sequence impedance of the source
Z_{S0}	zero sequence impedance of the source
V_{1F}	positive sequence voltage of the fault
V_{2F}	negative sequence voltage of the fault
V_{0F}	zero sequence voltage of the fault
R_f	fault resistance
I_r	residual current
I_a	phase A current
I_b	phase B current
I_c	phase C current
Z_m	mutual impedance between the two conductors
I_{fault}	fault current on the protected line
k_0	zero sequence current compensating factor
k_{0M}	mutual coupling factor
$I_{0parallel}$	zero sequence current of the parallel line
ρ	resistivity of the ground in Ω/m
f	frequency in Hz

Where subscripts differ, these have been defined where they are used.

TABLE OF FIGURES

LIST OF TABLES

CHAPTER 1
INTRODUCTION

A power system's core functionality is to generate, transmit and distribute electrical energy to its customers. The aim of the power system is to supply this generated energy to the customer in a reliable and economical manner, which presents a huge task since there usually exists a compromise between these two requirements. These three sectors of generation, transmission and distribution comprise many diverse items of equipment that are very expensive, requiring a big capital investment. It is therefore important to protect these pieces of equipment at all costs.

The discipline of protection goes hand in hand with the concept of reliability of a power system in meeting its requirements. These two important factors are dependent on proper design, installation, testing, repair and precaution. Although every effort is made to prevent faults and abnormal conditions in a system, they are often inevitable and it is here that the purpose of protective relays and relaying becomes evident.

A transmission line is a fundamental element in the core functionality of a power system. Power, at high voltages, is transmitted to various parts of the power system through these transmission lines. It is these transmission lines that terminate on transmission substations, feeding numerous customers from that point. It is crucial that this transmission stage be reliable since these transmission lines usually feed critical parts of the network.

Transmission lines, more particularly parallel and double-circuit transmission lines utilised over long distances, are widely used in modern transmission systems. With their numerous different topologies, configuration, design and factors affecting the network, the effective protection of parallel and double-circuit transmission lines is often more complicated than other parts of the network [1]. These challenges can negatively affect the performance of protection schemes, since not all the factors and dynamic characteristics of the network that influence the correct functioning of the protection schemes may have been taken into consideration in their settings design or even be properly known and understood.

The proper documentation of these practical operating conditions, and their effect on protection schemes and the network, are of great importance to the design engineer to adequately compensate for these factors where the protection scheme is concerned. This will allow for these factors to be given due consideration in order to effectively enhance the performance of the protection scheme and reduce the effect of the fault on the rest of the network.

Although the influences on the measurements made by protection relays of issues associated with complex transmission line topologies have in fact been well documented over the years [1-3], the tools required by protection engineers to study these phenomena, and properly consider

their impact under different practical conditions have not, until more recently, been commonly available. However, recent trends toward using detailed electromagnetic transient simulations and fully-dynamic models of protection relays by utility protection engineers [4] has served to remind protection engineers of the actual extent to which these issues can impact on practical protection schemes in the field [5], as well as making it more feasible to take such issues into account when designing and setting protection schemes. Hence, in this thesis, it was considered timely and valuable to revisit the issue of protection of complex transmission line topologies under practical operating conditions using modern simulation and analysis tools, including detailed dynamic models of the relays, as well as using practical protection relay hardware. In particular, the thesis uses a real time digital simulator, and its software programme RSCAD, as the analysis tool.

RSCAD was chosen to model the system, run the necessary simulations and generate results for the following reasons [2]:

RSCAD provides the capability to simulate the behaviour of power systems and control the simulation in real time on the real time digital simulator. It also allows for interface with hardware for closed loop testing of actual protection relays, as well as providing a library of generic, but representative dynamic simulation models of protection relays [6].

1.1. Background and Importance of Research

At both transmission and distribution voltage levels in South Africa, the use of permissive over-reaching distance protection schemes is widespread, and the characteristics of such schemes are well understood for the majority of operating and fault conditions. However, there are particular practical operating challenges facing such protection schemes in South Africa that, although their existence is well known and they are often discussed, they are not thoroughly documented or fully understood.

Presently, in South Africa, there are many double circuit lines travelling over long distances, but only a handful of these lines have been properly investigated where due consideration is given to practical operating conditions. Faults on these transmission lines sometimes cause unexplained trips due to the lack of proper knowledge of the effects of these operating conditions on the protection scheme. The information deficiency in this area of transmission line protection makes conditions difficult for the protection engineer to properly design the protection scheme.

One such issue is the mutual coupling between parallel and double circuit transmission lines, where interaction between two transmission lines' electro-magnetic fields occurs when the lines are routed sufficiently close to each other. Present practice often ignores the effects of mutual

coupling between the transmission lines, causing incorrect settings to be designed for the protection scheme given the operating condition that the line is subjected to. Mutual impedance between the transmission lines is known to affect distance protection schemes, causing effective reach errors of impedance relays' measurements. The availability of the real time digital simulator makes investigation of this phenomenon promising.

Another phenomenon that will be investigated is the effect of the untransposed nature of many of the transmission lines in parts of South Africa. The question of whether non-transposition presents further challenges to the performance of the distance protection schemes on these lines needs to be studied, as the full extent of the effect of untransposed lines on the protection scheme is often not fully appreciated. This issue, again, can be addressed by a thorough real time simulator study using practical protection relays and detailed modelling of the transmission plant in question.

The final issue is that of cross country faults, where two separate short circuit faults (for example an A-phase to ground fault and a C-phase to ground fault) occur simultaneously, or near-simultaneously on adjacent lines. In South Africa, transmission line faults can be attributed to the following sources [3]:

- Bird pollution (30%)
- Fires (27%)
- Lightning (25%)
- Other (18%)

Where parallel and double circuit transmission lines are concerned, fires are of great concern as in most instances fire and resultant smoke can cause faults in both the transmission line circuits. Because, by their very nature, permissive over-reaching protection schemes have overlapping zones of protection on adjacent lines, cross country faults present particular challenges to this form of protection. It has been reported that, when trying to account for unexpected operation or mal-operation of the relays following system faults, cross country faults are often used as a catch-all category when no other specific explanation can be found. With the emergence of facilities such as real time digital simulators, where actual protection relays can be tested on very realistic simulation models of the transmission and distribution network, it is possible to study the phenomenon of cross country faults in a systematic and through manner so as to remove some of the misunderstanding and misrepresentation of what problems can, and cannot, be attributed to cross country faults.

1.2. Research Question

What is the true influence of mutual coupling of parallel and double circuit transmission lines on the performance of distance protection relays?

What is the extent of the effect of untransposed transmission lines on the impedance of a faulted transmission line measured by a protection relay and how will this degrade the performance of the distance protection relays?

What is the effect of cross country faults on the distance protection scheme and its decision making elements that comprise the protection scheme typically used for parallel and double circuit transmission lines?

1.3. Aims and Objectives

The objective is to present a well-documented and thorough research study into the performance of permissive over-reaching distance protection schemes under particular practical operating conditions where such schemes are known to have weaknesses, but where the true extent of these weaknesses are often not fully documented or understood. With respect to mutual coupling and cross country faults, the objective is to be able to understand definitively, exactly how standard permissive over-reaching protection schemes respond to these faults. Similarly, for untransposed transmission lines, the objective is to quantify the influence of un-transposed lines, and their unbalanced impedance characteristics, on the performance of distance protection relays for practical examples of such lines in South Africa.

1.4. Methodological Approach

The approach adopted was to develop detailed real time simulator models of particular transmission lines, in the South African grid, susceptible to each of the issues described above, and connect these models to physical distance protection relays used in practice in the field. The foundations of this method of study are by now well documented and proven over numerous projects at this institution, of which [3] and [4] are but two recent examples; in this case the approach is to be used for further practical research questions in the field of protection as outlined above. Through consultation with industry protection specialists, the appropriate parameters and fault scenarios were developed to study and each of these phenomena were documented in detail.

1.5. Thesis Layout

Chapter One of this thesis includes a general introduction to the background and importance of the research, presenting the objectives of the study and an outline of the thesis.

Chapter Two provides a literature review of studies surrounding the research topic. A presentation of the theory required to understand the fundamental elements used in this research will be included. A general scope of functionality of the resources used and the vital associated theory on which these resources are based will be detailed here.

Chapter Three outlines the fundamental theory of transmission lines and the calculation of the transmission line impedances and mutual impedances between transmission lines from first principles. Various typical transmission line topologies will be investigated and a base case for use throughout the research will be established.

Chapter Four further investigates the mutual coupling of transmission lines using real time simulation. The effect of mutual coupling of transmission lines on the protection scheme is investigated with a generic software model of an impedance protection relay as well as with physical distance protection relays employing hardware in-loop testing with the real time digital simulator.

Chapter Five explores the effect of untransposed transmission lines versus ideally transposed transmission lines. The theoretical justification of the effects of un-transposed transmission lines will be presented with derivations from first principles. These theoretical results will then be evaluated using real time digital simulation.

Chapter Six presents typical practical operating scenarios encompassing each of the issues that are considered, in isolation, earlier in the thesis (mutual coupling between transmission lines and untransposed transmission lines) and examines how these issues interact, and influence one another, in practice and their combined effects on distance protection. The impact of these challenging operating scenarios on the protection scheme will be assessed.

Chapter Seven presents the classical definition of a cross country fault and the practical evaluation of this is studied using real time digital simulation. The effect of a cross country fault on the protection scheme is then examined using both a generic software version of a distance protection relay as well as actual distance protection relay hardware. The design of a protection scheme to minimise the effects of a cross country fault is discussed, developed, implemented and tested. Thereafter the scheme is tested under a very challenging operating condition combining the effects of mutual coupling between transmission lines and untransposed transmission lines with the presence of a cross country fault on the system.

Chapter Eight consolidates all main research points into a final summary and conclusion, and presents suggestions for further work.

1.6. Research Publications

Some of the findings of this research have been published at local [7] and international [8, 9] conferences.

CHAPTER 2
BACKGROUND THEORY AND LITERATURE REVIEW

2.1. Introduction to protection schemes

The basic function of a protection scheme is to detect the presence of a fault on a power system and to remove the fault from the system as quickly and efficiently as possible in order to minimize the effects of the fault on the system. This is generally accomplished by the protection equipment which includes current transformers, voltage transformers, circuit breakers and protection relays. Collectively, the protective equipment functions to detect the fault and ideally to isolate only that particular part of the power system network responsible for the fault from the rest of the power system [10]. In this way, minimising the impact of the fault on the power system is achieved. The protection scheme also serves to monitor the behaviour of the system. Figure 2.1 shows the typical arrangement of the protective equipment making up the protection scheme.

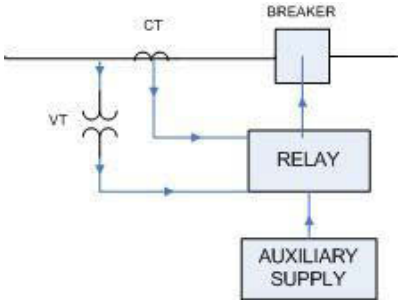

Figure 2.1: A basic protection scheme

The protection relay forms the most important part of the protection scheme, as a result its capability and functionality plays a central role in how the protection scheme operates. An electrical relay is the decision making element in the protection scheme. It is prompted by current and voltage measurements obtained from current transformers and voltage transformers [10]. The relay must then decide if an abnormal condition exists, if the abnormal condition is large enough to endanger the system, and if so, what preventative action should be taken. The relay's function in the protection scheme can be described by the following flow diagram:

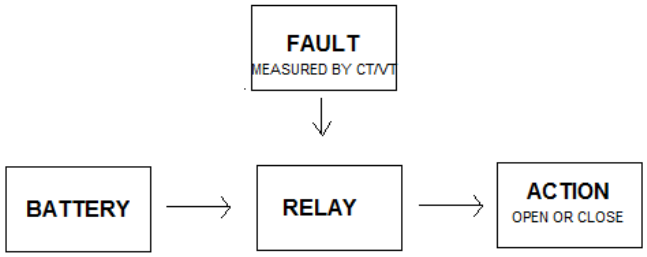

Figure 2.2: Flow diagram of the relay logic

It is important to note that one particular concern here is the accuracy of the instrument transformers (CTs and VTs) [10]. In the application of protection, the consequence of inaccuracy will cause the protection scheme to perform delayed operations or unnecessary operations.

2.2. Requirements of a Protection Scheme

A scheme, such as the one above, needs to adhere to five basic requirements of a protection system. These are [11]:

- Reliability: This is the most important protection requirement and involves the ability of the protection scheme to always operate when required.
- Selectivity (or Discrimination): This involves correct identification of the location of the fault and selectively isolating the fault, or the part of the system experiencing the fault, from the rest of the network.
- Speed: This involves the time the protection scheme takes to operate and to successfully isolate the fault. The desired factor is for the fault to be cleared as fast as possible, to minimise the damage to equipment and to minimise the likelihood of system instability due to a fault being present on the system for a longer than desired duration.
- Security (or Stability): This requirement of a protection scheme becomes important where unit protection is concerned. It involves the ability of the protection scheme to remain stable for out of zone faults.
- Sensitivity: This is the ability for the protection scheme to detect incipient faults (faults at a low level) as well as large high current faults without compromising the four requirements of the protection scheme mentioned above.

2.3. Faults

The type of failure of the electrical system that causes the greatest concern is represented by a short circuit and usually known as a ‘fault’. Faults can be grouped into three categories. These are:

- Transient: caused by lightning, field fires, bird droppings and industrial (smoke) pollution.
- Permanent: caused by mechanical or electrical faults which require repairs when they occur.
- Persistent faults: caused by transient and permanent faults and would cause a breaker to lockout.

No matter how well designed the system is, faults are likely to occur, and these faults represent a risk to life and property if they are not dealt with swiftly and correctly. These categories of faults result in three phase faults, single phase to ground faults, phase to phase faults, phase to phase to ground faults and cross country faults [11]. Faults involving ground are often also referred to as ground faults.

2.4. Transmission Line Electromagnetic Field (EMF)

In order to design a protection scheme to detect and remove faults from transmission lines that are on their own zones of protection, and to refrain from operating in response to faults on out of zone lines, the knowledge of the specific characteristics of each of these types of faults is required. This in-turn depends on accurate knowledge of the parameters in the transmission line and appropriate modelling of the lines in protection studies.

When current flows through a transmission line at a rated voltage, the presence of an electro-magnetic field exists [12]. It is important to understand that the electro-magnetic field is comprised of two components, the electric field and the magnetic field. The electric field (E) is associated with the voltage of the transmission line and the magnetic field (H) is associated with the current of the transmission line. Figure 2.3 gives an indication of the orientation of the electric and magnetic fields. Understanding the interaction between two current carrying conductors is vitally important for later explanations of mutual coupling between transmission lines.

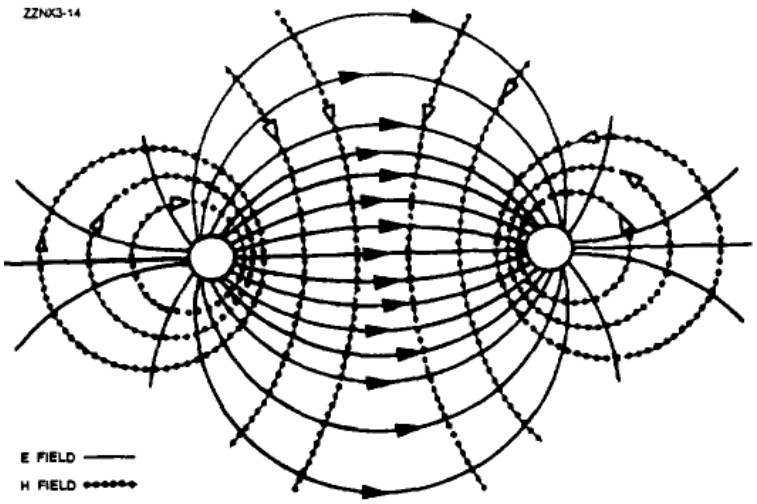

Figure 2.3: Electric and magnetic field between two parallel conductors [12]

2.5. Basic Transmission Line Mathematical Models

A transmission line can be represented using two distinct types of mathematical models, namely lumped-parameter and distributed-parameter models. A lumped-parameter model represents the

resistance, capacitance and inductance of the whole transmission line as single, lumped circuit elements. A distributed-parameter model of the transmission line more properly describes the resistance, capacitance and inductance of the line as functions of distance along the line, by means of partial differential equations. The latter of these two methods of transmission line modelling is more commonly used for longer transmission lines to more accurately represent the actual transmission line behaviour. This type of model is also often referred to as a travelling wave model, since it represents the propagation of signals along the line at the speed of light.

The RTDS simulation software RSCAD allows the user the option to choose between using a lumped circuit model or a travelling wave model to represent transmission lines in a particular scenario. In the RSCAD family of tools, transmission lines are defined by using the TLINE support programme. Here the parameters of the travelling wave transmission line model can be input either by the geometry of the line or by the RLC data of the line [13].

A basic transmission line conductor has resistance per unit of length. In addition to the resistance of the transmission line, in accurately observing the behaviour of the line, one needs to consider the inductance and capacitance, also distributed along the line per unit of length. Current flowing through a transmission line causes an electro-magnetic field to be setup around the conductor. The energy stored by the electro-magnetic field collapsing back into the wire tends to keep the current flowing in the same direction. This occurrence represents the inductance of the transmission line [14]. In addition, the conductors of a parallel transmission line act as plates of a capacitor, with the air between them acting as the dielectric. This gives rise to the capacitance between the conductors. Each of these important parameters of inductance and capacitance of each conducting element of a transmission line can be calculated from first principles in order to appropriately model the behaviour of the line as a whole. In particular, the study of electro-magnetic field theory [13] gives the inductance (L) per meter lengths of a conductor as:

$$\frac{L}{l} = \frac{\mu}{\pi} \ln \frac{D}{a} \; henrys/meter \qquad (1)$$

Where: $\frac{L}{l}$ is the inductance per meter

D is the distance between the centres of the two conductors

a is the radius of the conductor

μ is the permeability in henrys/meter ($\mu = \mu_r \mu_o$)

μ_r is the relative permeability

μ_o is the permeability of free space ($\mu_o = 4\pi \times 10^{-7}$henrys/meter)

Similarly, the capacitance (C) per meter length of a conductor is given as:

$$\frac{C}{l} = \frac{\pi\varepsilon}{\ln^{D}/_{a}}\ farads/meter \quad (2)$$

Where: $\frac{C}{l}$ is the capacitance per meter

D is the separation between the centres of the two conductors

a is the radius of the conductor

ε is the permittivity in farads/meter ($\varepsilon = \varepsilon_r \varepsilon_o$)

ε_r is the relative permittivity

ε_o is the permeability of free space ($\varepsilon_o = 8.85 \times 10^{-12}$farads/meter)

2.6. Distance Protection Relays

Distance protection relays (also known as impedance relays) operate on the fundamental principle of constantly monitoring the impedance measured on a transmission line under protection. The impedance is monitored by means of a current transformer (CT) and voltage transformer (VT) at the point of observation on the transmission line, and it is the outputs of the CT and VT that are fed as measurement inputs to the relay. The relay will then use these input measurements to internally calculate an impedance measurement from the combination of these currents and voltages. A simple distance relay can be viewed as a device that carries out a measurement of impedance from the point of observation of the relay (as in eqn. (3) below) and then checks if that impedance lies inside some geometric shape that governs the reach of the protected zone [15]. When imputing the desired reach of a particular protection zone setting to the relay, the ohmic reach must be converted to a secondary or primary value depending on the relay being used and the format of the relay algorithms internally in the relay. This can be converted using eqn. (3) or the converse of this equation.

$$Z_{primary} = \frac{VT\ Ratio}{CT\ Ratio} \times \frac{V_{measured}}{I_{measured}} = \frac{VT\ Ratio}{CT\ Ratio} \times Z_{secondary} = \frac{V_{pri}/V_{sec}}{I_{pri}/I_{sec}} \times Z_{secondary} \quad (3)$$

Where $V_{measured}$ is the voltage measured by the relay in terms of the VT secondary value

$I_{measured}$ is the current measured by the relay in terms of the CT secondary value

$Z_{secondary}$ is the ohmic secondary impedance measured by the relay

$Z_{primary}$ is the ohmic primary impedance measured by the relay

I_{pri}/I_{sec} is the CT ratio where I_{pri} is the primary current and I_{sec} is the associated secondary current

V_{pri}/V_{sec} is the VT ratio where V_{pri} is the primary voltage and V_{sec} is the associated secondary voltage

The geometric shape that governs the reach of the relay is used as the benchmark to determine if there is a fault on the transmission line that is being protected. If there exists a fault on the transmission line that is protected by the relay, the impedance seen by the relay would be measured from the point of observation to the point of fault. If the fault impedance seen by the relay is smaller than the impedance of the line, this will flag a condition of a fault. The geometric shapes that govern the reach of the different zones of protection will be used to decide which zone of protection contains the fault. This is the simple principle that distance protection works on, using the current and voltage inputs to the relay of the line under protection. The simple relationship representation in eqn. (3) is merely a principle that is used to explain the basic concept of a distance protection relay. In modern numeric distance relays, relay manufacturers have endeavoured to mathematically model the operating characteristics of legacy electromechanical distance protection relays, making the actual computation of the impedance somewhat more involved that what has been presented in eqn. (3). Later sections of this chapter give an indication of the full complexity of the internal workings of the relay to establish the presence of a fault on the transmission line.

The apparent impedance equation of the fault loops that the relay measures can be depicted by the equations below [15]:

A-g fault loop: $V_a/[I_a + k0 \cdot I_r]$ (4)

B-g fault loop: $V_b/[I_b + k0 \cdot I_r]$ (5)

C-g fault loop: $V_c/[I_c + k0 \cdot I_r]$ (6)

A-B fault loop: $[V_a - V_b]/[I_a - I_b]$ (7)

B-C fault loop: $[V_b - V_c]/[I_b - I_c]$ (8)

C-A fault loop: $[V_c - V_a]/[I_c - I_a]$ (9)

Where V_a, V_b and V_c are the phase-neutral voltages measured by the relay, I_a, I_b and I_c are the phase currents measured by the relay and I_r is the residual current (or sum of the currents I_a, I_b and I_c) measured by the relay. Thus, the phase impedance elements of the relay measure the currents and voltages in two adjacent phases of the transmission line to calculate a loop impedance. By contrast, the ground impedance elements of the relay measure the current and voltage in one phase of the line, and a k_0 factor is used to determine the impedance of the fault loop.

This k_0 is necessary if the relay manufacturer uses the positive sequence impedance of the line for the apparent impedance calculation [16]. The actual value of k_0 used in practice is dependent on the sequence component current distribution for faults including ground and varies according to relay manufacturer.

For a phase A-g fault, the voltage at the relay is [17]:

$$V_a = V_1 + V_2 + V_0 \tag{10}$$

Where V_a is the voltage at the relay's point of measurement

V_1 is the positive sequence voltage

V_2 is the negative sequence voltage

V_0 is the zero sequence voltage

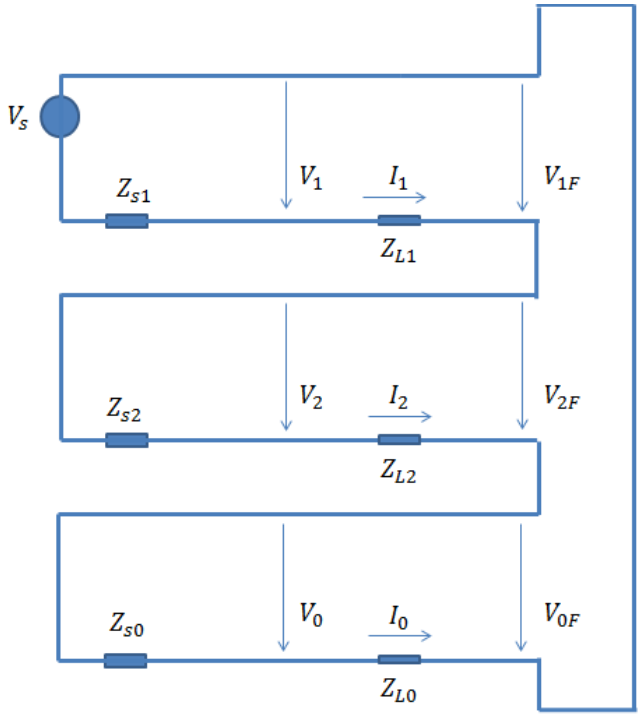

Figure 2.4: Sequence network for an A-g fault

In Figure 2.4: I_1 is the positive sequence current

I_2 is the negative sequence current

I_0 is the zero sequence current

Z_{L1} is the positive sequence impedance of the line

Z_{L2} is the negative sequence impedance of the line

Z_{L0} is the zero sequence impedance of the line

Z_{S1} is the positive sequence impedance of the source

Z_{S2} is the negative sequence impedance of the source

Z_{S0} is the zero sequence impedance of the source

V_{1F} is the positive sequence voltage of the fault

V_{2F} is the negative sequence voltage of the fault

V_{0F} is the zero sequence voltage of the fault

From Figure 2.4, the following derivation is made:

$$V_1 = I_1 Z_{L1} + V_{1F} \quad (11)$$

$$V_2 = I_2 Z_{L1} + V_{2F} \quad (12)$$

$$V_0 = I_0 Z_{L0} + V_{0F} \quad (13)$$

since $Z_{L1} = Z_{L2}$.

Substituting eqn. (11), eqn. (12) and eqn. (13) in eqn. (10):

$$V_a = I_1 Z_{L1} + V_{1F} + I_2 Z_{L1} + V_{2F} + I_0 Z_{L0} + V_{0F} \quad (14)$$

$$V_a = I_1 Z_{L1} + I_2 Z_{L1} + I_0 Z_{L0} + (V_{1F} + V_{2F} + V_{0F}) \quad (15)$$

Since $V_{1F} + V_{2F} + V_{0F} = 0$

$$V_a = I_1 Z_{L1} + I_2 Z_{L1} + I_0 Z_{L0} \quad (16)$$

$$V_a = (I_1 + I_2) Z_{L1} + I_0 Z_{L0} \quad (17)$$

$$I_a = I_1 + I_2 + I_0 \quad (18)$$

If the reach of the relay for ground faults is set using the positive sequence impedance of the line (as in the case for most manufacturers' relays [18], [19], [20]),

$$IZ = (I_1 + I_2) Z_{L1} + I_0 Z_{L1} \quad (19)$$

From eqn. (17) and eqn. (19), note that $V_a \neq IZ$. IZ must be multiplied by a ratio of zero sequence impedance to positive sequence impedance ($k_0 = \frac{Z_{L0}}{Z_{L1}}$) so that $V_a = IZ$ [17]. The compensated current is therefore:

$$I_{comp} = I_1 + I_2 + k_0 I_0 \quad (20)$$

$$IZ = (I_1 + I_2) Z_{L1} + k_0 I_0 Z_{L1} \quad (21)$$

$$IZ = (I_1 + I_2) Z_{L1} + I_0 Z_{L0} \quad (22)$$

k_0 is known as the zero sequence current compensating factor which allows users to set the distance protection relay's reach settings in terms of the positive sequence impedance of the protected line. The value of k_0 and the equation used to calculate this value is dependent on the relay manufacturer and the design of the zone polygons of the relay [21]. The typical expression for k_0 is [17]:

$$k_0 = \frac{Z_{0L} - Z_{1L}}{K \times Z_{0L}} \tag{23}$$

Where the variable K in eqn. (23) is equal to 1 or 3, as specified by relay manufacturers. Other versions of k_0 are presented in [22]. The k_0 factor is considered a constant for a particular line and is independent of the length of the line. To summarise this concept, the basic components that a typical k_0 factor compensates are the relationships between the impedance of the phase to phase loop and the impedances of the phase to ground loop. The general approach to the k_0 factor is to find a relationship between [21]:

1) The half of a phase to phase loop for a fully transposed line (the impedance of one line) referred to as the Positive Sequence Impedance Z_1;
2) Three times the impedance of the ground loop consisting of the three phase conductors;
3) Three times the ground return path referred to as the Zero Sequence Impedance Z_0, to reflect the single phase model.

The apparent impedances depicted by eqns. (4)-(9) are not as simply computed by the relay as it may appear. The actual deciphering of the impedance that the relay performs is complex.

Taking the A-g fault loop into account as an example, consider the following system where an A-g fault is present on a simple radial system.

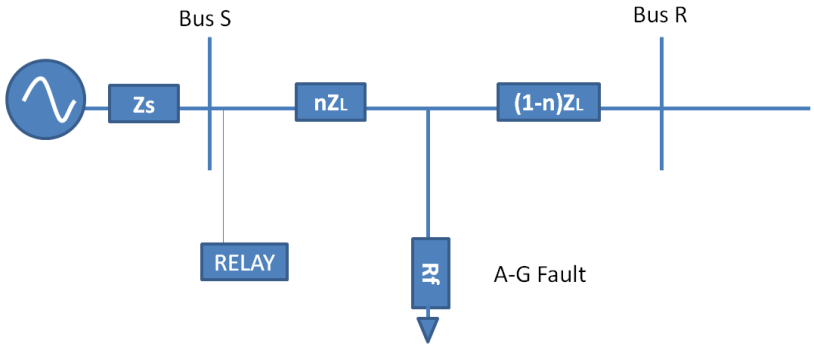

Figure 2.5: Single line diagram for a ground fault

For the single line diagram in Figure 2.5, if the fault were an A-g fault, the voltage at bus S would be [15]:

$$V = n \cdot Z_L(I_a + k_0 \cdot I_r) + R_f I_f \tag{24}$$

Where:

V is the voltage at bus S

n is the per unit distance to the fault from bus S

Z_L is the positive sequence line impedance

I_a is the current measured at bus S

k_0 is the zero sequence current compensating factor

I_r is the residual current measured at bus S

R_f is the fault resistance

I_f is the initial current flowing through the fault resistance

If eqn. (24) is converted into an impedance measurement by dividing every term by I, where $I = (I_a + k_0 \cdot I_r)$ one will obtain:

$$Z = \frac{V}{I} = mZ_L + R_f \frac{I_f}{I} = mZ_L + R_f \frac{I_f}{I_a + k_0 \cdot I_r} \quad (25)$$

The relationship in eqn. (25) can be expressed graphically as shown in Figure 2.6 below.

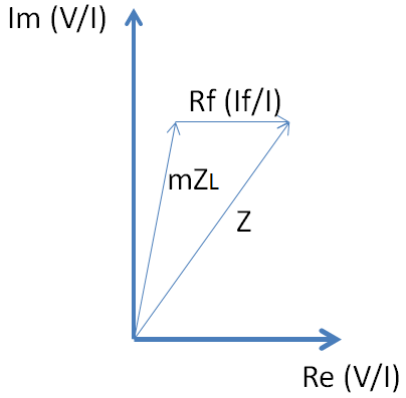

Figure 2.6: Impedance showing composition of resistance and reactance

From Figure 2.6, note how the relay will determine whether or not the impedance is within the reach of the zones of protection.

Since the impedance of the transmission line is proportional to its length, this method of protection will also give a good indication of the vicinity of the fault once the impedance seen by the relay is known.

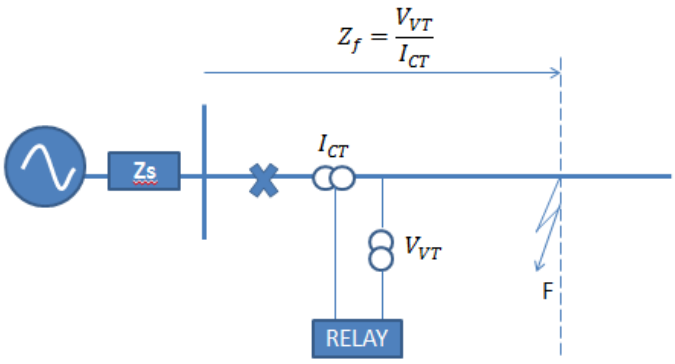

Figure 2.7: Basic distance protection principle

As with most protection schemes some degree of inaccuracy is inevitable, irrespective of the care taken in the design stages of the protection scheme. These inaccuracies could stem from CT and VT errors, inaccuracy of the line impedance parameters used to set the relay, measuring errors, etc. [10]. As with all protection schemes, the aim is to trip the breaker closest to the fault in the fastest possible time, so as to isolate the fault from the system, causing minimal disruption to other parts of the network. Due to the uncertainties and errors that are inevitably present, instantaneous tripping for faults near 100% of the line length becomes risky, since, due to the inaccuracies that exist, it is very possible for the relay to pick up for a fault on the next transmission line, either adjacent to or downstream to the line that is being protected. Instantaneous, unsupervised tripping is therefore undesirable for a protection zone set to cover 100% of the line.

To counteract this problem, more than one protection zone is used to protect a transmission line. The reach of the fast tripping zone is intentionally restricted to less than 100% of the line: the first protection zone (zone 1) of the relay is commonly set with a reach of approximately 80% of the line impedance with unsupervised instantaneous tripping. The value of 80% zone 1 reach is chosen since in theory 20% is considered to be the worst case combination of errors that will be present in the protection scheme. In other words at the furthest reach of the instantaneous zone 1 element, even if a 20% measurement error occurs, the element should still not trip incorrectly for faults that are, in reality, beyond 100% of the actual line length. Since this zone of protection is generally set to 80% of the line length, this zone is commonly called the under-reaching stage of the distance protection scheme.

The rest of the line is protected by a second zone of protection, (zone 2) commonly called the over-reaching zone. Introducing this zone of protection allows the remaining part of the transmission line (that cannot, for security, be covered by the instantaneous zone 1 element) to be covered. However in the case of this element security is ensured by making it slower-acting, with an intentional time delay to avoid unwanted trips for faults beyond 100% of the protected

line. The second zone of protection is intentionally set to cover 120% of the transmission line. Again, the additional 20% coverage arises from the theory that the worst-case combination of errors present in the protection scheme would be less than 20%. Setting this zone of protection to 120% will ensure that any fault that is actually on the transmission line that is being protected will be picked up by the relay even in the presence of a 20% measurement error. Setting this zone of protection to 120% will eliminate the risk of actual faults on the line being missed because of inaccuracies, but this will also mean that some faults on the transmission lines neighbouring the protected the line will be picked up. For this reason the intentional time delay is utilised for this protection zone in conjunction with supervision from other relay elements (other relay elements must be flagged in addition to the zone 2 element for a permissive trip to occur, in which the time delay is bypassed). It also implies that a relay operating a breaker closer to the fault will be given a chance to operate first.

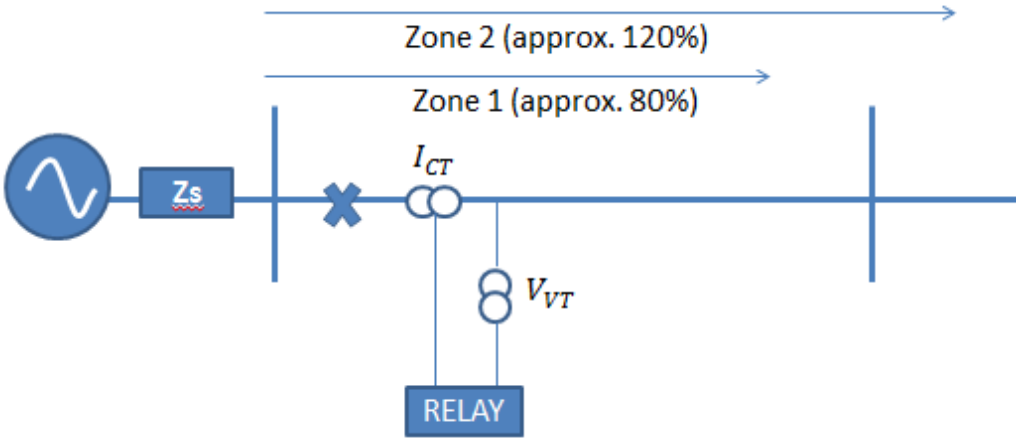

Figure 2.8: Illustration of zones of protection

2.7. Mho Impedance Diagrams

Distance protection relays use the impedance seen by the relay to make critical decisions with regard to the operation of the protection scheme as a whole. To make sense of the impedances seen by the relay, the impedance diagram is essential for evaluation purposes. Impedances are usually represented in the complex R-X plane. To understand the impedance plot it is important to first understand the definition of a phasor. A phasor $\bar{A}$ can be expressed as:

$$\bar{A} = A \cdot e^{j\varphi} = A \cdot [cos\varphi + jsin\varphi] = B + jC \quad (26)$$

This phasor $\bar{A}$ is therefore a vector quantity consisting of real and imaginary components.

Consider the impedance diagram in Figure 2.9, which represents the load and short circuit impedance of the transmission line using the phasor notation as described in eqn. (26). Note the load impedance and the short circuit impedance (fault impedance) represented in Figure 2.10 in

relation to the impedance representation on the impedance plot on Figure 2.9. During normal system conditions the impedance of the system would be the load impedance (Z_{LOAD}) [10], where:

$$Z_{LOAD} = \frac{{V_{LINE}}^2}{P_{LOAD}} \tag{27}$$

The angle between the current and voltage during this system condition (or load angle) can be represented as:

$$\varphi_{LOAD} = \text{atan}\left[\frac{P_{reactive}}{P_{real}}\right] \tag{28}$$

When a fault is present on the system (with or without a fault resistance) the measured impedance is no longer governed by the load, but rather by the short circuit impedance. As noted from Figure 2.10, this impedance corresponds to the impedance of the line between the location of the relay and the point of the fault (Z_{F1}). Where there exists a fault resistance, a resistive component (R_f) is added onto the impedance (Z_{F2}). This will be discussed in the next section.

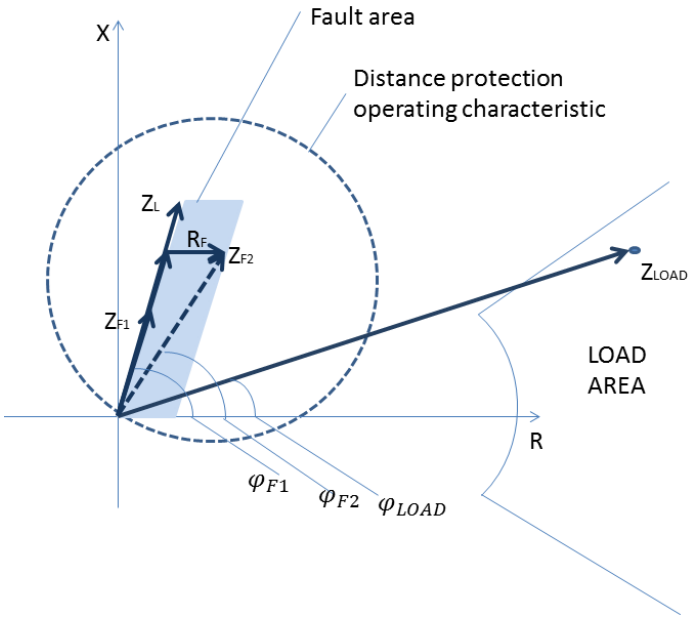

Figure 2.9: Impedance plot

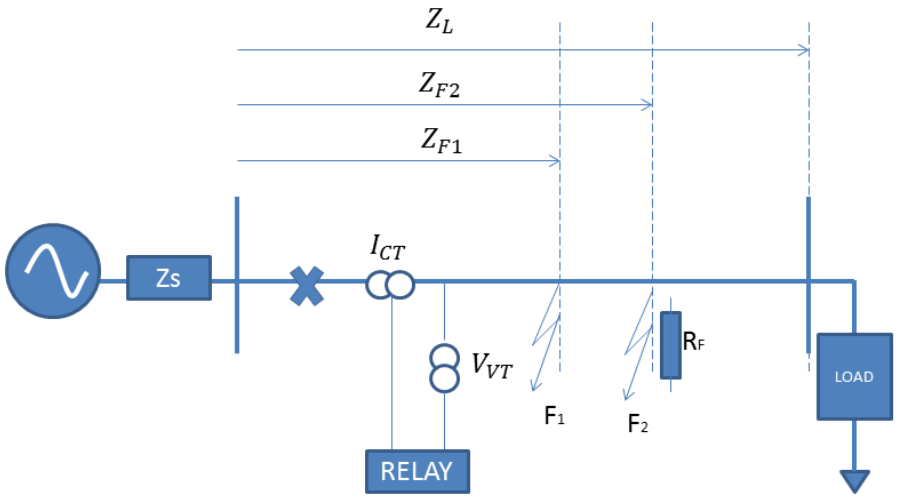

Figure 2.10: Faults and zones of protection

The distance protection is governed by the operating characteristic of the relay as defined by the user. This operating characteristic is fixed according to this user-defined input.

The impedance diagram shown in Figure 2.9 is known to be a self-polarised mho relay. This relay characteristic displays a weakness in that under close-up fault conditions, when the relay voltage falls to zero or near-zero, this characteristic (the self-polarised mho relay) may fail to operate when required to do so [11]. It is here that the fully cross-polarised mho characteristic becomes important. This mho characteristic employs an addition of a percentage voltage from the healthy phases to the main healthy voltage. This serves as a substitute phase reference. The addition of this percentage of voltage allows the relay to detect the close-in faults. This method of cross polarising enhances the conventional properties of the mho characteristic.

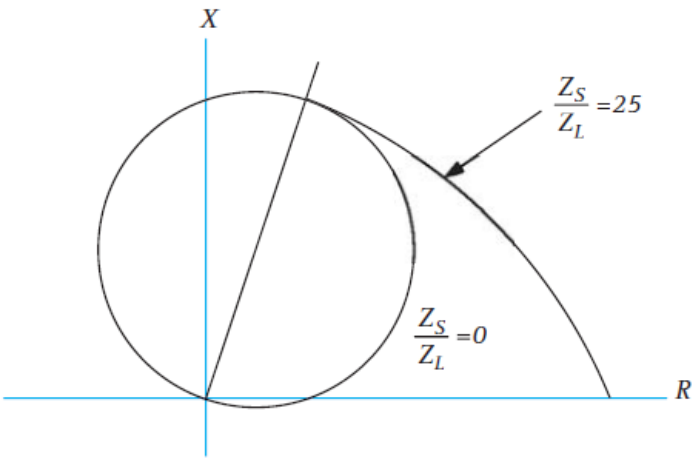

Figure 2.11: The ohmic effect of cross-polarisation of the mho characteristic [11]

2.8. Resistive Ground Faults

A high resistance ground fault is commonly known as a fault having a low fault current, where the resistance of the ground path is generally high. This causes the impedance seen by a relay to be larger than it actually is. This type of fault is of great importance where the application of distance protection relays is concerned, since the relays' decision elements rely on the impedance seen by the relay. Any error in the seen impedance will cause the distance protection relay to undergo reach errors. It is therefore important to properly investigate the effects of high resistance faults on transmission line networks.

Of all the faults recorded in South Africa, by Eskom (the main energy utility in the country), 16% of the faults are classified as high resistance faults [23]. According to the statistics presented in Section 1.1, more than a quarter of all faults arise due to fires under the transmission lines. The dynamic characteristics of a fire burning under a transmission line and the production of arcs burning in the air, result in changes in arc length and resultant fault resistances [24].

The arcing resistance can be calculated using Warrington's formula [11]

$$R_a = \frac{28710}{I^{1.4}} L \tag{29}$$

Where: R_a is the arc resistance in Ω

I is the arc current in A

L is the arc length in meters

In addition to the arc resistance, ground faults are largely affected by the ground resistivity. In South Africa this becomes a particular problem due to the high soil resistivity in most regions of the country due to the dry ground conditions. High soil resistivity provides a high fault resistance in the ground path, similar to the manner that the arc resistance does, but with greater effects [25].

Referring back to the example in Figure 2.9, where the additional resistance R_f is present in the fault branch, a change in the nature of the impedance seen by the relay is noted when comparing Z_{F1} to Z_{F2}. A closer look at this impedance plot will illustrate the problems presented by resistive faults to distance protection relays more clearly.

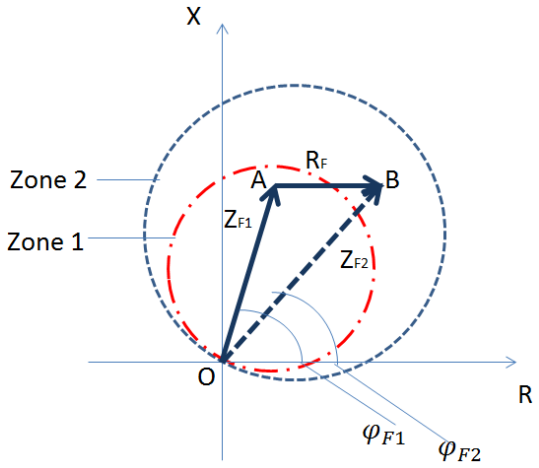

Figure 2.12: Effect of resistance faults on the impedance plot

For the fault Z_{F2} shown in Figure 2.12, the fault location is actually at point A, within zone 1. Due to the effect of the resistance of the fault, the relay will see the apparent impedance OB, and therefore the fault at point B, in zone 2. The problem then arises that the relay will trip for a zone 2 fault after a time delay, when the fault is actually in zone 1. Due to the intentional time delay of the zone 2 elements, the fault could remain on the system for a longer time, causing possible damage to the transmission line and other infrastructure connected to this line. This is referred to as under-reaching of the relay i.e. the relay will see the fault further away than it actually is.

Consider the case where the fault resistance is so high that the apparent fault impedance is pushed outside the boundaries of both zone 1 and zone 2. The fault would then need to be cleared by the back-up protection which usually also has a substantial delay causing possible damage to the transmission line. In addition to the time delay, the fault current through the ground path gets amplified by the effect of in-feed current from the remote end. This has the effect of causing the fault resistance seen by the relay to be much greater that the actual fault resistance, i.e. $R_{Fseen} > R_F$.

2.9. Permissive Signalling

Permissive signalling is used to achieve selective clearing of faults without time delay over the entire length of the line to be protected. Where permissive signalling is not present in the scheme, if a fault is present within zone 1, an instantaneous trip will be initiated by the relay, but if the fault is present in zone 2, the relay initiates a trip only after an intentional time-delay has elapsed. This delay is not ideal, since the fault will remain on the protected transmission line for a period of time, causing possible damage to plant and equipment; however, as explained earlier, the delay is necessary to allow coordination with the zone and elements of other lines' protection schemes, because of the over-reaching nature of the zone 2 element. Nevertheless,

with additional supervision logic, it is possible to bypass the zone 2 time delay under certain conditions without compromising the security of the protection scheme. This is the so-called permissive signalling - i.e. zone 2 can be given permission to trip without waiting for the zone 2 time delay if certain supervisory logic conditions can be satisfied.

A scheme that employs permissive signalling requires a communication link between the two relays that comprise the protection scheme. This communication link can be pilot wire, power-line carrier, microwave or fibre optic. As discussed in Section 2.6, the under-reaching zone will generally cause the breaker to trip instantaneously and the over-reaching zone will cause the breaker to trip after an intentional time delay. In the case of a permissive signalling scheme the relays on either end of the protected zone will communicate, via the communication link, with each other to provide near-instantaneous tripping. If certain supervisory logic conditions are satisfied, these communicated signals can be used to block, trip or transfer a trip signal, dependent on the protection engineer and the application he/she requires.

Permissive signalling schemes can be [10]:

- Direct under-reaching transfer trip (DUTT)
- Permissive under-reaching transfer trip (PUTT) with starter (fault detector)
- Permissive under-reaching transfer trip (PUTT) with zone extension
- Permissive over-reaching transfer trip (POTT)

The POTT scheme will be discussed and studied in this thesis since it is the main method of permissive signalling used for distance protection schemes in South Africa. The permissive over-reaching scheme derives its name from the fact that the over-reaching zone governs the permissive signalling. The POTT is the most popular distance scheme used in protecting transmission lines due to the greater protective coverage and resistive coverage offered by the zone 2 elements [11]. Consider the diagram in Figure 2.13, which shows a line between busbars A and B, protected by a permissive over-reaching protection scheme. This trip scheme (POTT) is known to initiate a near-instantaneous trip when the relays at both busbar A and B detect a fault in the over-reaching zone.

Consider a transmission line to be protected with relays at busbar A and busbar B with both relays having their zone 1 and zone 2 elements activated.

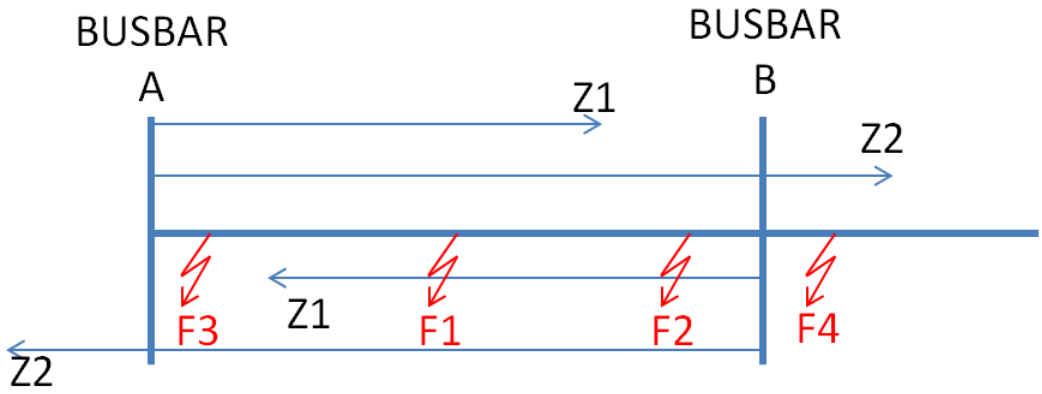

Figure 2.13: Permissive over-reaching transfer trip scheme

Consider a fault F1 in Figure 2.13, the relays at busbars A and B will see the fault in their respective zone 1. Both relays will initiate an instantaneous trip.

For faults F2 and F3, one relay will see the fault in zone 1 and the other relay will see the fault in zone 2. For F3, the relay at A will see the fault in both its zone 1 and 2 and the relay at B will see the fault in its zone 2. For F2, the relay at B will see the fault in both its zone 1 and 2, while and the relay at A will see the fault in its zone 2. It is these cases where the POTT scheme becomes important. For a fault such as that at F2 that is actually on the protected line and is seen by the relay A only in its zone 2, the relay B will see the fault in both zone 1 and zone 2. For a fault that is actually on the protected line, the zone 2 element of relay B then can be used to initiate a permissive signal to send to relay A. Relay B would trip the breaker B instantaneously. With the implementation of permissive over-reaching signalling relay B would trip instantaneously and concurrently send a permissive signal to the relay A. The relay A will now see the fault in zone 2 and additionally will receive the permissive signal sent by relay B. This received permissive signal will cause the breaker A to trip without further delay. Hence both breaker A and breaker B will trip at high speed. Alternatively if relay A only sees the fault in its zone 2 but relay B does not see the fault in its zone 2, this means that the fault is behind relay B (fault F4 in Figure 2.13) and it is not secure for relay A's zone 2 to trip faster that its zone 2 time delay. In this case no permissive signal is sent, since relay B does not see the fault in its zone 2, so the relay at A will wait until its delay is timed out before initiating a trip to the breaker A.

The principle depicted above can be illustrated by the logic circuit below:

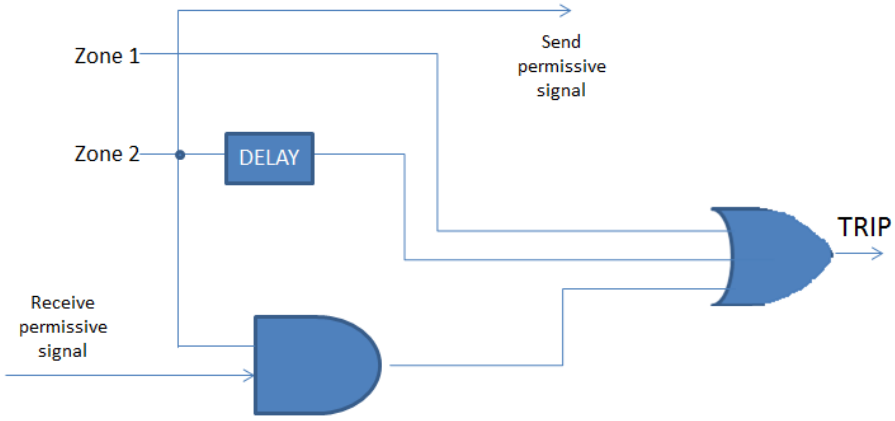

Figure 2.14: Logic circuit for POTT scheme

2.10. Double Circuit and Parallel Transmission Lines

Due to space and servitude constraints, enhancing power transfer, reliability and security [1], [26], the use of double circuit and parallel transmission lines has become widespread. A double circuit transmission line can be classified as two transmission lines constructed on the same tower and parallel transmission lines can be classified as two transmission lines constructed in the same right of way on separate towers. Double circuit and parallel transmission lines have many different topologies that cause varied influence to the power system depending on the geometry of tower and line construction. Due to the complexities that arise from double circuit and parallel transmission lines, the protection schemes protecting these lines often require enhanced performance [27] and require consideration of the specific operating conditions that the transmission line being protected is subjected to. One of the known factors that affect these parallel transmission lines is the mutual coupling been the two lines. The second challenge that is unique to parallel transmission lines is the possibility of cross country faults. Citations of the effects of mutual coupling on parallel transmission lines have been documented to some extent, but none contains a simple, consolidated approach to consider the extent of the effect on the protection scheme in a real time simulation environment.

2.11. Mutual Coupling

It is known that mutual coupling between transmission lines can lead to undesirable interaction phenomena, which may affect the protection scheme functionality [28].

Mutual coupling occurs when two or more current carrying conductors are sufficiently close to each other, allowing their electro-magnetic fields to interact. Note the interaction of the field lines in Figure 2.3. The coupling between the conductors will give rise to mutual impedance between the two conductors. This is known as the mutual zero sequence impedance which

allows one to calculate the zero sequence volt-drop in one line due to the circulation of zero sequence current on the other line [29].

Consider the two current carrying conductors in Figure 2.15, where Z_s is the self-impedance of each conductor and Z_m is the mutual impedance between the two conductors.

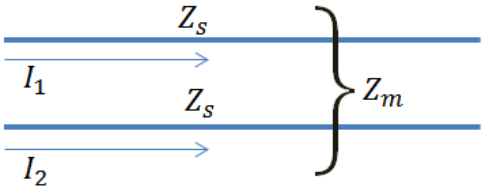

Figure 2.15: Mutual coupling between two conductors

Where the discipline of transmission line protection is concerned, these current carrying conductors are equivalent to double circuit transmission lines on the same tower or parallel lines on separate towers in the same right of way. Transmission lines with mutual coupling can have some of the following topologies [1]:

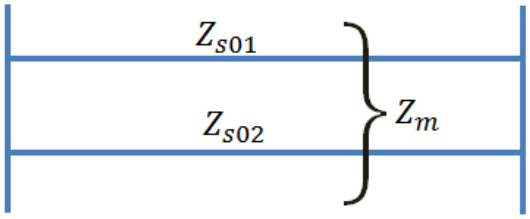

Figure 2.16: Transmission lines originating and terminating on common busbars

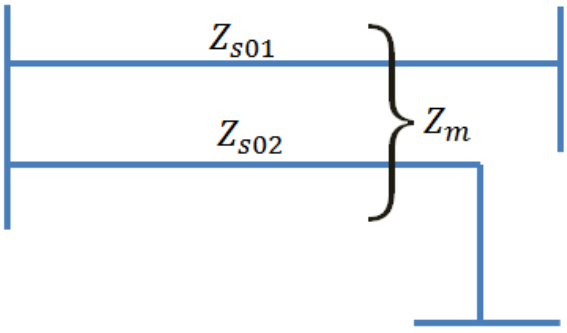

Figure 2.17: Transmission lines originating on common busbar, but terminating on different busbars

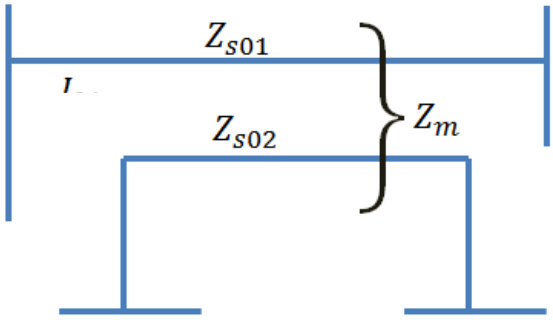

Figure 2.18: Transmission lines originating and terminating on different busbars

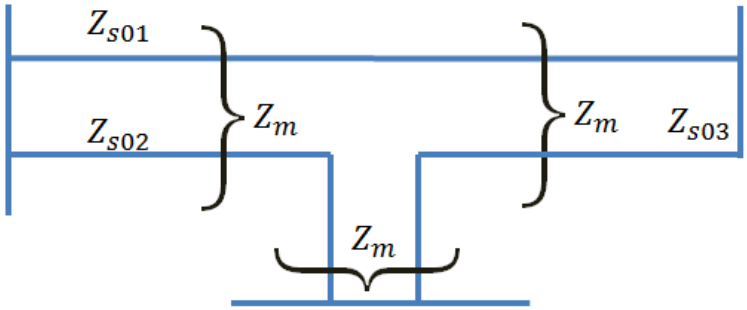

Figure 2.19: Multiple couplings

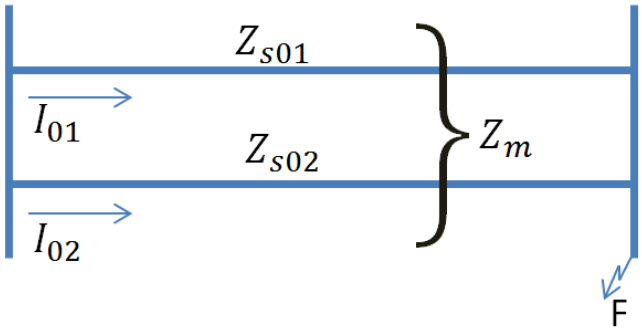

Figure 2.20: Parallel transmission lines with a fault

Considering the specific topology of parallel coupled line in Figure 2.20 for the case where there is a single-phase to ground fault F at the receiving end, the zero sequence volt-drop in the first line can be expressed as [29]:

$$V_{01} = Z_{s01}I_{01} + Z_mI_{02} \quad (30)$$

Where V_{01} is the zero sequence volt-drop

$Z_{s01}$is the zero sequence self-impedance of the line

$I_{01}$is the zero sequence current of the transmission line

$I_{02}$is the zero sequence current of the parallel transmission line

Z_m is the mutual impedance between the parallel lines.

According to [30] the self and mutual impedance between two transmission lines can be defined as:

$$Z_{ii} = r_i + 0.09530\left(\frac{f}{60}\right) + j0.07537\left(\frac{f}{60}\right)\left[\ln\left(\frac{1}{GMR_i}\right) + 6.74580\right]\Omega/km \quad (31)$$

$$Z_{ij} = 0.05919\left(\frac{f}{60}\right) + j0.07537\left(\frac{f}{60}\right)\left[\ln\left(\frac{1}{d_{ij}}\right) + 6.74580\right]\Omega/km \quad (32)$$

Where : r_i is the resistance of the line

GMR_i is the geometric mean radius of the line

d_{ij} is the distance between the two parallel lines

The subscript *i* denotes the parameters of the reference transmission line and subscript *j* denotes the parameters of the parallel line. These two equations however only apply to the simplest case of one ground wire, one conductor per phase and a ground resistivity of 100Ω/m^3. For a more complex system involving a different ground resistivity, more than one conductor per phase and the introduction of more than one ground wire, the mathematical computation of the impedance becomes complex.

For a single three-phase transmission line (with phases a, b c), the self-impedance of each phase and the mutual impedances between each phase of the transmission line can be expressed by the 3x3 impedance matrix:

$$Z_{abc} = \begin{bmatrix} Z_{aa} & Z_{ab} & Z_{ac} \\ Z_{ba} & Z_{bb} & Z_{bc} \\ Z_{ca} & Z_{cb} & Z_{cc} \end{bmatrix} \quad (33)$$

By contrast, the self and mutual impedances of two three-phase transmission lines (phases a, b, c and a', b', c') in an double-circuit configuration or on separate towers in the same right of way are described by a single 6x6 impedance matrix [30] as follows:

$$Z_{abc} = \begin{bmatrix} Z_{a\,a} & Z_{a\,b} & Z_{a\,c} & Z_{a\,a'} & Z_{a\,b'} & Z_{a\,c'} \\ Z_{b\,a} & Z_{b\,b} & Z_{b\,c} & Z_{b\,a'} & Z_{b\,b'} & Z_{b\,c'} \\ Z_{c\,a} & Z_{c\,b} & Z_{c\,c} & Z_{c\,a'} & Z_{c\,b'} & Z_{c\,c'} \\ Z_{aa'} & Z_{a'b} & Z_{a'c} & Z_{a'a'} & Z_{a'b'} & Z_{a'c'} \\ Z_{b'a} & Z_{bb'} & Z_{b'c} & Z_{b'a'} & Z_{b'b'} & Z_{b'c'} \\ Z_{c'a} & Z_{c'b} & Z_{cc'} & Z_{c'a'} & Z_{c'b'} & Z_{c'c'} \end{bmatrix} \quad (34)$$

To the protection engineer, the mutual coupling between the transmission lines becomes important where the design of the protection scheme is concerned. Consider the following

symmetrical component network for a simple A-g fault, Figure 2.21 not taking into account mutual coupling and Figure 2.22 taking into account mutual coupling.

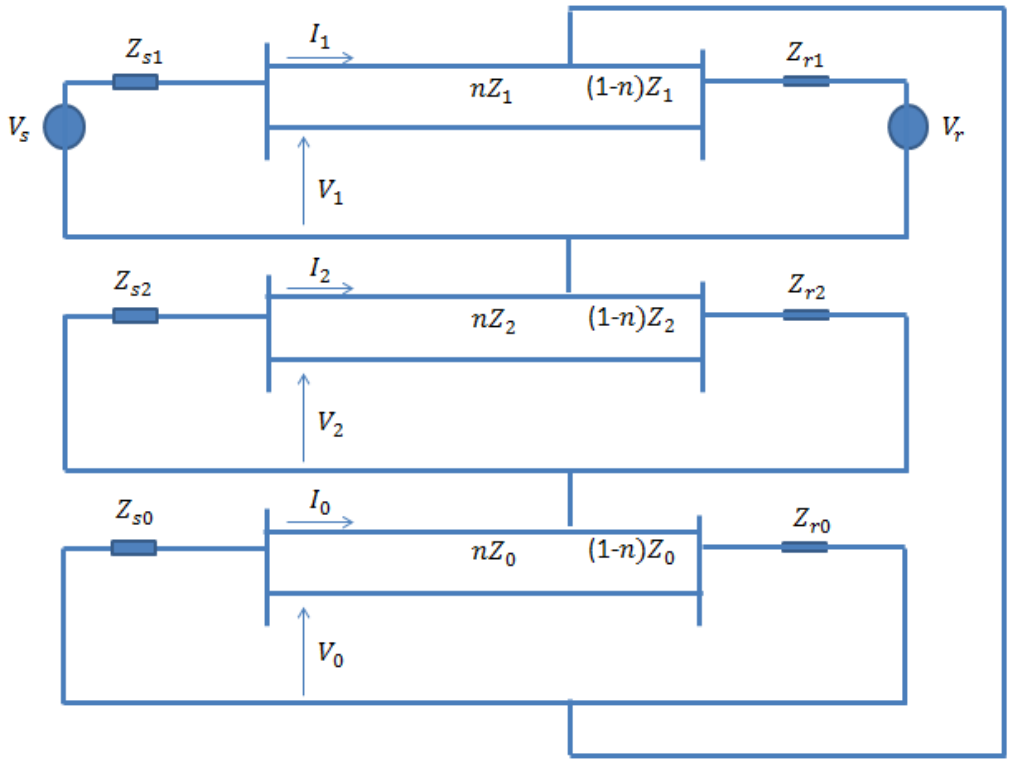

Figure 2.21: Symmetrical component network without mutual coupling

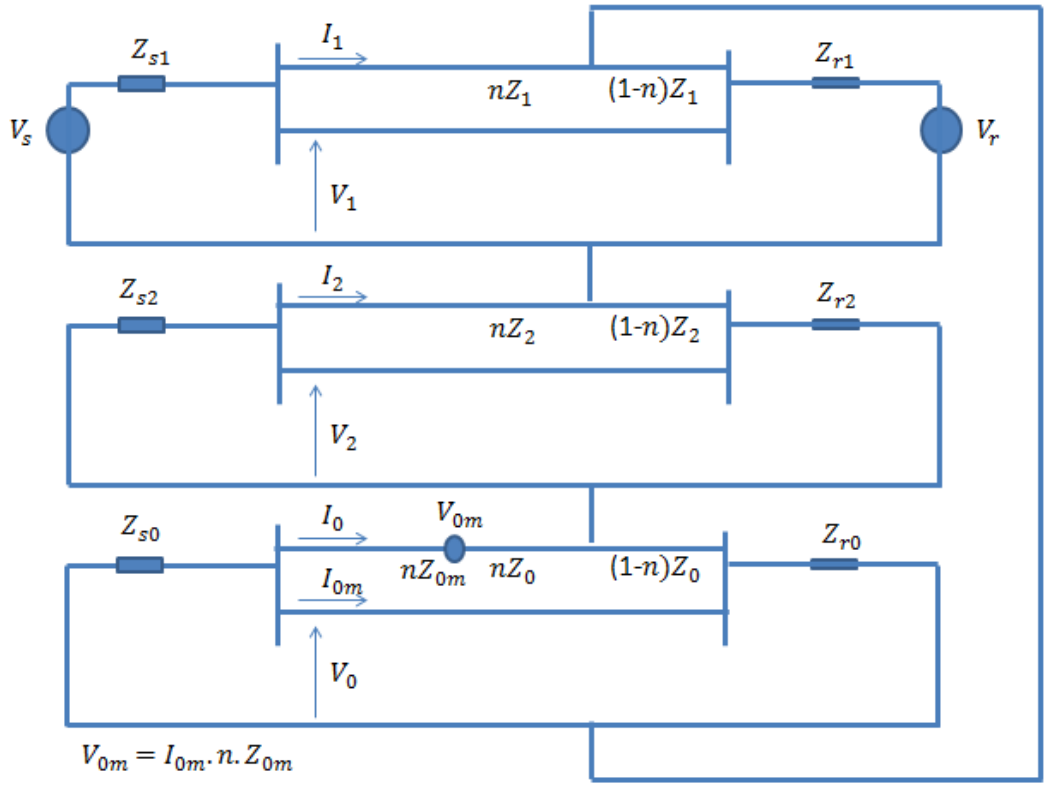

Figure 2.22: Symmetrical component network with mutual coupling [30]

To derive the phase voltage for this A-g fault where mutual coupling is present, using the sequence network of Figure 2.22, V_a can be calculated as follows [30]:

$$[V_1 - (nZ_1)I_1] + [V_2 - (nZ_2)I_2] + [V_0 - (nZ_0)I_0 - (nZ_{0m})I_{0m}] = 0 \quad (35)$$

$$V_1 + V_2 + V_0 = (nZ_1)I_1 + (nZ_2)I_2 + (nZ_0)I_0 + (nZ_{0m})I_{0m} \quad (36)$$

$$V_a = (nZ_1)[I_a + \frac{Z_0 - Z_1}{Z_1} I_0 + \frac{Z_0}{Z_1} I_{0m}] \quad (37)$$

$$nZ_1 = \frac{V_a}{I_a + \frac{Z_0 - Z_1}{Z_1} I_0 + \frac{Z_0}{Z_1} I_{0m}} \quad (38)$$

From eqn. (38), note that the impedance seen by the distance protection relay will be affected by the mutual impedance between the two transmission lines. This change in impedance seen by the protection relay will cause the relay to operate incorrectly. In the case of a distance protection relay, the change in impedance due to mutual coupling would cause the relay to under-reach or over-reach. This error in reach will be dependent on the direction of current flow in the healthy circuit [1].

The mutual coupling of the positive and negative sequence components between the feeders of the parallel transmission towers for symmetrical lines is usually small in comparison to the zero sequence components. For this reason the positive and negative sequence components of mutual coupling are typically neglected [1], [31]. Mutual coupling that affects the zero sequence networks is more significant and therefore the mutual coupling will have the greatest effect on faults involving ground. Where there exists a ground fault on one of the feeders and the parallel feeder is taken out of service and grounded at both ends, the effects of mutual coupling on the impedances measured by distance protection relays are even more significant [1], [5] [31], [32], [33]. The authors of [29] suggest that the error in the impedance seen by the relay for the condition of having one line out of service and ground at each end could reach as much as 11%.

Once the extent of the reach errors borne by the distance protection relay due to mutual coupling, according to the specific operating conditions, is known, compensation for this error can be designed. The presentation of methods to combat the effects of mutual coupling vary between publications and differ according to the protection scheme used [5], [24], [29], [31], [32], [34].

The zero sequence current compensating factor (k_0 factor) is one of the methods used in modern distance protection relays to ensure that the ground impedance measured is more precise and to eliminate unnecessary reach errors caused by mutual coupling [24]. The zero sequence current compensating factors (k_0 factors) do not have a specific format and are entirely dependent on the relay manufacturer and the algorithm that the relay is governed by as discussed in Section 2.6. Typically, distance protection relays make use of these different formats of the k_0 factor to

convert all phase-to-ground faults so that they can be assessed as if they were phase-to-phase faults [22].

For the purposes of using the k_0 factor to compensate for the mutual coupling of parallel transmission lines, a modified compensating factor must be used relevant to the operating condition of the parallel transmission line [1]. Caution must be exercised on how the specific relay that is being used defines its k_0 factor. The derivation of this k_0 factor used to compensate for the mutual coupling between two transmission lines is sometimes known as the mutual coupling factor (k_{0M}). The mutual coupling factor takes into account the mutual coupling between the transmission lines. The specific equation defining this factor again depends on the relay manufacturer.

Using these factors, the zero sequence current is internally compensated by the relay. Only the current measurement would need to be compensated since the voltage measurement already includes the effect of the coupling. The current compensation can be derived as follows [11]:

$$I = I_{fault} + \mathrm{k}_0 I_0 + k_{0M} I_{0parallel} \tag{39}$$

Where: I_{fault} is the fault current on the protected line

k_0 is the zero sequence current compensating factor

I_0 is the zero sequence current of the protected line

k_{0M} is the mutual coupling factor

$I_{0parallel}$ is the zero sequence current of the parallel line

A particular expression for k_{0M} is then defined by relay manufacturers where this method of mutual coupling compensation is employed. For example, various publications define k_{0M} in different ways as follows [24], [30], [32], [35].

$$k_{0M} = \frac{Z_{0M}}{3Z_{1L}} \tag{40}$$

$$k_{0M} = \frac{Z_{0L} - Z_{1L} - Z_{0M}}{3Z_{1L}} \tag{41}$$

$$k_{0M} = \frac{Z_{0M}}{Z_{1L}} \tag{42}$$

Where Z_{0M} is the zero sequence mutual impedance

Z_{1L} is the positive sequence impedance of the line

Z_{0L} is the zero sequence impedance of the line

In most instances the current of the parallel line must be available for input to the relay so that the relay can internally compute the zero sequence current of the parallel line, the zero sequence impedance of the parallel line or the zero sequence mutual impedance between the lines.

In cases where the currents of the parallel line are not available, or where a particular utility prefers not to adopt this current compensation approach, mutual coupling can also be compensated for by appropriately setting the ground fault reach settings of the protected line, such that the reach errors due to mutual coupling are adequately counteracted [1], [5]. For instance, if a fault on a parallel transmission line causes the relay to see the fault in zone 2 due to the mutual impedance, when the fault is actually in zone 1, the zone 1 reach can be extended to compensate for this. Figure 2.23 illustrates a condition where, a fault was placed at 80% of the line, and due to mutual coupling, the fault was seen in zone 2. The zone 1 reach can then be extended as shown to represent a new zone 1 reach.

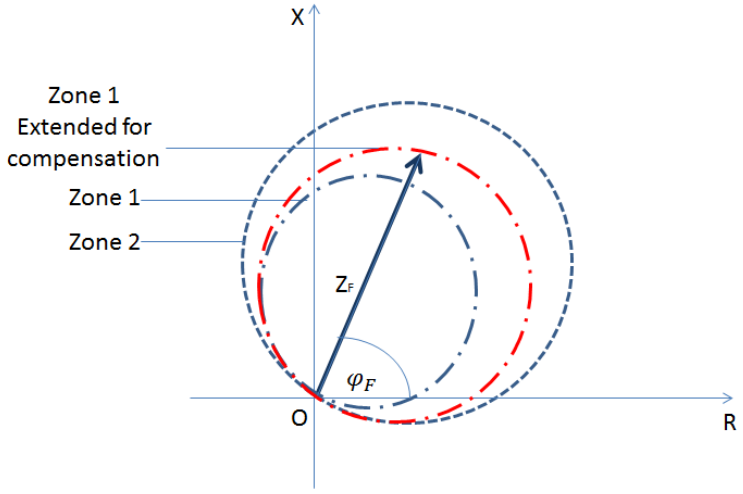

Figure 2.23: Impedance diagram showing an extended zone 1

The two methods of compensation for mutual coupling presented above are most often not adequate for the protection of a double circuit or parallel transmission line due the constant change in transmission line topology, e.g. one line taken out of service for maintenance. In practice, a fixed mutual coupling compensation method is undesirable as it makes protection settings for a variety of operating conditions unaccommodating since the effects of mutual coupling on the protection relays on a particular protected line can be different under different operating conditions. One way to approach this issue is to design settings (compensated zone reaches) for each envisaged operating condition and store these in different setting groups within the relay. In this way, when a particular closely coupled transmission line is taken out of service, the protection is switched to a different and more appropriate settings group. Automation of the selection between setting groups has also been investigated, allowing the

relay to select the appropriate setting to protect the line using inputs from the operating condition of the line [33].

Any form of mutual coupling compensation must be approached with caution since incorrect operation of the relay for close in faults on the adjacent feeder may be experienced [1].

2.12. Transposition of Transmission Lines

Transposition of transmission lines is practiced in transmission networks since it proposes to balance out the capacitive and inductive effects of the transmission lines [12] and thereby reduce unbalance in system currents and voltages [36]. Transposition of transmission lines can be defined as the conductors in each phase exchanging positions at regular intervals along the line such that each conductor occupies every position for equal distances [37]. Consider a three phase transmission line where the spacing between the conductors is known. One complete cycle arrangement of a transposed transmission line can be illustrated as:

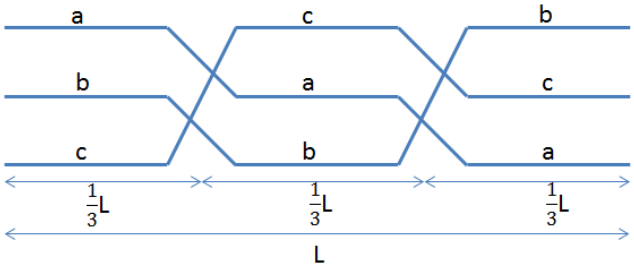

Figure 2.24: 1 cycle of transposed transmission lines [38]

Transmission lines that have undergone one complete transposition cycle would have balanced voltage drops in each phase since the capacitive and inductive effects in each phase with respect to the other two phases have been balanced.

Transposition of transmission lines introduces many complexities to the system physically and financially such as [36], [39]:

- Conductors crossing over each other giving rise to susceptibility to flashovers;
- Increase in the cost since transposition towers are required at regular intervals, these towers themselves being more expensive and the cost of their insulator strings being greater also;
- The total weight of supports will increase due to more insulator strings being introduced;
- Experience has proved that transposition towers introduce weakness into the system and reduce the performance of the transmission line.

For these reasons, transmission lines are, at times, untransposed to avoid the addition of weakness in the system. Where the transmission lines are untransposed, their effect on the distance protection relay must be noted and documented since the unbalanced capacitive and inductive effects will give rise to a change in the impedance seen by the relay.

In order to understand the unbalances that arise from an untransposed transmission line, it is important to understand the use of symmetrical components as described in the classical paper by C. L Fortesque [40] and more recently in [41]. The unbalances due to untransposed transmission lines have been widely covered by [42], and extensive studies have been done by Hesse in [43], [44], [45]. The effects of non-transposition of the transmission lines are well understood but the effect on the distance protection relay is not widely documented. A full mathematical investigation of the unbalance on the distance protection relay will be discussed in Chapter Five of this thesis.

2.13. Cross Country Faults

The term cross country fault is commonly used to refer to a case where a fault is present on a transmission line and at the same time a fault is present on a parallel transmission line at a location further down the line [46], [47], [48]. For example on a pair of parallel transmission lines, an A-g fault is present on one line and at the same time (or a very short time later such that both faults are present on the system at the same time) a B-g fault is present on an adjacent line. The term cross country fault is sometimes also used to refer to an evolving fault on a parallel transmission line. For example the A-g fault can occur just before the B-g fault in the illustration given below.

Figure 2.25: Illustration of a cross country fault

Cross country faults become of special interest where single pole tripping is concerned as operation of the phase selection elements at the sending end (relays R1 and R3) becomes complicated under such conditions [48]. Since the phases at the sending end are at the same electrical point on the system, the relays at points R1 and R3 will see an AB-g fault [46]. This will result in a three phase trip instead of a single phase trip as desired for a single pole tripping scheme, since a multi-phase fault will be seen by the relays' phase selectors. However the relays

at the receiving end will see the correct phase faults and trip correctly. If this three phase trip at the sending end occurs on both parallel feeders a disastrous loss of supply to a complete area can occur.

To understand this more clearly note the current distribution in Figure 2.26 due to an A-g fault on one line and a B-g fault on the parallel line, with both faults located close to the receiving end.

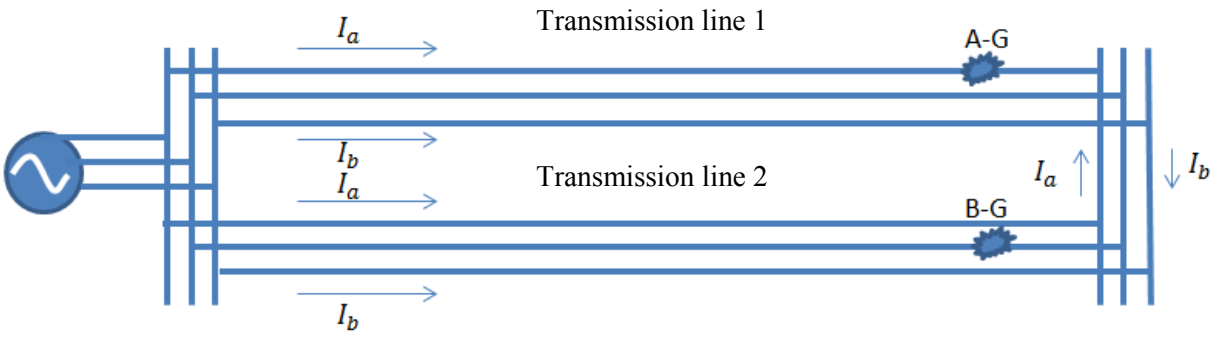

Figure 2.26: Current distribution of a cross country fault in parallel feeders

An A-g fault on the first transmission line will cause the fault to be fed from current on the second transmission line through the connecting busbar. At the same time if a B-g fault occurs on the second transmission line, the fault current will be fed from the current on the first transmission line through the connecting busbar. The relays protecting transmission lines 1 and 2 at their sending ends will see both A phase and B phase fault currents, thereby initiating a 3 phase trip as opposed to a single phase trip since more than one phase of fault current will be detected.

Generally this problem occurs where the faults are closer to the receiving (remote) end and tends to become less evident when the fault moves closer the midpoint of the line [47].

Due to the uncertain nature of cross country faults and the unclear effect this type of fault has on the relay, a properly documented extent of the consequences on the protection scheme is lacking. Many engineers propose methods and means to reduce the uncertain three pole tripping due to cross country faults. These include:

- The use of a permissive scheme that makes use of phase-segregated permissive signals from the remote end to provide selectivity at the sending end [1], [46].
- The use of modern relays that utilise advanced phase selection techniques [1].
- Use of a digital pilot communication channel to transmit multiple bits of information such as faulted phase selection in addition to permissive signalling [46].

- Use of a per phase line current differential protection scheme to correctly identify the internal line to ground fault. This method will however be insensitive to high resistive faults [46].
- The use of a delay for the permissive tripping signals in an attempt to allow the trip of the local end to isolate the fault first thereby stabilising the phase selectors [46].

2.14. SEL 421 relay

The SEL 421 is a relay manufactured by Schweitzer Engineering Laboratories and is an advanced, full-featured, single-pole reclose relay for transmission protection applications. Two such relays will be used for the purposes of distance protection on transmission lines in this research.

The Figure 2.27 gives an indication of the available functions as well as the variable names and numbers to be used to identify the settings class where programming the relay is concerned. These variable names and numbers are of great importance in the control of the bit logic used internally in the relay, giving rise to desired control of coupled equipment, such as a breaker. Configuration of the relays can be done in two ways, firstly by manually changing the setting by means of pushbuttons on the relay front panel, or more efficiently to use the customized software package AcSELerator QuickSet ®. This enables settings to be made on the software interface and to be sent via serial communication to the relay.

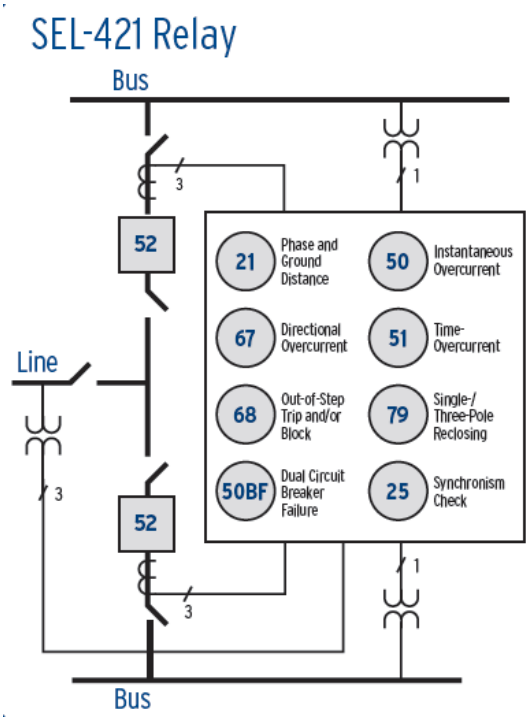

Figure 2.27: Applications and setting classes for the SEL 421 relay [48]

Inter relay tripping and relay to relay communication is an extremely important application in power systems that are reliant on the speed and efficiency of the communication channel between communicating relays. The transfer of data and timing coordination between relay terminals and the fastest possible tripping between these corresponding breakers becomes critical in any application. In the specific application of the SEL 421 relays in this research, relay to relay communication and the monitoring and control of particular word bits are of supreme importance. Different communication channels were investigated, which encompass simple and fast two directional logic communications. Basically, as shown below, virtual channels are required to transmit and receive information continuously between two relay terminals For this reason high voltage interface panels were used to achieve relay to relay communication, making use of input signals directly from the simulation models.

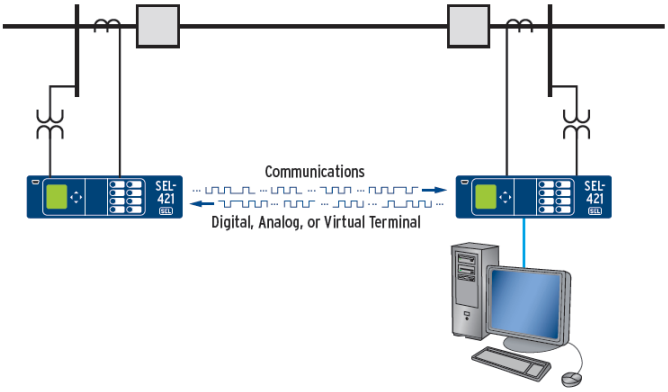

Figure 2.28: Relay to relay communication [48]

The SEL 421 distance protection relay provides the needed capabilities for a distance protection scheme and will be used in the various studies performed in this thesis where hardware protection relays are involved. The particular protection elements that are to be used in this thesis, that are provided by the relay are:

1) **Mho Ground Distance Elements**

The SEL 421 relay has five independent zones of mho ground distance protection. The mho ground distance protection operates only for single phase-to-ground faults. Each zone's reach can be set independently. Zone 1 and zone 2 are forward distance protection elements and zones 3, 4 and 5 can be set to either forward or reverse [18].

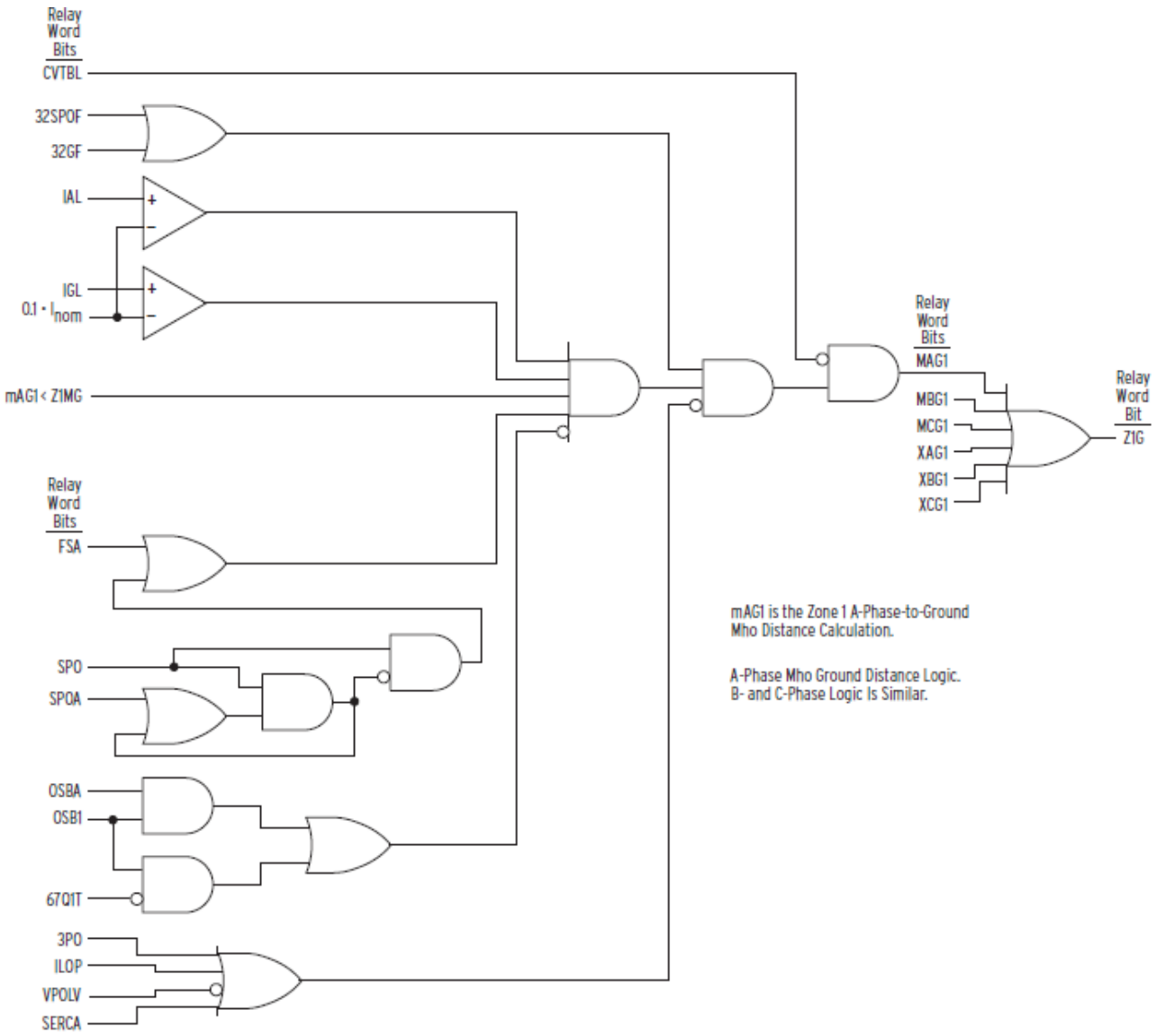

Figure 2.29: Mho ground distance element logic [18]

2) **Mho Phase Distance Elements**

The SEL 421 has five independent zones of mho phase distance protection. The mho distance protection operates for phase-to-phase, phase-to-phase-to-ground and three-phase faults. Each zone's reach can be set independently. Zone 1 and zone 2 are forward distance protection elements and zones 3, 4 and 5 can be set to either forward or reverse [18].

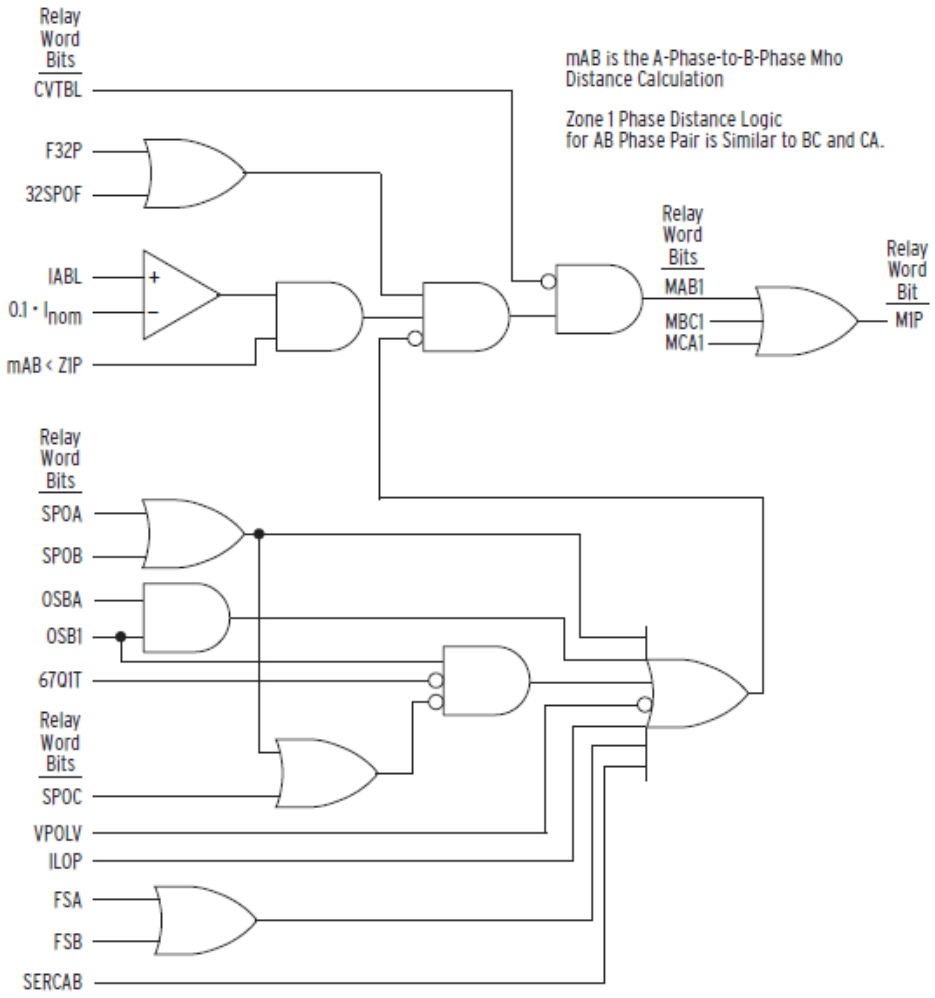

Figure 2.30: Mho phase distance element logic [18]

3) **Zero-sequence Current Compensation Factors**

The zero-sequence current compensation helps to keep the phase and ground distance elements at the correct reach. The SEL 421 relay has three zero-sequence current compensation factors. k_{01} is a dedicated zero sequence current compensation factor defined as [49]:

$$k_{01} = \frac{Z_{0\,line} - Z_{1\,line}}{3 \times Z_{1\,line}} \tag{43}$$

4) **Communications Assisted Tripping Logic**

The SEL 421 communications assisted tripping schemes provide unit protection for transmission lines without any need for external coordination devices [18]. POTT schemes for two terminal and three terminal line applications are available. The scheme, as discussed before operates according to the Figure 2.31.

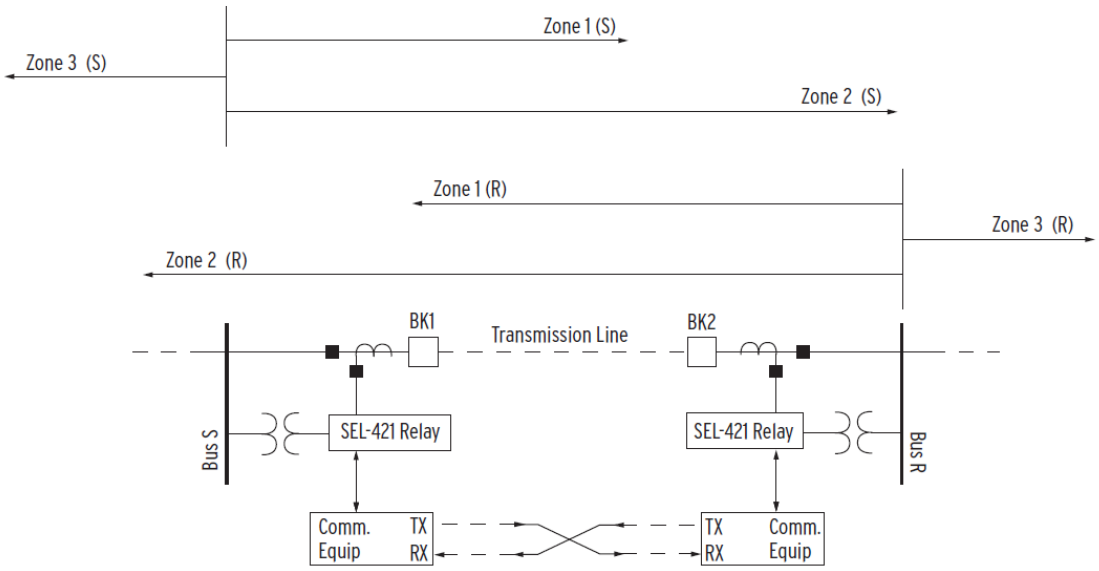

Figure 2.31: Communications assisted trip logic using the SEL 421 relay [18]

5) **Single Pole Tripping**

The SEL 421 relay provides single pole tripping if this function is activated. Single pole trip logic is activated for the following conditions [18]:

- Zone 1 ground distance protection asserts for a single phase-to-ground fault
- Zone 2 ground distance protection asserts for a single phase-to-ground fault and is permitted to trip via the communications assisted tripping logic
- Any of the three SELogic control equations if activated

6) **Cross-Country Fault Identification and Single Pole Tripping**

The SEL 421 relay provides a means of implementing simultaneous ground fault tripping logic for single-pole tripping applications in double-circuit tower applications [49]. The SEL 421 relay overcomes the mismatches that arise with cross country faults by making use of a minimum of two communication channels. One channel is used for transmitting a three-pole trip permission and another channel is used for any other permissive trips. If a relay receives both permissive signals, only then will a three-pole trip occur. With phase distance elements asserting one signal and ground distance elements asserting the other signal, unnecessary three pole tripping will be eliminated.

2.15. The Real Time Digital Simulator

The Real Time Digital Simulator (RTDS) is a power system simulator that solves electromagnetic transient simulations in real time [50]. The RTDS that will be used for this research project is located at the Real Time Power System Studies (RTPSS) Centre of the

Durban University of Technology (DUT), Steve Biko campus. RSCAD is the software that is used to run the simulations on the Real Time Digital Simulator. A very important application of the RTDS is the closed loop testing of protective relays and integration into a power system [51] that would be important in this project. The ability of the RTDS system to be connected to hardware through the available analogue and digital input and output channels provides a more thorough method of testing of power system protection schemes before commissioning and provides a reliable means for research. Closed loop testing is a method of taking the outputs of test equipment and feeding them back as inputs to the controlled plant in the system, which is beneficial since the actual performance of the equipment connected to the simulator will be realized. This makes provision for realistic test conditions which results in speed, accuracy, reliability and efficiency for the implementation of the modelled system in industry.

There are two important components to the real time simulation platform, namely hardware and software.

Software: The RTDS uses the RSCAD software that has been mentioned earlier. RSCAD is advantageous since this software allows for simulation models to be set up easily due to the user friendly graphical user interface. Modification to the simulated study system and desired control of the system can be achieved during the running of the simulation. RSCAD boasts an extensive range of component models available for use in the modelling process. This provides numerous solutions to any given problem, where the most economical and efficient solution can be achieved. New component models can also be created by combination of elementary component models, thus allowing flexibility in design. An important point to note, that will be referred to later in the thesis, is that the software comprises of two important subprograms. These are the DRAFT subprogram which is used to build the real time model of the plant and the RUNTIME subprogram which is used to run the simulation, view outputs and make changes to the simulation while the simulation is being run.

Hardware: The RTDS has the feature of running simulations in real time and allowing connection of external equipment in closed loop as mentioned before. The RTDS has the distinctive advantage of interfacing sophisticated equipment, such as a relay, in the design process allowing for full testing of the equipment in design stages. This provides vital information in predicting the operation of the equipment in real applications. RTDS hardware employs high-speed DSP (Digital Signal Processor) and RISC (Reduced Instruction Set Computer) chips that operate in parallel providing fast computation of results with diminutive simulation step sizes achieved. The closed loop also provides the most direct path possible from the processor to the input/output [52].

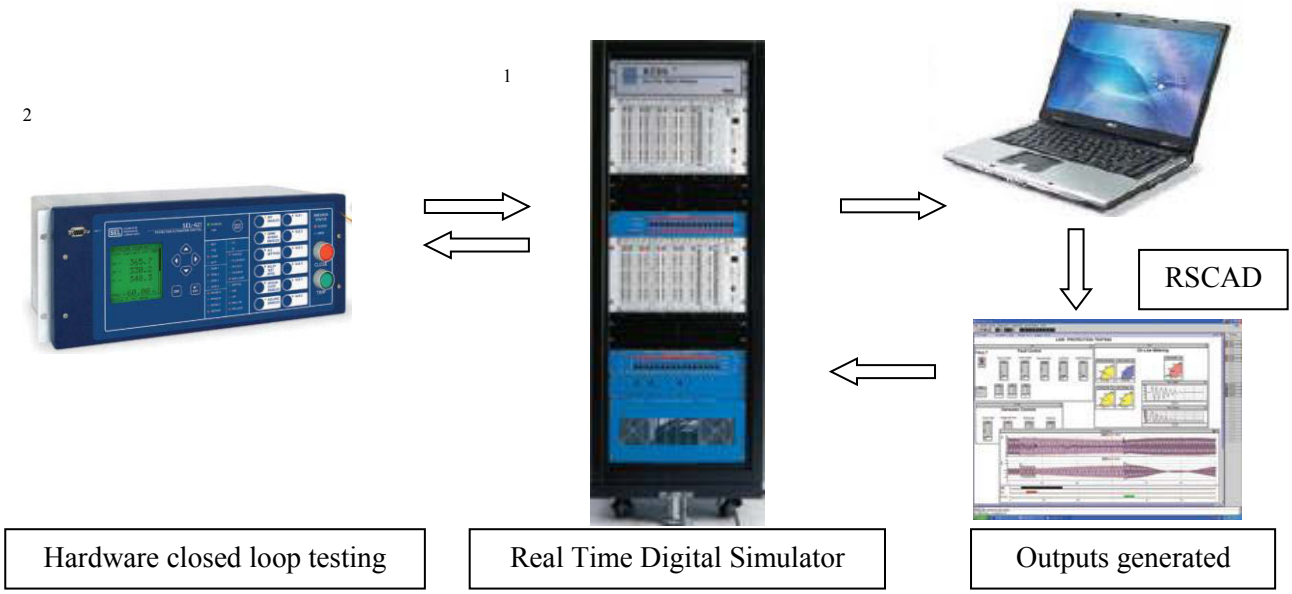

Figure 2.32: Pictorial overview of the integration of hardware and software

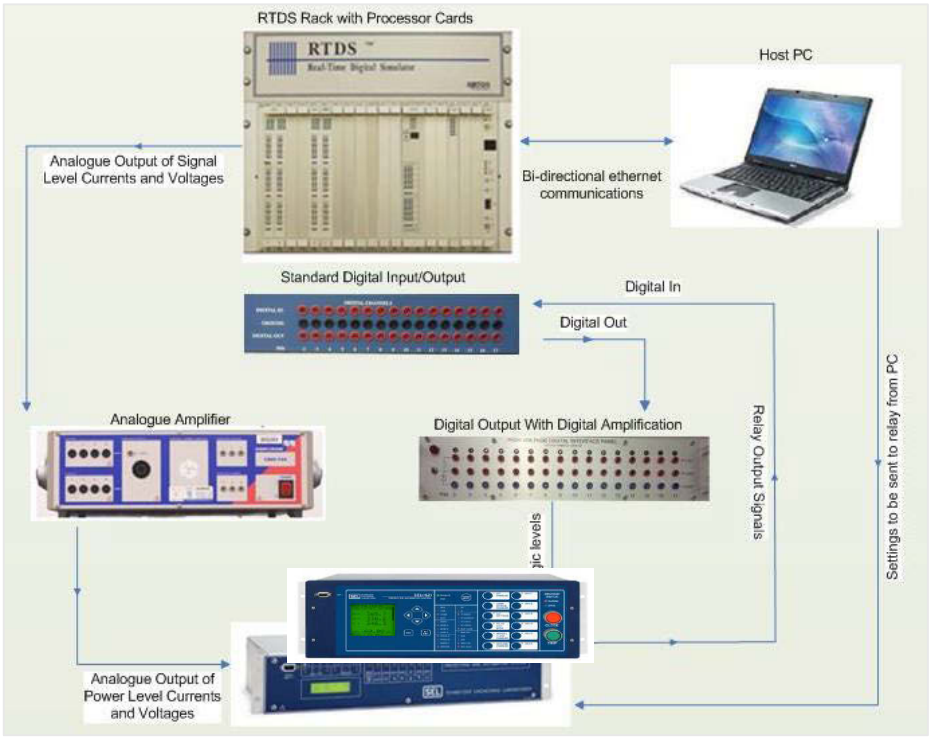

Figure 2.33: Closed loop connection between hardware components

Since the tool of real time digital simulation has emerged in recent years, it has proven to be extremely powerful for providing better understanding of protection relay performance [51]. The closed loop testing functionality allows complex real-world protection challenges to be studied in a representative manner, yet under controlled laboratory conditions [53], [54]. This

[1] Picture obtained from [52]
[2] Picture obtained from [48]

approach will be taken in the investigation of the operating challenges of distance protection relays in this thesis.

2.16. RSCAD Simulation Model of a Distance Protection Relay

Modelling of a distance protection relay in RSCAD has been implemented by various users and has been tested to provide successful representation of a real distance protection relay [3], [55]. RSCAD however, also provides the user with a host of pre-defined models in the user library. One such available simulation model is a mathematical representation of a generic distance relay [56]. The generic distance protection relay module is equipped to perform distance protection on single-pole transmission lines with [57]:

- Six impedance measuring loops (three phase to ground and three phase to phase)
- Phase selection elements that can be extracted from the relay
- Single and three pole tripping
- Communication aided tripping schemes
- Additional plot signals to provide information to extract various data for theoretical calculations
- Additional impedance measurement algorithm for theoretical calculations and plotting purposes

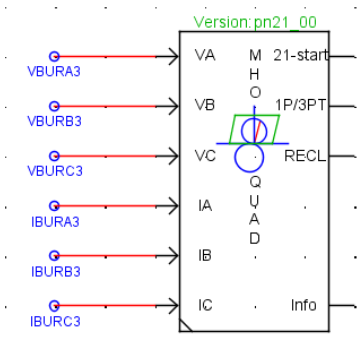

Figure 2.34: RSCAD software model of a generic distance protection relay

The approach adopted in this thesis has been to use both the hardware SEL 421 distance protection relays and the RSCAD generic distance protection relay model at different stages during the development of the research, and at times to use both the hardware relays and generic relay models in parallel at the same time. This latter approach, in particular, was used to provide greater insight into the reasons for the real relay hardware's response to each fault scenario, since the impedance seen by the generic relay model can be extracted as an output from the model and plotted on a mho impedance plot similar to that seen in Figure 2.35.

Since the input currents and voltages to the relay are the same when the SEL relay hardware and RSCAD generic relay models are connected in parallel, one can use the impedance plots of one

relay to give an idea of the impedance seen by the other relay. In this way the RSCAD software relay was used to give an indication of the impedance seen by the SEL 421 relay during detailed test studies.

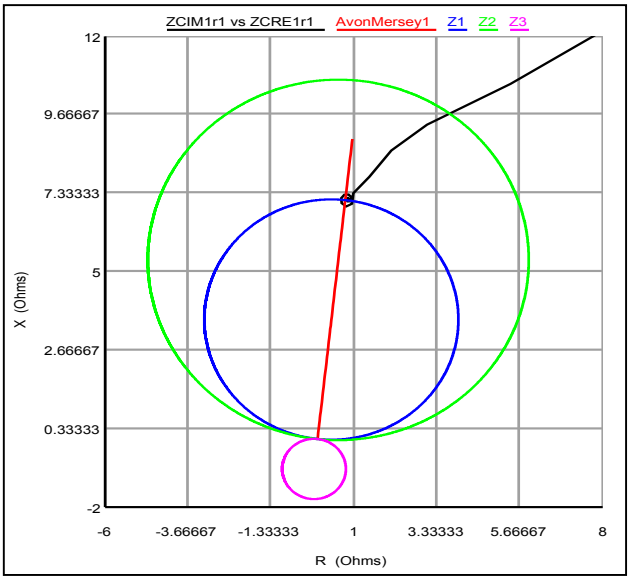

Figure 2.35: Impedance plot for RSCAD software relay

2.17. Study System Model for the Research Studies

The research problems outlined in this chapter were investigated using an actual transmission line with the same challenging practical operating conditions that are of interest in the thesis. The transmission network that was chosen for this study was the 275 kV lines between Mersey and Invubu substations. The transmission line network is as follows:

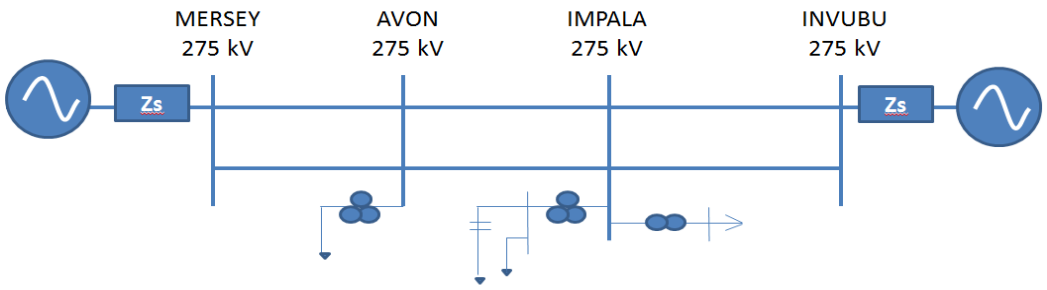

Figure 2.36: Transmission line network to be studied

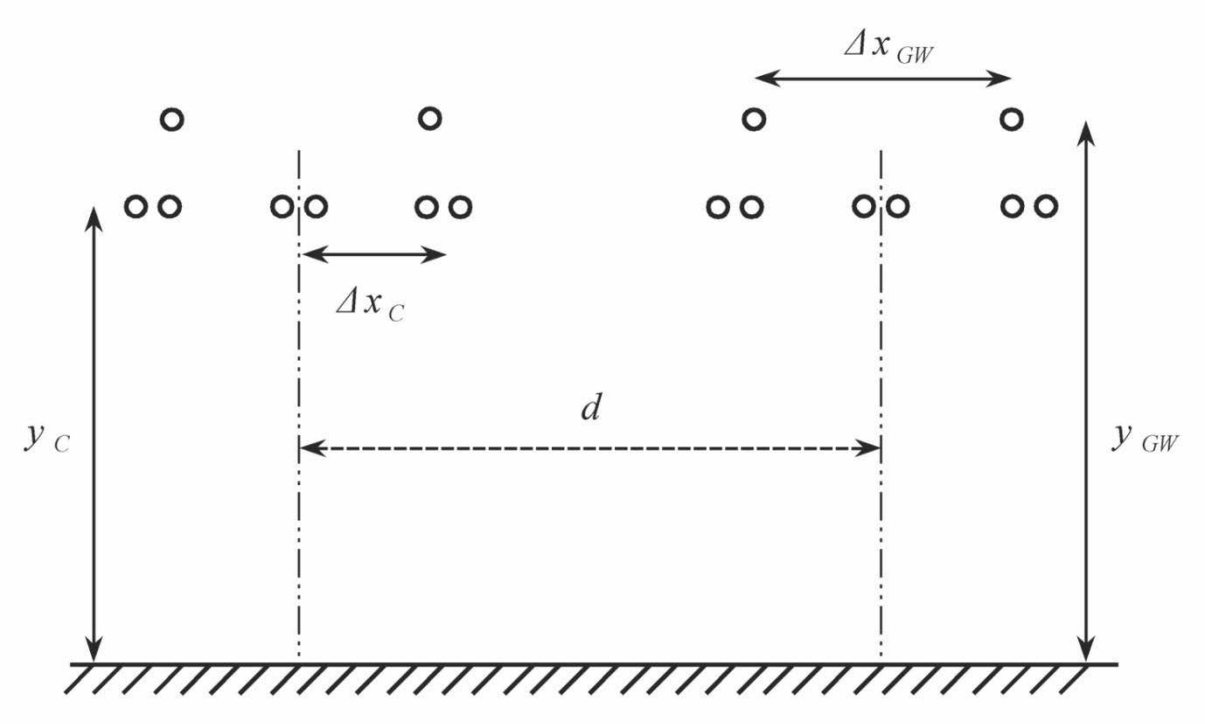

Figure 2.37: Transmission line topology to be studied

Transmission line data was obtained from the electrical utility, Eskom. For the study the portion of the transmission line between Mersey and Impala was modelled on the RSCAD DRAFT programme. The transmission lines were modelled using the TLINE programme in RSCAD using the parameters received from the Eskom data base. Once the network was successfully modelled, faults were placed at various parts of the network. It is desirable to be able to control the type of fault, duration of fault and location of the fault from the RUNTIME programme in a consistent and repeatable manner. A logic circuit needed to be implemented to achieve this. Simply, a switch is used to select between a ground fault and a line to line fault, a dial is used to decide the phases that are to be involved in the fault (e.g. A-g or A-B) and a dial is used to decide which bus the fault will be placed on. The circuit developed in the DRAFT programme to place faults on the network and the associated control functions used from the RUNTIME programme are as follows:

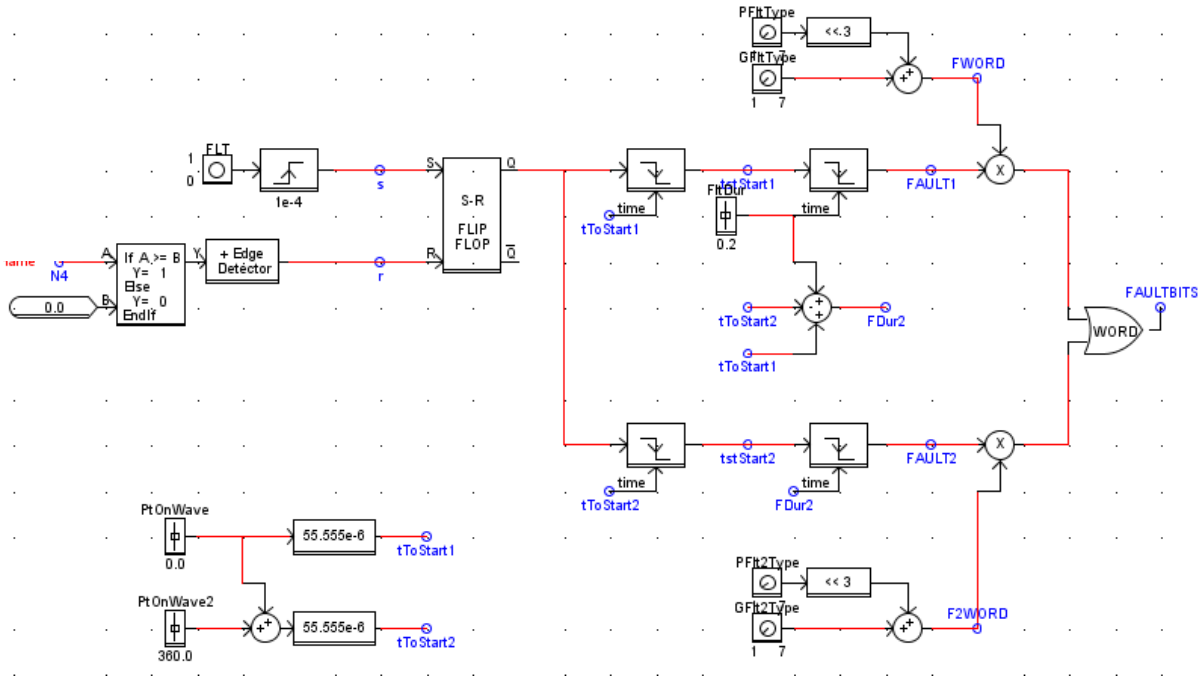

Figure 2.38: DRAFT model for fault logic

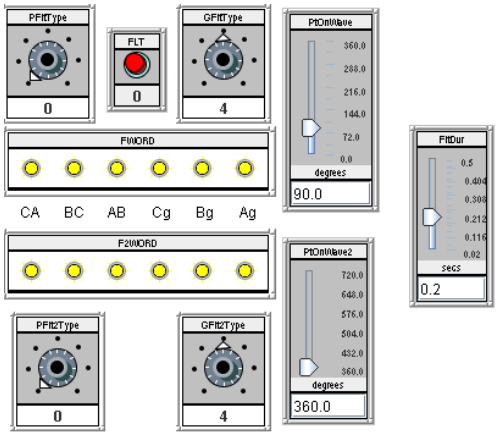

Figure 2.39: RUNTIME interface for fault control

This fault control logic makes provision for more than one kind of fault to be placed on the system at a time on any two points of the network. In addition a fault can be initiated at a specific point on wave of a chosen reference voltage. This allows for more reliable fault control. The transmission line model was then tested with the faults at different locations in the network in preparation for further study.

2.18. Conclusion

This chapter has presented the fundamental theory and prior research on which this thesis is based, paying specific attention to distance protection schemes and the challenges faced in the protection of overhead transmission lines. Each proposed research aspect (mutual coupling between double circuit and parallel transmission lines, non-transposition of transmission lines

and cross country faults) has been individually addressed and the importance of revisiting these practical operating challenges, using new resources such as the real time digital simulator, has been outlined. Methods for the compensation and correction of such interesting conditions have also been presented.

Successive chapters will present these operating conditions in more detail which will include derivations from first principles, real time simulation results and an interpretation of these. The next chapter will go on to derive the equations for calculation of the impedances of a double circuit and parallel transmission line where mutual coupling is present between the transmission lines. Chapter three will derive the impedance of a transmission line progressively, from a fundamental single three-phase transmission line example to a double-circuit (or parallel) three phase transmission line system including ground wires, from first principles.

CHAPTER 3
CALCULATION OF IMPEDANCES OF MUTUALLY COUPLED TRANSMISSION LINES

As mentioned in Section 2.11, mutual coupling occurs when two or more current carrying conductors are constructed significantly close to each other, such that their electro-magnetic fields interact. Protection of transmission lines today is performed by protection relays that make use of the transmission lines' positive and zero sequence impedances in their decision making algorithms. The notion that this simplicity fully describes the transmission line under normal operating conditions is incorrect. The transmission line, in fact, comprises a host of impedances, (self-impedances of the particular line and mutual impedance contributions of adjacent lines) that make up the impedance matrix of the transmission line [30].

The series inductance that arises from mutual coupling is of importance in the study of protection systems in mutually coupled parallel transmission lines. The fundamental mathematics of the computation of this mutual inductance, and hence the impedance matrix, has been understood for many years [59] but is rarely documented exhaustively in modern texts. Even in some texts, such as [30], where the actual equations for self and mutual impedances of coupled lines are presented, these equations have typically been derived using specific values of ground resistivity, system frequency and ground wire topology and are not applicable if any of these conditions change. Because of the complexity of the derivations behind these equations, the relationship between any one parameter (e.g. ground resistivity) and the coefficients of the final equation is not clear, so they have limited use outside of the narrow conditions they were derived for.

Although modern simulation tools are perfectly capable of calculating the impedance matrix of coupled transmission lines from geometric data entered by the user, this does not typically provide much insight to the user as to the influence of specific line parameters and topology on the final impedances, and again the underlying assumptions and equations used in these packages are typically not known. It is therefore useful to revisit the fundamental theory behind line impedance calculations to examine how the full impedance matrices of mutually coupled lines are derived from first principles. This provides some insight into the reasons for the final answers, but also, importantly, allows one to check numerical answers obtained from simulation tools against hand calculations, at least for some basic cases to get an understanding of what assumptions and methods have been used in these packages' numerical parameter calculation.

This chapter focuses on the derivation of the equations used to calculate the impedance matrices of coupled transmission lines in a step by step manner in an attempt to allow the reader of this text to be able to follow the application of theoretical concepts such that these derivations can be applied to all operating conditions and transmission line topologies. The parameters of different transmission line topologies obtained by hand calculation using these derived equations are compared against those obtained using RSCAD real time simulation software so that validation of these derivations can be established.

3.1. Derivation from first principles

Consider the classical simple starting example, shown in Figure 3.1, of a single-phase two-wire transmission line, where the two wires are solid cylindrical conductors *x* and *y*. The radius of each conductor is r_x and r_y respectively.

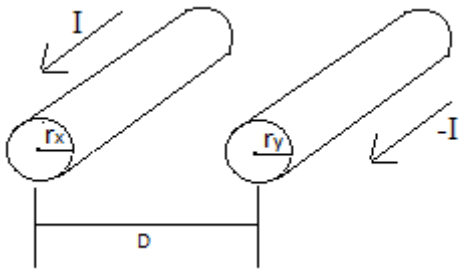

Figure 3.1: Single-phase two-wire line

We note that the currents in conductor *x* and *y* are $I_x = I$ and $I_y = -I$ respectively, therefore the sum of the two currents is zero and the flux linkage, λ_x, of conductor *x* is [58]:

$$\lambda_x = 2 \times 10^{-7} \left(I_x \ln \frac{1}{D_{xx}} + I_y \ln \frac{1}{D_{xy}} \right)$$

$$= 2 \times 10^{-7} \left(I \ln \frac{1}{r'_x} - I \ln \frac{1}{D} \right)$$

$$= 2 \times 10^{-7} \; I \; \ln \frac{D}{r'_x} \quad (\text{Wb} - \text{t})/\text{m} \tag{44}$$

Where: D_{xy} is the GMD (Geometric Mean Distance) between conductor *x* and *y*

r'_x is the GMR (Geometric Mean Radius) of conductor *x*

In this instance $r'_x = e^{-1/4} \; r_x = 0.7755 \; r_x$ (45)

The inductance of conductor *x* is therefore:

$$L_x = \frac{\lambda_x}{I_x} = \frac{\lambda_x}{I} = 2 \times 10^{-7} \ln \frac{D}{r'_x} \quad H/m \; per \; conductor \tag{46}$$

The impedance due to the above inductance of conductor *x* is:

$$X_{L_x} = 2\pi f\ L_x$$
$$= 2\pi f(2 \times 10^{-7}) \ln \frac{D}{r'_x} \quad \Omega/m$$
$$= 2\pi f(2 \times 10^{-7}) \ln \frac{D}{r'_x} \times 10^3 \quad \Omega/km \tag{47}$$

The above equations can be adapted to calculate the inductive reactances of bundled conductors if the geometry is known such that the GMR and GMD can be established.

The GMD between two conductors, for the case where each conductor (namely conductors *x* and *y*) consists of bundled sub-conductors, is [58]:

$$\text{GMD} = \sqrt[MN]{\prod_{k=1}^{N} \prod_{m=1'}^{M} D_{km}} = D_{xy} \tag{48}$$

Where: N is the number of sub-conductors of conductor *x*

M is the number of sub-conductors of conductor *y*

k is the index counting the individual sub-conductors of conductor *x*

m is the index counting the individual sub-conductors of conductor *y*

D_{km} is the distance between each sub-conductor of conductor *x* and every sub-conductor of conductor *y*

The GMR of a conductor, for the case where the conductor can consist of bundled sub-conductors, is [58]:

$$\text{GMR} = \sqrt[N^2]{\prod_{k=1}^{N} \prod_{m=1}^{N} D_{km}} = D_{xx} \tag{49}$$

Where: N is the number of sub-conductors of the conductor

k and *m* are both indices counting the individual sub-conductors of the conductor *x*

D_{km} is the distance between each sub-conductor of conductor *x* and all other sub-conductors of the same conductor *x*

The GMR for the conductor *y* follows from eqn. (49) as:

$$D_{\text{yy}} = \sqrt[M^2]{\prod_{k=1}^{M} \prod_{m=1}^{M} D_{km}} \tag{50}$$

These mathematics can be extended further to a suitable format such that one can calculate the inductive reactances for three-phase bundled conductors. Consider the example of a three phase

transmission line with grounded neutral conductors constructed in an arbitrary geometry as shown in the top half of Figure 3.2. This arbitrary line example has three phase conductors, labelled a, b and c in Figure 3.2, and N neutral conductors, labelled n1, n2 and nN; the diagram and nomenclature in Figure 3.2 are taken from [58]. Assume that the neutral conductors are grounded to earth at regular intervals and the equivalent GMRs of the bundled conductors are known and that all conductors are insulated from each other. Under normal load conditions, this three phase transmission line system will have only three current carrying conductors at any given time regardless of the number of neutral conductors in the system. In the event of an unbalanced fault or when the phase currents are unbalanced for any reason, there will be a return zero-sequence current in both the neutral conductors and in the ground in some combination (depending on the lowest impedance path), which will give rise to a zero sequence impedance for that particular fault condition [39].

In the classic paper published by John R. Carson [59], a method describing electromagnetic wave propagation in overhead wires with ground return is presented. This fundamental paper shows how the above mentioned ground can be replaced with fictitious "ground return conductors" below the surface of the earth at a distance dependent on the resistivity of the ground. Previously we would have considered a very large area seeking the lowest resistance path back to the source, but the method described by Carson considers the return through the "ground return conductors". Each fictitious ground return conductor in the bottom half of Figure 3.2 carries the negative of its overhead conductor current and has the following parameters [58]:

$$D_{k'k'} = D_{kk} \quad \text{m} \tag{51}$$

$$D_{kk'} = 658.5\sqrt{\rho/f} \quad \text{m} \tag{52}$$

$$R_{k'} = 9.869 \times 10^{-7} f \quad \Omega/m \tag{53}$$

Where: $D_{k'k'}$ is the GMR of the ground return conductor *k'*

D_{kk} is the GMR of the conductor *k*

$D_{kk'}$ is the distance of each fictitious ground return conductor *k'* below its overhead conductor *k'*

ρ is the resistivity of the ground in Ω/m

f is the frequency in Hz

$R_{k'}$ is the resistance of the fictitious ground return conductors

Note that the GMR of each fictitious ground return conductor is the same as the GMR of its corresponding overhead conductor.

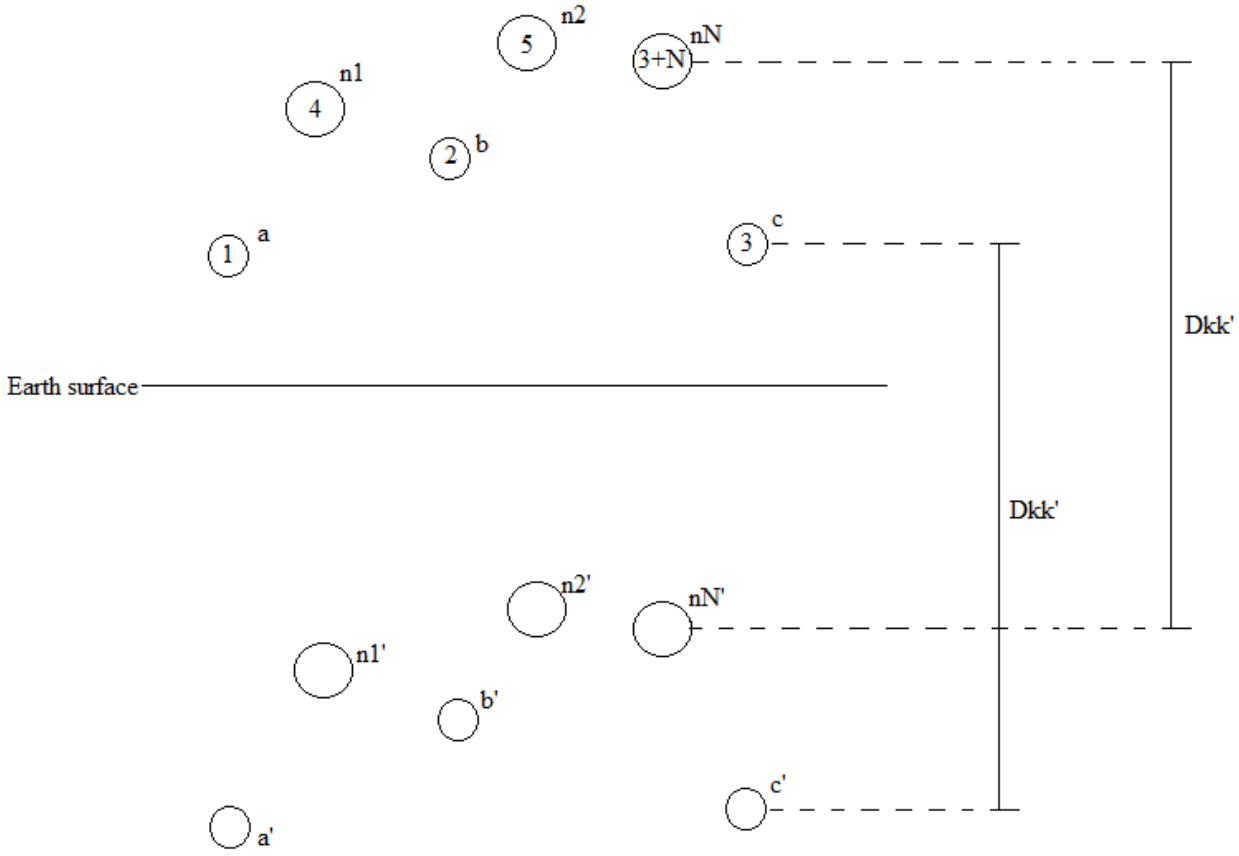

Figure 3.2: Three phase transmission line with ground replaced by ground return conductors

It is also important to note that the distance $D_{kk'}$ between each fictitious ground return conductor and its corresponding overhead conductor is the same for all such conductors as this distance is only dependent on the resistivity of the ground and the frequency of the system. Each fictitious ground return conductor also will have the same resistance, $R_{k'}$.

The above theory is fundamental to the procedure used in the calculation of the impedance of mutually coupled transmission lines. For a three phase circuit, the volt drops across conductors are [58]:

$$\begin{bmatrix} E_{Aa} \\ E_{Bb} \\ E_{Cc} \\ 0 \\ 0 \\ \vdots \\ 0 \end{bmatrix} = (\boldsymbol{R} + j\omega \boldsymbol{L}) \begin{bmatrix} I_a \\ I_b \\ I_c \\ I_{n1} \\ I_{n2} \\ \vdots \\ I_{nN} \end{bmatrix} \tag{54}$$

Where: E is the volt drop across the phase conductors

R is the matrix of conductor resistances

L is the matrix of conductor inductances

I is a vector of phase and neutral currents

The resistance matrix R includes the resistances of the overhead conductors R_{kk} and the resistance of the ground return conductors $R_{kk'}$. Number all the conductors from 1 to (3+N) for a three phase system as shown in Figure 3.2, and from eqn. (54), one can obtain the following matrix equation [58]:

$$\begin{bmatrix} E_{Aa} \\ E_{Bb} \\ E_{Cc} \\ 0 \\ \dots \\ 0 \end{bmatrix} = \left[\begin{array}{ccc:ccc} Z_{11} & Z_{12} & Z_{13} & Z_{14} & \dots & Z_{1(3+N)} \\ Z_{21} & Z_{22} & Z_{23} & Z_{24} & \dots & Z_{2(3+N)} \\ Z_{31} & Z_{32} & Z_{33} & Z_{34} & \dots & Z_{2(3+N)} \\ \hdashline Z_{41} & Z_{42} & Z_{43} & Z_{44} & \dots & Z_{1(3+N)} \\ \vdots & \vdots & \vdots & \vdots & \vdots & \vdots \\ Z_{(3+N)1} & Z_{(3+N)2} & Z_{(3+N)3} & Z_{(3+N)4} & \dots & Z_{(3+N)(3+N)} \end{array}\right] \begin{bmatrix} I_a \\ I_b \\ I_c \\ I_{n1} \\ \vdots \\ I_{nN} \end{bmatrix} \quad (55)$$

The diagonal elements of the impedance matrix in eqn. (55) are [58]:

$$Z_{kk} = R_k + R_{k'} + j\omega(2 \times 10^{-7} \ln \frac{D_{kk'}}{D_{kk}}) \quad \Omega/m \quad (56)$$

The off-diagonal elements of the impedance matrix in eqn. (55) are [58]:

$$Z_{km} = R_{k'} + j\omega(2 \times 10^{-7} \ln \frac{D_{km'}}{D_{km}}) \quad \Omega/m \quad (57)$$

To simplify eqn. (55), partitioning of the impedance matrix can be made as follows:

$$\begin{bmatrix} \overbrace{\begin{matrix} Z_{11} & Z_{12} & Z_{13} \\ Z_{21} & Z_{22} & Z_{23} \\ Z_{31} & Z_{32} & Z_{33} \end{matrix}}^{Z_A} & \overbrace{\begin{matrix} Z_{14} & \dots & Z_{1(3+N)} \\ Z_{24} & \dots & Z_{2(3+N)} \\ Z_{34} & \dots & Z_{2(3+N)} \end{matrix}}^{Z_B} \\ \begin{matrix} Z_{41} & Z_{42} & Z_{43} \\ \vdots & \vdots & \vdots \\ Z_{(3+N)1} & Z_{(3+N)2} & Z_{(3+N)3} \end{matrix} & \begin{matrix} Z_{44} & \dots & Z_{1(3+N)} \\ \vdots & \vdots & \vdots \\ Z_{(3+N)4} & \dots & Z_{(3+N)(3+N)} \end{matrix} \\ \underbrace{\qquad\qquad}_{Z_C} & \underbrace{\qquad\qquad}_{Z_D} \end{bmatrix}$$

Therefore:

$$\begin{bmatrix} E_P \\ 0 \end{bmatrix} = \begin{bmatrix} Z_A & Z_B \\ Z_C & Z_D \end{bmatrix} \begin{bmatrix} I_P \\ I_n \end{bmatrix} \quad (58)$$

Where: $E_P = \begin{bmatrix} E_{Aa} \\ E_{Bb} \\ E_{Cc} \end{bmatrix}$, $I_P = \begin{bmatrix} I_a \\ I_b \\ I_c \end{bmatrix}$, and $I_n = \begin{bmatrix} I_{n1} \\ \vdots \\ I_{nN} \end{bmatrix}$

If eqn. (58) is written out as two separate equations, solving for E_P is then carried out as follows:

$$E_P = Z_A I_P + Z_B I_n \quad (59)$$

$$0 = Z_C I_P + Z_D I_n \quad (60)$$

Solving eqn. (60) for I_n:

$$I_n = -Z_D^{-1} Z_C I_P \tag{61}$$

Substituting eqn. (61) in eqn. (59)

$$E_P = [Z_A - Z_B Z_D^{-1} Z_C] I_P = Z_P I_P \tag{62}$$

Where $Z_P = [Z_A - Z_B Z_D^{-1} Z_C]$ (63)

Thus eqn. (55) shows that the full phase impedance matrix of any arbitrary three phase transmission line geometry, including the effects of ground wires and ground return, can be assembled from first principles using the well-known formulae for a pair of conductors [viz. eqn. (44-50)], together with the concept of fictitious ground return conductors [viz. eqn. (51-53)]. This mathematical representation of the transmission line includes the magnetic coupling between each pair of conductors, and in the format in eqn. (55) it is still possible to explicitly see the relationship between the impedances of each conductor and the geometrical properties of these conductors. In other words, every element in the impedance matrix in eqn. (55) can be written as a closed-form expression derived (once Carson's method is understood) from simple first principles. However, although simple to derive, because the impedance matrix equation in eqn. (55) retains explicit representations of the variables associated with every conductor in the geometry, it is of large dimension (even for this simple example) and it does not present the impedances of the particular line in the format used in fault analysis (either by hand or by most protection relay algorithms).

By contrast, eqn. (63) which follows from eqn. (55), shows that the parameters of any line can be further reduced into the more commonly used format in which the total impedance of the line presented to each electrical phase of the power system is calculated to form a 3 x 3 impedance matrix Z_P. The impedances of this 3 x 3 matrix Z_P in eqn. (63) still include the effects of all the ground wires and ground return, and all the magnetic coupling between these conductors, but, as a result of applying the reduction method, the variables associated with ground wires and ground return currents are no longer represented or solved explicitly. Because the reduction method used to arrive at eqn. (63) is carried out numerically, it also means that the impedance terms in the 3 x 3 matrix Z_P cannot be written as closed-form expressions in which the contribution of each coupled conductor in the line to the overall lumped impedance in each phase of the line can still be seen explicitly in the form of separate terms of an equation. The parameters of the matrix Z_P in eqn. (63) represent all these effects, but they are now in the form of numerical values for the particular line rather than specialized formulae.

Nevertheless, the theory in eqns. (44-63) can be used to derive from first principles, and then calculate numerically, the phase impedance matrix of any transmission line, including parallel transmission lines where magnetic coupling between the currents of these two lines is significant. This theory can be used both to verify the methods and assumptions being used in simulation packages used to study protection systems in such lines, as well as to gain better understanding of the factors that influence the impedances of coupled transmission lines.

The following analysis therefore considers some simple examples in which the theory in eqns. (44-63) is used to verify the parameters obtained from RSCAD's TLINE support programme, starting with deliberately simple cases and finishing with a full representation of two coupled, three-phase lines with ground wires and ground return as considered in the actual example study system of this thesis.

3.2. Calculation of mutual impedances between parallel transmission lines and verification using a real time digital simulator

Three phase conductors with single sub-conductor per phase

Consider a simple case of a three phase transmission line where no ground wires are present, there exists a single conductor per phase and the effect of conductor sag is ignored. Using the actual data for the Avon-Mersey transmission line, and these simplifying assumptions, the following transmission line parameters exist, where Figure 3.3 shows the actual data entered into RSCAD's TLINE support programme.

Conductor Data

Bundle #	Bundle 1	Bundle 2	Bundle 3
Conductor Name	2Zebra50	2Zebra50	2Zebra50
Conductor Type (AC or DC)	AC	AC	AC
V(kV)(AC:L--L,rms/DC:L--G,pk)	275.0	275.0	275.0
V Phase(Deg)	0.0	-120.0	120.0
Line I(kA)(AC:rms/DC:pk)	1.284	1.284	1.284
Line I Phase(Deg)	20.0	-100.0	140.0
Num of Sub-Conductors	1	1	1
Sub-Cond Radius(cm)	1.155819	1.155819	1.155819
Sub-Cond Spacing(cm)	38.0	38.0	38.0
Horiz. Dist. X(m)	-7.9	0.0	7.9
Height at Tower Y(m)	19.995	19.995	19.995
Sag at Midspan(m)	0.0	0.0	0.0
DC Resistance per Sub-Cond(ohms/km)	0.0674	0.0674	0.0674

Line Length(km): 68.59 Ground Resistivity (ohm-m): 700.0

Figure 3.3: Phase conductor data

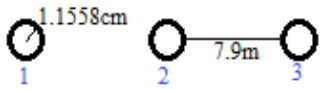

Figure 3.4: Conductor geometry

Using eqn. (51-53) and eqn. (56-57) and the conductor data above:

$$D_{kk'} = D_{km'} = 658.5\sqrt{\rho/f} = 658.5 \times \sqrt{700/50} = 2463.88 \quad m$$

$$R_{k'} = 9.869 \times 10^{-7} f = 9.869 \times 10^{-7}(50) = 4.9345 \times 10^{-5} \quad \Omega/m$$

$$D_{kk} = e^{-1/4}\, r_x = 0.7755\, r_x = e^{-1/4} \times \frac{1.155819}{100} = 9.002 \times 10^{-3}\ m$$

$$R_k = 0.0674 \quad \Omega/km = 6.74 \times 10^{-5} \quad \Omega/m$$

$$Z_{kk} = R_k + R_{k'} + j\omega(2 \times 10^{-7} \ln \frac{D_{kk'}}{D_{kk}}) \quad \Omega/m$$

$$= R_k + R_{k'} + j\omega(2 \times 10^{-7} (\ln \frac{1}{D_{kk}} + \ln D_{kk}')) \quad \Omega/m$$

Hence,

$$Z_{11} = 6.74 \times 10^{-5} + 4.9345 \times 10^{-5} + j\omega(2 \times 10^{-7} (\ln \frac{1}{9.002 \times 10^{-3}} + \ln 2463.88)) \quad \Omega/m$$

$$= 0.116745 \times 10^{-3} + j0.78665 \times 10^{-3} \quad \Omega/m$$

$$= Z_{22} = Z_{33}$$

$$Z_{km} = R_{k'} + j\omega(2 \times 10^{-7} \ln \frac{D_{km}'}{D_{km}}) \quad \Omega/m$$

$$= R_{k'} + j\omega(2 \times 10^{-7} (\ln \frac{1}{D_{km}} + \ln D_{km}')) \quad \Omega/m$$

Hence,

$$Z_{12} = 4.9345 \times 10^{-5} + j\omega(2 \times 10^{-7} (\ln \frac{1}{7.9} + \ln 2463.88)) \quad \Omega/m$$

$$= 0.49345 \times 10^{-4} + j0.36082 \times 10^{-3} \quad \Omega/m$$

$$= Z_{21} = Z_{23} = Z_{32}$$

Likewise,

$$Z_{13} = 4.9345 \times 10^{-5} + j\omega(2 \times 10^{-7} (\ln \frac{1}{2 \times 7.9} + \ln 2463.88)) \quad \Omega/m$$

$$= 0.49345 \times 10^{-4} + j0.31727 \times 10^{-3} \quad \Omega/m$$

$$= Z_{31}$$

The impedance matrix Z for this simple example using hand calculations derived from first principles as shown above is thus:

$$Z = \begin{bmatrix} 0.116745 \times 10^{-3} + j0.78665 \times 10^{-3} & 0.49345 \times 10^{-4} + j0.36082 \times 10^{-3} & 0.49345 \times 10^{-4} + j0.31727 \times 10^{-3} \\ 0.49345 \times 10^{-4} + j0.36082 \times 10^{-3} & 0.116745 \times 10^{-3} + j0.78665 \times 10^{-3} & 0.49345 \times 10^{-4} + j0.36082 \times 10^{-3} \\ 0.49345 \times 10^{-4} + j0.31727 \times 10^{-3} & 0.49345 \times 10^{-4} + j0.36082 \times 10^{-3} & 0.116745 \times 10^{-3} + j0.78665 \times 10^{-3} \end{bmatrix}$$

in Ω/m

The phase impedance matrix obtained from the TLINE support programme used to model the line under the same assumptions in the RSCAD programme is shown below.

```
THE PHASE IMPEDANCE MATRIX ( Z(I,J) , OHMS/M ):
   0.11729E-03,0.79264E-03   0.48688E-04,0.36637E-03   0.48687E-04,0.32282E-03
   0.48688E-04,0.36637E-03   0.11729E-03,0.79264E-03   0.48688E-04,0.36637E-03
   0.48687E-04,0.32282E-03   0.48688E-04,0.36637E-03   0.11729E-03,0.79264E-03
```

These two matrices show that there is close agreement between the impedance parameters calculated by hand from first principles and those obtained from RSCAD's TLINE programme.

Three phase conductors with two sub-conductors per phase

To extend this study further, consider the case where there are now two sub-conductors per phase. As before there are no ground wires present and the effect of conductor sag is ignored.

Conductor Data

Bundle #	Bundle 1	Bundle 2	Bundle 3
Conductor Name	2Zebra50	2Zebra50	2Zebra50
Conductor Type (AC or DC)	AC	AC	AC
V(kV)(AC:L--L,rms/DC:L--G,pk)	275.0	275.0	275.0
V Phase(Deg)	0.0	-120.0	120.0
Line I(kA)(AC:rms/DC:pk)	1.284	1.284	1.284
Line I Phase(Deg)	20.0	-100.0	140.0
Num of Sub-Conductors	2	2	2
Sub-Cond Radius(cm)	1.155819	1.155819	1.155819
Sub-Cond Spacing(cm)	38.0	38.0	38.0
Horiz. Dist. X(m)	-7.9	0.0	7.9
Height at Tower Y(m)	19.995	19.995	19.995
Sag at Midspan(m)	0.0	0.0	0.0
DC Resistance per Sub-Cond(ohms/km)	0.0674	0.0674	0.0674

Line Length(km): 68.59 Ground Resistivity (ohm-m): 700.0

Figure 3.5: Phase conductor data

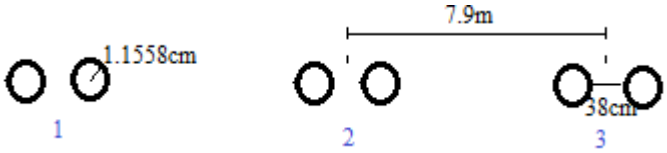

Figure 3.6: Conductor geometry

Using the conductor parameters above:

$$D_{kk'} = 658.5\sqrt{\rho/f} = 658.5 \times \sqrt{700/50} = 2463.88 \quad m$$

$$R_{k'} = 9.869 \times 10^{-7} f = 9.869 \times 10^{-7}(50) = 4.9345 \times 10^{-5} \quad \Omega/m$$

For two sub-conductors per phase the equivalent diameter of the conductor is

$$D_{kk} = \sqrt{e^{-1/4} r_x} = \sqrt{0.7755 r_x \times d_{sub-conductor}} = \sqrt{e^{-1/4} \times \frac{1.155819}{100} \times \frac{38}{100}}$$

$$= 5.8486 \times 10^{-2} \quad m$$

$$R_k = \frac{0.0674}{2} \quad \Omega/km = 3.37 \times 10^{-5} \quad \Omega/m$$

$$Z_{kk} = R_k + R_{k'} + j\omega(2 \times 10^{-7} \ln \frac{D_{kk'}}{D_{kk}}) \quad \Omega/m$$

$$= R_k + R_{k'} + j\omega(2 \times 10^{-7} (\ln \frac{1}{D_{kk}} + \ln D_{kk'})) \quad \Omega/m$$

Hence,

$$Z_{11} = 3.37 \times 10^{-5} + 4.9345 \times 10^{-5} + j\omega(2 \times 10^{-7} (\ln \frac{1}{5.8486 \times 10^{-2}} + \ln 2463.88)) \ \Omega/m$$

$$= 0.83045 \times 10^{-4} + j0.66906 \times 10^{-3} \quad \Omega/m$$

$$= Z_{22} = Z_{33}$$

Since the distance between the centre and outside phases is 7.9 m, which is significantly larger than the spacing between the sub-conductors (38 cm), for simplicity one can ignore sub-conductor spacing when calculating the mutual impedances since this spacing is negligible in comparison with distances between the phases. Therefore assume $D_{km} = 7.9$ m in the calculation:

$$Z_{km} = R_{k'} + j\omega(2 \times 10^{-7} \ln \frac{D_{km'}}{D_{km}}) \quad \Omega/m$$

$$= R_{k'} + j\omega(2 \times 10^{-7} (\ln \frac{1}{D_{km}} + \ln D_{km}')) \quad \Omega/m$$

Hence,

$$Z_{12} = 4.9345 \times 10^{-5} + j\omega(2 \times 10^{-7} (\ln \frac{1}{7.9} + \ln 2463.88)) \quad \Omega/m$$

$$= 0.49345 \times 10^{-4} + j0.36082 \times 10^{-3} \quad \Omega/m$$

$$= Z_{21} = Z_{23} = Z_{32}$$

In the same way, since the distance between the outer phases is 2×7.9 m, which is significantly larger than the sub-conductor spacing, assume $D_{kk} = 2 \times 7.9$ m in the calculation of the mutual impedances between these phases, giving:

$$Z_{13} = 4.9345 \times 10^{-5} + j\omega(2 \times 10^{-7} (\ln \frac{1}{2 \times 7.9} + \ln 2463.88)) \quad \Omega/m$$

$$= 0.49345 \times 10^{-4} + j0.31727 \times 10^{-3} \quad \Omega/m$$

$$= Z_{31}$$

The impedance matrix Z for this simple example using hand calculations derived from first principles as shown above is thus:

$$Z = \begin{bmatrix} 0.83045 \times 10^{-4} + j0.66906 \times 10^{-3} & 0.49345 \times 10^{-4} + j0.36082 \times 10^{-3} & 0.49345 \times 10^{-4} + j0.31727 \times 10^{-3} \\ 0.49345 \times 10^{-4} + j0.36082 \times 10^{-3} & 0.83045 \times 10^{-4} + j0.66906 \times 10^{-3} & 0.49345 \times 10^{-4} + j0.36082 \times 10^{-3} \\ 0.49345 \times 10^{-4} + j0.31727 \times 10^{-3} & 0.49345 \times 10^{-4} + j0.36082 \times 10^{-3} & 0.83045 \times 10^{-4} + j0.66906 \times 10^{-3} \end{bmatrix}$$

in Ω/m

The phase impedance matrix obtained from the TLINE support programme used to model the line under the same assumptions in the RSCAD programme is shown below.

```
THE PHASE IMPEDANCE MATRIX ( Z(I,J) , OHMS/M ):
   0.82991E-04,0.67484E-03   0.48688E-04,0.36637E-03   0.48687E-04,0.32282E-03
   0.48688E-04,0.36637E-03   0.82991E-04,0.67484E-03   0.48688E-04,0.36637E-03
   0.48687E-04,0.32282E-03   0.48688E-04,0.36637E-03   0.82991E-04,0.67484E-03
```

These two matrices show that there is close agreement between the impedance parameters calculated by hand from first principles and those obtained from RSCAD's TLINE programme.

In these first two example cases, the geometry of the transmission line conductors is still simple enough that each term in the final 3x3 impedance matrix Z of the transmission line can be described in terms of a closed-form equation for its resistance and inductance, even in the case of multiple sub-conductors per phase. However, when the transmission line has one or more ground wires, the dimensions of the full impedance matrix (eqn.(55)) increases to include

coupling between conductors and ground wires, and matrix reduction techniques are required to derive the final 3x3 impedance matrix Z_P in eqn. (63) representing the line. The following sub-section shows a numerical example case to illustrate this process.

Three phase conductors with single sub-conductor per phase and ground wires

The studies above have ignored the effect of ground wires. We now introduce two ground wires, each with a single conductor per phase, and with the effect of conductor sag once again ignored.

Conductor Data

Bundle #	Bundle 1	Bundle 2	Bundle 3
Conductor Name	2Zebra50	2Zebra50	2Zebra50
Conductor Type (AC or DC)	AC	AC	AC
V(kV)(AC:L--L,rms/DC:L--G,pk)	275.0	275.0	275.0
V Phase(Deg)	0.0	-120.0	120.0
Line I(kA)(AC:rms/DC:pk)	1.284	1.284	1.284
Line I Phase(Deg)	20.0	-100.0	140.0
Num of Sub-Conductors	1	1	1
Sub-Cond Radius(cm)	1.155819	1.155819	1.155819
Sub-Cond Spacing(cm)	38.0	38.0	38.0
Horiz. Dist. X(m)	-7.9	0.0	7.9
Height at Tower Y(m)	19.995	19.995	19.995
Sag at Midspan(m)	0.0	0.0	0.0
DC Resistance per Sub-Cond(ohms/km)	0.0674	0.0674	0.0674

Line Length(km): 68.59 Ground Resistivity (ohm-m): 700.0

Figure 3.7: Phase conductor data

Ground Wire #	Conductor 1	Conductor 2
Conductor Name	S19	S19
Conductor Radius(cm)	0.664	0.664
Horiz. Dist. X(m)	-7.1	7.1
Height at Tower Y(m)	24.309	24.309
Sag at Midspan(m)	0.0	0.0
DC Resistance(ohms/km)	1.88	1.88

Figure 3.8: Ground wire data

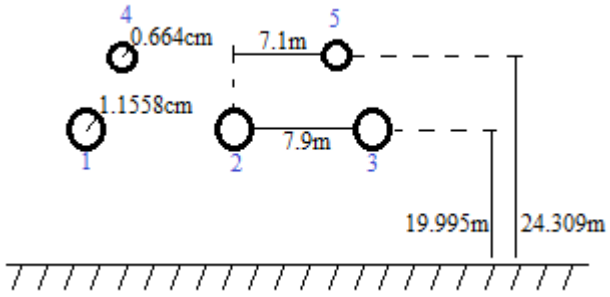

Figure 3.9: Conductor geometry

The mathematics for this scenario is more complicated than the two scenarios presented earlier due to the addition of the ground wires. It is now necessary to obtain each term of the full impedance matrix in the form $\begin{bmatrix} Z_A & Z_B \\ Z_C & Z_D \end{bmatrix}$ before finally employing numerical methods to reduce this to the 3x3 matrix $[Z_A - Z_B Z_D^{-1} Z_C]$.

As calculated previously, the self-impedances of the phase conductors are as follows:

$$D_{kk'} = 658.5\sqrt{\rho/f} = 658.5 \times \sqrt{700/50} = 2463.88 \quad m$$

$$R_{k'} = 9.869 \times 10^{-7} f = 9.869 \times 10^{-7}(50) = 4.9345 \times 10^{-5} \quad \Omega/m$$

$$D_{kk} = e^{-1/4} r_x = 0.7755 r_x = e^{-1/4} \times \frac{1.155819}{100} = 9.002 \times 10^{-3} \quad m$$

$$R_k = 0.0674\ \Omega/km = 6.74 \times 10^{-5} \quad \Omega/m$$

$$Z_{kk} = R_k + R_{k'} + j\omega(2 \times 10^{-7} \ln \frac{D_{kk'}}{D_{kk}}) \quad \Omega/m$$

$$= R_k + R_{k'} + j\omega(2 \times 10^{-7} (\ln \frac{1}{D_{kk}} + \ln D_{kk}')) \quad \Omega/m$$

Hence,

$$Z_{11} = 6.74 \times 10^{-5} + 4.9345 \times 10^{-5} + j\omega(2 \times 10^{-7} (\ln \frac{1}{9.002 \times 10^{-3}} + \ln 2463.88)) \quad \Omega/m$$

$$= 0.116745 \times 10^{-3} + j0.78665 \times 10^{-3} \quad \Omega/m$$

$$= Z_{22} = Z_{33}$$

The mutual impedances between the phase conductors are also calculated in the same manner as in the previous example as follows:

$$Z_{km} = R_{k'} + j\omega(2 \times 10^{-7} (\ln \frac{1}{D_{km}} + \ln D_{km}')) \quad \Omega/m$$

Hence,

$$Z_{12} = 4.9345 \times 10^{-5} + j\omega(2 \times 10^{-7} (\ln \frac{1}{7.9} + \ln 2463.88)) \quad \Omega/m$$

$$= 0.49345 \times 10^{-4} + j0.36082 \times 10^{-3} \quad \Omega/m$$

$$= Z_{21} = Z_{23} = Z_{32}$$

Similarly,

$$Z_{13} = 4.9345 \times 10^{-5} + j\omega(2 \times 10^{-7} (\ln \frac{1}{2 \times 7.9} + \ln 2463.88) \ ) \quad \Omega/m$$

$$= 0.49345 \times 10^{-4} + j0.31727 \times 10^{-3} \quad \Omega/m$$

$$= Z_{31}$$

With the introduction of the ground wires, the distances between each phase conductor and each ground wire need to be calculated. From a study of the geometry in Figure 3.9, the calculation of the distance D_{km} for each phase and ground conductor is summarised in Table 3.1 below:

Table 3.3: Table of distances D_{km} between phase and ground conductors

Distance	Geometry	x (m)	y (m)	$\sqrt{x^2 + y^2}$ (m)
D14=D41	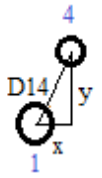	4.314	0.8	4.3876
D15=D51	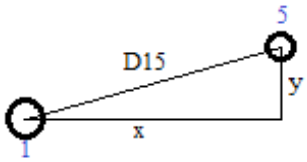	4.314	15	15.6080
D24=D42	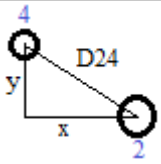	4.314	7.1	8.3079
D25=D52	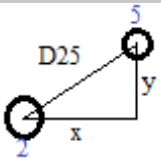	4.314	7.1	8.3079
D34=D43	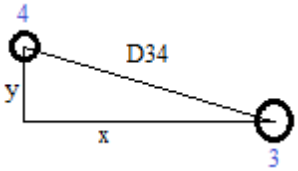	4.314	0.8	4.3876
D35=D53		4.314	15	15.6080

The self-impedances of the ground wires are then calculated using the parameters in Figure 3.8 and eqn. (56).

$D_{kk'} = 658.5\sqrt{\rho/f} = 658.5 \times \sqrt{700/50} = 2463.88 \quad m$

$R_{k'} = 9.869 \times 10^{-7} f = 9.869 \times 10^{-7}(50) = 4.9345 \times 10^{-5} \quad \Omega/m$

$D_{kk} = e^{-1/4}\ r_x = 0.7755\ r_x = e^{-1/4} \times \frac{0.664}{100} = 5.171 \times 10^{-3} \quad m$

$R_k = 1.88\,\Omega/km = 1.88 \times 10^{-3} \quad \Omega/m$

$Z_{kk} = R_k + R_{k'} + j\omega(2 \times 10^{-7} \ln\frac{D_{kk'}}{D_{kk}}) \quad \Omega/m$

$= R_k + R_{k'} + j\omega(2 \times 10^{-7} (\ln\frac{1}{D_{kk}} + \ln D_{kk}')\ ) \quad \Omega/m$

Hence,

$Z_{44} = 1.88 \times 10^{-3} + 4.9345 \times 10^{-5} + j\omega(2 \times 10^{-7} (\ln\frac{1}{5.171 \times 10^{-3}} + \ln 2463.88)\ ) \quad \Omega/m$

$= 0.19293 \times 10^{-4} + j0.82147 \times 10^{-3} \quad \Omega/m$

$= Z_{55}$

The mutual impedance of the ground wires in relation to the other conductors in the system can be calculated using the geometries and distances calculated in Table 3.1and eqn. (57) as follows:

$Z_{km} = R_{k'} + j\omega(2 \times 10^{-7} (\ln\frac{1}{D_{km}} + \ln D_{km}')\ ) \quad \Omega/m$

Hence,

$Z_{14} = 4.9345 \times 10^{-5} + j\omega(2 \times 10^{-7} (\ln\frac{1}{4.3876} + \ln 2463.88)\ ) \quad \Omega/m$

$= 0.49345 \times 10^{-4} + j0.39777 \times 10^{-3} \quad \Omega/m$

$= Z_{41} = Z_{34} = Z_{43}$

$Z_{15} = 4.9345 \times 10^{-5} + j\omega(2 \times 10^{-7} (\ln\frac{1}{15.6080} + \ln 2463.88)\ ) \quad \Omega/m$

$= 0.49345 \times 10^{-4} + j0.31804 \times 10^{-3} \quad \Omega/m$

$= Z_{51} = Z_{35} = Z_{53}$

$$Z_{24} = 4.9345 \times 10^{-5} + j\omega(2 \times 10^{-7} (\ln \frac{1}{8.3079} + \ln 2463.88) \ ) \quad \Omega/m$$

$$= 0.49345 \times 10^{-4} + j0.35766 \times 10^{-3} \quad \Omega/m$$

$$= Z_{42} = Z_{25} = Z_{52}$$

$$Z_{45} = 4.9345 \times 10^{-5} + j\omega(2 \times 10^{-7} (\ln \frac{1}{2 \times 7.1} + \ln 2463.88) \ ) \quad \Omega/m$$

$$= 0.49345 \times 10^{-4} + j0.32398 \times 10^{-3} \quad \Omega/m$$

$$= Z_{54}$$

From the values calculated above, one can derive matrices Z_A, Z_B, Z_C, and Z_D as defined earlier in eqn. (55) and eqn. (58).

$$Z_A = \begin{bmatrix} Z_{11} & Z_{12} & Z_{13} \\ Z_{21} & Z_{22} & Z_{23} \\ Z_{31} & Z_{32} & Z_{33} \end{bmatrix}$$

$$= \begin{bmatrix} 0.1167 + j0.7866 & 0.0493 + j0.3608 & 0.0493 + j0.3173 \\ 0.0493 + j0.3608 & 0.1167 + j0.7866 & 0.0493 + j0.3608 \\ 0.0493 + j0.3173 & 0.0493 + j0.3608 & 0.1167 + j0.7866 \end{bmatrix} \times 10^{-3} \quad \Omega/m$$

$$Z_B = \begin{bmatrix} Z_{14} & Z_{15} \\ Z_{24} & Z_{25} \\ Z_{34} & Z_{35} \end{bmatrix}$$

$$= \begin{bmatrix} 0.0493 + j0.3978 & 0.0493 + j0.3180 \\ 0.0493 + j0.3577 & 0.0493 + j0.3577 \\ 0.0493 + j0.3180 & 0.0493 + j0.3978 \end{bmatrix} \times 10^{-3} \quad \Omega/m$$

$$Z_C = \begin{bmatrix} Z_{41} & Z_{42} & Z_{43} \\ Z_{51} & Z_{52} & Z_{53} \end{bmatrix}$$

$$= \begin{bmatrix} 0.0493 + j0.3978 & 0.0493 + j0.3577 & 0.0493 + j0.3180 \\ 0.0493 + j0.3180 & 0.0493 + j0.3577 & 0.0493 + j0.3978 \end{bmatrix} \times 10^{-3} \quad \Omega/m$$

$$Z_D = \begin{bmatrix} Z_{44} & Z_{45} \\ Z_{54} & Z_{55} \end{bmatrix}$$

$$= \begin{bmatrix} 0.0192 + j0.8214 & 0.0493 + j0.3239 \\ 0.0493 + j0.3239 & 0.0192 + j0.8214 \end{bmatrix} \times 10^{-3} \quad \Omega/m$$

The impedance matrix Z_P using hand calculations derived from first principles as shown above is thus:

$$Z_P = [Z_A - Z_B Z_D^{-1} Z_C]$$

$$= \begin{bmatrix} 0.1979 + j0.7044 & 0.1288 + j0.2790 & 0.1273 + j0.2359 \\ 0.1288 + j0.2790 & 0.1962 + j0.7049 & 0.1288 + j0.2790 \\ 0.1273 + j0.2359 & 0.1288 + j0.2790 & 0.1979 + j0.7044 \end{bmatrix} \times 10^{-3} \quad \Omega/m$$

The phase impedance matrix obtained from the TLINE support programme used to model the line under the same assumptions in the RSCAD programme is shown below.

```
THE PHASE IMPEDANCE MATRIX ( Z(I,J) , OHMS/M ):
   0.20107E-03,0.70835E-03   0.13082E-03,0.28255E-03   0.12930E-03,0.23937E-03
   0.13082E-03,0.28255E-03   0.19936E-03,0.70886E-03   0.13082E-03,0.28255E-03
   0.12930E-03,0.23937E-03   0.13082E-03,0.28255E-03   0.20107E-03,0.70835E-03
```

These two matrices show that there is close agreement between the impedance parameters calculated by hand from first principles and those obtained from RSCAD's TLINE programme.

Two sets of parallel three phase conductors with two sub-conductors per phase and ground wires

Consider now the full representation of two coupled three phase transmission lines with ground wires and ground return that has been chosen as the example study system in this thesis. Each of these three phase sets of conductors includes two ground wires per three phase set. The impedance matrix taking into account mutual coupling between conductors with the effects of conductor sag ignored must then be calculated.

Conductor Data

Bundle #	Bundle 1	Bundle 2	Bundle 3
Conductor Name	2Zebra50	2Zebra50	2Zebra50
Conductor Type (AC or DC)	AC	AC	AC
V(kV)(AC:L--L,rms/DC:L--G,pk)	275.0	275.0	275.0
V Phase(Deg)	0.0	-120.0	120.0
Line I(kA)(AC:rms/DC:pk)	1.284	1.284	1.284
Line I Phase(Deg)	20.0	-100.0	140.0
Num of Sub-Conductors	2	2	2
Sub-Cond Radius(cm)	1.155819	1.155819	1.155819
Sub-Cond Spacing(cm)	38.0	38.0	38.0
Horiz. Dist. X(m)	-7.9	0.0	7.9
Height at Tower Y(m)	19.995	19.995	19.995
Sag at Midspan(m)	0.0	0.0	0.0
DC Resistance per Sub-Cond(ohms/km)	0.0674	0.0674	0.0674

Line Length(km): 68.59 Ground Resistivity (ohm-m): 700.0

Figure 3.10: Phase conductor 1-3 data

Conductor Data

Bundle #	Bundle 4	Bundle 5	Bundle 6
Conductor Name	2Zebra50	2Zebra50	2Zebra50
Conductor Type (AC or DC)	AC	AC	AC
V(kV)(AC:L--L,rms/DC:L--G,pk)	275.0	275.0	275.0
V Phase(Deg)	0.0	-120.0	120.0
Line I(kA)(AC:rms/DC:pk)	1.284	1.284	1.284
Line I Phase(Deg)	20.0	-100.0	140.0
Num of Sub-Conductors	2	2	2
Sub-Cond Radius(cm)	1.155819	1.155819	1.155819
Sub-Cond Spacing(cm)	38.0	38.0	38.0
Horiz. Dist. X(m)	26.1	34.0	41.9
Height at Tower Y(m)	19.995	19.995	19.995
Sag at Midspan(m)	0.0	0.0	0.0
DC Resistance per Sub-Cond(ohms/km)	0.0674	0.0674	0.0674

Line Length(km): 68.59 Ground Resistivity (ohm-m): 700.0

Figure 3.11: Phase conductor 4-6 data

Ground Wire Data

Ground Wire #	Conductor 1	Conductor 2	Conductor 3	Conductor 4
Conductor Name	S19	S19	S19	S19
Conductor Radius(cm)	0.664	0.664	0.664	0.664
Horiz. Dist. X(m)	-7.1	7.1	26.9	41.1
Height at Tower Y(m)	24.309	24.309	24.309	24.309
Sag at Midspan(m)	0.0	0.0	0.0	0.0
DC Resistance(ohms/km)	1.88	1.88	1.88	1.88

Figure 3.12: Ground conductor data

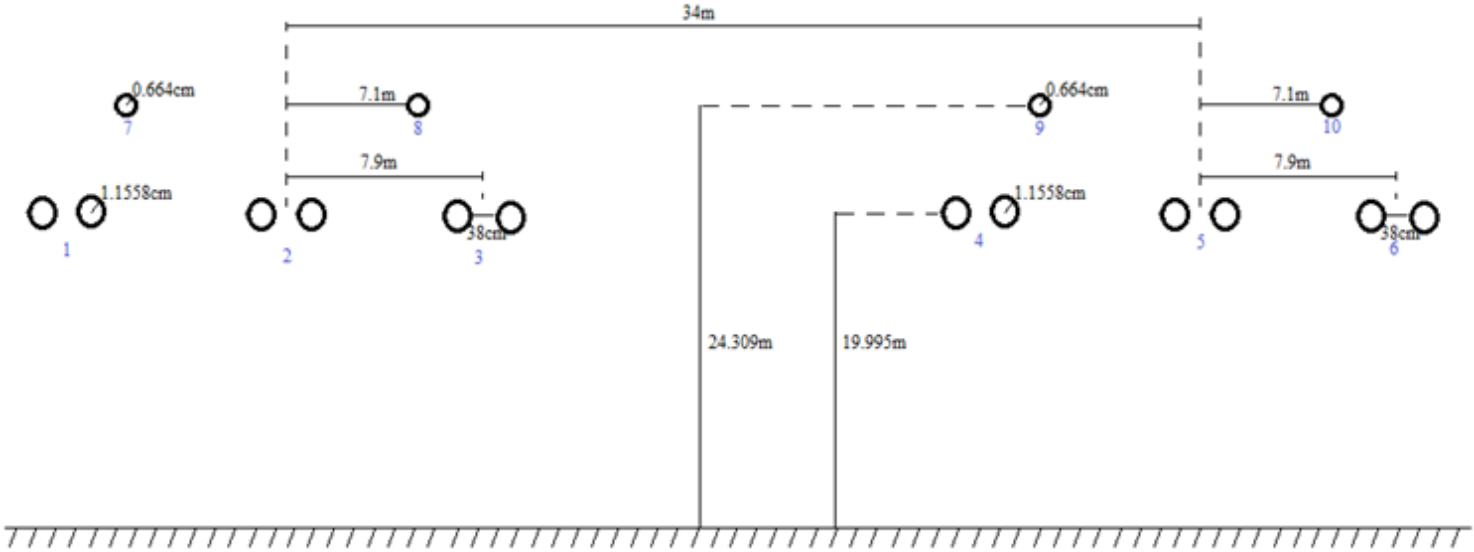

Figure 3.13: Conductor geometry

Again, in order to work toward the impedance matrices in the format of $\begin{bmatrix} Z_A & Z_B \\ Z_C & Z_D \end{bmatrix}$ and ultimately $Z_P = [Z_A - Z_B Z_D^{-1} Z_C]$ the associated parameters are calculated.

As calculated previously, the self-impedances of the phase conductors are as follows:

$D_{kk'} = 658.5\sqrt{\rho/f} = 658.5 \times \sqrt{700/50} = 2463.88 \quad m$

$R_{k'} = 9.869 \times 10^{-7} f = 9.869 \times 10^{-7}(50) = 4.9345 \times 10^{-5} \ \ \Omega/m$

$D_{kk} = \sqrt{e^{-1/4} \times r_x \times d_{subconductor}}$

$= \sqrt{0.7755 \times r_x \times d_{subconductor}}$

$= \sqrt{e^{-1/4} \times \frac{1.155819}{100} \times \frac{38}{100}}$

$= 0.0585 \ \ m$

$R_k = 0.0674 \ \ \Omega/km = 6.74 \times 10^{-5} \ \ \Omega/m$

$Z_{kk} = 0.5R_k + R_{k'} + j\omega(2 \times 10^{-7} \ln\frac{D_{kk'}}{D_{kk}}) \quad \Omega/m$

$= 0.5R_k + R_{k'} + j\omega(2 \times 10^{-7} (\ln\frac{1}{D_{kk}} + \ln D_{kk}') \ ) \quad \Omega/m$

Hence,

$Z_{11} = 0.5(6.74 \times 10^{-5}) + 4.9345 \times 10^{-5} + j\omega(2 \times 10^{-7} (\ln\frac{1}{0.0585} + \ln 2463.88) \ ) \quad \Omega/m$

$= 0.08304 \times 10^{-3} + j0.66906 \times 10^{-3} \ \ \Omega/m$

$= Z_{22} = Z_{33} = Z_{44} = Z_{55} = Z_{66}$

The mutual impedances between the phase conductors are also calculated as done previously as follows:

$Z_{km} = R_{k'} + j\omega(2 \times 10^{-7} (\ln\frac{1}{D_{km}} + \ln D_{km}') \ ) \quad \Omega/m$

Hence,

$Z_{12} = 4.9345 \times 10^{-5} + j\omega(2 \times 10^{-7} (\ln\frac{1}{7.9} + \ln 2463.88) \ ) \quad \Omega/m$

$= 0.49345 \times 10^{-4} + j0.36082 \times 10^{-3} \ \ \Omega/m$

$= Z_{21} = Z_{23} = Z_{32} = Z_{45} = Z_{54} = Z_{56} = Z_{65}$

$Z_{13} = 4.9345 \times 10^{-5} + j\omega(2 \times 10^{-7} (\ln\frac{1}{2 \times 7.9} + \ln 2463.88) \ ) \quad \Omega/m$

$$= 0.49345 \times 10^{-4} + j0.31727 \times 10^{-3} \ \ \Omega/m$$

$$= Z_{31} = Z_{46} = Z_{64}$$

$$Z_{14} = 4.9345 \times 10^{-5} + j\omega(2 \times 10^{-7} (\ln\frac{1}{34} + \ln 2463.88)) \ \ \Omega/m$$

$$= 0.49345 \times 10^{-4} + j0.26912 \times 10^{-3} \ \ \Omega/m$$

$$= Z_{41} = Z_{25} = Z_{52} = Z_{36} = Z_{63}$$

$$Z_{15} = 4.9345 \times 10^{-5} + j\omega(2 \times 10^{-7} (\ln\frac{1}{34 + 7.9} + \ln 2463.88)) \ \ \Omega/m$$

$$= 0.49345 \times 10^{-4} + j0.25599 \times 10^{-3} \ \ \Omega/m$$

$$= Z_{51} = Z_{26} = Z_{62}$$

$$Z_{16} = 4.9345 \times 10^{-5} + j\omega(2 \times 10^{-7} (\ln\frac{1}{34 + 7.9 + 7.9} + \ln 2463.88)) \ \ \Omega/m$$

$$= 0.49345 \times 10^{-4} + j0.24514 \times 10^{-3} \ \ \Omega/m$$

$$= Z_{61}$$

$$Z_{24} = 4.9345 \times 10^{-5} + j\omega(2 \times 10^{-7} (\ln\frac{1}{34 - 7.9} + \ln 2463.88)) \ \ \Omega/m$$

$$= 0.49345 \times 10^{-4} + j0.28573 \times 10^{-3} \ \ \Omega/m$$

$$= Z_{42} = Z_{35} = Z_{53}$$

$$Z_{34} = 4.9345 \times 10^{-5} + j\omega(2 \times 10^{-7} (\ln\frac{1}{34 - 7.9 - 7.9} + \ln 2463.88)) \ \ \Omega/m$$

$$= 0.49345 \times 10^{-4} + j0.30838 \times 10^{-3} \ \ \Omega/m$$

$$= Z_{34}$$

With the ground wires represented, the distances between each phase conductor and each ground wire needs to be calculated. From a study of the geometry in Figure 3.13, the calculation of the distance D_{km} for each phase and ground conductor is summarised in Table 3.2 below.

Table 3.4: Table of distances D_{km} between phase and ground conductors

Distance	Geometry	y (m)	x (m)	$\sqrt{x^2+y^2}$ (m)
D17=D71 **D38=D83** **D49=D94** **D6 10=D10 6**	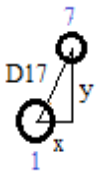	4.314	0.8	4.3876
D18=D81 **D37=D73** **D4 10=D10 4** **D69=D96**	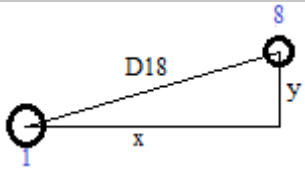	4.314	15	15.6080
D27=D72 **D28=D82** **D59=D95** **D5 10=D10 5**	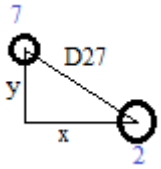	4.314	7.1	8.3079
D19=D91 **D68=D86**	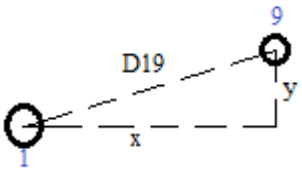	4.314	34.8	35.0664
D1 10=D10 1 **D67=D76**	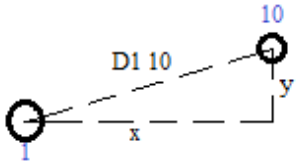	4.314	49	49.1895
D29=D92 **D58=D85**	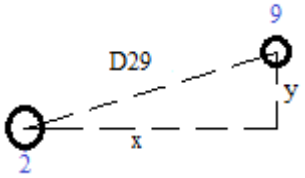	4.314	26.9	27.2437
D2 10=D10 2 **D57=D75**	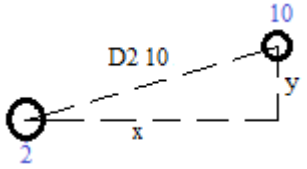	4.314	41.1	41.3258
D39=D93 **D48=D84**	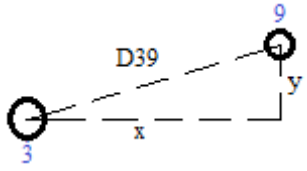	4.314	19	19.4836

D 3 10=D10 3 **D47=D74**	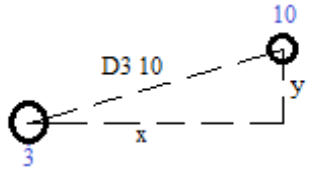	4.314	33.2	33.4791

The self-impedances of the ground wires are then calculated using the parameters in Figure 3.12.

$D_{kk'} = 658.5\sqrt{\rho/f} = 658.5 \times \sqrt{700/50} = 2463.88 \ \ m$

$R_{k'} = 9.869 \times 10^{-7} f = 9.869 \times 10^{-7}(50) = 4.9345 \times 10^{-5} \ \ \Omega/m$

$D_{kk} = e^{-1/4} \ r_x = 0.7755 \ r_x = e^{-1/4} \times \frac{0.664}{100} = 5.171 \times 10^{-3} \ \ m$

$R_k = 1.88 \ \ \Omega/km = 1.88 \times 10^{-3} \ \ \Omega/m$

$Z_{kk} = R_k + R_{k'} + j\omega(2 \times 10^{-7} \ln \frac{D_{kk'}}{D_{kk}}) \ \ \Omega/m$

$= R_k + R_{k'} + j\omega(2 \times 10^{-7} (\ln \frac{1}{D_{kk}} + \ln D_{kk}') \ ) \ \ \Omega/m$

Hence,

$Z_{77} = 1.88 \times 10^{-3} + 4.9345 \times 10^{-5} + j\omega(2 \times 10^{-7} (\ln \frac{1}{5.171 \times 10^{-3}} + \ln 2463.88) \ ) \ \ \Omega/m$

$= 0.19293 \times 10^{-4} + j0.82147 \times 10^{-3} \ \ \Omega/m$

$= Z_{88} = Z_{99} = Z_{10\,10}$

The mutual impedance of the ground wires in relation to the other ground wires in the system is calculated as follows:

$Z_{km} = R_{k'} + j\omega(2 \times 10^{-7} (\ln \frac{1}{D_{km}} + \ln D_{km}') \ ) \ \ \Omega/m$

Hence,

$Z_{78} = 4.9345 \times 10^{-5} + j\omega(2 \times 10^{-7} (\ln \frac{1}{2 \times 7.1} + \ln 2463.88) \ ) \ \ \Omega/m$

$= 0.49345 \times 10^{-4} + j0.32398 \times 10^{-3} \ \ \Omega/m$

$= Z_{87} = Z_{9\,10} = Z_{10\,9}$

$Z_{79} = 4.9345 \times 10^{-5} + j\omega(2 \times 10^{-7} (\ln \frac{1}{34} + \ln 2463.88) \ ) \ \ \Omega/m$

$$= 0.49345 \times 10^{-4} + j0.26912 \times 10^{-3}\ \Omega/m$$

$$= Z_{97} = Z_{8\,10} = Z_{10\,8}$$

$$Z_{7\,10} = 4.9345 \times 10^{-5} + j\omega(2 \times 10^{-7}\,(\ln\frac{1}{48.2} + \ln 2463.88)\ )\ \ \Omega/m$$

$$= 0.49345 \times 10^{-4} + j0.24719 \times 10^{-3}\ \ \Omega/m$$

$$= Z_{10\,7}$$

$$Z_{89} = 4.9345 \times 10^{-5} + j\omega(2 \times 10^{-7}\,(\ln\frac{1}{19.8} + \ln 2463.88)\ )\ \ \Omega/m$$

$$= 0.49345 \times 10^{-4} + j0.30309 \times 10^{-3}\ \Omega/m$$

$$= Z_{98}$$

The mutual impedance of the ground wires in relation to the phase conductors in the system can be calculated using the geometries and distances calcualted in Table 3.2 as follows:

$$Z_{km} = R_{k'} + j\omega(2 \times 10^{-7}\,(\ln\frac{1}{D_{km}} + \ln D_{km}')\ )\ \ \Omega/m$$

$$Z_{17}\ = 4.9345 \times 10^{-5} + j\omega(2 \times 10^{-7}\,(\ln\frac{1}{4.3876} + \ln 2463.88)\ )\ \ \Omega/m$$

$$= 0.49345 \times 10^{-4} + j0.0.39777 \times 10^{-3}\ \ \Omega/m$$

$$= Z_{71} = Z_{38} = Z_{83} = Z_{49} = Z_{94} = Z_{6\,10} = Z_{10\,6}$$

$$Z_{18}\ = 4.9345 \times 10^{-5} + j\omega(2 \times 10^{-7}\,(\ln\frac{1}{4.3876} + \ln 2463.88)\ )\ \ \Omega/m$$

$$= 0.49345 \times 10^{-4} + j0.31804 \times 10^{-3}\ \ \Omega/m$$

$$= Z_{81} = Z_{37} = Z_{73} = Z_{4\,10} = Z_{10\,4} = Z_{69} = Z_{96}$$

$$Z_{27}\ = 4.9345 \times 10^{-5} + j\omega(2 \times 10^{-7}\,(\ln\frac{1}{8.3079} + \ln 2463.88)\ )\ \ \Omega/m$$

$$= 0.49345 \times 10^{-4} + j0.35766 \times 10^{-3}\ \ \Omega/m$$

$$= Z_{72} = Z_{28} = Z_{82} = Z_{59} = Z_{95} = Z_{5\,10} = Z_{10\,5}$$

$$Z_{19}\ = 4.9345 \times 10^{-5} + j\omega(2 \times 10^{-7}\,(\ln\frac{1}{35.0664} + \ln 2463.88)\ )\ \ \Omega/m$$

$$= 0.49345 \times 10^{-4} + j0.26718 \times 10^{-3}\ \Omega/m$$

$$= Z_{91} = Z_{68} = Z_{86}$$

$$Z_{1\,10} = 4.9345 \times 10^{-5} + j\omega(2 \times 10^{-7}\,(\ln\frac{1}{49.1895} + \ln 2463.88)\ )\ \Omega/m$$

$$= 0.49345 \times 10^{-4} + j0.24591 \times 10^{-3}\ \Omega/m$$

$$= Z_{10\,1} = Z_{67} = Z_{76}$$

$$Z_{29} = 4.9345 \times 10^{-5} + j\omega(2 \times 10^{-7}\,(\ln\frac{1}{27.2437} + \ln 2463.88)\ )\ \Omega/m$$

$$= 0.49345 \times 10^{-4} + j0.28304 \times 10^{-3}\ \Omega/m$$

$$= Z_{92} = Z_{58} = Z_{85}$$

$$Z_{2\,10} = 4.9345 \times 10^{-5} + j\omega(2 \times 10^{-7}\,(\ln\frac{1}{41.3258} + \ln 2463.88)\ )\ \Omega/m$$

$$= 0.49345 \times 10^{-4} + j0.25686 \times 10^{-3}\ \Omega/m$$

$$= Z_{10\,2} = Z_{57} = Z_{75}$$

$$Z_{39} = 4.9345 \times 10^{-5} + j\omega(2 \times 10^{-7}\,(\ln\frac{1}{19.4836} + \ln 2463.88)\ )\ \Omega/m$$

$$= 0.49345 \times 10^{-4} + j0.30410 \times 10^{-3}\ \Omega/m$$

$$= Z_{93} = Z_{48} = Z_{84}$$

$$Z_{3\,10} = 4.9345 \times 10^{-5} + j\omega(2 \times 10^{-7}\,(\ln\frac{1}{33.4791} + \ln 2463.88)\ )\ \Omega/m$$

$$= 0.49345 \times 10^{-4} + j0.27009 \times 10^{-3}\ \Omega/m$$

$$= Z_{10\,3} = Z_{47} = Z_{74}$$

From the values calculated above, one can derive the matrices Z_A, Z_B, Z_C, and Z_D as defined earlier in eqn. (55) and eqn. (58):

$$Z_A = \begin{bmatrix} Z_{11} & Z_{12} & Z_{13} & Z_{14} & Z_{15} & Z_{16} \\ Z_{21} & Z_{22} & Z_{23} & Z_{24} & Z_{25} & Z_{26} \\ Z_{31} & Z_{32} & Z_{33} & Z_{34} & Z_{35} & Z_{36} \\ Z_{41} & Z_{42} & Z_{43} & Z_{44} & Z_{45} & Z_{46} \\ Z_{51} & Z_{52} & Z_{53} & Z_{54} & Z_{55} & Z_{56} \\ Z_{61} & Z_{62} & Z_{63} & Z_{64} & Z_{65} & Z_{66} \end{bmatrix}$$

$$= \begin{bmatrix} 0.0830 + j0.6691 & 0.0493 + j0.3608 & 0.0493 + j0.3173 & 0.0493 + j\,0.2691 & 0.0493 + j0.2560 & 0.0493 + j0.2451 \\ 0.0493 + j0.3608 & 0.0830 + j0.6691 & 0.0493 + j0.3608 & 0.0493 + j0.2857 & 0.0493 + j\,0.2691 & 0.0493 + j0.2560 \\ 0.0493 + j0.3173 & 0.0493 + j0.3608 & 0.0830 + j0.6691 & 0.0493 + j0.3084 & 0.0493 + j0.2857 & 0.0493 + j\,0.2691 \\ 0.0493 + j0.2691 & 0.0493 + j0.2857 & 0.0493 + j0.3084 & 0.0830 + j0.6691 & 0.0493 + j0.3608 & 0.0493 + j\,0.3173 \\ 0.0493 + j0.2560 & 0.0493 + j0.2691 & 0.0493 + j0.2857 & 0.0493 + j0.3608 & 0.0830 + j0.6691 & 0.0493 + j0.3608 \\ 0.0493 + j0.2451 & 0.0493 + j0.2560 & 0.0493 + j0.2691 & 0.0493 + j\,0.3173 & 0.0493 + j0.3608 & 0.0830 + j0.6691 \end{bmatrix}$$

$\times 10^{-3} \quad \Omega/m$

$$Z_B = \begin{bmatrix} Z_{17} & Z_{18} & Z_{19} & Z_{1\,10} \\ Z_{27} & Z_{28} & Z_{29} & Z_{2\,10} \\ Z_{37} & Z_{38} & Z_{39} & Z_{3\,10} \\ Z_{47} & Z_{48} & Z_{49} & Z_{4\,10} \\ Z_{57} & Z_{58} & Z_{59} & Z_{5\,10} \\ Z_{67} & Z_{68} & Z_{69} & Z_{6\,10} \end{bmatrix}$$

$$= \begin{bmatrix} 0.0493 + j0.3978 & 0.0493 + j0.3180 & 0.0493 + j0.2672 & 0.0493 + j0.2459 \\ 0.0493 + j0.3577 & 0.0493 + j0.3577 & 0.0493 + j0.2830 & 0.0493 + j0.2569 \\ 0.0493 + j0.3180 & 0.0493 + j0.3978 & 0.0493 + j0.3041 & 0.0493 + j0.2701 \\ 0.0493 + j0.2701 & 0.0493 + j0.3041 & 0.0493 + j0.3978 & 0.0493 + j0.3180 \\ 0.0493 + j0.2569 & 0.0493 + j0.2830 & 0.0493 + j0.3577 & 0.0493 + j0.3577 \\ 0.0493 + j0.2459 & 0.0493 + j0.2672 & 0.0493 + j0.3180 & 0.0493 + j0.3978 \end{bmatrix} \times 10^{-3} \quad \Omega/m$$

$$Z_C = \begin{bmatrix} Z_{71} & Z_{72} & Z_{73} & Z_{74} & Z_{75} & Z_{76} \\ Z_{81} & Z_{82} & Z_{83} & Z_{84} & Z_{85} & Z_{86} \\ Z_{91} & Z_{92} & Z_{93} & Z_{94} & Z_{95} & Z_{96} \\ Z_{10\,1} & Z_{10\,2} & Z_{10\,3} & Z_{10\,4} & Z_{10\,5} & Z_{10\,6} \end{bmatrix}$$

$$= \begin{bmatrix} 0.0493 + j0.3978 & 0.0493 + j0.3577 & 0.0493 + j0.3180 & 0.0493 + j0.2701 & 0.0493 + j0.2569 & 0.0493 + j0.2459 \\ 0.0493 + j0.3180 & 0.0493 + j0.3577 & 0.0493 + j0.3978 & 0.0493 + j0.3041 & 0.0493 + j0.2830 & 0.0491 + j0.2672 \\ 0.0491 + j0.2672 & 0.0493 + j0.2830 & 0.0493 + j0.3041 & 0.0493 + j0.3978 & 0.0493 + j0.3577 & 0.0493 + j0.3180 \\ 0.0493 + j0.2459 & 0.0493 + j0.2569 & 0.0493 + j0.2701 & 0.0493 + j0.3180 & 0.0493 + j0.3577 & 0.0493 + j0.3978 \end{bmatrix}$$

$\times 10^{-3} \quad \Omega/m$

$$Z_D = \begin{bmatrix} Z_{77} & Z_{78} & Z_{79} & Z_{7\,10} \\ Z_{87} & Z_{88} & Z_{89} & Z_{8\,10} \\ Z_{97} & Z_{98} & Z_{99} & Z_{9\,10} \\ Z_{10\,7} & Z_{10\,8} & Z_{10\,9} & Z_{10\,10} \end{bmatrix}$$

$$= \begin{bmatrix} 0.01929 + j0.82147 & 0.04934 + j0.32398 & 0.04934 + j0.26912 & 0.04934 + j024719 \\ 0.04934 + j0.32398 & 0.01929 + j0.82147 & 0.04934 + j0.30309 & 0.04934 + j0.26912 \\ 0.04934 + j0.26912 & 0.04934 + j0.30309 & 0.01929 + j0.82147 & 0.04934 + j0.32398 \\ 0.04934 + j024719 & 0.04934 + j0.26912 & 0.04934 + j0.32398 & 0.01929 + j0.82147 \end{bmatrix} \times 10^{-3} \quad \Omega/m$$

$$Z_P = [Z_A - Z_B Z_D^{-1} Z_C]$$

$$\begin{bmatrix} 0.1678 + j0.5453 & 0.1338 + j0.2353 & 0.1340 + j0.1894 & 0.1283 + j0.1432 & 0.1246 + j0.1335 & 0.1217 + j0.1253 \\ 0.1338 + j0.2353 & 0.1689 + j0.5414 & 0.1372 + j0.2302 & 0.1315 + j0.1570 & 0.1277 + j0.1439 & 0.1246 + j0.1335 \\ 0.1340 + j0.1894 & 0.1372 + j0.2302 & 0.1747 + j0.5350 & 0.1315 + j0.1760 & 0.1315 + j0.1570 & 0.1283 + j0.1432 \\ 0.1283 + j0.1432 & 0.1315 + j0.1570 & 0.1356 + j0.1760 & 0.1747 + j0.5350 & 0.1372 + j0.2302 & 0.1340 + j0.1894 \\ 0.1246 + j0.1335 & 0.1277 + j0.1439 & 0.1315 + j0.1570 & 0.1372 + j0.2302 & 0.1689 + j0.5414 & 0.1338 + j0.2353 \\ 0.1217 + j0.1253 & 0.1246 + j0.1335 & 0.1283 + j0.1432 & 0.1340 + j0.1894 & 0.1338 + j0.2353 & 0.1678 + j0.5453 \end{bmatrix}$$

$\times 10^{-3} \ \ \Omega/m$

The phase impedance matrix obtained from the TLINE support programme used to model the line under the same assumptions in the RSCAD programme is shown over the page.

```
THE PHASE IMPEDANCE MATRIX ( Z(I,J) , OHMS/M ):
  0.17320E-03,0.54276E-03  0.13713E-03,0.22030E-03  0.13031E-03,0.14781E-03  0.13031E-03,0.14781E-03  0.13031E-03,0.14781E-03
  0.13713E-03,0.22030E-03  0.17320E-03,0.54276E-03  0.13713E-03,0.22030E-03  0.13031E-03,0.14781E-03  0.13031E-03,0.14781E-03
  0.13713E-03,0.22030E-03  0.13713E-03,0.22030E-03  0.17320E-03,0.54276E-03  0.13031E-03,0.14781E-03  0.13713E-03,0.22030E-03
  0.13031E-03,0.14781E-03  0.13031E-03,0.14781E-03  0.13031E-03,0.14781E-03  0.17320E-03,0.54276E-03  0.13713E-03,0.22030E-03
  0.13031E-03,0.14781E-03  0.13031E-03,0.14781E-03  0.13713E-03,0.22030E-03  0.13713E-03,0.22030E-03  0.17320E-03,0.54276E-03
```

These two matrices show that there is close agreement between the impedance parameters calculated by hand from first principles and those obtained from RSCAD's TLINE programme.

Finally, when considering the theory and derivations presented thus far, it is important to note the difference between the individual phase-impedance matrices used to represent two parallel three-phase transmission lines when interaction between the lines is not taken into account, and the unitary phase-impedance matrix used to represent the same pair of lines when the full interaction between the two lines is taken into account. When no mutual coupling between the parallel lines is represented, each line is modelled using its own resultant 3x3 phase impedance matrix equation according to eqn. (62), as follows:
$E_{P_{L1}} = Z_{P_{L1}} I_{P_{L1}}$ and $E_{P_{L2}} = Z_{P_{L2}} I_{P_{L2}}$.

When mutual coupling between the lines is represented, a single 6x6 matrix Z_P that represents the two three-phase systems as a unitary, coupled electrical and magnetic system, $E_{P_{L1L2}} = Z_{P_{L1L2}} I_{P_{L1L2}}$ is obtained. Upon examining the resultant 6x6 matrix equation for such a system, $E_{P_{L1L2}}$ can be re-written as:

$$\begin{bmatrix} E_{P_{L1A}} \\ E_{P_{L1B}} \\ E_{P_{L1C}} \\ E_{P_{L2A}} \\ E_{P_{L2B}} \\ E_{P_{L2C}} \end{bmatrix} = \begin{bmatrix} [Z_{11}] & [Z_{12}] \\ [Z_{21}] & [Z_{22}] \end{bmatrix} \begin{bmatrix} I_{P_{L1A}} \\ I_{P_{L1B}} \\ I_{P_{L1C}} \\ I_{P_{L2A}} \\ I_{P_{L2B}} \\ I_{P_{L2C}} \end{bmatrix}$$

where $Z_{11}, Z_{12}, Z_{21}, Z_{22}$ are 3x3 sub-matrices of the full 6x6 matrix $Z_{P_{L1L_2}}$. Note that the 3x3 sub-matrices Z_{11}, and Z_{22} of the full, coupled system model are not simply the 3x3 phase-impedance matrices $Z_{P_{L1}}$ and $Z_{P_{L2}}$ obtained for the two individual lines when mutual coupling is ignored (except for special cases when both lines have no ground wires).

3.3. Conclusion

This chapter has presented the fundamental theory required to derive, by hand calculation, the phase-domain impedances of mutually coupled transmission lines. In all the scenarios investigated in this chapter, it has been seen that the transmission line parameters calculated by hand from first principles agree closely with those obtained from RSCAD's TLINE support programme. The small differences seen in the transmission line parameters derived from first principles and those obtained from the TLINE program could arise from differences in the way the resistance is represented under AC conditions (e.g. skin effect) in the TLINE program and the specific formulae used for Carson's method within the TLINE program, both of which may differ from the assumptions used here in the first-principles derivations. Nevertheless, the

agreement between the parameters is sufficiently close to provide confidence between the results obtained using the real time simulator models of coupled transmission lines in subsequent chapters of this thesis

The next chapter presents the results of a real time simulation investigation into the effects of mutual coupling in transmission lines, paying specific attention to the impact mutual coupling has on the impedance seen by a distance protection relay and the response of a distance protection relay as a result of this phenomenon.

CHAPTER 4

INVESTIGATING THE IMPACT OF MUTUAL COUPLING ON DISTANCE PROTECTION RELAYS USING A REAL TIME DIGITAL SIMULATOR

In Southern Africa, the approach of having double circuit or parallel transmission lines in the same servitude is widely used. Historically, when setting protection relays on adjacent transmission lines running in the same servitude, separated by distances of 35 meters or more, the effects of mutual coupling in the design stages of the protection settings have been ignored. Recent experience however, has called for a review of this practice [5].

The use of permissive over-reaching distance protection schemes on overhead high voltage transmission lines is common practice in South Africa. Such schemes allow isolation of a fault on a transmission line almost instantaneously. In the event of the distance protection relay making an incorrect decision based on the current and voltage measurement inputs that it is fed, the effect of such is potentially very serious. Chapter 3 has explained the nature of mutual coupling, and the effect that it has on the impedances of transmission lines, but the impact that these mutual coupling effects have on the measurements made by a protection scheme is complex and dependent on a variety of different factors and operating conditions. It is not always possible to easily understand the effect of mutual coupling on a particular transmission line's protection scheme in the design stages, without the use of specialised simulation tools. One particular simulation tool that has been discussed in Chapter 2 is the Real Time Digital Simulator which allows the user to gain a better understanding of a protection scheme's performance, since it allows for the actual protection relays to be connected hardware-in-loop. In this way a detailed real time model of the power system can be used to test the actual protection relays to be used on site, with the designed protection settings for the protection scheme. This chapter presents the results of an investigation into the use of a Real Time Digital Simulator to quantify the effects of mutual coupling on a distance protection relay.

The studies performed in this chapter will be based on the Avon to Impala section of the transmission system described in Section 2.17 and Figure 2.36, where the two transmission lines that run in parallel are on separate towers in the same servitude and are connected to common busbars at either end.

4.1. Theory

For the transmission system topology used in this study, Figure 4.1 will be used to examine the theory, where Bus S is the sending end busbar and Bus R the receiving end busbar. The circuit breakers at the sending ends of the two transmission lines are labelled A and C in Figure 4.1 whilst the breakers at the receiving end of these transmission lines are labelled B and D. If both transmission lines are constructed sufficiently close to each other, mutual coupling will be present between the two transmission lines. This will create the scenario where the zero sequence current associated with a ground fault in one circuit will induce a significant zero sequence voltage in the parallel circuit [1].

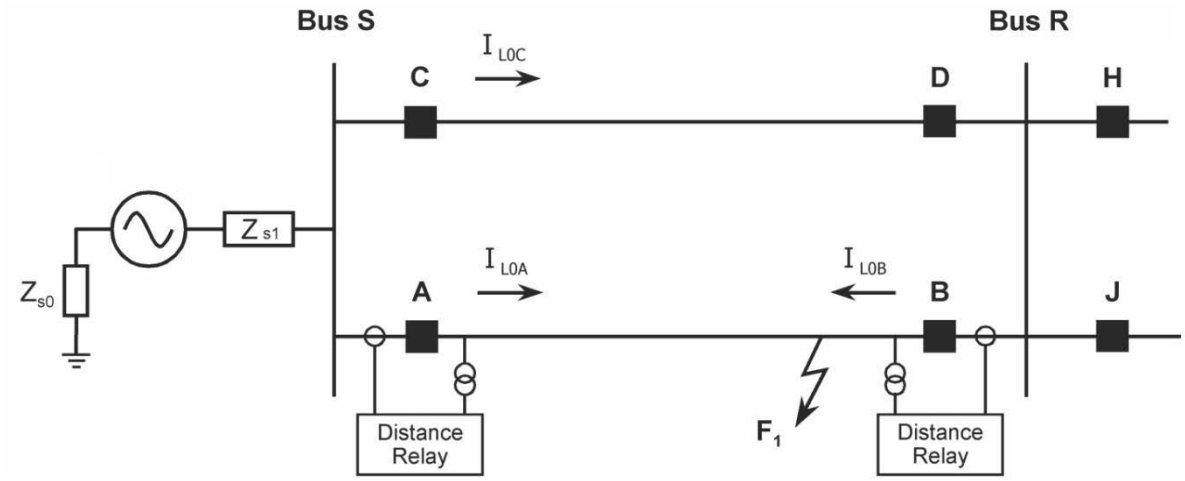

Figure 4.1: Double Circuit Transmission Line System

For a phase to ground fault located close to bus R on one of the transmission lines (F_1 in Figure 4.1), I_{L0A} and I_{L0B} are the zero sequence currents seen by the relays on the faulted line at A and B respectively. Note the direction of the zero sequence currents in the faulted line. For this fault scenario, the zero sequence current in the parallel healthy line, I_{L0C}, is in the same direction as I_{L0A} but in the opposite direction to I_{L0B}. This zero sequence current in the healthy line induces, via mutual coupling, a zero sequence voltage in the line with the fault. For the particular zero sequence current directions in this scenario, this induced zero sequence voltage will be of a polarity such that it adds to the voltage at point A and opposes the voltage at B which will cause the relay at A to see an increase in impedance and the relay at B to see a decrease in impedance. The expected response of the relays to this scenario will be to under-reach at A and over-reach at B.

The challenge that this places on the distance protection scheme is reliability and selectivity of the protection scheme to operate. In a typical permissive over-reaching transfer trip (POTT) protection scheme, both transmission lines in Figure 4.1 will be protected by an unsupervised (instantaneous tripping) forward looking zone 1 element set to protect 80% of the transmission

line, and a time-delayed forward looking zone 2 element set to protect 120% of the transmission line (with additional supervisory logic used to override the time delay on conditions of the remote end relay confirming the fault on the protected line). In the event of either an over-reach or under-reach of the relay, the selectively or stability of the protection scheme maybe compromised.

The particular concern for an over or under-reach of zone 1 is that this is an instantaneous, unsupervised zone. High speed mal-operation of the protection scheme can take place causing either widespread outage or widespread equipment damage if a fault is not cleared as quickly as possible. Zone 2 mal-operation is also of concern as any under-reach of the of the zone 2 element will have the effect of increasing the risk that the protection scheme may not trip for faults near the ends of the protected line until other relays operate to clear this fault. The reliability of the protection scheme maybe compromised.

Methods for mutual coupling compensation in distance protection relay settings have been discussed in Chapter 2.11. These include the use of a mutual coupling compensation factor (k_{0M}), together with measurement of the zero sequence current of the parallel transmission line, so that the relay can internally compensate for mutual coupling, as well as adjustment of the reach settings of the zones of protection to compensate for the mutual coupling effects under different operating conditions in the transmission line. The practical implementation of each of these two methods will also be described in this chapter. The following section describes a RTDS model that has been developed to study the impact of mutual coupling on distance protection relays.

4.2. Setup of model used to research mutual coupling between transmission lines

A real time model of the system to be studied was developed using RSCAD. The Avon to Impala transmission lines were two 275 kV transmission lines (of length 69 km between Avon and Mersey) with the distance between the two towers being 37 meters, measured between the mid-points of each tower as shown in Figure 2.37. The transmission line and power system data was acquired from Eskom. The power system was modelled in DRAFT. Two versions of the power system were modelled: in the first model each of the two transmission lines was described using its own distinct distributed parameter model such that no mutual coupling between the transmission lines was represented; in the second model the two transmission lines were described together using a single distributed parameter model so that the full interaction and mutual coupling between the transmission lines was represented. The purpose of this approach was to examine the effect of mutual coupling against a control case. In both models all

parameters were exactly the same (with the exception of the representation of mutual coupling) such that any differences between the results that were observed can be attributed to mutual coupling alone. In the studies carried out in this chapter of the thesis, the transmission lines were assumed to be ideally transposed.

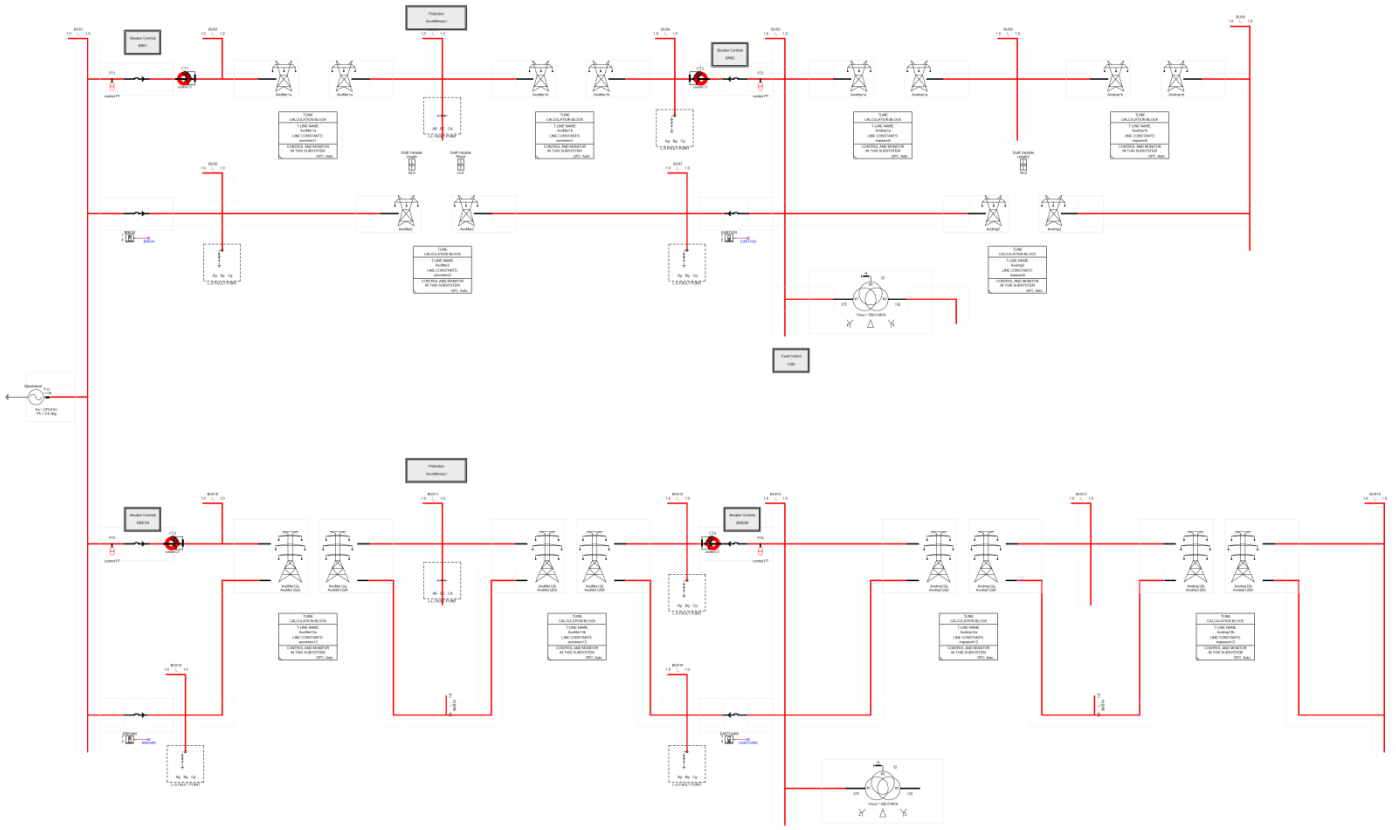

Figure 4.2: DRAFT model of the power system without mutual coupling (above) and with mutual coupling (below)

From the DRAFT model in Figure 4.2, note that the parallel transmission lines in the top part of the figure are independent from each other (two distinct distributed-parameter transmission line models) and the parallel transmission lines at the bottom part of the figure are represented using coupled-circuit transmission line tower symbols (a combined distributed-parameter transmission line model used to represent the parallel lines). In each case, the details of the tower construction, as well as the distance between the towers and other electrical and mechanical details of the conductors and ground wires need to be known so that the electrical parameters of the two sets of travelling-wave transmission line models (with mutual coupling ignored and mutual coupling represented) can be developed using the TLINE support program as shown in Figure 4.3 and 4.4.

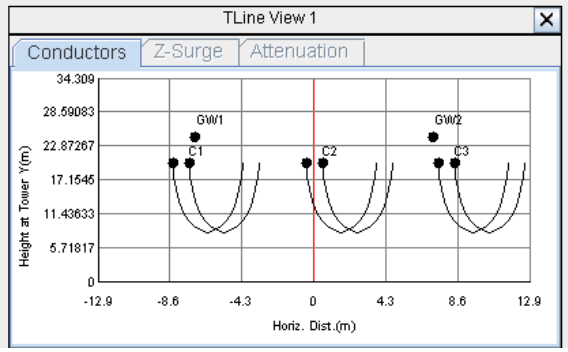

Figure 4.3: TLINE model for one transmission line without mutual coupling

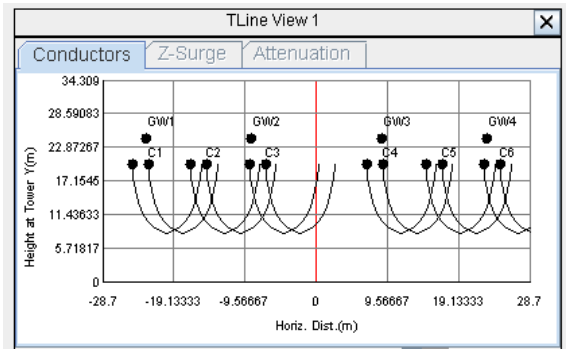

Figure 4.4: TLINE model for two transmission lines with mutual coupling

At each location A and B in the real-time model of the system in Figure 4.2, SEL 421 hardware protection relays were used to perform conventional distance protection where zone 1 was set to protect 80% of the line and zone 2 was set to protect 120% of the line. A simple POTT scheme was designed, implemented and tested. In addition, RSCAD generic software distance protection relays were run in parallel with the SEL 421 relays, with identical settings to the hardware relays, and were used to gain insight into the impedance that the hardware relays were seeing and hence to allow a better understanding of the reasons for the hardware relays' responses to each fault scenario. A simple POTT scheme was also implemented using the RSCAD software relays as shown in Figure 4.7. The decision making elements of the software relays were also monitored in order to gain a proper understanding of how and why the trip signals of the hardware relays were issued. The digital and analogue inputs to the RSCAD software relays were the same inputs that were sent to the SEL hardware relays.

In order to make hardware in loop connections between the external SEL 421 hardware relays and the real time simulation, the DRAFT model of the system had to be configured to export and import digital signals between the relays and the model. Figure 4.5 shows the approach used to export analogue measurements from the DRAFT model to the external relays.

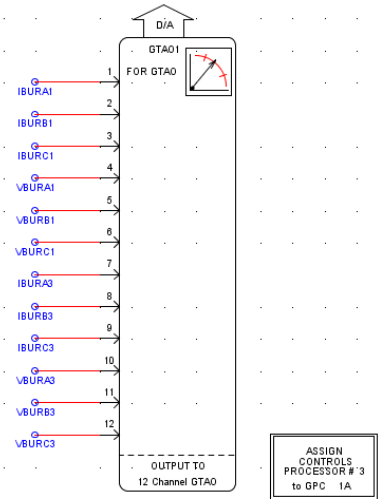

Where :

IBURx is the CT2 secondary current for input to the relay

VBURx is the VT2 secondary voltage for input to the relay

Figure 4.5: GTAO card used for exporting signals

Figure 4.6 shows the approach used to export and import digital signals between the real time model and external relays in DRAFT.

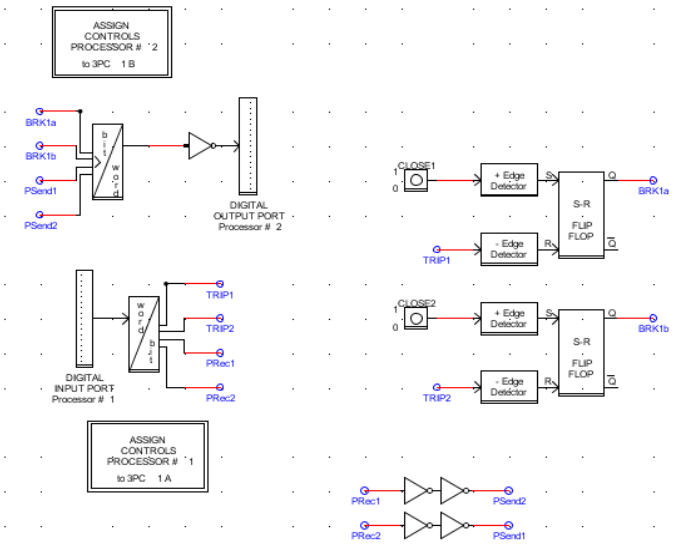

Figure 4.6: Additional logic required to import and export digital signals between the SEL relay and the RTDS model

The GTAO card shown in Figure 4.5 is a 12 channel digital to analogue converter through which analogue signals are exported and scaled before being amplified and input to the hardware relays. The signal-level analogue outputs from the GTAO card are interfaced with a high-bandwidth voltage-voltage and voltage-current power amplifier, in this case an Omicron CMS 156. It is important to note the gain of the amplifier, per signal level volt in order to configure the above DAC (Digital to Analogue Converter). The CMS 156 has the following gains [50]:

5 A/V for the voltage-current signals

50V/V for the voltage-voltage signals

This was used to calculate the scale factors required for the DAC as follows:

$$\frac{I_{Simulation}}{I_{Physical}} = 1 = \frac{5}{S_x} \times 5 = \frac{25}{S_x} \rightarrow S_x = 25 \text{ for the voltage to current channels} \quad (64)$$

$$\frac{V_{Simulation}}{V_{Physical}} = 1 = \frac{5}{S_x} \times 50 = \frac{250}{S_x} \rightarrow S_x = 250 \text{ for the voltage to voltage channels} \quad (65)$$

Careful checking was carried out in order to ensure that the currents and voltages output from the Omicron amplifier were scaled correctly and were within the safe operating range for connection to the hardware relays' measurement inputs. The relays were then driven from the amplifiers, and open-loop testing was done to verify that the zones of protection of the relay were correctly set for both phase and ground faults. Closed loop testing (signals sent both to and from the simulation to the relay) was then performed with the addition of digital input and output ports as shown in Figure 4.6.

Both the RSCAD software and SEL hardware relays' settings were designed with mho characteristics. In the RUNTIME interface these mho characteristics and the impedances measured by the software relay models can be viewed on graphs displaying the transmission line characteristics and the zones of protection.

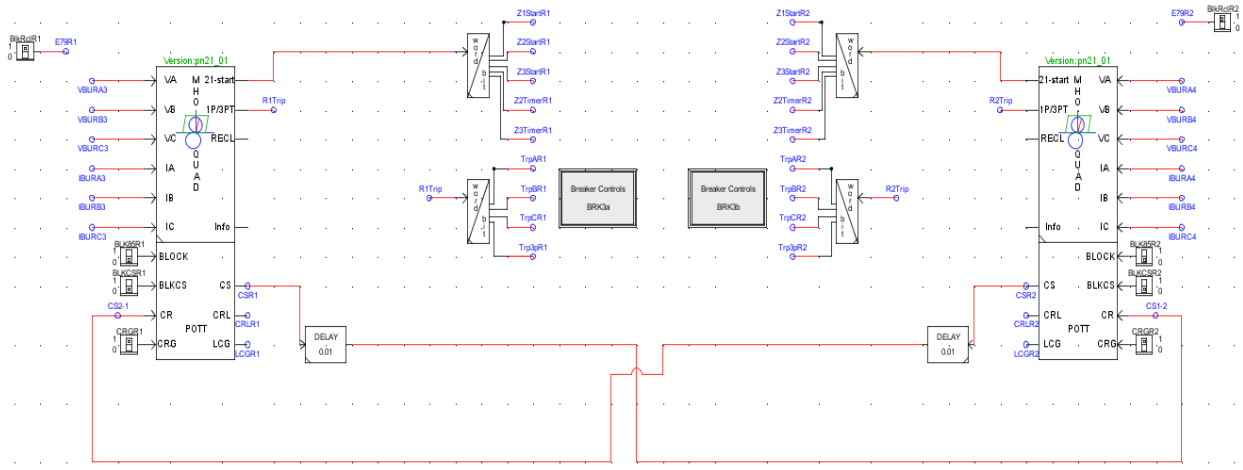

Figure 4.7: POTT scheme implemented using the RCSAD software relays

Once the DRAFT model, TLINE model, RUNTIME interface, relay settings and connection between hardware and software had been setup, an investigation into the effects of mutual coupling on the distance protection relay was made. Figure 4.8 shows the full hardware-in-loop connections that were used at the DUT RTDS laboratory.

Figure 4.8: Hardware-in-loop connections between the SEL 421 relays and the RTDS simulator used for the research

4.3. Results

4.3.1. Testing a base case

Once the real time model of the power system was set up, tests were carried out on the base case (control) model in which no mutual coupling was represented. For this portion of the research, conditions in the power system were chosen to be as simple as possible such that there was intentionally no load transfer down the transmission lines and no source beyond bus S was considered. The transmission lines were ideally transposed thus eliminating any additional complicating factors. In order to produce clean impedance plots and to ascertain where exactly the impedance locus settles in each test, the breakers were held closed for the initial studies. In other words, initially the system was studied open loop such that the trip signals from the relays were simply monitored via the hardware-in-loop connection, but they were prevented from actually operating the circuit breakers.

Once this base case was set up, the real time model of the power system and the protection settings were tested and verified. Faults were placed along the transmission line to verify the zone 1 and 2 reach settings for both the SEL 421 and the RSCAD generic model relays. Figure

4.9 shows the impedance seen by the RSCAD generic relay model of the relay connected at A in Figure 4.2 following a C-g fault situated 80% along the line from A. The red straight line is the transmission line impedance characteristic, the blue mho circle represents the reach of zone 1 set to 80%, the green mho circle represents the reach of zone 2 set to 120% and the pink mho circle represents the reach of the reverse looking zone 3 set to 20%. From this impedance plot, note that the impedance locus settles correctly on the intersection of the line impedance characteristic and the edge of zone 1 in the phase C to ground impedance measurement element of the relay.

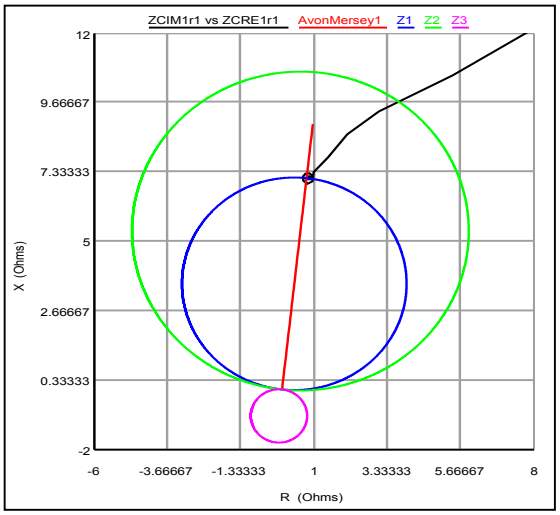

Figure 4.9: Impedance measured by the C phase ground element of the relay at A for a C-g fault located at 80% along the line AB with no mutual coupling between the lines

These results are as one would expect for a simple case where no mutual coupling or other complicating factors exist. The RSCAD generic relay issues an instantaneous zone 1 trip for this fault location. The SEL 421 relay also issues a zone 1 instantaneous trip. To test the reach of zone 1 a fault was placed just past the zone 1 reach at 81%. Both the hardware and software relays issued a zone 2 trip, indicating that the zone 1 protection setting was correct. This exercise was then repeated for the zone 2 reach and this was also verified to be correct.

4.3.2. Both lines in service with mutual coupling between the lines

Once the base case was established it provided a reference to compare all future results with. The case where mutual coupling was represented between the transmission lines was then considered, initially with the distance between the transmission lines in the model set to 37 metres which is the actual distance between the two transmission lines as they stand in service. Figure 4.10 shows the impedance seen by the RSCAD model of the relay at A in Figure 4.2 for

a C-g fault located 80% along the line from A when mutual coupling is represented between the transmission lines.

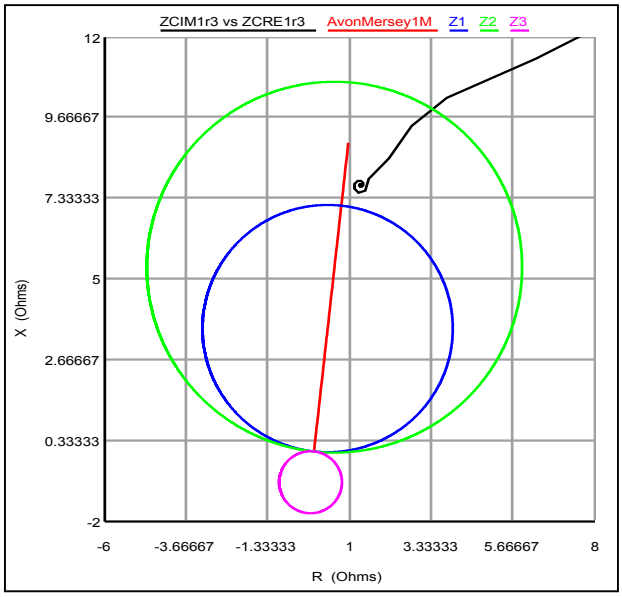

Figure 4.10: Impedance measured by the C phase ground element of the relay at A for a C-g fault located at 80% along the line AB with mutual coupling between the lines

In Figure 4.10 the impedance locus now settles on a point somewhat to the right of the line characteristic well beyond the boundary of zone 1. Comparing the impedance loci of Figure 4.9 and Figure 4.10, note that for the exact same scenario and fault, as soon as mutual coupling is present between the transmission lines, the relay at A under-reaches. This was verified with the SEL 421 relays and the RSCAD generic distance relay as both relays issued a zone 2 trip for a fault at 80% when mutual coupling was represented in the model. This verifies the statement made earlier that the zero sequence current in the healthy line induces a zero sequence voltage in the faulted line with the effect of adding to the voltage at A causing an increase in the impedance seen by the relay at A.

To test the converse of this, for the relay at B, a fault was placed at 20% along the line from the relay at A which was 80% down the line from the relay at B. Figure 4.11 shows the impedance seen by the RSCAD model of the relay at B in Figure 4.2 for a C-g fault located 20% along the line from A when mutual coupling is represented between the transmission lines.

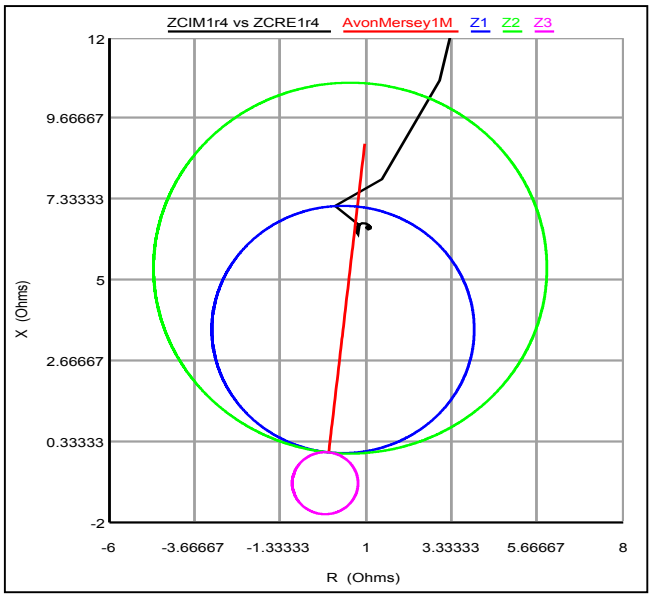

Figure 4.11: Impedance measured by C phase ground element of the relay at B for a C-g fault located at 20% along the line AB with mutual coupling between the lines

The results in Figure 4.11 once again demonstrate the effect of mutual coupling on the impedance that the distance protection relay sees. Figure 4.11 shows that in the case of the relay at B, the impedance locus again settles on a point somewhat to the right of the line characteristic but now well inside the boundary of zone 1 proving that the relay at B over-reaches as a result of the mutual coupling. The SEL 421 relays and the RSCAD generic distance relays both issued zone 1 trip for a fault at 81%. This verifies the statement made earlier that the zero sequence current in the healthy line induces a zero sequence voltage in the faulted line with the effect of opposing the voltage at B, causing a decrease in the impedance seen by the relay at B.

The behaviour of the relays at both A and B is consistent with that expected from the analysis presented earlier for mutually coupled parallel lines under these test conditions.

To quantify the extent of the under-reaching of the zone 1 elements at A due to mutual coupling when both transmission lines are in service, the distance between the transmission lines in the study system model was varied and the difference between the results of the base case (mutual coupling ignored) and the results from the case where mutual coupling is present were calculated. The distance between the midpoints of each tower was varied from 15.8 meters to 1000 meters so that the true extent of mutual coupling could be quantified as the separation between the transmission lines increases (and the influence of mutual coupling diminishes). At each assumed distance between the transmission lines, in order to calculate the error in zone 1 reach at A as a result of mutual coupling effects, the fault placed on the transmission line (C-g in this study) was moved from 80% along the line progressively closer toward the relay in order

to find the distance to fault at which the hardware relay at A issued a zone 1 trip. This was also supervised with the software relay models operating in parallel. The error in zone 1 reach was then calculated as:

$$Z_{1\ reach\ error} = \frac{Distance\ for\ Z_1\ Trip - Z_1\ Distance\ Setting}{Z_1\ Distance\ Setting} \times 100\% \quad (66)$$

This test, and calculation of the zone 1 reach error, was repeated for each assumed distance between the mutually coupled transmission lines. The error in the zone 1 reach of the relay at A was then plotted as a function of the distance between the transmission lines, with the results shown in Figure 4.12.

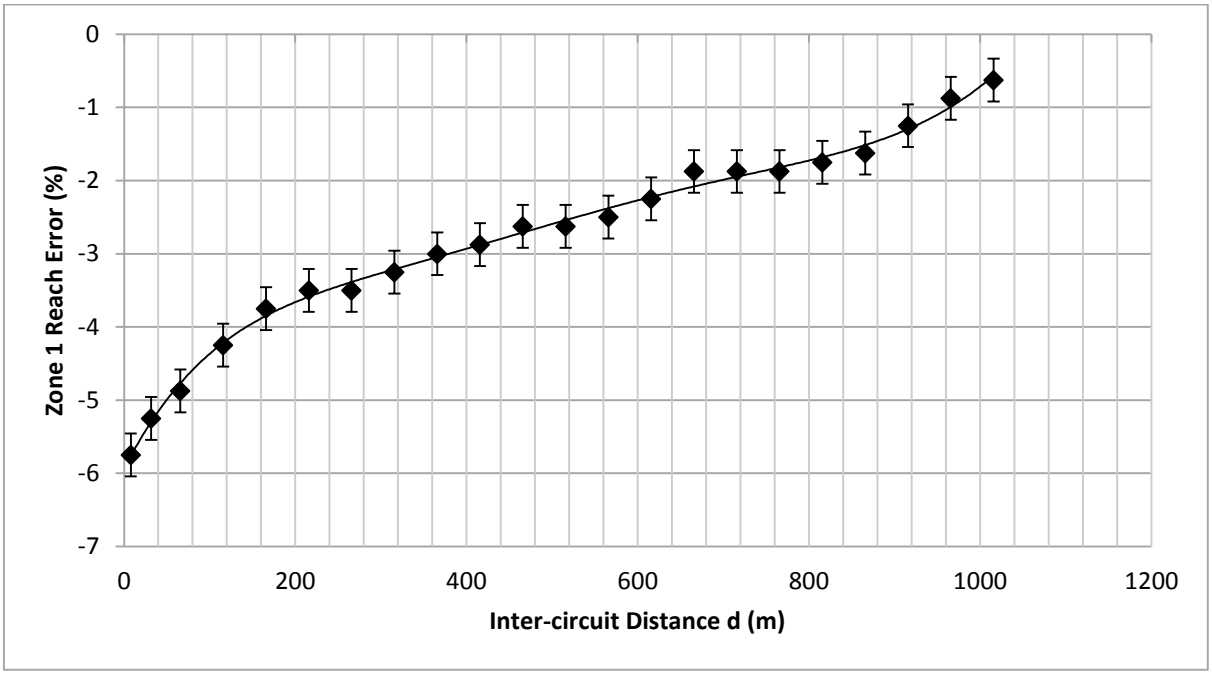

Figure 4.12: Error in zone 1 reach at relay A for different distances between the mutually coupled parallel transmission lines.

Figure 4.12 shows that, as expected, as the distance between the parallel transmission lines increases and the strength of the magnetic coupling effects between them diminishes, the error in the reach of the relay also decreases. From the results it can be seen that the maximum under-reach error of the relay for this test environment is around 6%. An error of this magnitude may prove not to be of significant concern for a fault at 80% along the line, but this will play an important factor in the decision making elements of relay for an end of line fault. The likelihood of the relay not providing guaranteed coverage of the transmission line it is protecting and the possibility of the relay not operating for a zone 2 fault therefore needs to be investigated.

To examine the impact of relay A under-reaching for an end of line fault, a C-g fault was placed at 100% of the line, with the distance between the transmission lines set to 37 meters (the actual distance between the lines in service). Figure 4.13 shows the impedance seen by the RSCAD model of the relay at A for a C-g fault at the remote end of the line.

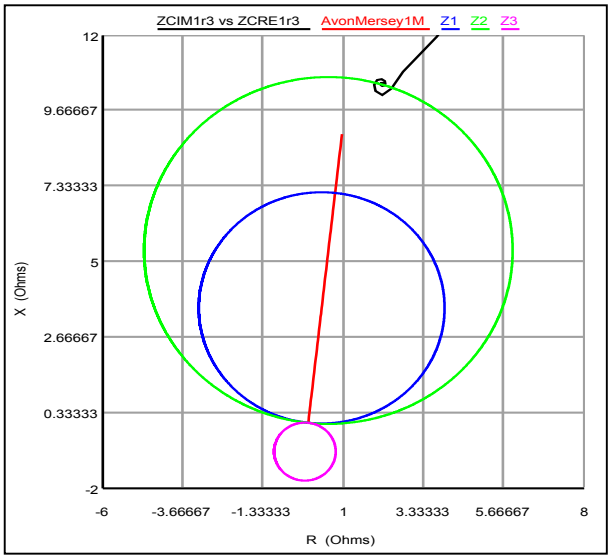

Figure 4.13: Impedance measured by the C phase ground element of the relay at A for a C-g fault located at 100% along the line AB with mutual coupling between the lines

Note for this fault scenario the impedance locus settles just outside the edge of zone 2, only entering zone 2 momentarily during the transient path of the locus. This result confirms that the extent of under-reaching of the relay at A due to mutual coupling is sufficiently large that it could potentially result in a lack of operation of the main protection scheme.

Since this case poses the possibility of non-operation of the protection scheme, it is therefore useful to include the results of testing this scenario with the full POTT protection scheme in operation and with the relays operating in closed loop (that is, the relays allowed to trip the breaker in the real-time model). The study was performed with a full POTT scheme implemented on both the hardware and software relays, both lines in service with the distance between the transmission lines set at 37 meters and a C-g fault applied at 100% of the line. Figures 4.14 and 4.15 show some of the results of this test.

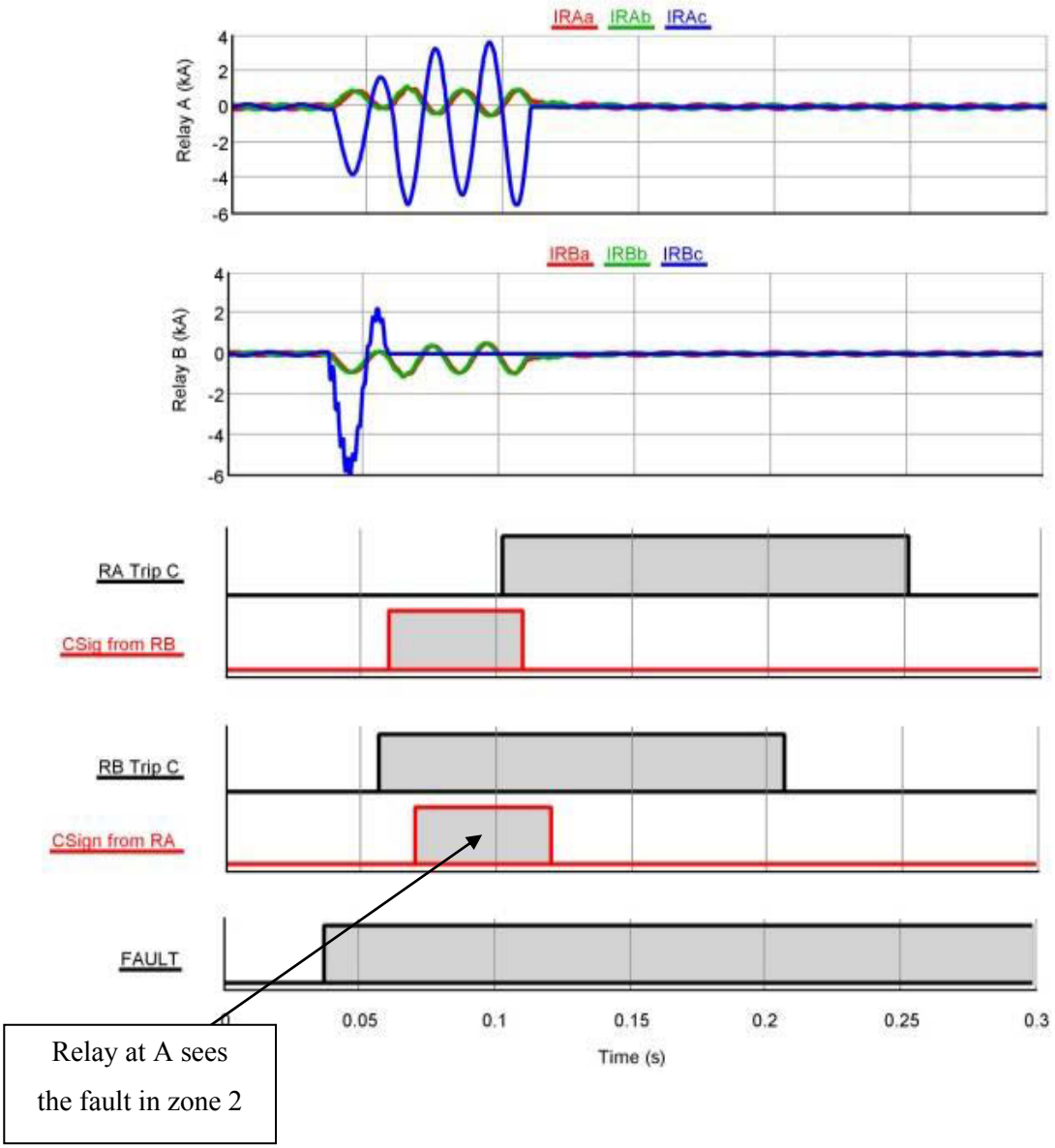

Figure 4.14: Response of the RSCAD software relays at A and B for a C-g fault at 100% of the line AB with a full POTT scheme

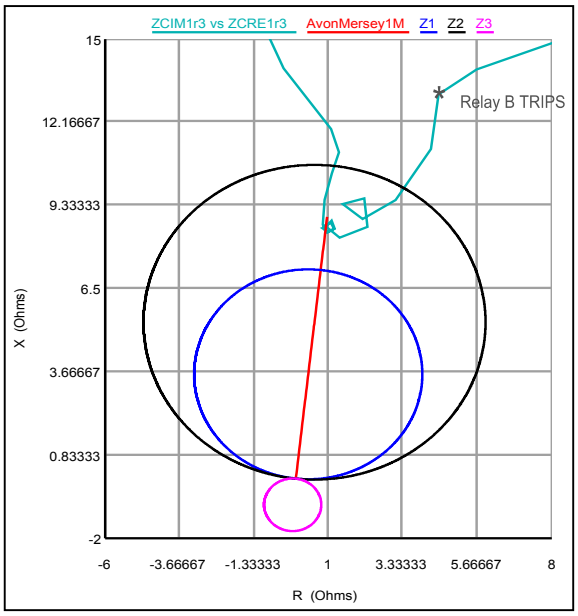

Figure 4.15: Impedance measured by the C phase ground element of the relay at A for a C-g fault located at 100% along the line AB with a full POTT scheme

The top part of Figure 4.14 shows the currents seen by the relays at A (first plot) and B (second plot) and the bottom part shows the digital signals from the relays A and B. The digital signals presented are:

- The trip signal from the relay at A (RA Trip C),
- The trip signal from relay at B (RB Trip C),
- The carrier signal sent from relay B to relay A indicating that the fault falls in zone 2 of relay B (CSig from RB)
- The carrier signal sent from relay A to relay B indicating that the fault falls in zone 2 of relay A (CSig from RA)
- The control signal used to apply the fault in the real time model (Fault)

From Figure 4.14, it appears as through the protection scheme operates as desired for an end of line fault in line AB. The relay at B issues an instantaneous trip and a permission to trip to the remote end. The relay at A issues a trip some time after it receives a permission to trip from the relay at B. Thus, at least in terms of the order of events, it appears as though the protection relays are tripping according to normal POTT logic for an end-of-line fault. However, upon closer inspection of the signals of Figure 4.14, note that the relay at A does not initially see the fault in zone 2 due to the effects of mutual coupling. The relay at A only issues its carrier signal after the relay at B has tripped, meaning that the relay at A only sees the fault in zone 2 after the current feeding the fault from the remote end has been cleared. Clearing the fault at the remote end has the effect of eliminating any zero sequence current in the parallel line, and hence the

mutual coupling effect. Once the remote end has tripped, conditions revert back to the base case (where no mutual coupling is present) and the relay at A is now able to see the fault in zone 2 since the zero sequence contribution from the adjacent line is now zero. Since relay A has already received permission to trip from the remote end and now sees the fault in its zone 2, relay A overrides its zone 2 time delay and trips.

Figure 4.15 is the impedance locus of the relay at A for the study discussed above. The impedance locus initially follows the same trajectory of the impedance locus in Figure 4.13 for the same fault condition, but in which the breakers were held closed. However, in Figure 4.15 at the instant that the relay at B trips, the impedance locus changes trajectory and moves towards the true location of the fault, at the end of the line characteristic. When the impedance locus moves to the true location of the fault in zone 2, the relay at A issues a trip and the impedance locus moves back out of the fault zone. Although the relays at both ends of the line are ultimately able to clear the fault in this case, concern still exists around the possibility of the breaker at B not opening for some reason, (trip circuit of trip coil failure, breaker failure, etc.) and the relay at A therefore not detecting the fault in zone 2 at all as a result of the effects of mutual coupling. Such a failure would lead to extensive damage of equipment if the back-up protection fails to clear this fault thus proving that mutual coupling between parallel transmission lines is indeed a phenomenon that needs to be taken into account in the design of distance protection settings.

4.3.3 One line out of service and grounded at both ends with mutual coupling between the lines

As mentioned in Chapter 2, there are other practical contingencies where the impact of mutual coupling on the distance protection relay is more extensive. One such contingency is when one of the parallel lines is taken out of service (for various reasons e.g. maintenance) and grounded on either end as in Figure 4.16. In the event of a ground fault on line AB, this fault can induce zero-sequence current in the coupled line because of the closed loop formed by the out of service line grounded at both ends.

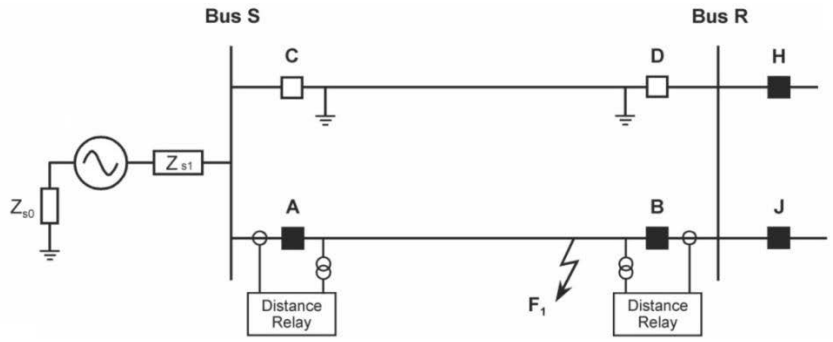

Figure 4.16: Double circuit transmission line system with one line out of service and grounded on either end

This scenario was investigated using the real time model of the study system with mutual coupling represented between the two transmission lines. As before, faults were placed on the system and the results of such were observed.

The results of Figure 4.17 show the impedance seen by the relay at A for the case where a C-g fault was placed at 80% along the transmission line AB while line CD is disconnected and grounded at each end. Figure 4.17 shows the impedance plot illustrating that the impedance locus settles to the left of the line characteristic, but now well inside the boundary of the zone 1 reach. The SEL 421 relay and the RSCAD distance relay model both issued a zone 1 trip for a fault at 81%. The relay at A over-reaches for a fault close to the receiving end when one line is taken out of service and grounded at both ends.

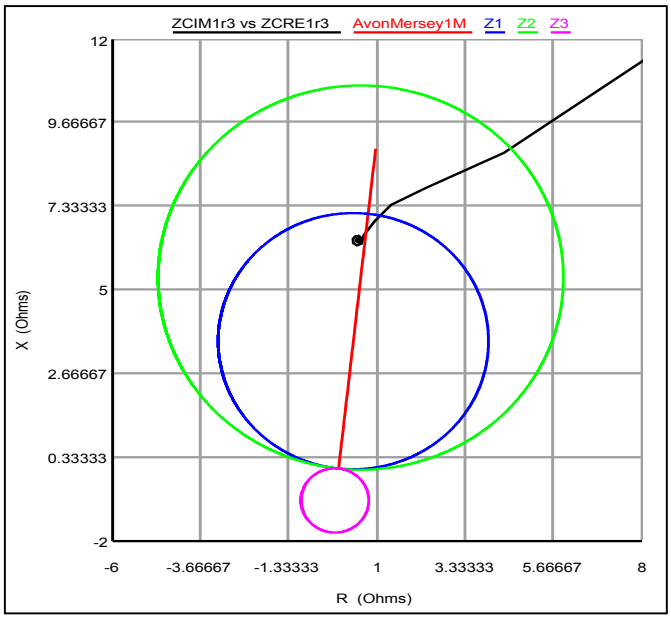

Figure 4.17: Impedance measured by C phase ground element of the relay at A for a C-g fault located at 80% along the line AB with line CD out of service and grounded at both ends

As undertaken previously for the case when both lines were in service, the extent of the over-reaching of the zone 1 element at A due to mutual coupling with the adjacent line out of service was investigated for different distances between the lines. For this operating condition where one transmission line is taken out of service and grounded at both ends the relay at A now under-reaches. To quantify the extent of the under-reaching of the zone 1 elements at A due to mutual coupling, the location of the fault at which zone 1 ceased to issue a trip was compared to the reach setting of zone 1 to calculate the reach error of zone 1 as shown below:

$$Z_{1\ reach\ error} = \frac{Distance\ for\ no\ Z_1\ trip - Z_1\ Distance\ Setting}{Z_1\ Distance\ Setting} \times 100\% \quad (67)$$

The distance between the midpoints of each tower was varied from 15.8 meters to 1000 meters so that the true extent of mutual coupling could be quantified as the separation between the transmission lines increases (and the influence of mutual coupling diminishes). At each assumed distance between the transmission lines, in order to calculate the error in zone 1 reach at A as a result of mutual coupling effects, the fault placed on the transmission lines (C-g in this study) was moved progressively away from the relay in order to find the distance to fault at which the hardware relay at A stopped issuing a zone 1 trip and began issuing a zone 2 trip. This was also supervised with the RSCAD software relay models in parallel. The error in zone 1 reach was then calculated as in eqn. (67).

This test, and calculation of the zone 1 reach error, was repeated for each assumed distance between the mutually coupled transmission lines. The error in the zone 1 reach of the relay at A was then plotted as a function of the distance between the transmission lines, with the results shown in Figure 4.18.

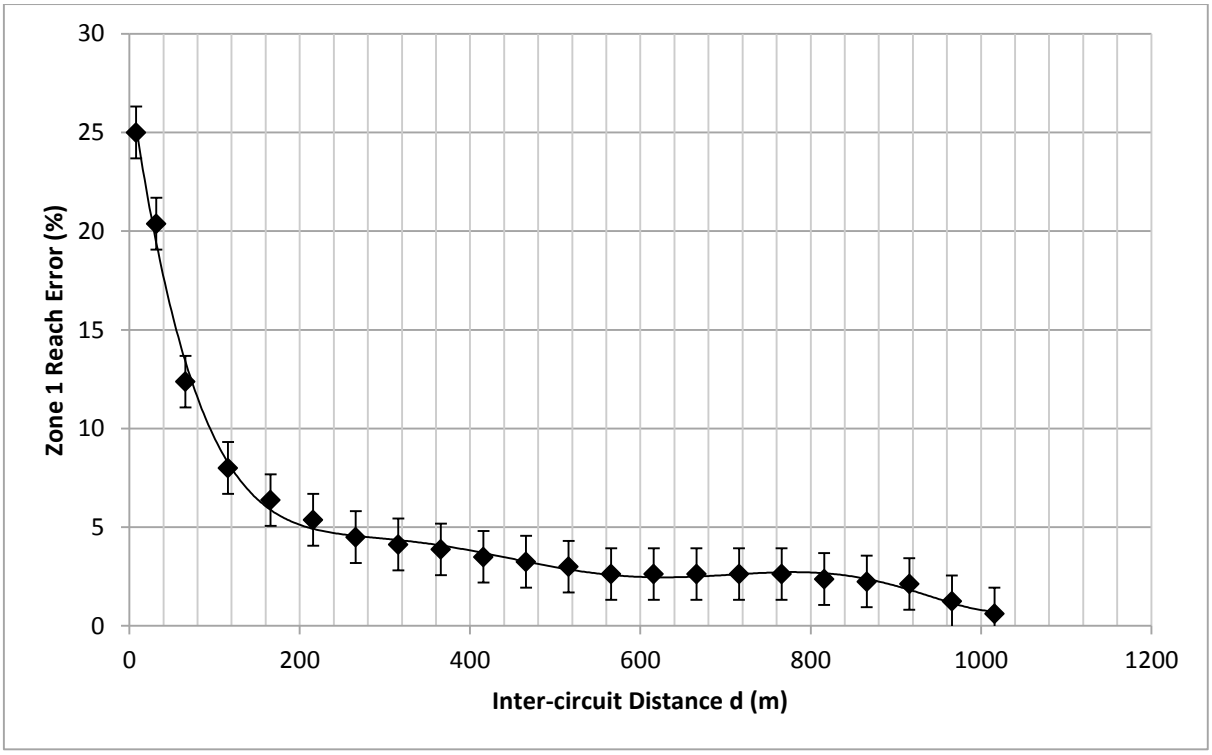

Figure 4.18: Error in zone 1 reach at relay A for different distances between the mutually-coupled parallel transmission lines when one line is taken out of service and grounded at both ends

Figure 4.18 shows that, as expected, as the distance between the parallel transmission lines increases and the strength of the magnetic coupling effects between them diminishes, the error in the reach of the relay also decreases. From the results it can be seen that the maximum over-

reach error of the relay for this test environment can reach as high as 25%. An error of this magnitude is significant when compared to the base case results and proves to be much more of a concern than the case where both transmission lines are in service. For the range of the typical distances between transmission lines used in South Africa (20-40 meters) the effect of mutual coupling on these transmission lines can reach as much as a 20% error in the zone 1 reach according to the graphical results in Figure 4.18. The concern here is that the zone 1 element is an unsupervised instantaneously tripping element. The consequence of this may result in the relay issuing an instantaneous trip for faults beyond the protected line which could lead to a serious threat of system security.

The results presented in Figure 4.18 show the potentially critical effects of mutual coupling on the distance protection scheme, enforcing the notion that mutual coupling should be taken into account when designing protection settings, not for just the known case where both lines are in service, but also for other practical operating conditions that the transmission lines are likely to be subjected to.

4.4. Mutual Coupling Compensation

Sections 4.2 and 4.3 have demonstrated the extent to which mutual coupling can affect the performance of distance protection schemes under practical operating conditions in a study system whose parameters are taken from actual utility transmission lines in South Africa. The findings in these sections demonstrate the practical importance of taking mutual coupling effects into consideration when designing the settings of distance protection schemes, even in cases where the parallel lines are tens of meters apart but in the same servitude. Chapter Two has reviewed various methods through which mutual coupling effects can be taken into account. The choice of which of these methods to use depends on the options available on the particular relay used and consideration for which method is most suitable for the protection scheme.

Once such method that was investigated and tested using the RSCAD software relays, was the use of current measurements from the parallel line as additional inputs to the relay. In some instances, the relay internally calculates the zero sequence currents of the parallel line from the three phase currents measured on the parallel line. This internally calculated zero sequence current is then used to adjust the measurements of the currents made on the line actually being protected. Once the currents measured on the transmission line being protected are adequately compensated, the short circuit impedance calculated by the relay and used by its zone decision making elements will in-turn be compensated for mutual coupling. In the real time simulation model, the generic RSCAD software relay model has a readymade function to calculate the protected transmission line's zero sequence current and this current is available as a value that

can be monitored by other RSCAD relay models protecting adjacent lines. The RSCAD relay model protecting a particular transmission line used this pre-calculated zero sequence value of current from the parallel transmission line to internally compensate for mutual coupling (i.e. the relay does not take a three phase current measurement from the parallel line but rather just the zero sequence current measurement from the parallel line).

Figure 4.19 shows the effectiveness of this method when both lines are in service. A phase C to ground fault was placed at 80% along transmission line A-B when both parallel transmission lines were in service, and the impedance plot for this case is shown on the left of Figure 4.19; the impedance plot shows the under-reaching effect at relay A for the fault under this particular operating condition as already seen earlier in Figure 4.10, with the impedance locus settling to the right of the transmission line characteristic and outside the boundary of the zone 1 reach. The impedance plot on the right of Figure 4.19 is the response of the RSCAD relay model to the same fault under the same operating condition but when mutual coupling compensation is used in the relays. The impedance locus now settles at the intersection of the transmission line characteristic and the edge of the boundary of the zone 1 reach. This compensated impedance locus now behaves similarly to the impedance locus in the base case study system in which no mutual coupling is present between the lines as seen in Figure 4.9. Hence, this method of compensating the relay for the effects of mutual coupling compensation is effective.

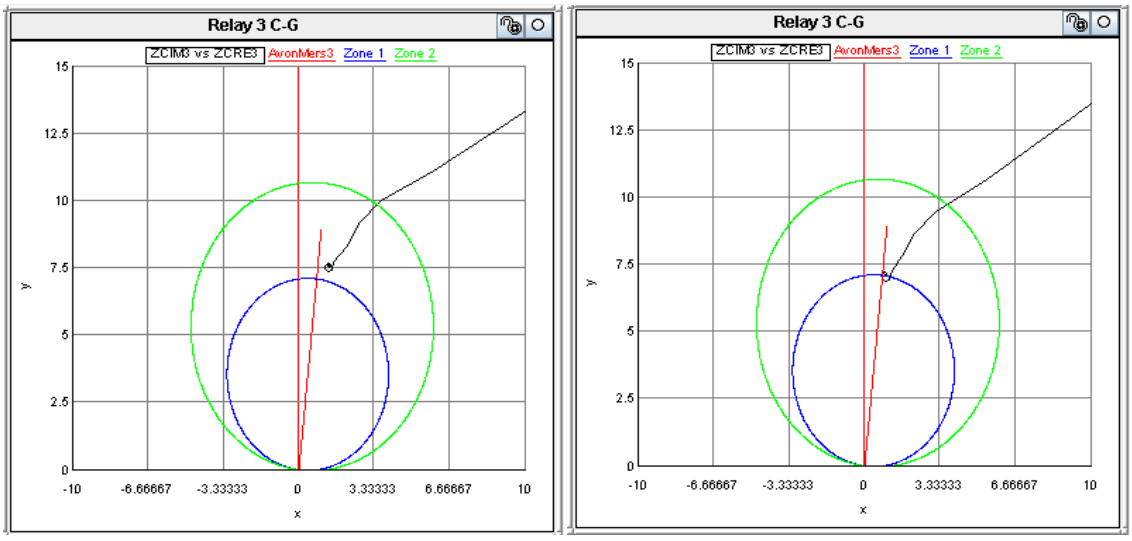

Figure 4.19: Impedance measured by the C phase ground element of the relay at A for a C-g fault located at 80% along the line AB when mutual coupling and without mutual coupling compensation (left) and with mutual coupling compensation (right) between the parallel lines is represented in the study: left plot – no compensation for mutual coupling used in relay settings; right plot – compensation for mutual coupling used in relay settings.

This form of compensation for the effects of mutual coupling within distance relays is not always permitted by utilities [11], as it cannot provide correct compensation in all circumstances and careful study has to be taken during the design of these settings to avoid further reach errors in the relay and hence nuisance tripping. Take for instance the case where one line is out of service and grounded at both ends. Under these conditions, the relay protecting the adjacent line receives no current inputs from the relays connected to the parallel line (since the line is out of service) and mutual coupling compensation is therefore not effective for this operating condition.

The most effective and safe approach is to adjust the reach of the protective zones according to the extent of mutual coupling for the particular line that is being protected. For different operating contingencies, e.g. one line out of service and grounded at both ends, alternative setting groups can be activated with uniquely adjusted zone reaches designed to suit that specific contingency.

4.5. Conclusion

Mutual coupling between transmission lines and the effect it has on distance protection schemes are well known phenomena and documentation of the mutual coupling effects on the impedance measurements made by distance protection relays has been carried out before. However, what has been shown in this chapter is that both the nature and the extent of the effects on distance relays of mutual coupling varies depending on both the fault scenarios encountered, as well as the particular operating conditions prevailing (lines out of service) and the design and spacing of the parallel lines themselves, which varies from installation to installation. In particular, this chapter has shown the extent to which mutual coupling can influence the protection relay measurements even in lines separated by several tens of meters: this is a common occurrence in transmission line servitudes in South Africa and such inter-line distances are often (mistakenly as evident from these results) considered to be sufficiently far apart that mutual coupling can be ignored.

In carrying out these studies this chapter has also further established the validity of the modelling of closely coupled parallel transmission lines on the Real Time Digital Simulator. Chapter 3 verified the correctness of the steady state phase impedances of coupled transmission line models obtained from RSCAD's TLINE support programme by direct comparison with hand derivations of these parameters from first principles. This chapter has now shown that the dynamic characteristics of the impedances measured on such lines by protection relays under fault conditions agree with the theory in the literature.

The difference in this study from those previously undertaken is the real time nature of the results and the ability to replicate actual power system parameters and operating conditions whilst the study system is connected to actual hardware relays in closed loop. This approach solidifies the research carried out in this chapter as it has been possible to gain insight into the actual performance of the protection system as it would operate in real life scenarios which is much more robust than anticipating how the protection scheme will react from effective studies, however detailed.

Although, as mentioned above, the theory behind the issues investigated in this chapter is not new, a further advantage of re-examining them on the particular platform used for these studies is that the RTDS real time simulators allow the detailed quantitative analysis to be carried out using actual protection relay hardware in a realistic closed-loop connection with the simulated plant, and with all the important inter-relay communication functions relevant to the study also included. In this way, not only can the impact of mutual coupling on a particular power system and a particular relay's algorithms be studied accurately, but also its impact on a full protection relay scheme can be evaluated directly on the physical protection relays.

The following chapter considers the impact of a second important practical issue in a real power system (untransposed transmission lines) and its effect on practical protection schemes using the RTDS simulator.

CHAPTER 5

THE IMPACT OF UNTRANSPOSED TRANSMISSION LINES ON THE DISTANCE PROTECTION SCHEME

As discussed in Chapter 2, a transposed transmission line is defined as one whose conductors exchange positions at regular intervals along the line such that each conductor occupies every position for equal distances. This transposition balances out the capacitive and inductive effects of the transmission line and balances the voltage drops in each phase. Due to the physical complexities that are present in transposed transmission systems, and the susceptibility to flashovers at transposition points, the use of untransposed transmission lines has become widespread [39]. The effect of this untransposed nature of a transmission line is investigated in this chapter, with specific attention being paid to its effect on the distance protection relay.

As with the issue of mutual coupling considered in previous chapters, to study the impact of untransposed transmission lines, one needs to understand, from first principles, how the untransposed nature of transmission line conductors influences its mathematical model. However, when considering the impact that transposition versus non-transposition of the lines has on the measurements made by distance protection relays, it is also important to understand how the phase-domain model of the transmission line appears in the positive, negative and zero sequence domain in which the relays operate. Hence, the chapter starts by revisiting the models of untransposed lines derived earlier from first principles in order to understand how they differ from transposed lines, and importantly, to be able to explain what effect they have on the impedances measured by a distance protection relay in the sequence domain.

5.1. Derivation from first principles

The phase impedance matrix of a transmission line is defined as follows:

$$Z = \begin{bmatrix} Z_{aa} & Z_{ab} & Z_{ac} \\ Z_{ba} & Z_{bb} & Z_{bc} \\ Z_{ca} & Z_{cb} & Z_{cc} \end{bmatrix} \tag{68}$$

Where the diagonal elements represent the self-impedance of each phase and the off-diagonal elements represent the mutual impedance between phases.

For perfectly transposed transmission lines, note that the self-impedance elements of each phase are equal, such that:

$$Z_s = Z_{aa} = Z_{bb} = Z_{cc} \tag{69}$$

The off-diagonal elements, which are the mutual impedances between phases, are also equal for a transposed line, such that:

$$Z_m = Z_{ab} = Z_{bc} = Z_{ac} \tag{70}$$

Hence, replacing each element in the impedance matrix with either Z_s or Z_m respectively one can obtain the phase impedance matrix for a perfectly transposed line as:

$$Z = \begin{bmatrix} Z_s & Z_m & Z_m \\ Z_m & Z_s & Z_m \\ Z_m & Z_m & Z_s \end{bmatrix} \tag{71}$$

The symmetrical component matrix can then be derived from the phase impedance matrix of the transposed transmission line [39]. The voltage drops due to the currents in each phase can be written as:

$$V_a = Z_{aa}I_a + Z_{ab}I_b + Z_{ac}I_c \tag{72}$$
$$V_b = Z_{ba}I_a + Z_{bb}I_b + Z_{bc}I_c \tag{73}$$
$$V_c = Z_{ca}I_a + Z_{cb}I_b + Z_{cc}I_c \tag{74}$$

Equations (72) to (74) can be written in matrix formation as:

$$\begin{bmatrix} V_a \\ V_b \\ V_c \end{bmatrix} = \begin{bmatrix} Z_{aa} & Z_{ab} & Z_{ac} \\ Z_{ba} & Z_{bb} & Z_{bc} \\ Z_{ca} & Z_{cb} & Z_{cc} \end{bmatrix} \begin{bmatrix} I_a \\ I_b \\ I_c \end{bmatrix} \tag{75}$$

The symmetrical components of the voltages are as follows:

$$V_{a0} = \frac{1}{3}(V_a + V_b + V_c) \tag{76}$$
$$V_{a1} = \frac{1}{3}(V_a + aV_b + a^2V_c) \tag{77}$$
$$V_{a2} = \frac{1}{3}(V_a + a^2V_b + aV_c) \tag{78}$$

Equations (76) to (78) can be written in matrix formation as:

$$\begin{bmatrix} V_{a0} \\ V_{a1} \\ V_{a2} \end{bmatrix} = \frac{1}{3}\begin{bmatrix} 1 & 1 & 1 \\ 1 & a & a^2 \\ 1 & a^2 & a \end{bmatrix}\begin{bmatrix} V_a \\ V_b \\ V_c \end{bmatrix} \quad (79)$$

In the same way the symmetrical component matrix of the line currents can be obtained:

$$I_{a0} = \frac{1}{3}(I_a + I_b + I_c) \quad (80)$$

$$I_{a1} = \frac{1}{3}(I_a + aI_b + a^2 I_c) \quad (81)$$

$$I_{a2} = \frac{1}{3}(I_a + a^2 I_b + aI_c) \quad (82)$$

$$\begin{bmatrix} I_{a0} \\ I_{a1} \\ I_{a2} \end{bmatrix} = \frac{1}{3}\begin{bmatrix} 1 & 1 & 1 \\ 1 & a & a^2 \\ 1 & a^2 & a \end{bmatrix}\begin{bmatrix} I_a \\ I_b \\ I_c \end{bmatrix} \quad (83)$$

Since $A = \frac{1}{3}\begin{bmatrix} 1 & 1 & 1 \\ 1 & a & a^2 \\ 1 & a^2 & a \end{bmatrix}$, the symmetrical component matrices of the line currents and voltage are:

$$I_{sym} = AI \quad (84)$$

$$V_{sym} = AV \quad (85)$$

Re-writing eqn. (75) in compact format matrix notation gives:

$$V = ZI \quad (86)$$

And solving for V and I and substituting in eqn. (86) one can obtain:

$$A^{-1}V_{sym} = ZA^{-1}I_{sym}$$

$$V_{sym} = (AZA^{-1})I_{sym} \quad (87)$$

Equation (87) can be re-written as:

$$V_{sym} = Z_{sym}I_{sym} \quad (88)$$

Where $Z_{sym} = AZA^{-1}$ (89)

From eqn. (71) and eqn. (87), the symmetrical component impedances for an ideally transposed transmission line can be calculated as follows:

$$Z_{sym} = \frac{1}{3}\begin{bmatrix}1 & 1 & 1\\ 1 & a & a^2\\ 1 & a^2 & a\end{bmatrix}\begin{bmatrix}Z_s & Z_m & Z_m\\ Z_m & Z_s & Z_m\\ Z_m & Z_m & Z_s\end{bmatrix}\begin{bmatrix}1 & 1 & 1\\ 1 & a^2 & a\\ 1 & a & a^2\end{bmatrix}$$

$$= \frac{1}{3}\begin{bmatrix}1 & 1 & 1\\ 1 & a & a^2\\ 1 & a^2 & a\end{bmatrix}\begin{bmatrix}(Z_s + 2Z_m) & (Z_s + a^2Z_m + aZ_m) & (Z_s + aZ_m + a^2Z_m)\\ (Z_s + 2Z_m) & (Z_m + a^2Z_s + aZ_m) & (Z_m + aZ_s + a^2Z_m)\\ (Z_s + 2Z_m) & (Z_m + a^2Z_m + aZ_s) & (Z_m + aZ_m + a^2Z_s)\end{bmatrix}$$

$$= \frac{1}{3}\begin{bmatrix}(3Z_s + 6Z_m) & 0 & 0\\ 0 & (3Z_s - 3Z_m) & 0\\ 0 & 0 & (3Z_s - 3Z_m)\end{bmatrix}$$

$$= \begin{bmatrix}(Z_s + 2Z_m) & 0 & 0\\ 0 & (Z_s - Z_m) & 0\\ 0 & 0 & (Z_s - Z_m)\end{bmatrix} \quad (90)$$

From the symmetrical component impedance matrix in eqn. (90) above, note that the diagonal elements represent the zero, positive and negative sequence components of the line impedance respectively, where:

$$Z_0 = Z_s + 2Z_m \quad (91)$$

$$Z_1 = Z_s - Z_m \quad (92)$$

$$Z_2 = Z_s - Z_m \quad (93)$$

The off-diagonal elements are zero indicating that there is no coupling between the positive, negative and zero sequence networks for a perfectly transposed transmission line [39].

For an untransposed transmission line, where the capacitive and inductive effects have not been balanced out, the mutual impedances between each phase are not equal, thus

$Z_{ab} \neq Z_{ac} \neq Z_{bc}$

However, in the untransposed line case it still holds that $Z_{ab} = Z_{ba}$, $Z_{ac} = Z_{ca}$ and $Z_{bc} = Z_{cb}$

Under these conditions if we calculate the matrix AZA^{-1} defined in eqn. (89), it will be seen that the impedance matrix Z_{sym} that emerges no longer has non-zero off-diagonal elements. In the case of distance protection relays that base their calculations only on positive sequence components and assume perfectly transposed lines, this could affect the accuracy of the relay measurements of fault loop impedances.

To investigate the likely impact of these effects, a three phase transmission line was studied, for both transposed and untransposed cases, and the results compared. Initially, for simplicity, a

three phase transmission line without ground wires was investigated, with conductor sag ignored, and with the transmission line ideally transposed. The parameters of this line are shown in Figures 5.1 and 5.2 below.

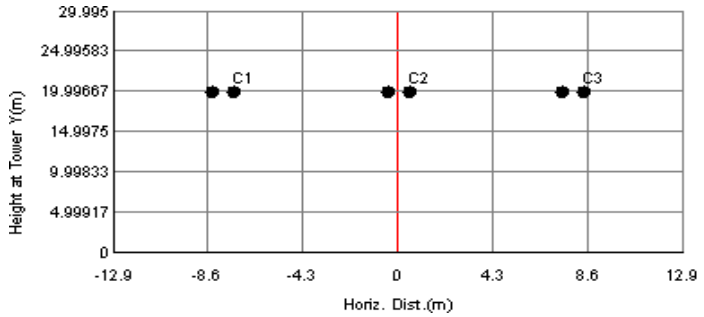

Figure 5.1: Transmission line geometry

Conductor Data

Bundle #	Bundle 1	Bundle 2	Bundle 3
Conductor Name	2Zebra50	2Zebra50	2Zebra50
Conductor Type (AC or DC)	AC	AC	AC
V(kV)(AC:L--L,rms/DC:L--G,pk)	275.0	275.0	275.0
V Phase(Deg)	0.0	-120.0	120.0
Line I(kA)(AC:rms/DC:pk)	1.284	1.284	1.284
Line I Phase(Deg)	20.0	-100.0	140.0
Num of Sub-Conductors	2	2	2
Sub-Cond Radius(cm)	1.155819	1.155819	1.155819
Sub-Cond Spacing(cm)	38.0	38.0	38.0
Horiz. Dist. X(m)	-7.9	0.0	7.9
Height at Tower Y(m)	19.995	19.995	19.995
Sag at Midspan(m)	0.0	0.0	0.0
DC Resistance per Sub-Cond(ohms/km)	0.0674	0.0674	0.0674

Line Length(km): 68.65 Ground Resistivity (ohm-m): 700.0

Figure 5.2: Transmission line phase conductor data

The theory presented previously in Chapter 3 showed how to derive the phase impedance matrix of such a line from first principles by hand calculation and it was verified that the phase impedance matrix obtained from the RSCAD TLINE programme matches that obtained by hand calculation from first principles in the most general case of an untransposed line. Thus, for the purposes of these analyses, and for simplicity, the RSCAD TLINE programme has been used to determine the phase impedance matrix of the example line chosen for this study directly, without starting from first principles in each case.

Initially, the line was assumed to be ideally transposed, and with this assumption the phase impedance matrix obtained from the RSCAD TLINE programme was as follows:

```
THE PHASE IMPEDANCE MATRIX ( Z(I,J) , OHMS/M ):
   0.82991E-04,0.67484E-03   0.48687E-04,0.35186E-03   0.48687E-04,0.35186E-03
   0.48687E-04,0.35186E-03   0.82991E-04,0.67484E-03   0.48687E-04,0.35186E-03
   0.48687E-04,0.35186E-03   0.48687E-04,0.35186E-03   0.82991E-04,0.67484E-03
```

Then, the next step is to calculate Z_{sym} using eqn. (89) and the numerical values in the phase impedance matrix above in which the impedances are given in ohms/meter, calculated at 50Hz. This calculation was done on the mathematical software package, MATLAB, with the following result:

$$Z_{sym} = AZA^{-1}$$

$$= \begin{bmatrix} 1.8036 \times 10^{-4} + j1.3785 \times 10^{-3} & 0 & 0 \\ 0 & 3.4304 \times 10^{-5} + j3.2298 \times 10^{-4} & 0 \\ 0 & 0 & 3.4304 \times 10^{-5} + j3.2298 \times 10^{-4} \end{bmatrix} \Omega/\mathrm{m}$$

The diagonal elements of the matrix Z_{sym} above denote the sequence components of the transmission line impedance (in this case in ohms/meter) as mentioned earlier, for the case when the transmission line is ideally transposed. Since there is no coupling between the positive negative and zero sequence elements, one can expect the impedance as seen by the relay to display a perfect symmetry between all three phases. If we apply a three phase fault at 100% of the line, we can expect to see the loci of the fault impedances measured by the distance protection relay settling at a point corresponding to 100% of the line impedance in each phase. This will be due the fact that the voltage drops seen by each phase are balanced.

Figure 5.3 shows the impedance loci of the distance protection relay in each phase for a three phase fault applied at the end of the line. Note that the impedance locus settles on a point at exactly 100% of the line characteristic in each phase as expected. One can deduce that the distance protection elements work correctly, as expected, when a transmission line is perfectly transposed.

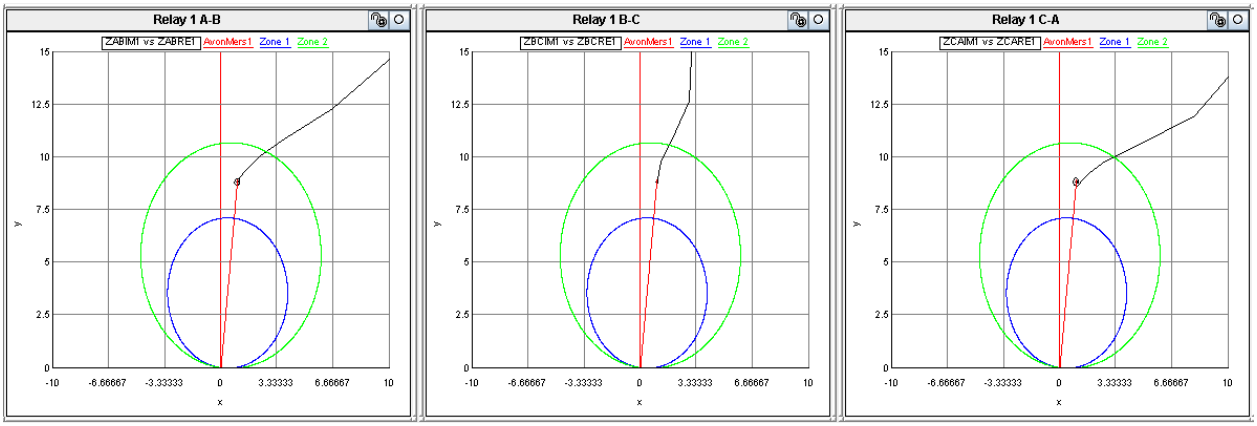

Figure 5.3: Impedance plots for a three phase, end of line fault on the ideally transposed transmission line with ground wires ignored

To investigate the performance of the relay's impedance measurements when the transmission line is untransposed, the phase impedance matrix of the same line is once again obtained from the output of the RSCAD TLINE software for this untransposed condition; the phase impedance matrix is as follows:

```
THE PHASE IMPEDANCE MATRIX ( Z(I,J) , OHMS/M ):
   0.82991E-04,0.67484E-03   0.48688E-04,0.36637E-03   0.48687E-04,0.32282E-03
   0.48688E-04,0.36637E-03   0.82991E-04,0.67484E-03   0.48688E-04,0.36637E-03
   0.48687E-04,0.32282E-03   0.48688E-04,0.36637E-03   0.82991E-04,0.67484E-03
```

Using MATLAB to calculate the symmetrical component impedance matrix $Z_{sym} = AZA^{-1}$ from the above phase impedance matrix now yields:

$$AZA^{-1}$$

$$= \begin{bmatrix} 1.80366 \times 10^{-4} + j1.37854 \times 10^{-3} & 1.25716 \times 10^{-5} - j7.25862 \times 10^{-5} & -1.25719 \times 10^{-5} - j7.25804 \times 10^{-6} \\ -1.25719 \times 10^{-5} - 7.25804 \times 10^{-6} & 3.43033 \times 10^{-5} + j3.22986 \times 10^{-4} & -2.51432 \times 10^{-5} + 1.45172 \times 10^{-5} \\ 1.25716 \times 10^{-5} - j7.25862 \times 10^{-6} & 2.51439 \times 10^{-5} + j1.45160 \times 10^{-5} & 3.43033 \times 10^{-5} + j3.22986 \times 10^{-4} \end{bmatrix} \Omega/_m$$

Note that the off-diagonal elements of Z_{sym} are now non-zero indicating that there exists coupling between the sequence networks for all fault types. If the relay uses sequence components and assumes an ideally transposed transmission line, one would expect to see errors in the impedance seen by the relay due to the different inductive and capacitive effects experienced by each phase and the associated unbalanced voltage drops experienced by each phase. The impedance loci seen by the distance protection relay for an end of line, three phase fault in the case of this untransposed line are shown in Figure 5.4. Note that for this three phase fault and this transmission line configuration, the effect of non-transposition is to cause the A-B phase and B-C phase loop impedance measurements to over-reach and the C-A phase loop impedance measurement to under-reach.

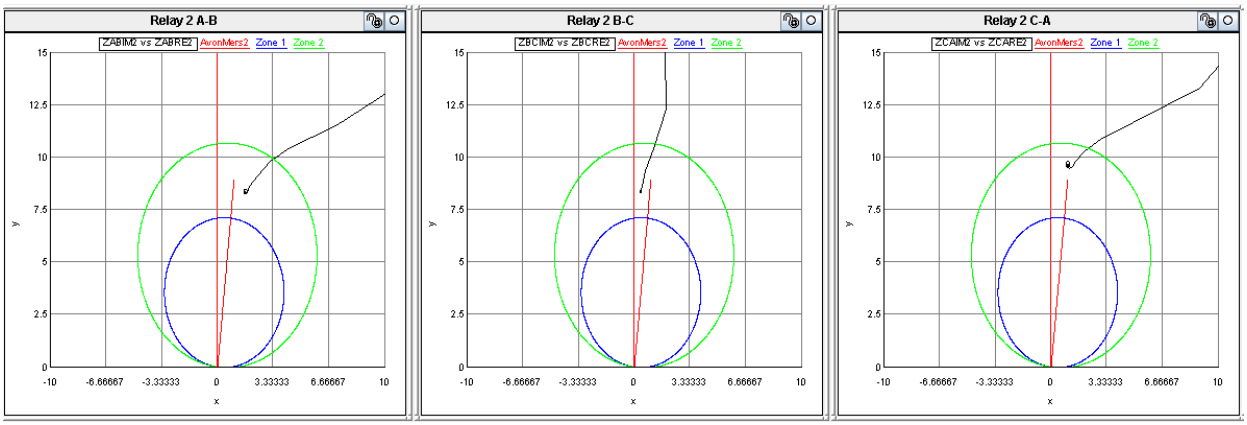

Figure 5.4: Impedance plots for a three phase, end of line fault on the untransposed transmission line with ground wires ignored

Next, the effects of the ground wires were considered, but with the effect of conductor sag still ignored such that the transmission line conductor geometry appears as in Figure 5.5: with the addition of ground wires to the transmission line model, a three phase fault was again applied at the end of line for both the untransposed and ideally transposed cases, and the impedances seen by the relay are shown for each of these tests in Figures 5.6 and 5.7. A comparison of Figures 5.3 and 5.6 shows that with the addition of the ground wires to the system, the impedances observed by the relay for the three-phase fault at the end of the ideally transposed line do not change significantly.

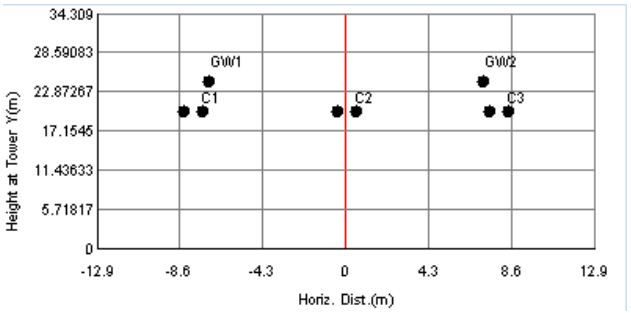

Figure 5.5: Conductor geometry

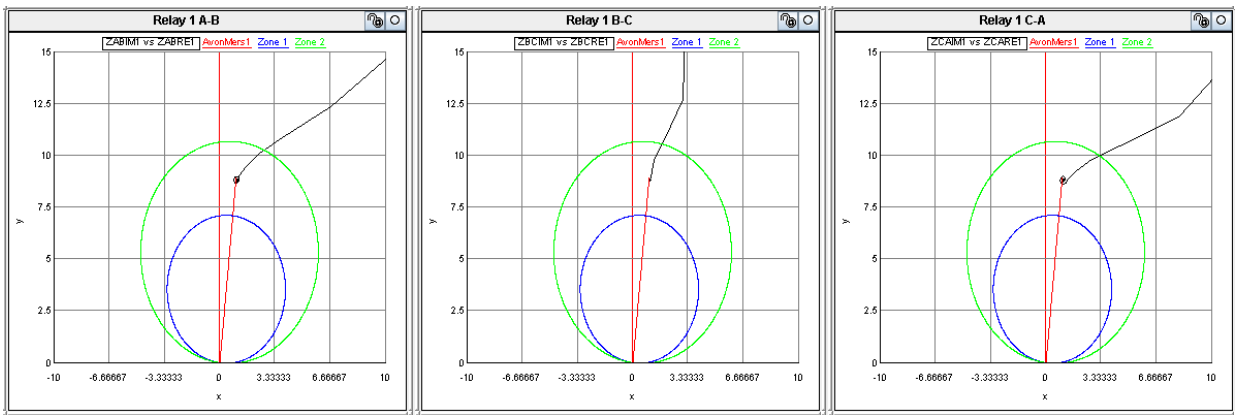

Figure 5.6: Impedance plots for a three phase, end of line fault on the transposed transmission line with ground wires

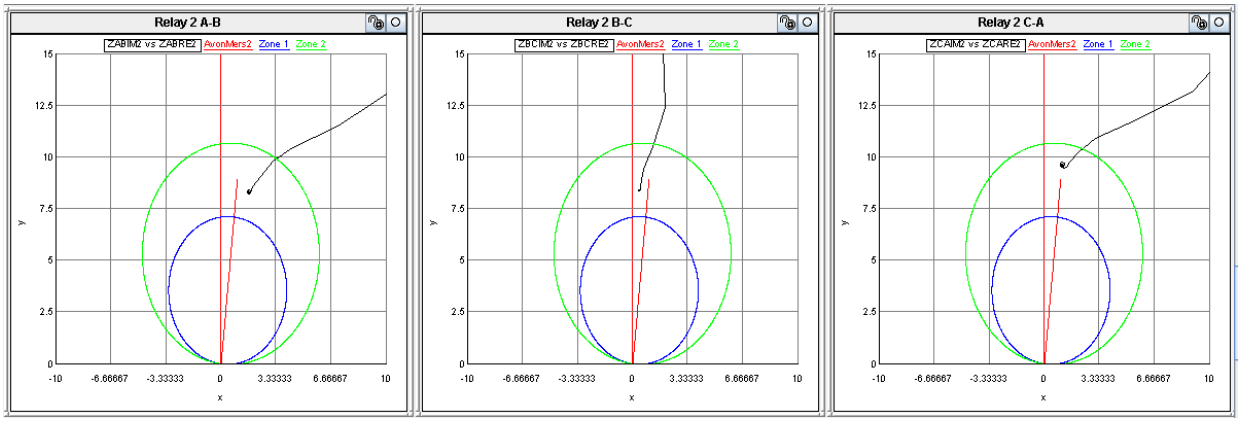

Figure 5.7: Impedance plots for a three phase, end of line fault on the untransposed transmission line with ground wires

Similarly, comparison of the results in Figures 5.4 and 5.7 shows that the impedances seen by the relay for a three phase fault at the end of the untransposed line do not change significantly with or without ground wires present. The results in Figures 5.3 to 5.7 thus confirm that the presence (or absence) of ground wires does not affect the impedances seen by the distance protection relay for phase faults, whether the transmission line is transposed or not.

Having shown that non-transposition of the transmission line affects the impedance measurements in the phase loops of a distance protection relay, it is necessary to quantify the extent of the errors seen in these measured impedances. Using the same transmission line data and parameters displayed previously, we first prove mathematically that there will exist no error in the impedance seen by the distance protection relay for an ideally transposed transmission line. For the case where the transmission line is perfectly transposed, and the effects of its ground wires are included, the phase impedance matrix of the transmission line obtained from the RSCAD TLINE programme is shown below:

```
THE PHASE IMPEDANCE MATRIX ( Z(I,J) , OHMS/M ):
   0.16620E-03,0.59072E-03   0.13031E-03,0.26816E-03   0.13031E-03,0.26816E-03
   0.13031E-03,0.26816E-03   0.16620E-03,0.59072E-03   0.13031E-03,0.26816E-03
   0.13031E-03,0.26816E-03   0.13031E-03,0.26816E-03   0.16620E-03,0.59072E-03
```

Converting from ohms/meter to ohms the phase impedance matrix for the full line length is:

$$Z = \begin{bmatrix} 11.4096 + j40.5529 & 8.9458 + j18.4092 & 8.9458 + j18.4092 \\ 8.9458 + j18.4092 & 11.4096 + j40.5529 & 8.9458 + j18.4092 \\ 8.9458 + j18.4092 & 8.9458 + j18.4092 & 11.4096 + j40.5529 \end{bmatrix} \Omega$$

To derive the sequence components from the above matrix, the formula $Z_{sym} = AZA^{-1}$ is applied to the above impedance matrix. The result is:

$$Z_{sym} = \begin{bmatrix} 29.3012 + j77.3713 & 0 & 0 \\ 0 & 2.4638 + j22.1437 & 0 \\ 0 & 0 & 2.4638 + j22.1437 \end{bmatrix} \Omega$$

The sequence components for the ideally transposed line impedances are therefore:

$$Z_0 = 29.3012 + j77.3713\Omega$$
$$Z_1 = 2.4638 + j22.1437\ \Omega$$
$$Z_2 = 2.4638 + j22.1437\ \Omega$$

Recall that for an ideally transposed transmission line:

$Z_{aa} = Z_{bb} = Z_{cc} = Z_m$ and,

$Z_{ab} = Z_{ac} = Z_{bc} = Z_{ba} = Z_{ca} = Z_{cb} = Z_m$

The positive sequence impedance seen by the relay in its A-B phase loop is then calculated from the voltages and currents measured by the relay from the following relationship:

$$Z_{1_{ab}} = \frac{V_a - V_b}{I_a - I_b} \tag{94}$$

From first principles, the voltages V_a and V_b are given by eqns. (72) and (73), which for the ideally transposed case, reduce to:

$$V_a = Z_s I_a + Z_m(I_b + I_c) \tag{95}$$
$$V_b = Z_s I_b + Z_m(I_a + I_c) \tag{96}$$

Substituting eqns. (95) and (96) in eqn. (94) gives:

$$Z_{1ab} = \frac{V_a - V_b}{I_a - I_b} = \frac{[Z_s I_a + Z_m(I_b + I_c)] - [Z_s I_b + Z_m(I_a + I_c)]}{I_a - I_b} \tag{97}$$

Since $I_a + I_b + I_c = 0$ we can substitute for I_c into eqn. (97).

$$\begin{aligned} Z_{1ab} &= \frac{Z_s I_a + Z_m(I_b + (-I_a - I_b)) - [Z_s I_b + Z_m(I_a + (-I_a - I_b))]}{I_a - I_b} \\ &= \frac{(Z_s - Z_m)I_a - [(Z_s - Z_m)I_b]}{I_a - I_b} \\ &= \frac{(Z_s - Z_m)(I_a - I_b)}{I_a - I_b} \\ &= (Z_s - Z_m) \end{aligned} \tag{98}$$

Thus, if one compares the positive sequence loop impedance Z_{1ab} that is measured by the relay in the phase A-B loop with the actual (known) positive sequence impedance parameter Z_1 of the line the result is:

$$\left|\frac{Z_{1ab}}{Z_1}\right| = \left|\frac{Z_s - Z_m}{Z_s - Z_m}\right| = 1 \tag{99}$$

In other words, in the ideally transposed case, the relay's measurement of the A-B phase loop impedance corresponds to the actual positive sequence impedance of the line.

Similarly, $Z_{1bc} = (Z_s - Z_m)$ and $Z_{1ca} = (Z_s - Z_m)$.

Therefore $\left|\frac{Z_{1bc}}{Z_1}\right| = 1$ and $\left|\frac{Z_{1ca}}{Z_1}\right| = 1$

The above analysis can be extended to the case of an untransposed transmission line, by carrying out a similar calculation of the impedance actually measured by the relay on an untransposed line, where $Z_{ab} \neq Z_{ac} \neq Z_{bc} \neq Z_{ba} \neq Z_{ca} \neq Z_{cb}$.

For the case where the transmission line is untransposed and the effects of its ground wires are included, the phase impedance matrix of the transmission line obtained from the TLINE programme is shown below:

```
THE PHASE IMPEDANCE MATRIX ( Z(I,J) , OHMS/M ):
   0.16676E-03,0.59054E-03   0.13082E-03,0.28255E-03   0.12930E-03,0.23937E-03
   0.13082E-03,0.28255E-03   0.16506E-03,0.59106E-03   0.13082E-03,0.28255E-03
   0.12930E-03,0.23937E-03   0.13082E-03,0.28255E-03   0.16676E-03,0.59054E-03
```

Converting from ohm/meter to ohms, the following phase impedance matrix for the full line length is obtained:

$$Z = \begin{bmatrix} 11.4481 + j40.5406 & 8.9808 + j19.3971 & 8.8764 + j16.4279 \\ 8.9808 + j19.3971 & 11.3314 + j40.5763 & 8.9808 + 19.3971 \\ 8.8764 + j16.4279 & 8.9808 + 19.3971 & 11.4481 + j40.5406 \end{bmatrix} \Omega$$

In the untransposed transmission line case, in order to compare the phase impedance measured by the relay with the actual positive sequence impedance of the line, it is necessary to consider a numerical example for a particular fault, rather than the generalised closed form analysis that was possible (and has just been presented) for the case of the ideally transposed line. To examine this, a three phase fault at the end of this untransposed transmission line is considered.

For a three phase fault at one end of this untransposed line, the phase currents that would be measured by the relay at the other end of this line can be calculated numerically from the line's phase impedance matrix Z, shown above, as follows:

$$\begin{bmatrix} I_a \\ I_b \\ I_c \end{bmatrix} = Z^{-1} \cdot \bar{V} \qquad (100)$$

where V is the vector of source voltages at the un-faulted end of the line.

For the untransposed line example being considered, the numerical values of the currents measured by the relay for the thee-phase fault at the end of the line were calculated by substituting the actual phase impedance matrix of the line shown above, and assuming balanced 275 kV source voltages follows:

$$Z = \begin{bmatrix} 11.4481 + j40.5406 & 8.9808 + j19.3971 & 8.8764 + j16.4279 \\ 8.9808 + j19.3971 & 11.3314 + j40.5763 & 8.9808 + 19.3971 \\ 8.8764 + j16.4279 & 8.9808 + 19.3971 & 11.4481 + j40.5406 \end{bmatrix} \Omega$$

$$Z^{-1} = \begin{bmatrix} 0.0048 - j0.0328 & -0.0006 + j0.0127 & 0.0004 + j0.0082 \\ -0.0006 + j0.0127 & 0.0049 - j0.0357 & -0.0006 + j0.0127 \\ 0.0004 + j0.0082 & -0.0006 + j0.0127 & 0.0048 - j0.0328 \end{bmatrix} \Omega$$

The currents were computed using MATLAB with the following equation:

$$\begin{bmatrix} I_a \\ I_b \\ I_c \end{bmatrix} = Z^{-1} \times \bar{V} = \begin{bmatrix} 2.406 - j11.666 \\ -11.281 + j5.356 \\ 10.367 + j6.290 \end{bmatrix} \times 10^3 A = \begin{bmatrix} 11.911\angle 78.35 \\ 12.488\angle 154.60 \\ 12.126\angle 31.25 \end{bmatrix} \times 10^3 \text{A}$$

The important observation to note in the above analysis is that the values of the currents now seen by the relay for the symmetrical three phase fault at the end of the line are unbalanced, as a consequence of the untransposed nature of the line.

As in the previous analysis of the ideally transposed line, for the particular fault being considered on this untransposed line, the impedance seen by the relay in its A-B phase loop can be determined from the relationship:

$$Z_{1ab} = \frac{V_a - V_b}{I_a - I_b}$$

However, in this case, substitutions of eqn. (72) and (73) which describe the volt drops in phases A and B of an untransposed line yield:

$$Z_{1ab} = \frac{V_a - V_b}{I_a - I_b}$$
$$= \frac{Z_s I_a + Z_{ab} I_b + Z_{ac} I_c - [Z_s I_b + Z_{ab} I_a + Z_{bc} I_c]}{I_a - I_b}$$

$$= \frac{Z_s I_a + Z_{ab} I_b + Z_{ac} I_c - Z_s I_b - Z_{ab} I_a - Z_{bc} I_c}{I_a - I_b}$$

$$= \frac{Z_s I_a + Z_{ab} I_b + Z_{ac}(-I_a - I_b) - Z_s I_b - Z_{ab} I_a - Z_{bc}(-I_a - I_b)}{I_a - I_b}$$

$$= \frac{Z_s I_a + Z_{ab} I_b - Z_{ac} I_a - Z_{ac} I_b - Z_s I_b - Z_{ab} I_a + Z_{bc} I_a + Z_{bc} I_b}{I_a - I_b}$$

$$= \frac{I_a(Z_s - Z_{ac} - Z_{ab} + Z_{bc}) + I_b(Z_{ab} - Z_{ac} - Z_s + Z_{bc})}{I_a - I_b}$$

Finally, substituting the actual values of I_a and I_b at the relay location that were determined by the direct numerical calculation of the fault current for this untransposed line example yields:

$$Z_{1ab} = 3.8729 + j20.9934 \quad \Omega$$

This value of the positive sequence impedance $Z_{1ab} = 3.8729 + j20.9934$ ohms measured by the relay for a fault at the far end of the untransposed line (100% of the line impedance in the fault loop) no longer corresponds to the value of the positive sequence impedance $Z_1 = 2.4638 + j22.1437$ ohms of the whole line for the ideal case where transposition is assumed.

Now, if one compares the relay's measurement of the impedance in the fault loop Z_{1ab} to the positive sequence impedance Z_1 in the loop, when the line is assumed to be ideally transposed one obtains:

$$\left|\frac{Z_{1ab}}{Z_1}\right| = \left|\frac{3.8729 + j20.9934}{2.4638 + j22.1437}\right| = 0.9581$$

In other words, for a three phase fault at the end of an untransposed line a relay that measures phase quantities calculates an impedance to the fault in the A-B loop that is smaller than the value of the positive sequence impedance of the line that is arrived at by assuming the line to be ideally transposed.

The results of the above analysis carried out by hand calculations using the phase impedance properties of the studied line agree qualitatively with the impedance locus actually measured by

the RSCAD software relay model for the same fault condition on the same transmission line case as seen in Figure 5.7.

From the equation shown at the end of the hand calculation above it can be seen that the magnitude of the loop impedance Z_{1ab} actually measured by the relay is smaller than the positive sequence impedance Z_1 of an ideally transposed line but the resistive component of Z_{1ab} is greater than that in this ideal impedance Z_1. This prediction is consistent with the locus of the impedance measured by the A-B phase element of the relay in the simulation study of Figure 5.7 which settles at a point to the right of the transmission line characteristic because of the extra measured resistance, but noticeably short of the true position of the fault at the end of the line impedance characteristic.

This analysis can be extended to calculate the impedance in the fault loop Z_{1bc} as follows:

$$Z_{1bc} = \frac{V_b - V_c}{I_b - I_c}$$

$$= \frac{Z_s I_b + Z_{ab} I_a + Z_{bc} I_b - [Z_s I_c + Z_{ac} I_a + Z_{bc} I_b]}{I_b - I_c}$$

$$= \frac{Z_s I_b + Z_{ab} I_a + Z_{bc} I_b - Z_s I_c - Z_{ac} I_a - Z_{bc} I_b}{I_b - I_c}$$

$$= \frac{Z_s I_b + Z_{ab}(-I_b - I_c) + Z_{bc} I_b - Z_s I_c - Z_{ac}(-I_b - I_c) - Z_{bc} I_b}{I_b - I_c}$$

$$= \frac{Z_s I_b - Z_{ab} I_b - Z_{ab} I_c + Z_{bc} I_b - Z_s I_c + Z_{ac} I_b + Z_{ac} I_c - Z_{bc} I_b}{I_b - I_c}$$

$$= \frac{I_b(Z_s - Z_{ab} - Z_{bc} + Z_{ac}) + I_c(Z_{bc} - Z_{ab} - Z_s + Z_{ac})}{I_b - I_c}$$

$$= 0.8157 + j21.1930 \quad \Omega$$

$$\left|\frac{Z_{1bc}}{Z_1}\right| = \left|\frac{0.8157 + j21.1930}{2.4638 + j22.1437}\right| = 0.9519$$

As in the case of the A-B measurement loop the results of the above analysis agree qualitatively with the characteristics of the impedance locus of this loop in the simulation study of Figure 5.7. As with the A-B impedance measurement loop, the analysis predicts that the B-C loop will actually measure a smaller magnitude of impedance for an end of line fault than the positive sequence impedance Z_1 of an ideally transposed line as well as measuring a smaller resistive component of this impedance. Both of these characteristics are confirmed in the results of Figure 5.7 (middle plot) which shows the locus of the impedance measured by the relay's B-C element for the fault at the end of an untransposed line lying to the left of the ideal line characteristic (smaller resistance than Z_1) and short of the end of the ideal Z_1 line characteristic.

Finally the analysis can be extended to calculate the impedance in the fault loop Z_{1ca} as follows:

$$Z_{1ca} = \frac{V_c - V_a}{I_c - I_a}$$

$$= \frac{Z_s I_c + Z_{ac} I_a + Z_{bc} I_b - [Z_s I_a + Z_{ab} I_b + Z_{ac} I_c]}{I_c - I_a}$$

$$= \frac{Z_s I_c + Z_{ac} I_a + Z_{bc} I_b - Z_s I_a - Z_{ab} I_b - Z_{ac} I_c}{I_c - I_a}$$

$$= \frac{Z_s I_c + Z_{ac} I_a + Z_{bc}(-I_c - I_a) - Z_s I_a - Z_{ab}(-I_c - I_a) - Z_{ac} I_c}{I_c - I_a}$$

$$= \frac{Z_s I_c + Z_{ac} I_a - Z_{bc} I_c - Z_{bc} I_a - Z_s I_a + Z_{ab} I_c + Z_{ab} I_a - Z_{ac} I_c}{I_c - I_a}$$

$$= \frac{I_c(Z_s + Z_{ab} - Z_{bc} - Z_{ac}) + I_a(Z_{ac} - Z_{bc} - Z_s + Z_{ab})}{I_c - I_a}$$

$$= 2.5716 + j24.1126 \quad \Omega$$

$$\left|\frac{Z_{1ca}}{Z_1}\right| = \left|\frac{2.5716 + j24.1126}{2.4638 + j22.1437}\right| = 1.0884$$

Once again, the characteristics of the impedance measured by the C-A loop predicted in the above analysis agree qualitatively with the results of the simulation study in Figure 5.7. The analysis predicts that the C-A loop will actually measure a larger magnitude of impedance for

an end of line fault than the positive sequence impedance Z_1 of an ideally transposed line, but with a resistive component slightly smaller than that of Z_1. Both of these characteristics are confirmed on the results of Figure 5.7 (right hand plot) which shows the locus of the impedance measured by the relay's C-A element for the fault at the end of an untransposed line lying beyond the end of, and slightly to the left of the Z_1 line characteristic.

The previous discussions have shown that the nature of the errors that occur in the individual phase impedance measurement elements of a relay for phase faults on an untransposed line agree qualitatively with the predictions from hand calculations presented for the specific case of a three phase fault at the end of the line. The analysis was then taken further by calculating the numerical value of the errors in the three impedance loop measurements of the RSCAD software relays by determining the R and X coordinates of the end points of the loci in Figure 5.7 and dividing these by the R and X coordinates of the end point of the positive sequence line impedance characteristic Z_1 of the ideally-transposed line in each case.

Using this approach, the three measurement elements of the RSCAD relay model in the simulated results in Figure 5.7 were found to have the following quantitative errors:

- The phase A-B element of the relay over reaches by 4.53%
- The phase B-C element of the relay over reaches by 5.28%
- The phase C-A element of the relay under reaches by 8.85%

These quantitative errors agree closely with the errors predicted by the hand calculation analysis carried out earlier, which can be re-expressed in percentage terms as follows:

- The predicted error of the phase A-B element of the relay will be to over reach by 4.19%
- The predicted error of the phase B-C element of the relay will be to over reach by 4.81%
- The predicted error of the phase C-A element of the relay will be to under reach by 8.84%

This quantitative error analysis for the end of line, three phase fault is summarised as case number 2 in Table 5.1 below; for reference comparison the same error analysis was done on the relay impedance loop measurements for a simulation study of an ideally transposed line, and Table 5.1 confirms that for these conditions in case 2 (three phase fault at 100% line length) the errors in an ideally transposed line are, as expected, negligible.

Similar studies were then carried out for a range of different fault types, and fault locations, and in each case the errors in the impedance measurement loops were quantified from detailed real time simulation studies using the RSCAD software relay model and compared for both untransposed and ideally transposed line conditions. The results of these additional studies are also shown in Table 5.1.

As explained previously, the percentage errors in the impedance measurement loop values in Table 5.1 were calculated by determining the R and X coordinates of the end points of the relay's actual measured phase impedance loci in the simulated results for each fault case, and dividing these by the R and X coordinates corresponding to the percentage distance of the fault (80%, 100% or 120%) along the positive sequence impedance characteristic of an ideally-transposed line in each case.

Table 5.1: Comparison of impedance loop measurement errors in RSCAD's software distance relay model for ideally transposed versus untransposed transmission line. Case 1; no ground wires, Case 2 to 13 with ground wires.

Case No.	Fault Type	Fault location (%)	Relay Impedance Measurement Loop	Impedance Measurement Loop Error (%)	
				Ideally Transposed	Untransposed
1	3 phase	100	A-B	0.13	4.11
			B-C	0.14	5.62
			C-A	0.16	8.98
2	3 phase	100	A-B	0.09	4.53
			B-C	0.09	5.28
			C-A	0.11	8.85
3	A-B	100	A-B	0.13	4.62
4	B-C	100	B-C	0.12	4.62
5	C-A	100	C-A	0.12	8.89
6	3 phase	80	A-B	0.34	4.17
			B-C	0.43	4.91
			C-A	0.42	9.24
7	A-B	80	A-B	0.39	4.24
8	B-C	80	B-C	0.39	4.24
9	C-A	80	C-A	0.44	9.25
10	3 phase	120	A-B	0.27	4.15
			B-C	0.30	5.01
			C-A	0.35	9.18
11	A-B	120	A-B	0.32	4.03
12	B-C	120	B-C	0.31	4.07
13	C-A	120	C-A	0.35	9.16

The results presented in Table 5.1 are included here to show the consistency in the errors of each phase impedance measurement loop, as a result of non-transposition, for a variety of fault locations and fault types. The percentage errors for the phase A-B and B-C impedance loops are

approximately 4.5% and the percentage error for the phase C-A impedance loops is approximately 9% in all cases. Furthermore, in all the cases displayed in Table 5.1 (as well as those not presented in this table, but identified in the testing phases during this part of the research studies) the worst-case relay impedance measurement errors were seen in the C-A impedance loops.

5.2. Testing phase element reach errors using hardware relays

Once the extent of the impact of untransposed transmission lines on a software distance protection relay's phase impedance measurement loops had been ascertained and verified against hand calculations, the impact of this was further verified using the SEL 421 hardware relay, with the RSCAD software relay's impedance plots then used solely as a monitoring tool.

When examining the reach errors in the hardware relay, the same case considered in the detailed hand calculation example of the previous section was considered (a fault at 100% of the untransposed transmission line with ground wires present), and the SEL 421 hardware relay was tested with a hypothetical zone reach setting of 100%. To monitor the performance of this hypothetical zone with 100% reach within the real time simulation, an additional distance protection zone with a 100% reach was also incorporated into the generic RSCAD distance relay models. When testing the hardware relay, the reach errors were determined in a similar way to the method used in Chapter 4, eqn. (66) and (67), where the fault placed on the transmission line was moved from the nominal study point on the line (100% of the line length in this study) progressively closer toward, or further away from, the relay in order to find the actual location of the fault at which the relay's hypothetical 100% reaching zone issues, or stops issuing, a trip.

Previous work has established that non-transposition of a transmission line only introduces errors within the phase impedance elements of a distance relay, so testing of each phase element of the SEL 421 relay was carried out separately to determine the reach error for that particular fault loop. The tests adopted a similar approach to that used to study the impact of mutual coupling in Chapter 4, with the DRAFT model for the study set up so as to include two distinct distributed-parameter modelling representations of the same transmission system: in one of these the transmission system was represented using ideally transposed transmission line models and in the other using models of an untransposed transmission line. These two scenarios were run concurrently to ensure reliability of the results obtained and to have the base case (the ideally transposed transmission line) run in the same environment, to compare with.

For an A-B fault at 100% of the transmission line, the A-B impedance plot obtained from RSCAD's software relay model is shown in Figure 5.8.

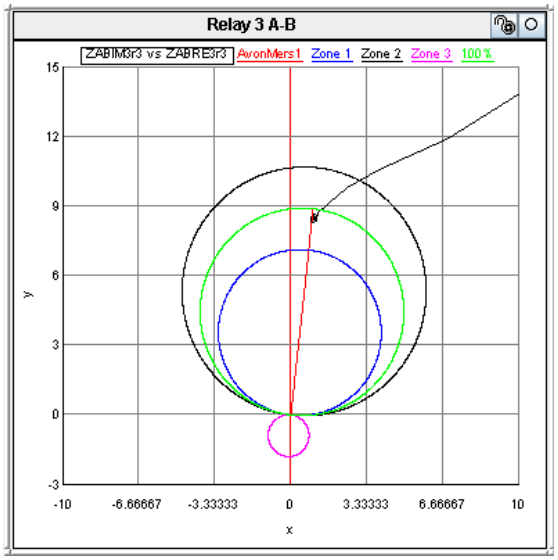

Figure 5.8: Impedance plot for a phase A-B end of line fault on an untransposed transmission line with ground wires, showing the additional, hypothetical 100% reaching zone used for testing purposes

From the impedance locus in Figure 5.8, it can be seen that the relay's A-B impedance measurement loop over reaches, with the impedance locus settling within the boundary of the 100% zone. The fault was thereafter moved progressively further away from the relay until the SEL 421 hardware relay stopped issuing a 100% zone trip, with this boundary point found to occur at approximately 104%. The hardware relay protecting the untransposed transmission line stopped issuing a 100% zone trip for the A-B phase fault at 104.1%, and it issued a zone 2 trip only for this fault at 104.2%. This boundary point was also tested for the RSCAD software relays which responded in the exact same way.

For a B-C fault at 100% of the transmission line, the B-C impedance plot obtained from RSCAD's software relay model is shown in Figure 5.9.

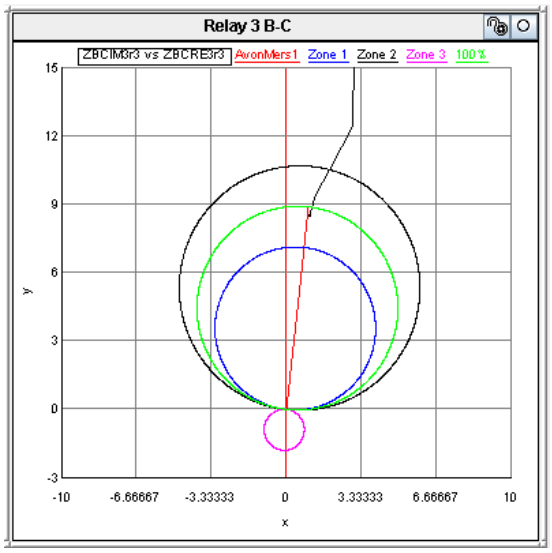

Figure 5.9: Impedance plot for a phase B-C end of line fault on an untransposed transmission line with ground wires, showing the additional, hypothetical 100% reaching zone used for testing purposes

From the impedance locus in Figure 5.9, the relay's B-C measurement loop also over reaches with the impedance locus settling within the boundary of the 100% zone in the same manner as seen for the A-B fault. The fault was again moved progressively further away from the relay until the SEL 421 hardware relay stopped issuing a 100% zone trip. This boundary point again occurred at approximately 104%. The hardware relay protecting the untransposed transmission line stopped issuing a 100% zone trip for the B-C phase fault at 104.2%, and it issued a zone 2 trip only for this fault at 104.3%. This boundary point was again tested for the RSCAD software relays which responded in the exact same way.

For a C-A fault at 100% of the transmission line, the C-A impedance plot obtained from RSCAD's software relay model is shown in Figure 5.10:

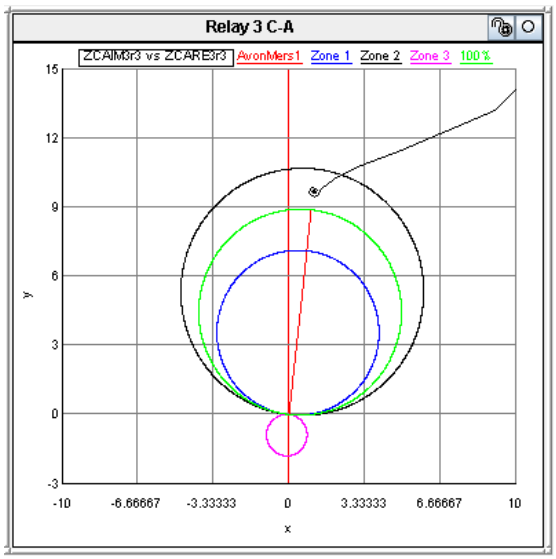

Figure 5.10: Impedance plot for a phase C-A end of line fault on an untransposed transmission line with ground wires, showing the additional, hypothetical 100% reaching zone used for testing purposes.

From the impedance locus in Figure 5.10, the relay's C-A measurement loop under reaches, with the impedance locus now settling outside the boundary of the 100% zone. The error in the reach of the C-A phase impedance measurement element was ascertained by moving the fault progressively toward the relay until the SEL 421 hardware relay began to issue a 100% zone trip. This boundary point was found to occur at approximately 92%. The hardware relay protecting the untransposed transmission line stopped issuing a 100% zone trip for the C-A phase fault at 91.5%, and it issued a zone 2 trip at 91.6%. This boundary point was again tested for the RSCAD software relays which once again were found to respond in the exact same way.

Testing of the SEL 421 hardware relay in conjunction with the RSCAD software relay provides further confirmation of the results presented earlier in this chapter: those earlier analyses, carried out from first principles via hand calculations, have subsequently been verified with both the RSCAD software relay (which is a generic distance protection relay model) as well as an actual hardware SEL 421 relay. Now that the extent to which non-transposition of transmission lines causes measurement errors in distance relays has been quantified and verified for a variety of fault locations and fault types, the impact of such errors on a full, permissive distance protection scheme is examined and discussed.

5.3. The effect of untransposed transmission lines on permissive distance protection trip schemes

In cases where permissive tripping schemes are used for the protection of untransposed transmission lines, further investigation of the effect of the errors seen by the impedance relays, due to the untransposed nature of the lines, must be made. The areas of concern for a permissive tripping scheme are those near the extremities of the zones of protection. Typically, zone 1 is set to cover 80% of the transmission line with instantaneous unsupervised tripping, and zone 2 is set to cover 120% of the transmission line with time delayed and/or supervised tripping to allow the breaker closest to the fault to open first. The reason for using these specific zone reaches is to cater for the accumulation of worst case errors that could be present in the power system, as explained in Chapter 2. For the purposes of this investigation these typical reaches will be used for both zones 1 and 2. As was the case in Chapter 4, a permissive over reaching transfer trip scheme will be considered in this study. To investigate the effect of the untransposed lines on the permissive tripping scheme, focus is placed on the ends of the various zones of protection.

Earlier results have established that the worst case fault scenario is a C-A phase fault. This will therefore be the fault to be investigated as this scenario will have the greatest impact on the POTT scheme. Examining the impact on the zone 2 elements first, where the reach is set to 120%, and applying a phase C-A fault at 120% of the line, the impedance plot for the phase C-A impedance loops of the RSCAD software relays is shown in Figure 5.11.

The impedance plot on the left of Figure 5.11 shows the response of a relay (relay 1) protecting a transmission line in which the phases are ideally transposed, while the plot on the right of Figure 5.11 shows the response of a relay (relay 3) protecting an untransposed transmission line for the fault considered. The two impedance plots are displayed side by side so that a clear comparison can be made, for the same fault, of the ideal case against the case where the transmission line is untransposed.

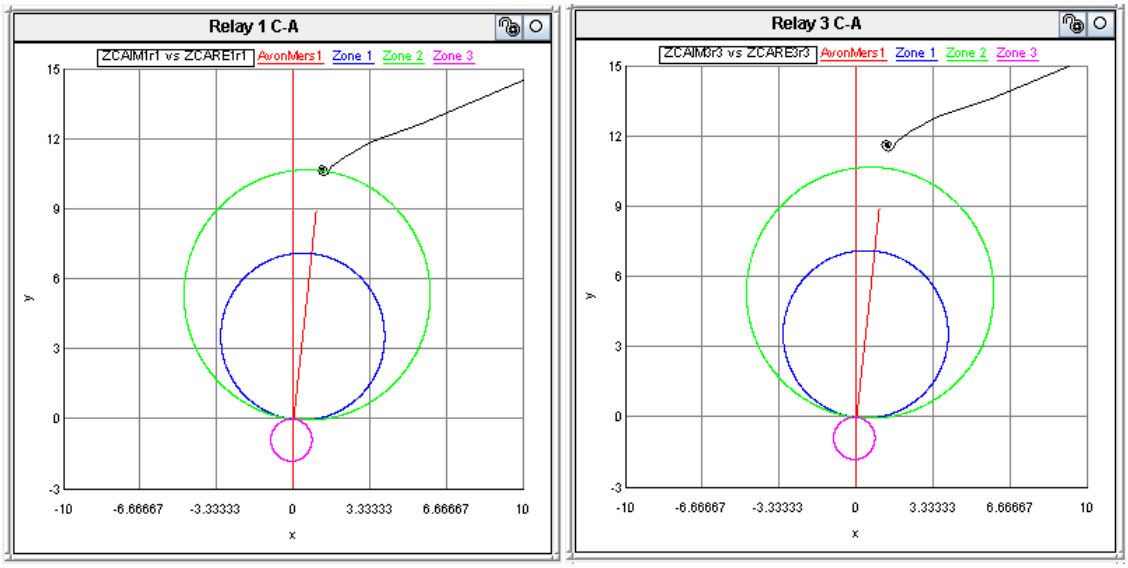

Figure 5.11: Impedance plots for a phase C-A fault at 120% of a line with ground wires: left plot – Relay 1 protecting the ideally transposed line; right plot – Relay 3 protecting the untransposed line

From the impedance plots in Figure 5.11, it can be noted that for an untransposed line with a fault at 120% of the line, protection of the transmission line may possibly no longer be achieved. The results show that the fault will not be seen by the distance protection relay's zone 2 which will therefore not issue a trip. In the event of the zone 1 element of the relay protecting this portion of the line being out of service for some reason, or the breaker being physically stuck, the fault will remain on the system until the secondary backup protection operates. This secondary backup protection is usually provided for by means of IDMT overcurrent relays which (depending on the setting) could take as long as 3 seconds [60] to clear the fault on a typical 275 kV network. This would lead to permanent damage of the equipment and extended outage time to repair damaged plant.

Where permissive overreaching transfer trip schemes are concerned, the ability of a distance protection relay to detect a fault in zone 2 is critical, since when a relay in a permissive scheme receives a permission to trip from its remote-end relay, a trip command cannot be issued since it is facilitated by a zone 2 element pick up. Reliability and selectivity of the protection scheme is compromised.

This issue was investigated further by applying a phase C-A fault well inside the zone 2 reach, at 112.5% of the line. The impedance plots from the RSCAD software relay for this test are displayed in Figure 5.12.

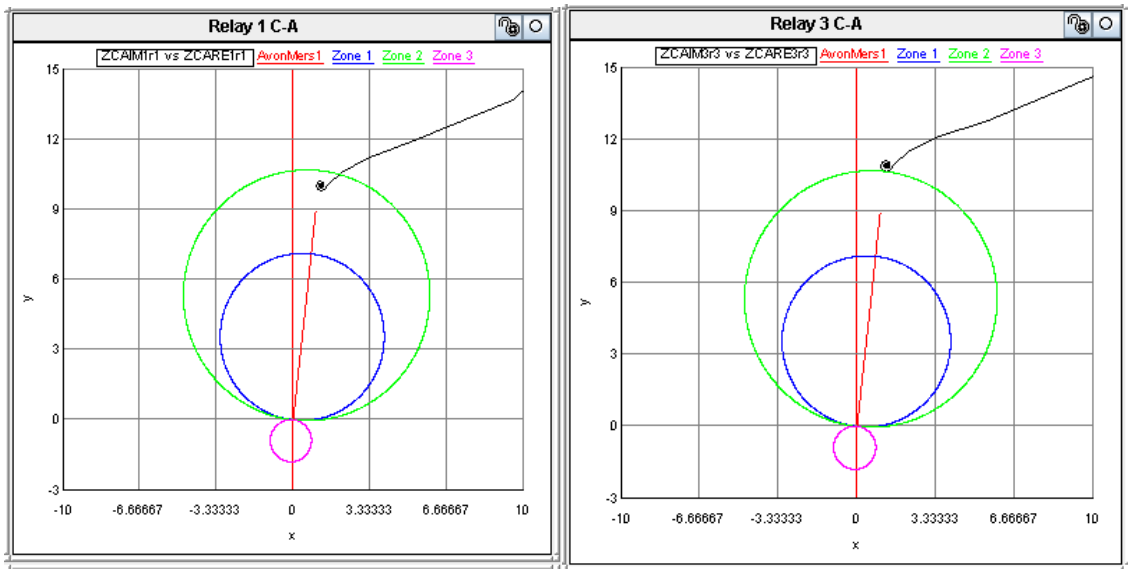

Figure 5.12: Impedance plots for a phase C-A fault at 112.5% of a line with ground wires: left plot – Relay 1 protecting the ideally transposed line; right plot – Relay 3 protecting the untransposed line

From the impedance plot in Figure 5.12, note that even for a fault that is actually 8.5% inside the boundary of the zone 2 reach, the relay protecting the untransposed transmission line still under-reaches, with the impedance locus settling just outside the zone 2 boundary. In order to look further into the relay operation, the start contacts of the two relays in Figure 5.12 are shown in Figure 5.13.

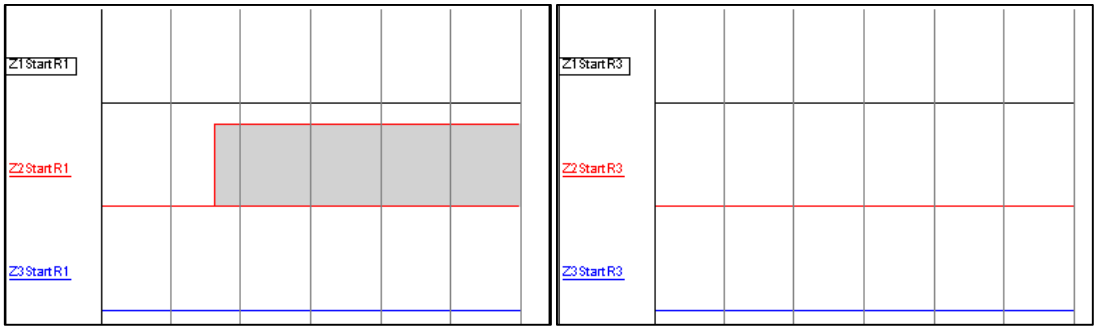

Figure 5.13: Start signals for the zones of Relay 1 and Relay 3 for the phase C-A fault at 112.5% of the line in the study of Figure 5.12

The signal labels in Figure 5.13 are defined as follows:

Z1StartR1- Zone 1 start signal for the sending-end Relay 1 protecting the ideally-transposed transmission line

Z2StartR1- Zone 2 start signal for the sending-end Relay 1 protecting the ideally-transposed transmission line

Z3StartR1- Zone 3 start signal for the sending-end Relay 1 protecting the ideally-transposed transmission line

Z1StartR3- Zone 1 start signal for the sending-end Relay 3 protecting the ideally-transposed transmission line

Z2StartR3- Zone 2 start signal for the sending-end Relay 3 protecting the ideally-transposed transmission line

Z3StartR3- Zone 3 start signal for the sending-end Relay 3 protecting the ideally-transposed transmission line

When considering the variables and decision making elements of the RSCAD software relays shown in Figure 5.13, note that Relay 3 does not see the fault in zone 2. In this case, if the other relay protecting this portion of the transmission line with its zone 1 element does not pick up the fault for any reason, the fault may not be cleared until the secondary backup overcurrent relay operates. As mentioned previously, this could result in damage of primary plant.

The consequence of the errors in the impedance measurement of an over reaching zone 2 element as a result of non-transposition have been considered in Figures 5.11 to 5.13. The effect of such errors on the zone 1 element of a distance protection relay will now be discussed.

Figure 5.14 shows the impedance plots obtained from the RSCAD software relays protecting ideally transposed and untransposed lines for a C-A phase fault at 80% of the transmission line length in each case.

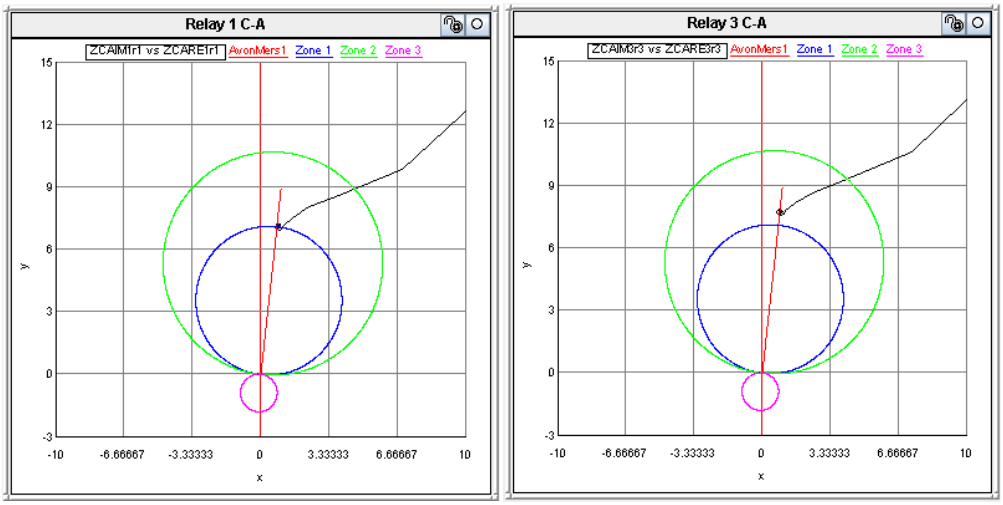

Figure 5.14: Impedance plots for a phase C-A fault at 80% of a line with ground wires: left plot – Relay 1 protecting the ideally transposed line; right plot – Relay 3 protecting the untransposed line

From the results in Figure 5.14, considering the zone 1 element, in which the reach is set to 80%, note that Relay 3 protecting the untransposed transmission line under-reaches. This fault would therefore not be detected in zone 1 for the case where the transmission lines are untransposed. As a result, it may no longer be possible for the relay at one end of the line to provide instantaneous tripping for this fault, even in the case of a permissive over-reaching scheme, since although the over-reaching zone 2 element of Relay 3 is still able to detect this fault, the communications link for the permissive signalling may not always be operational. The protection scheme now relies on zone 2 to clear the fault, provided that no other non-unit protection sees the fault and clears it first which would cause a larger outage unnecessarily.

The C-A phase fault was then moved progressively toward the relay until the relay protecting the untransposed line started issuing a zone 1 trip. Figure 5.15 shows the impedance plot of this condition. These results were included to show that the permissive transfer trip scheme will be compromised with an error of almost 8%.

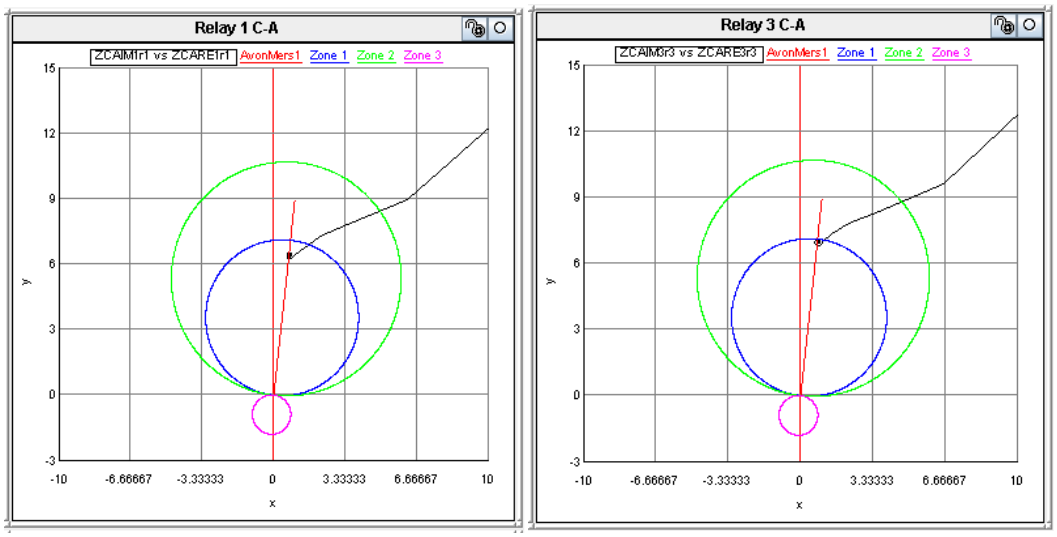

Figure 5.15: Impedance plot for a phase C-A fault at 72% of a line with ground wires: left plot – Relay 1 protecting the ideally transposed line; right plot – Relay 3 protecting the untransposed line

Where permissive under-reaching transfer trip schemes are used, zone 1 is used to send a permission to trip to the remote end relay. For this fault scenario presented in Figure 5.15, the relay at the sending end will not send a permission to trip to the remote end, which will render the permissive under-reaching transfer trip scheme inoperative. The distance protection relay continues to see the fault in zone 2 up until a fault that is placed at 72% of the line.

The results presented in this section have reinforced the notion that special precautions should be taken in the design of permissive transfer trip schemes for untransposed transmission lines, whether an over or under reaching transfer trip scheme is used.

5.4. Conclusion

The studies presented in this chapter show that in cases where the transmission lines in a power system are untransposed, their characteristics can have an impact where the distance protection relay is concerned. Mathematical evaluations have been presented to show that the symmetrical component matrix of the line impedance in an untransposed transmission line displays coupling between the sequence components of the transmission line impedance, thereby causing voltage imbalances and hence errors in the impedance measurement loops of a distance protection relay. The most significant effect is seen in the phase C-A loop for the detailed case studied in this report, for which the quantified errors can be as high as 8.85%.

The impact of these errors on permissive tripping schemes was considered and it was shown that reliability and selectivity may no longer be achieved at the edge of the zones of protection for a distance protection relay if the protection settings are designed assuming that the transmission lines are ideally transposed when they are in fact untransposed. The study highlights the effects on relay measurements of errors due to non-transposition and shows that, where untransposed transmission lines are concerned, special precaution needs to be taken to compensate for reach errors at the design stage of protection settings.

Compensation for this error in the protection settings can, in principle, be provided for by performing a hand calculation for the worst case error in the impedance that will be seen by the distance protection relay and to modify the zone reach accordingly. However, from the portion of the hand calculation that has been presented in Section 5.1, it can be seen that such calculations can be a lengthy process requiring mathematical software packages such as MATLAB to carry out. In this chapter, extensive studies have been presented to verify that the hand calculations agree with the results obtained from impedance loci measured by RSCAD's generic model of a distance relay. The real time digital simulator has thus been shown again to be an easier method of investigating the effect of practical operating conditions in a transmission line on the performance of a distance protection relay. By using the real time simulation studies when compensation for the effect of untransposed transmission lines is incorporated into the design of the protection settings, these compensated settings can be directly tested with the power system that is to be protected. The actual settings and hardware relays can be connected in closed-loop and used to verify that the compensation for

untransposed transmission lines has been designed correctly before the settings are applied in the field.

The next chapter examines the more challenging operating conditions described earlier in the thesis, in which both mutually coupled and non-transposed transmission lines make up the parallel lines in a servitude. The response of the distance protection relays to this complex operating condition is investigated and the results of this are examined.

CHAPTER 6

INVESTIGATING THE COMBINED EFFECTS OF MUTUAL COUPLING AND UNTRANSPOSED TRANSMISSION LINES ON THE DISTANCE PROTECTION RELAY, USING A REAL TIME DIGITAL SIMULATOR

The individual effects of mutual coupling between parallel transmission lines and non-transposition of transmission lines on the distance protection relay have been presented from first principles in Chapters 3, 4 and 5. The agreement between these theoretical derivations and the results obtained from the Real Time Digital Simulator (RTDS) prove that the RTDS is an accurate tool for the evaluation of these operating conditions on the distance protection relay. This chapter will investigate a more complex operating condition in which the effects of mutual coupling and untransposed transmission lines are considered together in the same study system.

6.1. Background

In the investigations presented in this chapter, the combined effects of mutual coupling and non-transposition of transmission lines on a distance protection relay, are studied directly using the real time simulator since the first principles theory of each contributing factor has already been developed earlier in the thesis to validate the use of the simulator as a tool for studying these issues. The chapter focuses on a single study case based on the actual parameters of the transmission lines between Mersey and Impala, where the distance between the transmission lines is 37 meters. No permissive trip schemes are implemented in this chapter and the SEL hardware relays under test are again studied in parallel with the RSCAD software relays, as a means to gain insight into the impedance measurements seen by the relays for each testing scenario as was the case in preceding chapters. The results in this chapter are presented purely in the form of impedance plots from the RSCAD model of the generic distance protection relay as the chapter aims to provide insight into the expected behaviour of a distance protection relay, and the dynamic impedances seen by the relay, under the various fault conditions. To provide a reference for comparison, a base case set of impedance plots were first obtained, for the various fault scenarios in which ideally-transposed lines with no mutual coupling were assumed in the studied power system. Thereafter, various challenging practical operating conditions are

presented and compared to the base case. The single line diagram in Figure 4.1 is referred to for all discussions of the study system topology.

In order for the combined effects of mutual coupling and non-transposition of transmission lines to be investigated, the type of faults to be placed on the network had to be carefully thought out so that both phenomena could be fully represented and studied together. Chapters 3 and 4 showed that mutual coupling affects the performance of the ground distance protection elements of the distance protection relay, while Chapter 5 showed that non-transposition of lines affects the performance of the phase distance protection elements of the relay. When the combined impact of the two operating conditions is tested, a combination of ground and phase faults should therefore be considered in order to examine the likely compounding and complex effects of these operating conditions on the distance protection relay. The chapter thus focuses mainly on three phase to ground faults as well as double line to ground faults in order for a practical combination of phase and ground faults to be tested.

As in previous chapters, two sets of parallel transmission line systems were represented in the same real time simulation model in this chapter to allow direct comparisons to be made more readily. The first parallel transmission line system, serving as the base case, made use of distinct distributed parameter models of each transmission line such that no mutual coupling was represented between the lines, and each transmission line was represented as being ideally transposed. In the second parallel transmission line system, the two transmission lines were modelled using a single distributed parameter model such that mutual coupling was fully represented between the conductors of the two transmission lines and both transmission lines were represented as being untransposed. The modelling of the transmission lines was done using the RSCAD TLINE program in both cases.

6.2. Three phase to ground fault at 100% of the transmission line

For the first fault scenario, the relay at A is observed when a three phase to ground fault (ABC-g) is placed at B (referring to Figure 4.1). The results of this end of line fault are displayed in Figures 6.1 and 6.2. For an ideally transposed transmission line where no mutual coupling is present, one would expect to see all impedance loci settling perfectly at the edge of the line characteristic for both the phase and ground impedance loop plots for this fault.

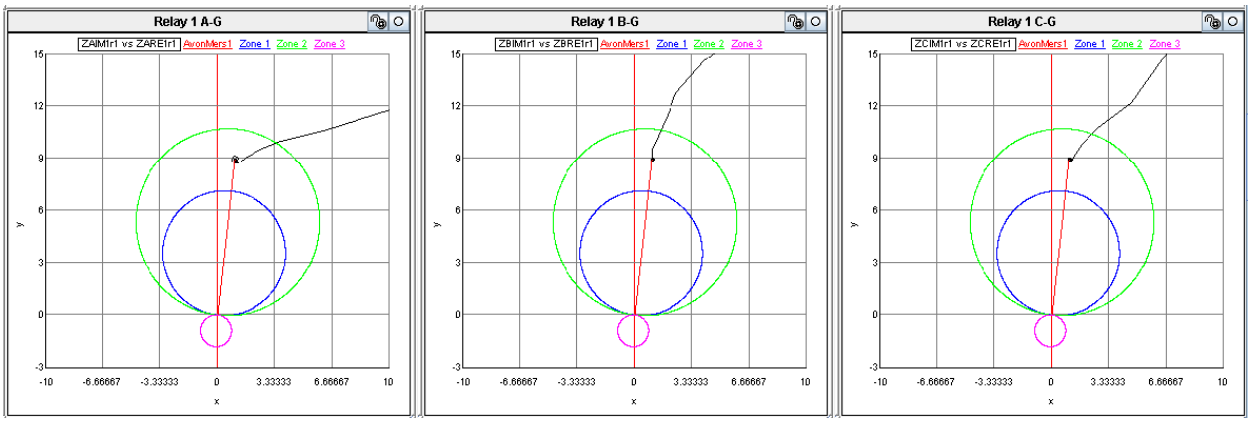

Figure 6.1: Phase to ground impedance plots for a three phase to ground fault at 100% of the line with ideally-transposed transmission lines and no mutual coupling present between the transmission lines with both transmission lines in service

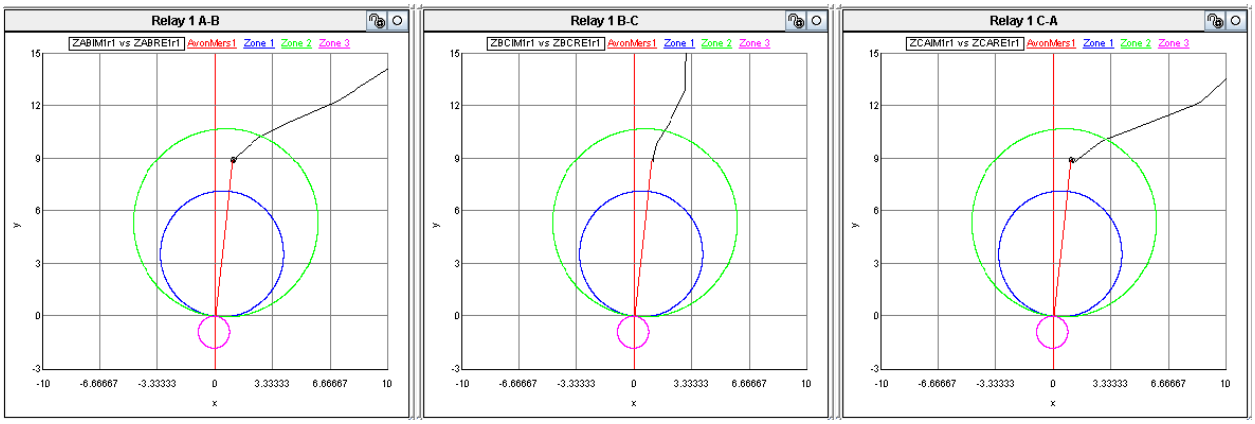

Figure 6.2: Phase to phase impedance plots for a three phase to ground fault at 100% of the line with ideally-transposed transmission lines and no mutual coupling present between the transmission lines with both lines in service

As expected, the impedance locus in each measurement loop settled at the end of the line characteristic as it should under ideal conditions. The impedance plots in Figures 6.1 and 6.2 will be referred back to for comparison purposes in all future fault studies.

Applying exactly the same three phase to ground fault on the system, but now with mutual coupling present between the transmission lines and with the transmission lines untransposed, the response of the impedance protection relay is shown in Figures 6.3 and 6.4. The deviation from the ideal case can be clearly noted when comparing each impedance locus to the corresponding locus in Figures 6.1 and 6.2.

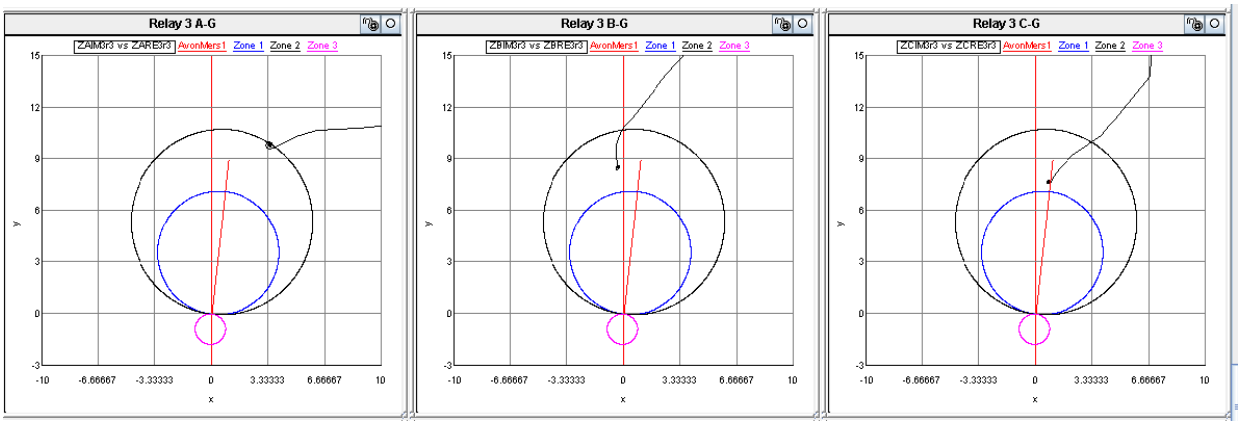

Figure 6.3: Phase to ground impedance plots for a three phase to ground fault at 100% of the line with untransposed transmission lines and mutual coupling present between the lines with both lines in service

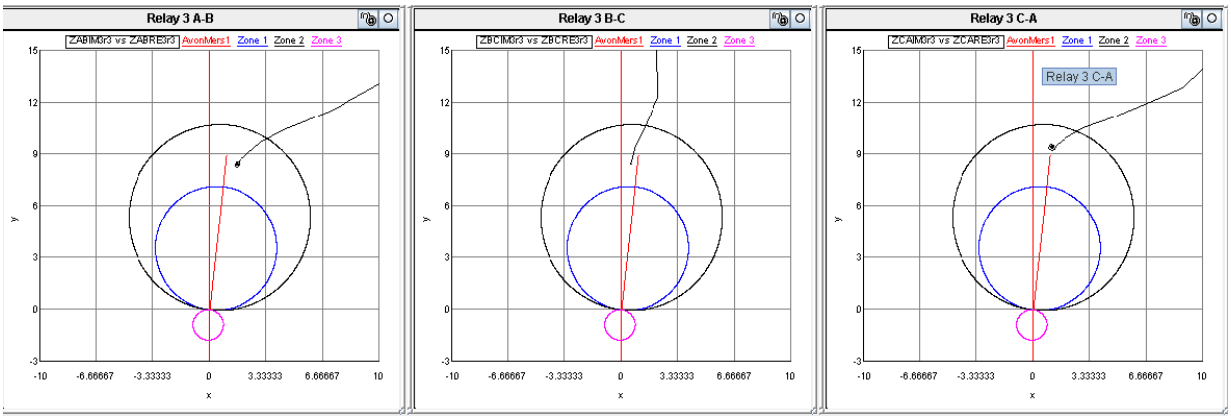

Figure 6.4: Phase to phase impedance plots for a three phase to ground fault at 100% of the line with untransposed transmission lines and mutual coupling present between the lines with both lines in service

Note now that as a result of the combined effects of mutual coupling (which affected only the phase to ground impedance loci for ground faults) and non-transposition of transmission lines (which affected primarily the phase to phase impedance loci for phase faults) both the phase to ground and the phase to phase impedance loci seen by the distance protection relay show noticeable changes. The fault applied on the system in this case is a three phase to ground fault which, ideally, behaves like a three phase fault, since the fault itself is balanced (fault current in all phases normally summing to zero) [11], so one would expect to see no change in the phase to ground impedance loci, but Figure 6.3 shows a contrary image. Chapter 5 showed that in the case of untransposed transmission lines, there exists coupling between the sequence networks for all fault types, which will introduce an associated unbalanced voltage drop in each phase. This unbalanced voltage drop, combined with the presence of mutual coupling, which in

Chapter 4 was shown to affect the zero sequence volt drop, causes the phase to ground impedance loci to deviate from the ideal impedance plots shown in Figure 6.1.

The most significant impact of the fault scenario presented above on the distance protection relay appears in the phase A to ground impedance loop in Figure 6.3: for this particular fault and complex operating condition, the A-g impedance locus settles at the edge of the zone 2 characteristic which is set to protect 120% of the line, indicating a 20% error in the A-g impedance loop measurement. Fortunately, for this fault scenario, the B-g and C-g impedance loops see the fault in zone 2 since their impedance loci settle within the zone 2 boundary of the reach of this relay so the relay will issue a three pole time delayed trip, provided that no POTT scheme is implemented.

The complex environment of the study was extended further by taking one transmission line out of service and grounding it at both ends and repeating the same fault study. The impedance loci are shown in Figures 6.5 and 6.6 for an ABC-g fault.

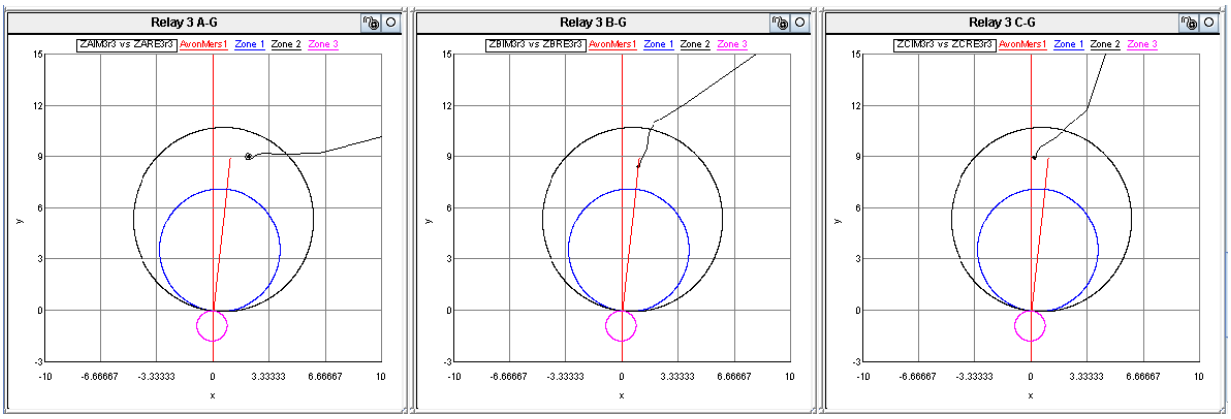

Figure 6.5: Phase to ground impedance plots for a three phase to ground fault at 100% of the line with untransposed transmission lines and mutual coupling present between the lines and with one line out of service and grounded at both ends

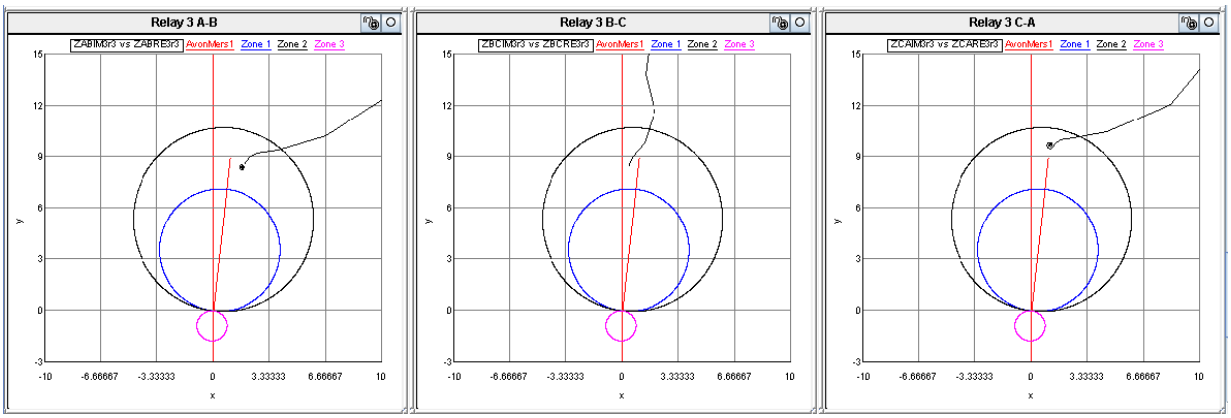

Figure 6.6: Phase to phase impedance plots for a three phase to ground fault at 100% of the line with untransposed transmission lines and mutual coupling present between the lines and with one line out of service and grounded at both ends

The results in Figure 6.5 show that with one line out of service and grounded at both ends, the phase to ground impedance loci move closer (when compared to Figure 6.3) toward the ideal locus trajectories seen in Figure 6.1. Recall that when one line was taken out of service and grounded at both ends in Chapter 4, the relay at A changed from under-reaching for single phase ground faults, when both lines were in service, to over-reaching when one line was taken out of service and grounded at each end (Figures 4.17 and Figure 4.18 illustrate this behaviour). In this case, for three phase to ground faults, the effect of taking one line out of service in the presence of both mutual coupling and untransposed lines is to cancel out some of the under-reaching effects seen in Figures 6.3 and 6.4. The impedance seen by the distance protection relay is now the combined result of both of these effects (under-reaching due to mutual coupling when one line is taken out of service and grounded at both ends, and over-reaching due to the transmission lines being untransposed).

6.3. Double line to ground faults at 100 % of the transmission line

In order to get a wider understanding of the relay's response under different fault scenarios, a double line to ground fault was applied on the transmission line. A double line to ground fault was selected so that the combined effects of phase to ground faults and phase to phase faults (investigated individually in Chapters 4 and 5 when mutual coupling and non-transposition of transmission lines were studied in isolation) could be understood. As with the earlier tests shown in this chapter, the ideal case was considered first, with no mutual coupling present between the transmission lines and the lines being ideally transposed. A phase AB-g fault at 100% of the transmission line was applied on the system and the impedance plots obtained at relay A for this fault condition are displayed in Figures 6.7 and 6.8.

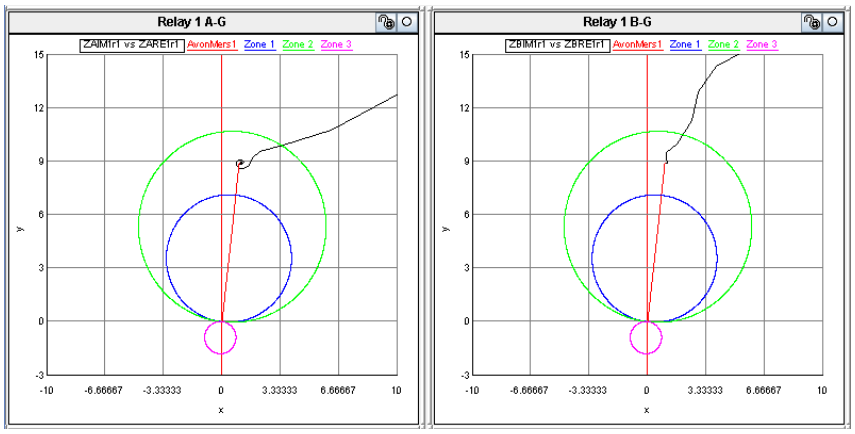

Figure 6.7: Phase to ground impedance plots for an AB-g fault at 100% of the line with ideally transposed transmission lines and no mutual coupling present between the lines with both lines in service

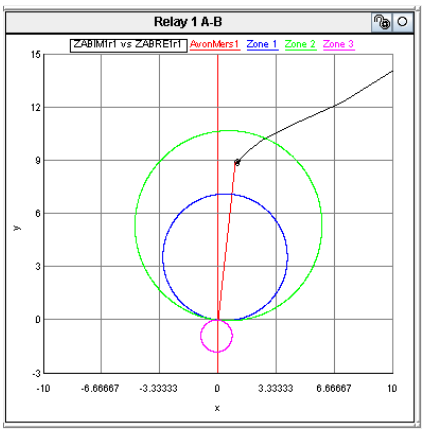

Figure 6.8: Phase to phase impedance plots for an AB-g fault at 100% of the line with ideally transposed transmission lines and no mutual coupling present between the lines with both lines in service

As expected, the impedance loci for both phase to phase and phase to ground elements settle at the end of the transmission line characteristic for this test. The complex operating condition in which both lines are untransposed and mutual coupling exists between them was then investigated and the results compared to those seen in Figures 6.7 and 6.8. The impedance plots for this scenario are presented in Figures 6.9 and 6.10 with an AB-g fault placed at 100% of the line.

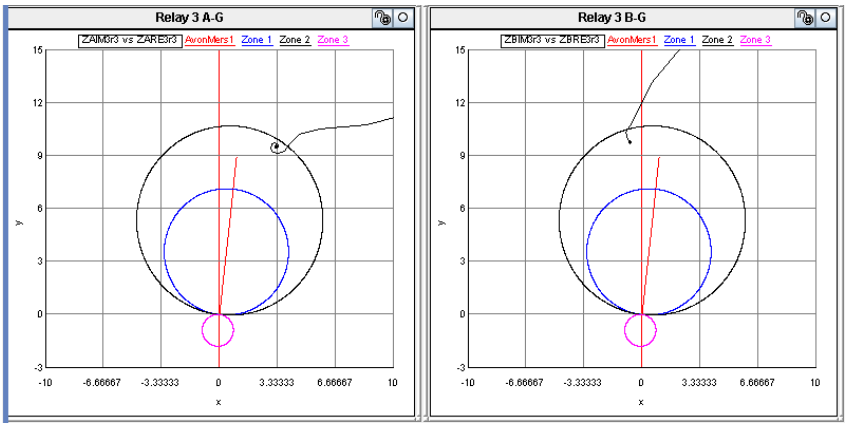

Figure 6.9: Phase to ground impedance plots for an AB-g fault at 100% of the line with untransposed transmission lines and mutual coupling present between the lines with both lines in service

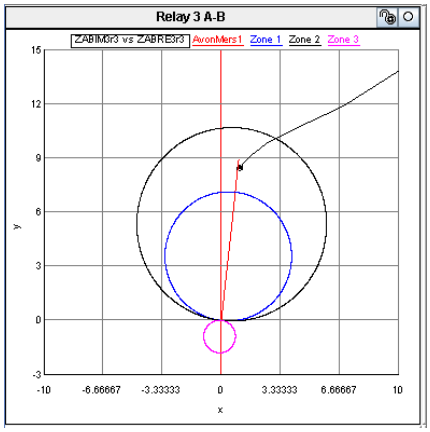

Figure 6.10: Phase to phase impedance plots for an AB-g fault at 100% of the line with untransposed transmission lines and mutual coupling present between the lines with both lines in service

Figures 6.9 and 6.10 show that under these operating conditions the phase to ground impedance loci significantly under reach and the phase to phase impedance locus minimally over reaches. The error seen by the distance protection relay's phase to ground elements under these conditions is significant. The possibility of the relay's ground impedance measurements not seeing the fault in zone 2 is evident from Figure 6.9 and the possibility of this would be more likely in the event of any further measurement errors in the system or if the transmission lines were positioned any closer to each other. In the event of a permissive trip scheme being implemented in the protection scheme that protects the transmission line concerned, if the fault has not been detected in zone 2 when the permissive signal is received from the remote end, the permissive scheme will not operate without a time delay. This could potentially lead to extensive damage of equipment if the fault is not cleared in the fastest possible time as well as

system instability. The reliability of the protection scheme is compromised for this operating condition.

A further investigation was carried out for this fault scenario for the condition when one line is out of service and grounded at both ends. The impedance plots for this condition are presented in Figures 6.11 and 6.12 for the AB-g fault at 100% of the line.

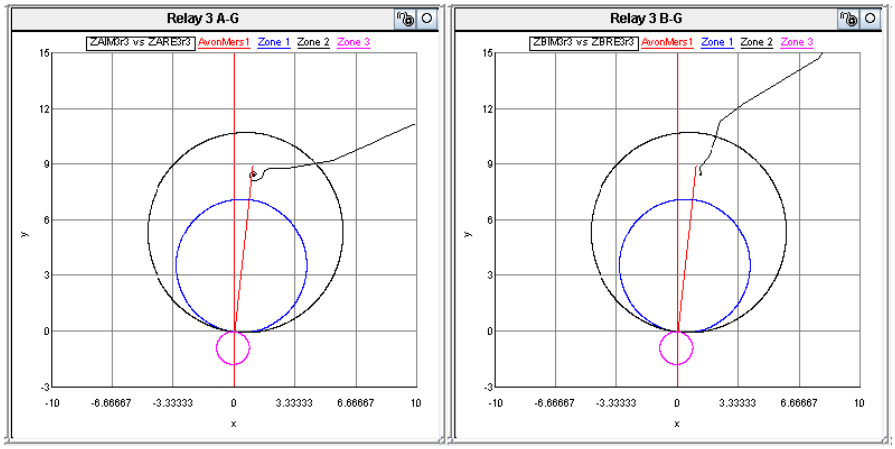

Figure 6.11: Phase to ground impedance plots for an AB-g fault at 100% of the line with untransposed transmission lines and mutual coupling present between the lines with one line out of service and grounded at both ends

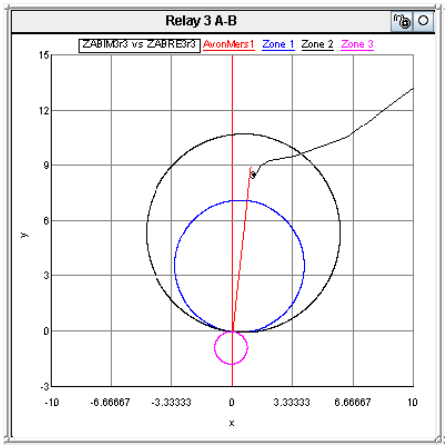

Figure 6.12: Phase to phase impedance plot for an AB-g fault at 100% of the line with untransposed transmission lines and mutual coupling present between the lines with one line out of service and grounded at both ends

From the impedance plots in Figures 6.11 and 6.12 it can once again be seen that with one line out of service and grounded at both ends, the combined effect of mutual coupling and non-transposition of the transmission lines is to make the impedance loci follow a more ideal

trajectory, thus reducing the errors in the distance protection relay loop measurements when compared to the same fault scenario with both lines in service (Figures 6.9 and 6.10)

These tests were repeated for a BC-g fault at 100% of the line and the results were found to be similar to those in Figures 6.9 to 6.12 for the AB-g fault. This finding is consistent with those in previous chapters where it was seen that the A-B and B-C impedance loops of the relay react in a similar manner to such fault scenarios.

The investigation into the effects of a double line to ground fault also considered an AC-g fault since the A-C impedance loop displayed the most significant changes under non-ideal conditions in earlier chapters. To investigate the combined effects of mutual coupling and non-transposition of transmission lines an AC-g fault was therefore applied at 100% of the transmission line. As in the previous tests a base case study was conducted with no mutual coupling and with ideally transposed transmission lines. The results of this study are shown in Figures 6.13 and 6.14.

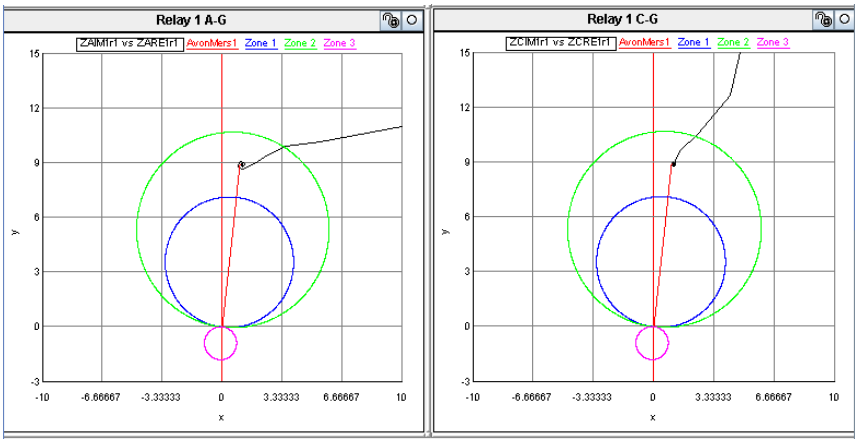

Figure 6.13: Phase to ground impedance plots for an AC-g fault at 100% of the line with ideally transposed transmission lines and no mutual coupling present between the lines with both lines in service

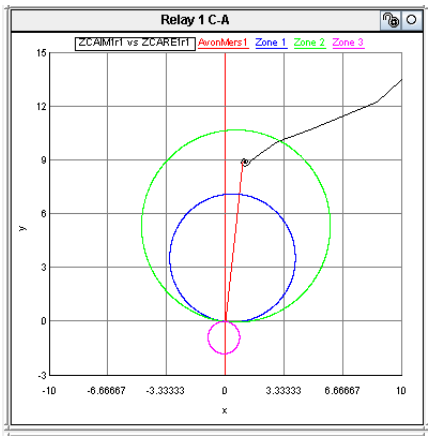

Figure 6.14: Phase to phase impedance plots for an AC-g fault at 100% of the line with ideally transposed transmission lines and no mutual coupling present between the lines with both lines in service

As in the previous studies, the impedance loci for this ideal case settle at the end of the transmission line characteristic. The impedance loci seen by the relay for the same AC-g fault when mutual coupling exists between the transmission lines and the lines are untransposed are presented in Figures 6.15 and 6.16.

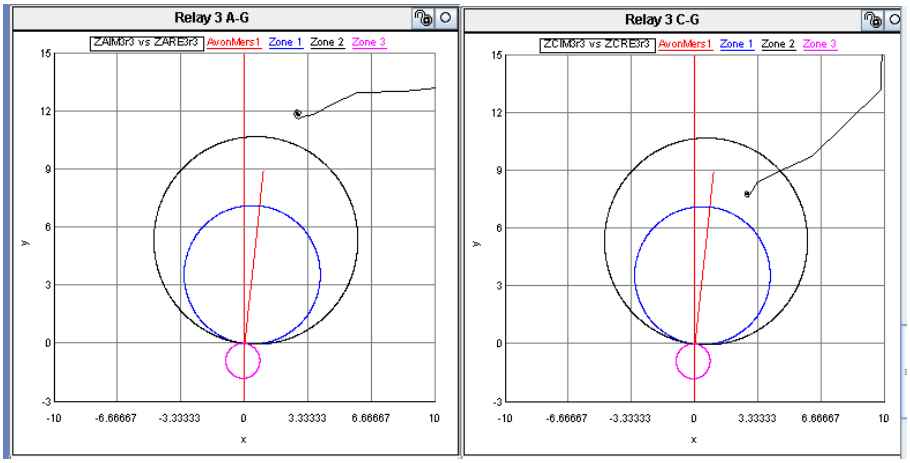

Figure 6.15: Phase to ground impedance plots for an AC-g fault at 100% of the line with untransposed transmission lines and mutual coupling present between the lines with both lines in service

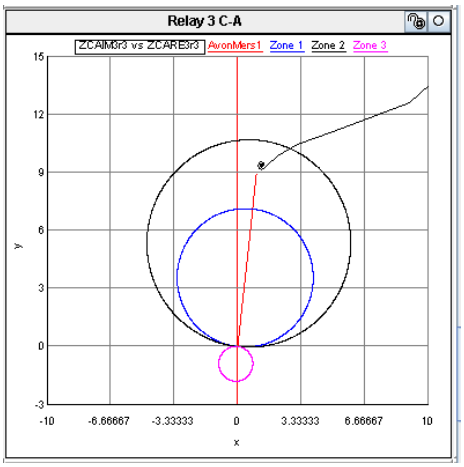

Figure 6.16: Phase to phase impedance plot for an AC-g fault at 100% of the line with untransposed transmission lines and mutual coupling present between the lines with both lines in service

The results for this particular double line to ground fault (AC-g) show that the error seen by the A-g impedance measurement loop is much greater than is the case for the previous double line to ground fault scenario. For the AC-g fault, the phase to ground impedance elements severely under reach and the phase to phase impedance element marginally over reaches. The phase A-g impedance loop measurement is of the greatest concern as the impedance locus for this fault settles significantly beyond the zone 2 reach of the impedance relay. Fortunately the relay will nevertheless issue a trip command due to the C-g and A-C impedance loops seeing the fault in zone 2.

In the case of the AC-g fault, when one transmission line is out of service and grounded at both ends the combined effects of non-transposition of the line and mutual coupling tend to reduce the errors in the impedance measurements as in the case with AB-g faults as seen in the results of Figures 6.17 and 6.18.

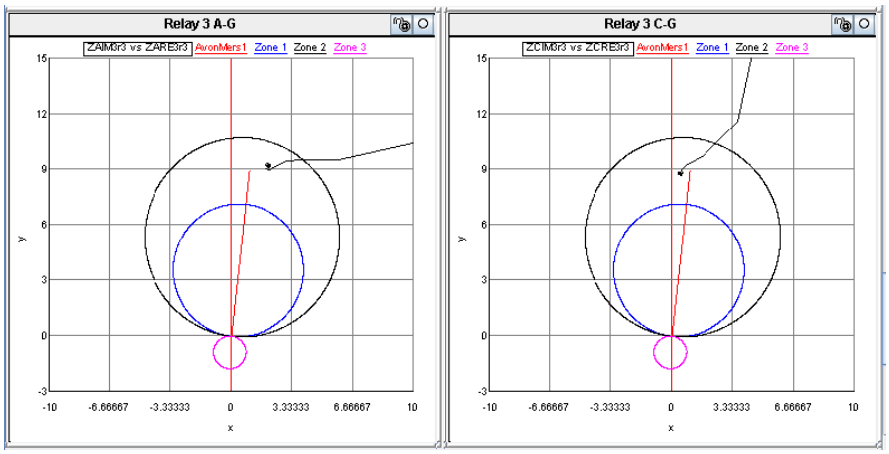

Figure 6.17: Phase to ground impedance plots for an AC-g fault at 100% of the line with untransposed transmission lines and mutual coupling present between the lines with one line out of service and grounded at both ends

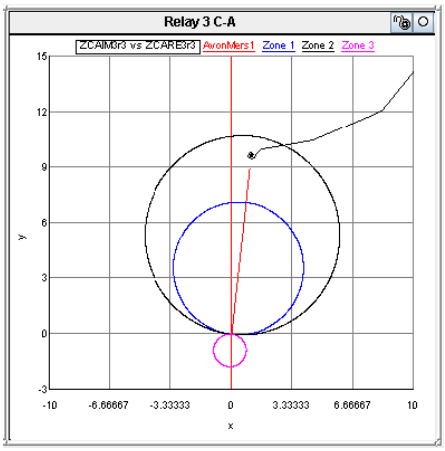

Figure 6.18: Phase to phase impedance plot for an AC-g fault at 100% of the line with untransposed transmission lines and mutual coupling present between the lines with one line out of service and grounded at both ends

6.4. Three phase to ground fault at 0% of the transmission line

The tests then considered the response of the relay at B in Figure 4.1 to a three phase to ground fault (ABC-g) placed at A. The results of this study are shown in Figures 6.19 and 6.20 for the base case when the transmission lines are ideally transposed and no mutual coupling exists between them. As expected, for perfectly transposed transmission lines with no mutual coupling, all impedance loci settle perfectly at the edge of the line characteristic of relay B for both the phase and ground impedance loop plots in Figures 6.19 and 6.20.

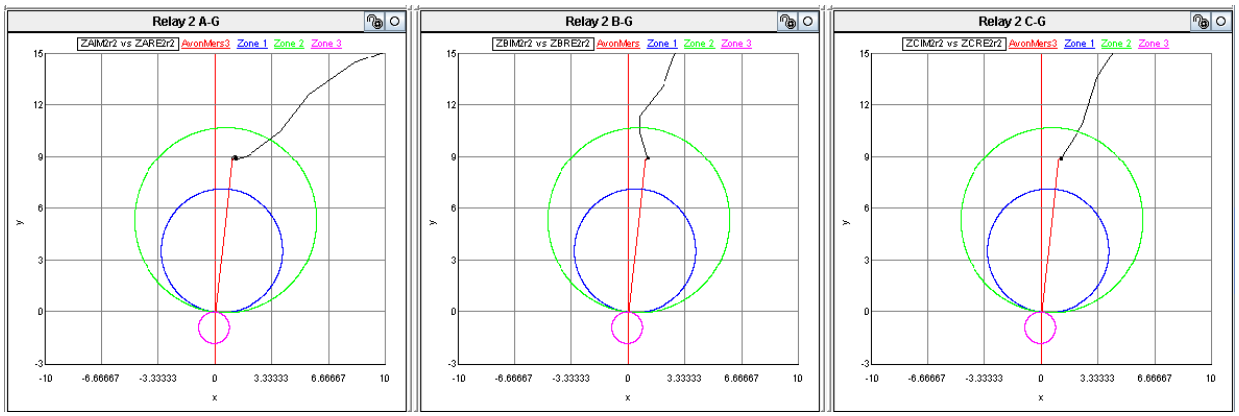

Figure 6.19: Phase to ground impedance plots at relay B for a three phase to ground fault at 0% of the line with ideally transposed transmission lines and no mutual coupling between the lines with both lines in service

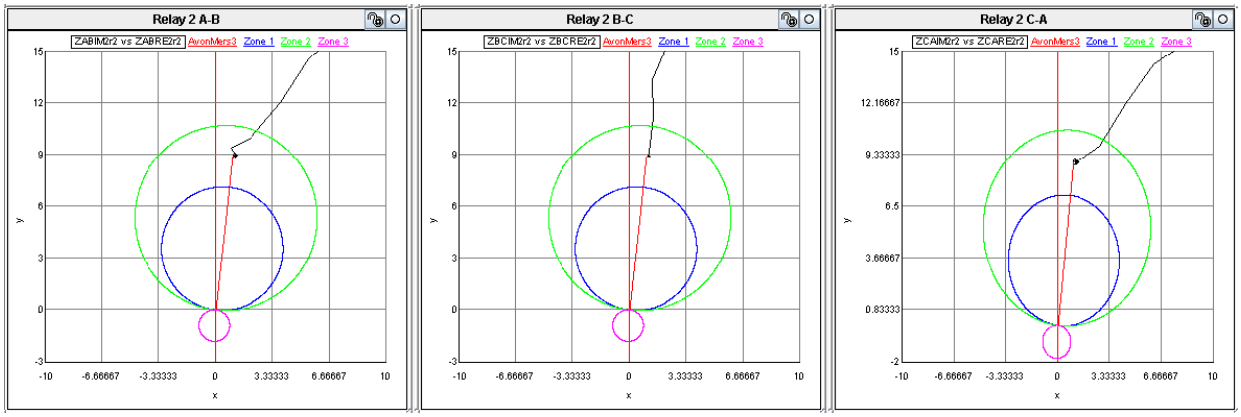

Figure 6.20: Phase to phase impedance plots at relay B for a three phase to ground fault at 0% of the line with ideally transposed transmission lines and no mutual coupling between the lines with both lines in service

The same fault study was then repeated with mutual coupling represented between the lines and with the lines untransposed with the results shown in Figures 6.21 and 6.22.

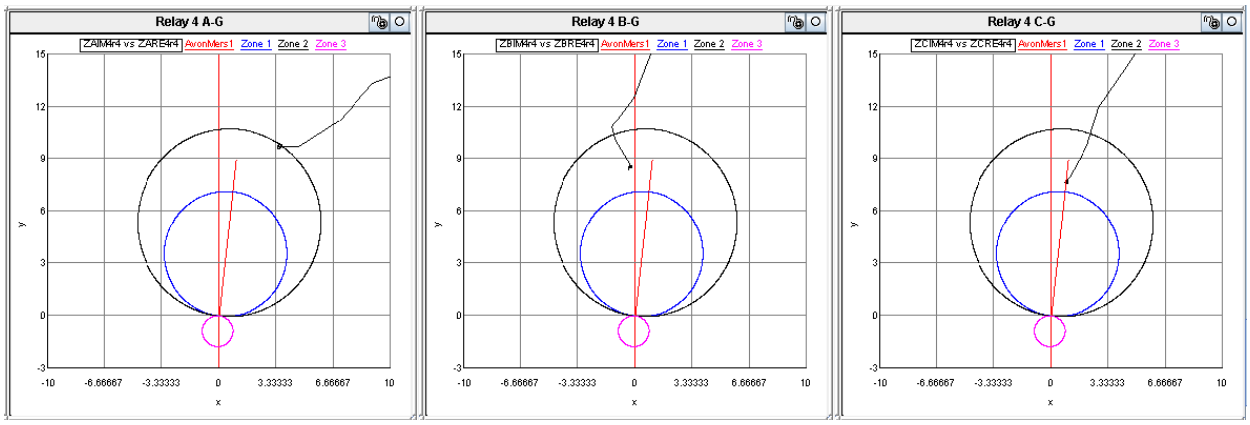

Figure 6.21: Phase to ground impedance plots at relay B for a three phase to ground fault at 0% of the line with untransposed transmission lines and mutual coupling between the lines with both lines in service

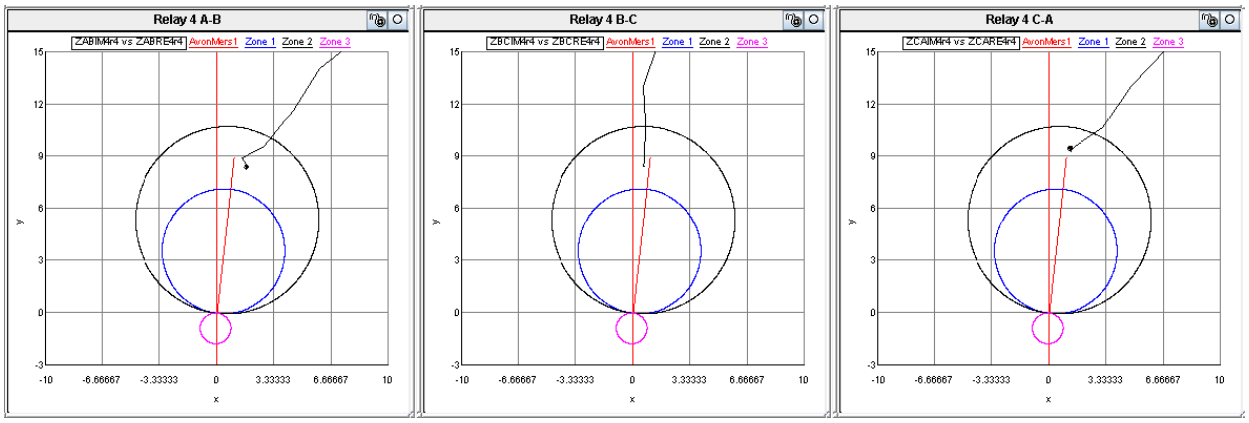

Figure 6.22: Phase to phase impedance plots at relay B for a three phase to ground fault at 0% of the line with untransposed transmission lines and mutual coupling between the lines with both lines in service

Note that the impedance plots in Figures 6.21 and 6.22 are the same as the impedance plots in Figures 6.3 and 6.4. This confirms that the relay at A and the relay at B each behave in the same way for a fault at their respective remote ends.

A further investigation was also carried out for this fault scenario when one line is out of service and grounded at both ends, the results of which are shown in Figures 6.23 and 6.24. Once again, it can be seen that the impedance plots of Figures 6.23 and 6.24 are the same as those in Figures 6.5 and 6.6. From this one can deduce that for the relay at A with the fault at 100% of the line and for the relay at B with the fault at 0% of the line, the impedances measured by the distance elements are the same, provided there is a source at both ends of the transmission line.

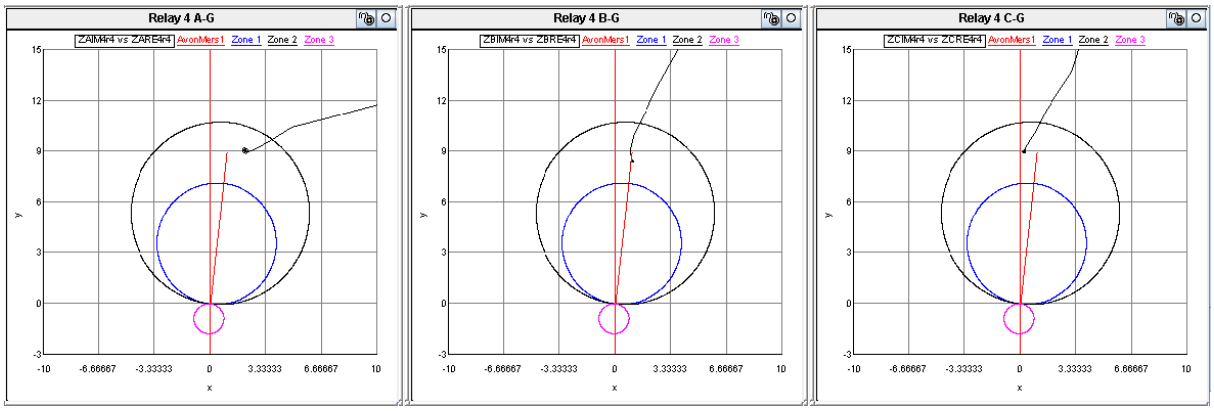

Figure 6.23: Phase to ground impedance plots at relay B for a three phase to ground fault at 0% of the line with untransposed transmission lines and mutual coupling between the lines with one line out of service and grounded at both ends

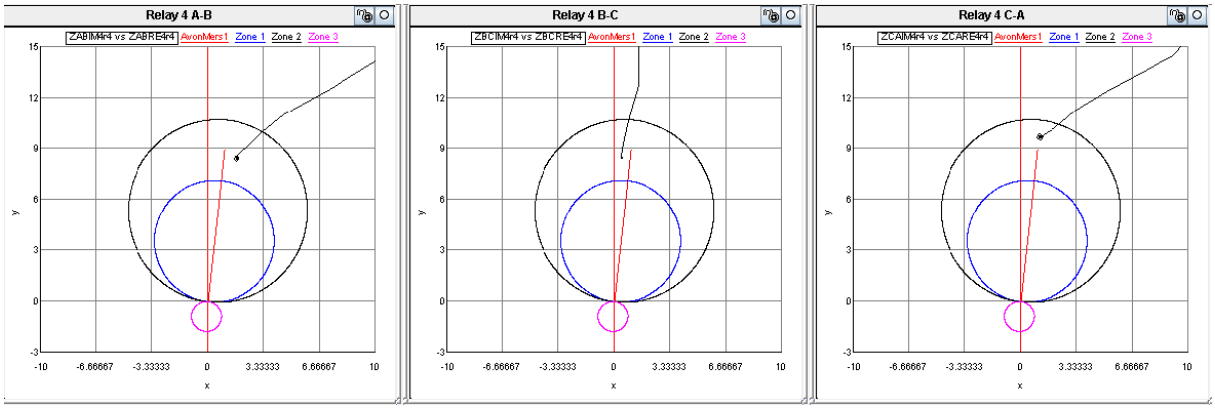

Figure 6.24: Phase to phase impedance plots at relay B for a three phase to ground fault at 0% of the line with untransposed transmission lines and mutual coupling between the lines with one line out of service and grounded at both ends

6.5. Faults involving ground resistance and resistance between the phases of the transmission line

The results in Figures 6.3, 6.9 and 6.15 have shown that for the fault scenarios considered, in complex operating environments, the reliability of the protection scheme may be compromised. In the above mentioned cases the impedance loci often settled at the edge of zone 2 of the distance protection relay. As discussed earlier, if any additional measurement errors were present in the system, or if the transmission lines were positioned closer together there would be no guarantee that the protection scheme would operate as designed under these complex conditions. Over and above these concerns, the presence of resistive faults is also known to cause an impedance relay to see the fault further along the R-axis of the impedance plane and possibly out of the zone 2 boundary as explained in Section 2.8. Hence the additional complexity of resistive faults together with mutual coupling between parallel untransposed

transmission lines could likely cause a very complex operating condition where the designed protection scheme might be unable to offer protection to the transmission line. The real time simulation studies were therefore used to investigate this possibility.

A typical resistance between the phases of the study system was calculated using Warrington's formula in eqn. (28) using the actual distances between the phase conductors. The ground fault resistance considered in these studies was a typical practical value based on the high ground resistivity of South African soil [25]. The following values were used:

Resistance between A and B phase conductors: 1.06Ω
Resistance between B and C phase conductors: 1.06Ω
Resistance between A and C phase conductors: 2.33Ω
Resistance between A phase conductor and ground: 10 Ω
Resistance between B phase conductor and ground: 10 Ω
Resistance between C phase conductor and ground: 10 Ω

Before the results of the full test scenario are presented, intermediate results are first considered to allow the response of the distance protection relay to be understood as the operating conditions of the transmission system become progressively more complex. Firstly, a three phase fault, with the above fault resistances, was placed at 100% of the transmission line with the lines untransposed but without mutual coupling represented. The impedances seen by the relay at A for this condition are shown in Figures 6.25 and 6.26.

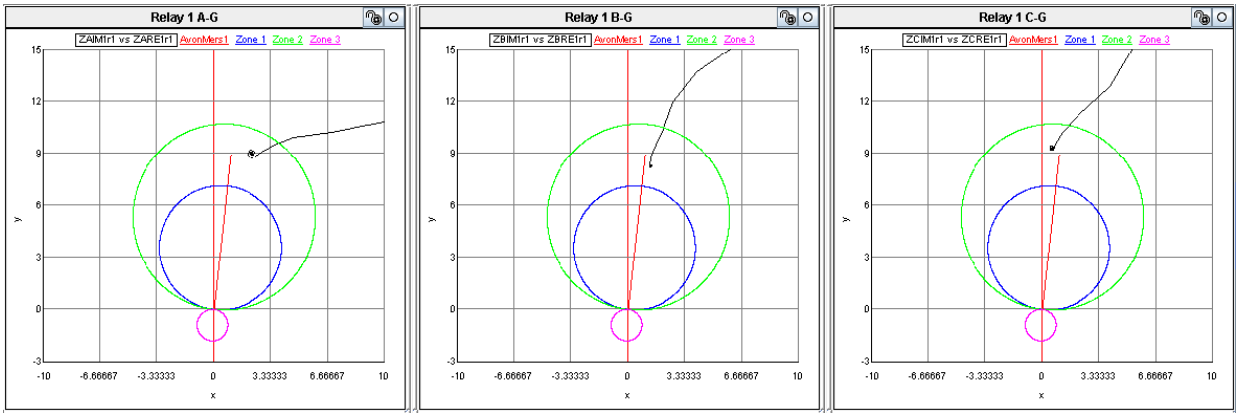

Figure 6.25: Phase to ground impedance plots at relay B for a three phase fault, including fault resistance, at 100% of the line; lines untransposed, no mutual coupling and both lines in service.

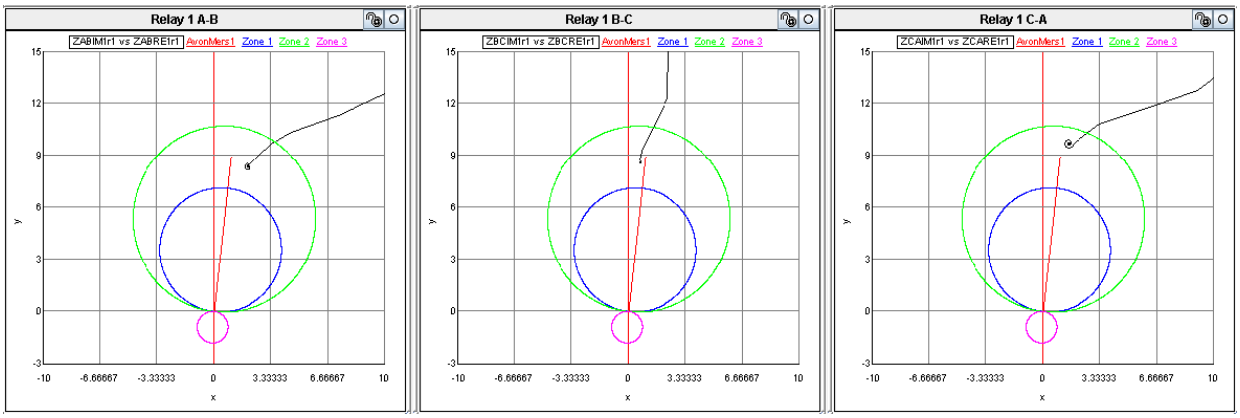

Figure 6.26: Phase to phase impedance plots at relay B for a three phase fault, including fault resistance, at 100% of the line; lines untransposed, no mutual coupling and both lines in service.

For this fault scenario, note that the impedance loci of all phase and ground impedance loops in Figures 6.25 and 6.26 deviate slightly from the ideal case, as expected. The RSCAD software distance protection relays all issued zone 2 trip commands. The SEL hardware distance protection relays were also tested in conjunction with the software relays and these relays also issued zone 2 trip commands. The effect of fault resistance in the presence of untransposed lines for a three phase fault, alone, is therefore not a substantial concern.

The operating condition was then made more complex with the inclusion of mutual coupling between the parallel transmission lines and the same three phase resistive fault was then applied to the system at 100% of the transmission lines. The results of this fault study are presented in Figures 6.27 and 6.28.

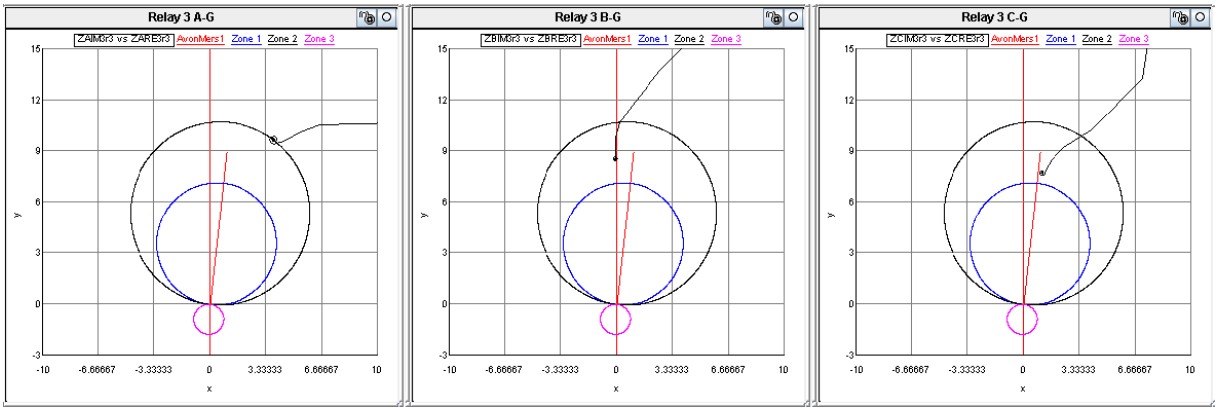

Figure 6.27: Phase to ground impedance plots at relay B for a three phase fault, including fault resistance, at 100% of the line; lines untransposed, mutual coupling represented and both lines in service.

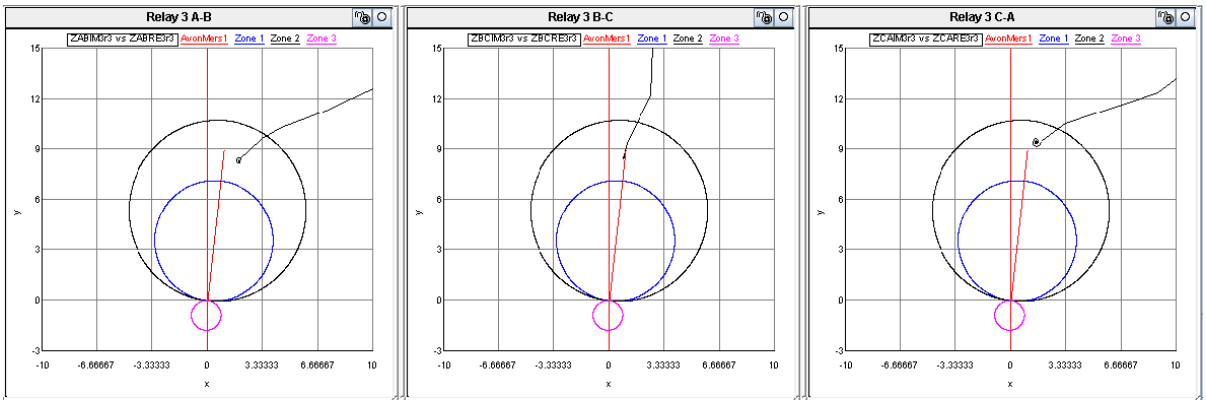

Figure 6.28: Phase to phase impedance plots at relay B for a three phase fault, including fault resistance, at 100% of the line; lines untransposed, mutual coupling represented and both lines in service.

The impedance loci seen in Figures 6.27 and 6.28 for this fault scenario and operating condition differ slightly when compared to the impedance loci for the same fault seen in Figures 6.25 and 6.26. For this fault scenario, note that the impedance loci of all phase and ground impedance loops in Figures 6.27 and 6.28 deviate slightly from the ideal case. The RSCAD software distance protection relays all issued zone 2 trip commands. The SEL hardware distance protection relays were also tested in conjunction with the software relays and these relays too also issued zone 2 trip commands. Again, the effect of fault resistance in the presence of untransposed lines with mutual coupling present for a three phase fault is also not a substantial concern.

The above two cases were presented to show that the fault resistances introduced into the system are not impractical or excessively large, such that they produce unrealistic results. These impedance plots will be used as a basis against which to assess the fault scenarios under the more complex conditions to come.

The next test scenario presented shows the compound effect on the distance protection relay of a number of complex operating conditions previously considered in this thesis. A three phase to ground fault (ABC-g) with fault resistance was placed at 100% of the transmission line with the transmission lines untransposed and with mutual coupling fully represented between the parallel transmission lines. The results of this ABC-g fault are displayed in Figures 6.29 and 6.30.

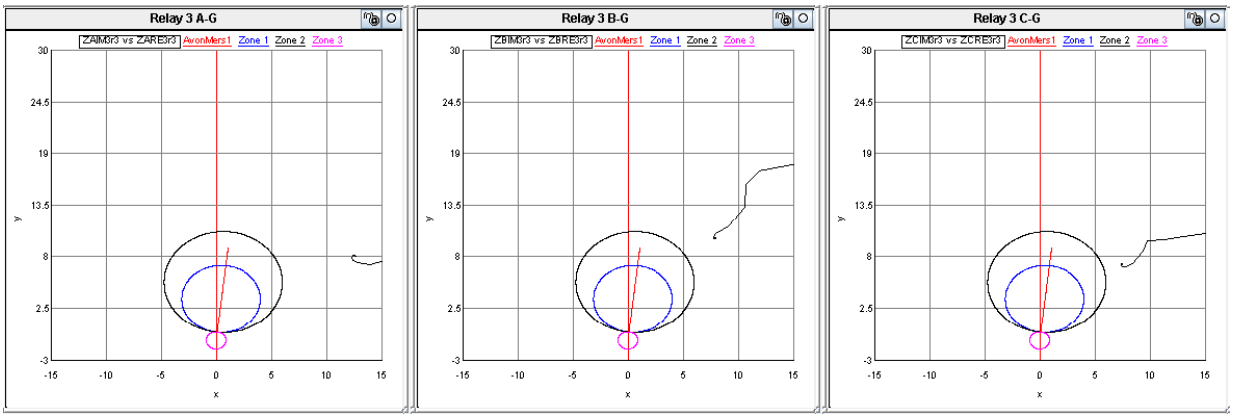

Figure 6.29: Phase to ground impedance plots at relay B for a three phase to ground (ABC-g) fault, including fault resistance, at 100% of the line; lines untransposed, mutual coupling represented and both lines in service.

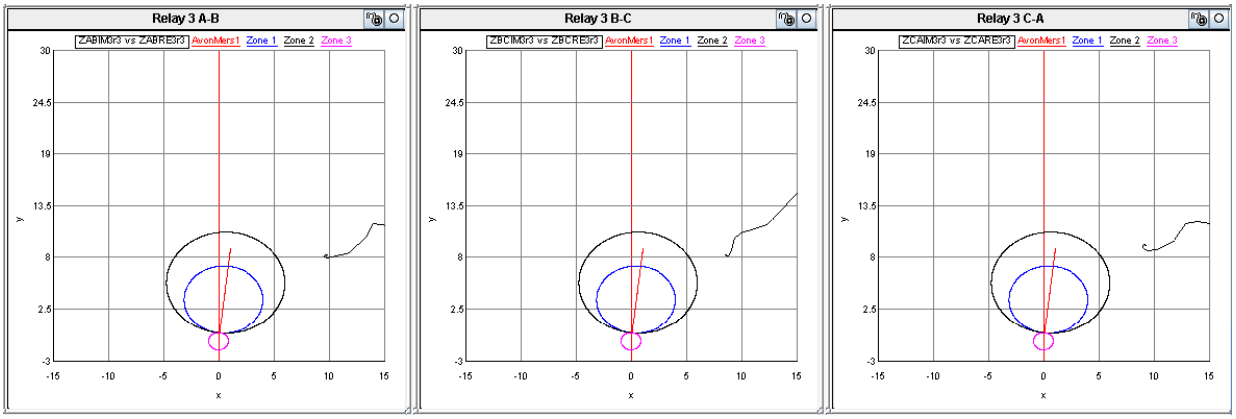

Figure 6.30: Phase to phase impedance plots at relay B for a three phase to ground (ABC-g) fault, including fault resistance, at 100% of the line; lines untransposed, mutual coupling represented and both lines in service.

Exactly the same fault scenario shown in Figures 6.29 and 6.30 was considered earlier in Figures 6.3 and 6.4, with the only difference being the addition of fault resistance in this latter test. Note the significant change in the impedance loci trajectory: with the addition of a modest amount of resistance in the fault branch, the relay at B no longer sees the fault in any of its zones, even though the fault is actually within zone 2. Recall earlier, Chapter 5 showed that due to non-transposition of transmission lines, coupling between the sequence networks for all fault types there exists, even for a balanced three phase to ground fault. This coupling between sequence networks will introduce an associated unbalanced voltage drop in each phase. This unbalanced voltage drop, when combined with the effects of mutual coupling between the lines (which in Chapter 4 was shown to affect the zero sequence volt drop) will cause the phase to ground impedance loci to deviate from the ideal impedance loci trajectory. This effect is further compounded by the presence of fault resistance, causing the impedance loci to settle far out of

the distance protection relay's protection zones. For this test scenario there is therefore no reliability of the protection scheme to operate for this fault. This statement was confirmed with both the trip indications of the RSCAD software distance protection relay as well as the SEL hardware distance protection relay as both relays issued no trip commands for this fault, under these operating conditions.

6.6 Conclusion

The studies presented in this chapter have considered the combined effects on distance relays of complex, practical operating conditions that can be present in typical parallel transmission lines. From the results in this chapter, one can clearly note the significant effects of a combination of mutual coupling and non-transposition of transmission lines when studied in combination. With the addition of a more complex, practical fault condition that includes fault resistance, one can note that the designed protection scheme could become inoperative for the transmission lines that it is intended to protect.

The results in this chapter reinforce the notion that these operating conditions must be taken into account in the design stages of a protection scheme for overhead parallel transmission lines as by ignoring these conditions (as current practice often does) the protection scheme may not adhere to the basic requirements of a protection scheme.

The following chapter will investigate further challenging conditions that parallel transmission lines can encounter in practice in the form of cross country faults.

CHAPTER 7

INVESTIGATING THE EFFECTS OF A CROSS COUNTRY FAULT ON THE DISTANCE PROTECTION RELAY USING A REAL TIME DIGITAL SIMULATOR

With the widespread use of parallel transmission lines in the South African transmission network, the consideration of cross country faults is a necessity in the design of protection systems used to protect these lines. The presence of a cross country fault on parallel transmission lines introduces complexities into the power system that would have otherwise been non-existent. From theory [1], [46], [47], a cross country fault is classified as a case where a fault is present on a transmission line and at the same time (or a very short space of time later), a fault is present on a parallel transmission line at the same location or at a location further down the line. The response of the distance protection relays during such fault scenarios is often distorted due to the distribution of current and the relay seeing current that feeds a fault on the parallel line. Due to the current distribution encountered during a cross country fault, proper phase identification in permissive schemes and single pole tripping are jeopardised [46], [47].

This chapter will focus on cross country faults and the effect they have on the distance protection relay. Firstly, based on the definition of a cross country fault that was presented in Chapter 2, a cross country fault will be replicated on the study system considered in the thesis using the Real Time Digital Simulator (RTDS) so that the distribution of fault current can be easily seen and the problems associated with cross country faults realised, in particular those that affect single pole trip schemes. Following this, the effect of a cross country fault on the POTT scheme will be investigated and the problems associated with this will be understood. Once the complexity of the mal-operation of the distance protection relay, in the presence of a cross country fault, is understood, a protection scheme to overcome this is designed using library components from the RSCAD DRAFT program. Testing of this scheme to show that it provides protection in the case of a cross country fault will be included in this chapter. Once it is established that a generic protection scheme can be designed to solve the problems experienced with cross country faults and the distance protection relay, the pre-defined POTT scheme available in the SEL hardware relays to prevent cross country faults from affecting the distance protection scheme was tested for functionality.

Once confidence is gained in the reliable operation of this protection scheme, full complex practical operating conditions are considered for this protection scheme in which mutual coupling is present between the transmission lines, and the transmission lines are untransposed.

7.1. Setup of the real time power system model used to investigate cross country faults

Before the response of the SEL hardware distance protection relays to a cross country fault is tested, the RSCAD software relays must be tested first to get an understanding of what impedances the relays will see and what factors will influence the response of the relays to the fault by observing the impedance plots of the RSCAD software relay. Initially, no consideration of the phenomena studied earlier (mutual coupling and untransposed lines) was taken into account. These factors are to be considered at a later stage. The purpose of this stage of study is purely to model and simulate cross country faults using a real time digital simulator.

The model shown in Figure 7.1 was used to perform the study.

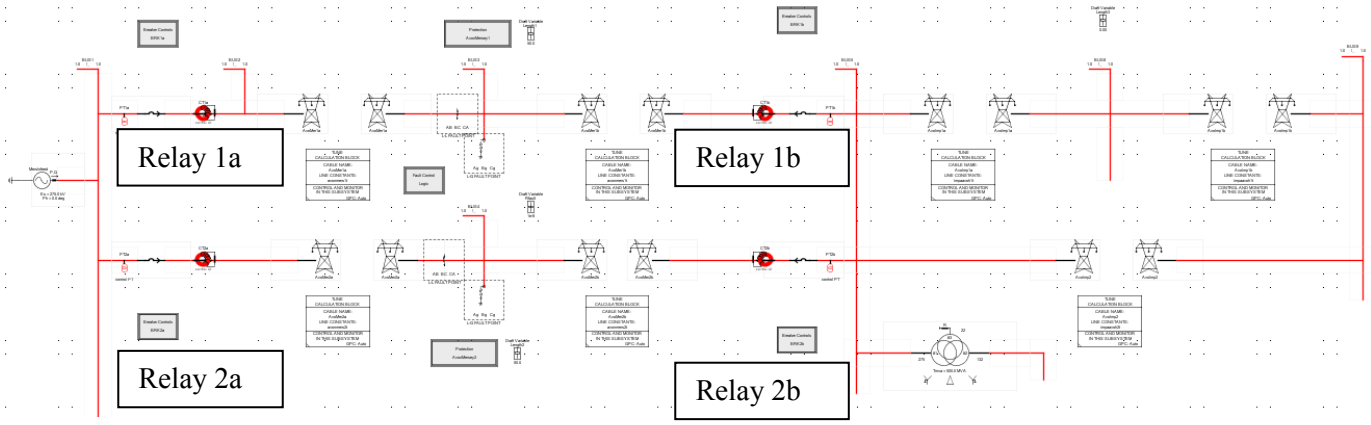

Figure 7.1: RSCAD DRAFT model of the transmission lines between Avon and Impala used to study cross country faults

The cross country fault was achieved by placing near-simultaneous faults on both transmission lines using the logic shown in Figure 7.2, where the fault types are selected and each line's fault is governed by the integer control words FAULT1 and FAULT2.

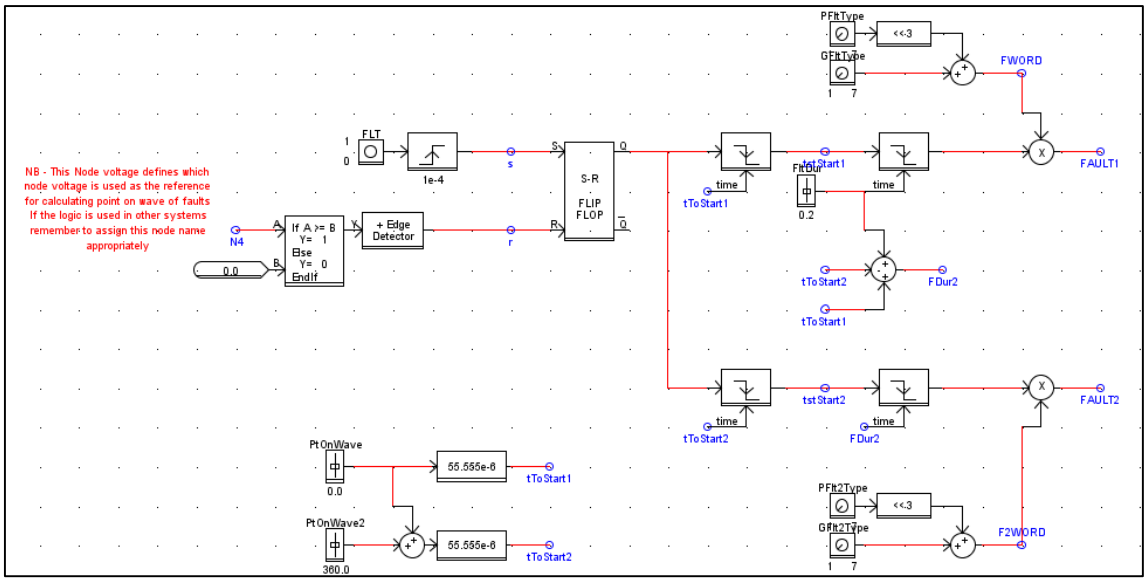

Figure 7.2: RSCAD DRAFT model of the fault logic used to apply two different faults on parallel transmission lines in order to model a cross country fault

For this stage of the study, the impedances at the sending and receiving ends of each transmission line are monitored, therefore four RSCAD generic models of a distance protection relay were required with four sets of corresponding VTs and CTs. These distance protection relays and their associated circuit breakers had to be set up for single pole tripping in the RSCAD DRAFT model. The arrangements in Figures 7.3 and 7.4 were used for the RSCAD software relays where the relays were configured to perform single pole tripping. These relays were set up to start on zone 1, zone 2 and a reverse looking zone 3 element so that the user can identify the relays' responses to each scenario.

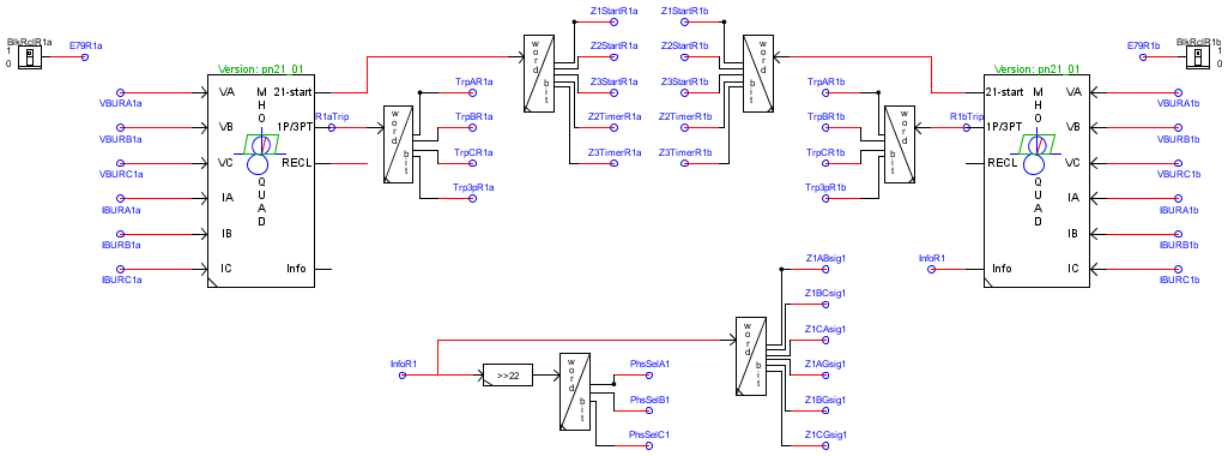

Figure 7.3: RSCAD models of generic distance protection relays configured to perform single pole tripping as used to protect transmission line 1 (relays 1a and 1b)

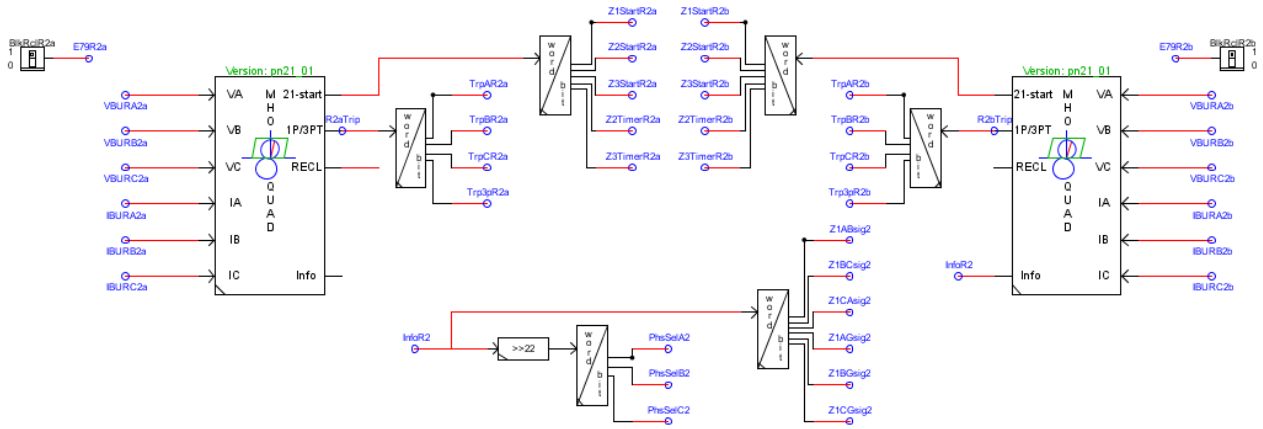

Figure 7.4: RSCAD models of generic distance protection relays configured to perform single pole tripping as used to protect transmission line 2 (relays 2a and 2b)

7.2. Investigating the effects of a cross country fault on the distance protection relay

The impedance (mho) diagrams for the relays in Figures 7.3 and 7.4 were plotted using the RSCAD RUNTIME program. Correct operation of the single pole tripping using a simple POTT scheme was first established using the DRAFT model in Figure 7.1. However, for the initial stage of testing presented here, the POTT scheme is not implemented since the response of the relay using a traditional instantaneous zone 1 set to 80% and a time delayed zone 2 set to 120% is investigated first.

Using only software relays, without the POTT scheme enabled, and with the breakers forced to stay closed, the following fault was placed on the system:
A-g fault at 95% on transmission line 1
B-g fault at 95% on transmission line 2

The fault on transmission line 2 was initiated 1 cycle after the fault appeared on transmission line 1, and the transmission lines were both ideally transposed with no mutual coupling represented between them. The impedance loci obtained for this fault are shown in Figures 7.5 to 7.6. These impedance plots were studied to ascertain the current distributions due to this cross country fault and what current distribution the relays will see. Figure 7.9 shows the fault control logic inputs and the single pole tripping logic outputs from the relays in this test.

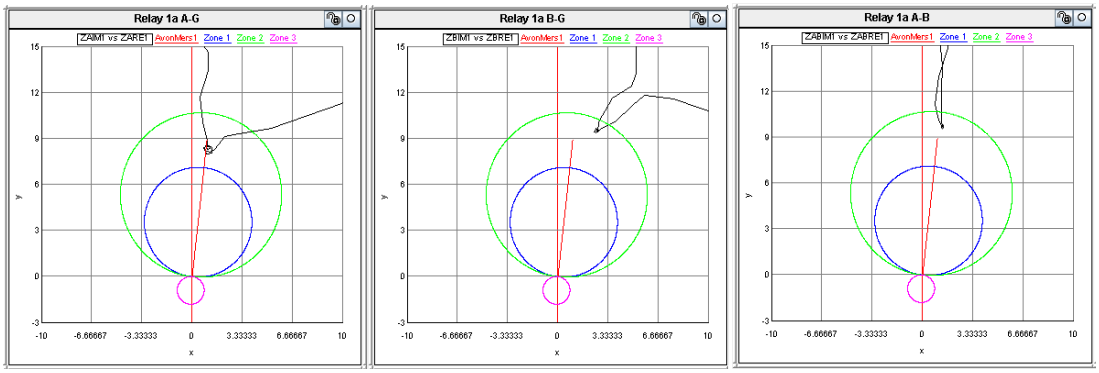

Figure 7.5: A-g, B-g and A-B impedance plots for relay 1a for a cross country fault at 95% of the line; ideally transposed lines with no mutual coupling, both transmission lines in service and no POTT scheme used

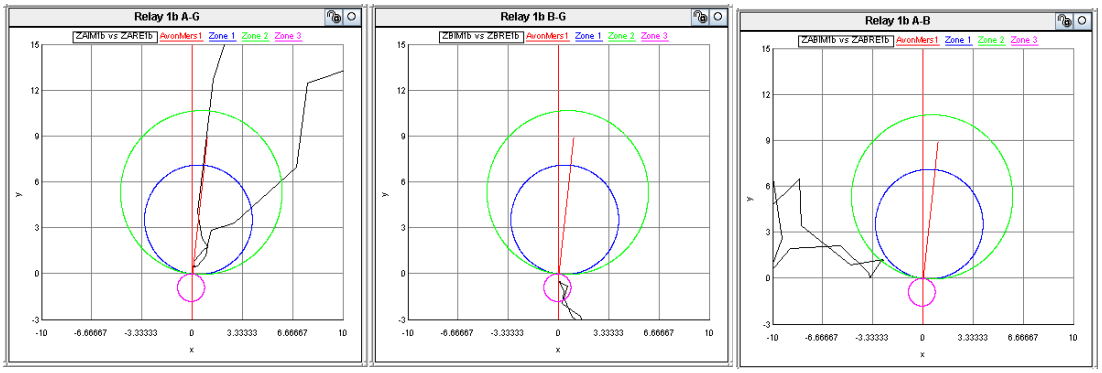

Figure 7.6: A-g, B-g and A-B impedance plots for relay 1b for a cross country fault at 95% of the line; ideally transposed lines with no mutual coupling, both transmission lines in service and no POTT scheme used

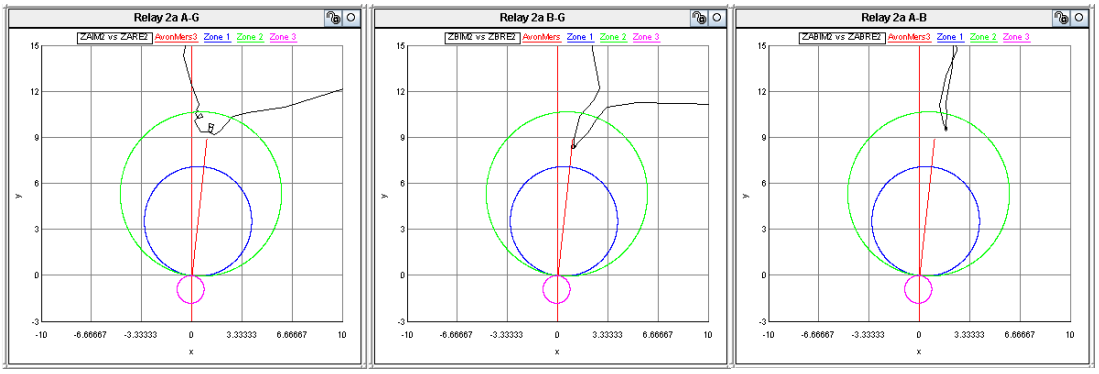

Figure 7.7: A-g, B-g and A-B impedance plots for relay 2a for a cross country fault at 95% of the line; ideally transposed lines with no mutual coupling, both transmission lines in service and no POTT scheme used

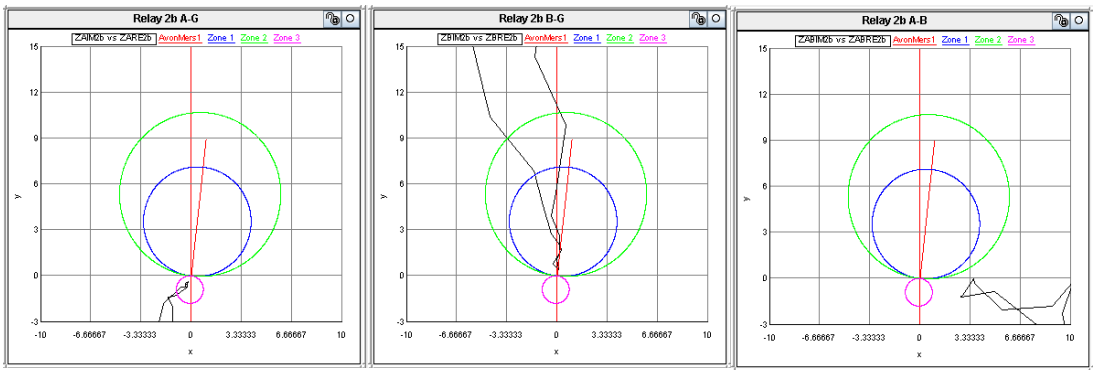

Figure 7.8: A-g, B-g and A-B impedance plots for relay 2b for a cross country fault at 95% of the line; ideally transposed lines with no mutual coupling, both transmission lines in service and no POTT scheme used

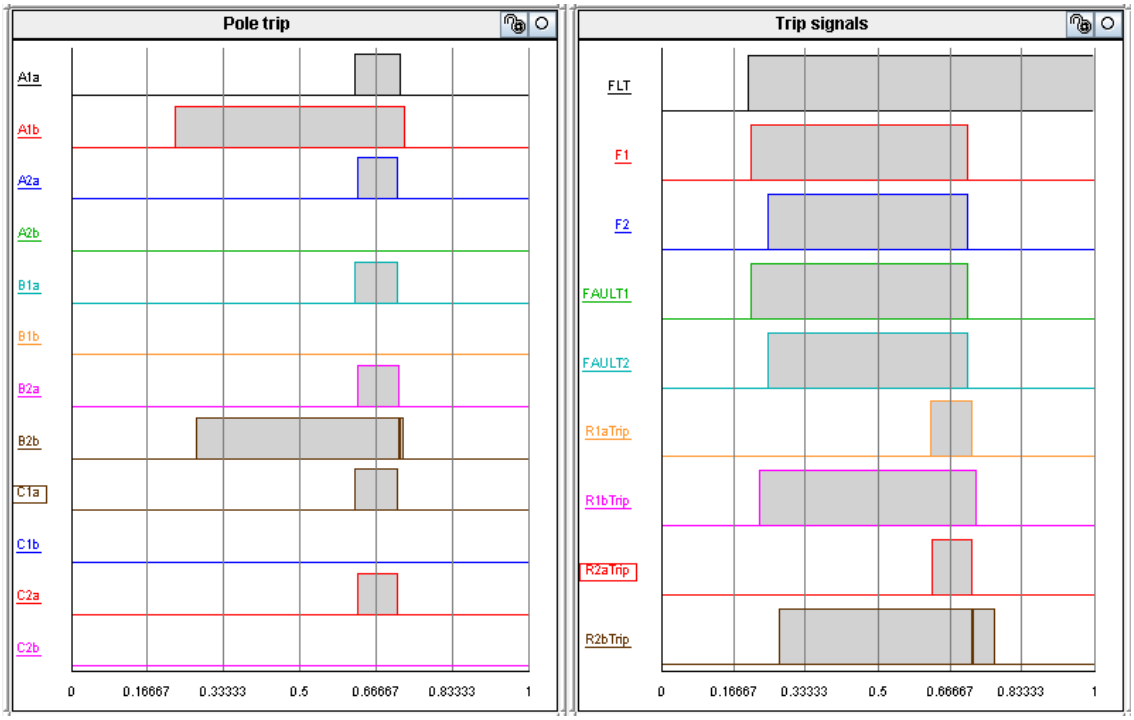

Figure 7.9: Relay single pole trip signal outputs (left) and real time model fault logic control inputs (right) for the cross country fault

The digital signals presented in Figure 7.9 have the following meaning:

Ax - Relay x (1a, 1b, 2a or 2b) issues a pole A trip

Bx - Relay x (1a, 1b, 2a or 2b) issues a pole B trip

Cx - Relay x (1a, 1b, 2a or 2b) issues a pole C trip

FLT- logic high when user initiates fault sequence

F1/FAULT 1 – logical high at the instant a fault is placed on line 1

F2/FAULT 2 – logical high at the instant a fault is placed on line 2

RxTrip – The instant relay x (1a, 1b, 2a or 2b) issues a trip

Upon inspection of the impedance plots in Figures 7.5-7.8 the following results are noted:

- Relay 1a sees impedance in the A-g, B-g and an A-B fault loops in zone 2,
- Relay 1b sees impedance in the A-g fault loop in zone 1 and B-g fault loop in zone 3,
- Relay 2a sees impedance in the A-g, B-g and an A-B fault loops in zone 2, and
- Relay 2b sees impedance in the B-g fault loop in zone 1 and A-g fault loop in zone 3.

These results demonstrate the classical problem experienced with a cross country fault that has been reprodued using the real time digital simulator. The relays at the sending end (relay 1a and relay 2a) see the faults as L-L-g faults when the faults are in fact L-g faults. Figure 7.10 shows a better illustration of the current distribution for this type of fault.

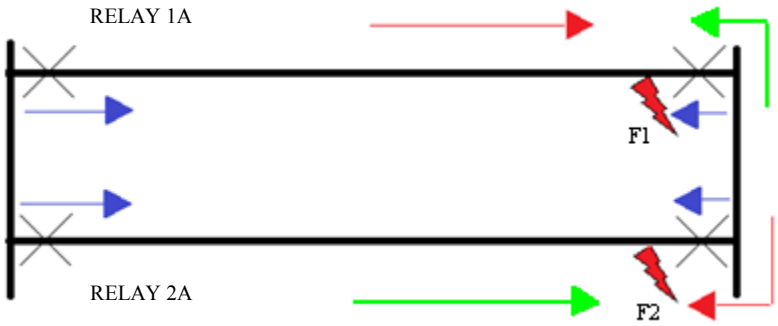

Figure 7. 10: Current distribution for a cross country fault on parallel transmission line circuits

From Figure 7.10, the blue arrows indicate the directions in which the actual current measurement is orientated at each relay from the forward looking zones 1 and 2. The red arrows show the direction of the fault current flowing towards faults F1 and F2 via line 1 and the green arrows represent currents flowing towards faults F1 and F2 via line 2. The relays at the receiving end will see a distinct current in the forward looking zone 1; however, the relays at the sending end (relay 1a and 2a) will see the resultant of the currents in both directions feeding the faults affecting the two phases. Where single pole tripping schemes are implemented, the relays at the sending end will operate incorrectly since they see a multi-phase fault. For this fault, the relays at the receiving end (relays 1b and 2b) issue a single pole trip and the relays at the sending end issue a three pole trip 400ms after the fault is placed on the network. For the protection scheme implemented for this fault, the operation is consistent with the definition of a cross country fault.

In a practical network application, where the breakers will operate on receipt of a trip signal from the relays, the current distribution will differ to a small extent. To investigate this, using only software relays, with the breakers now allowed to operate, the following fault was placed on the system:

A-g fault at 95% on transmission line 1

B-g fault at 95% on transmission line 2

The fault on transmission line 2 was again initiated 1 cycle after the fault appeared on transmission line 1, and the transmission lines were both ideally transposed with no mutual coupling between them. The results of this test are shown in Figures 7.11 to 7.15.

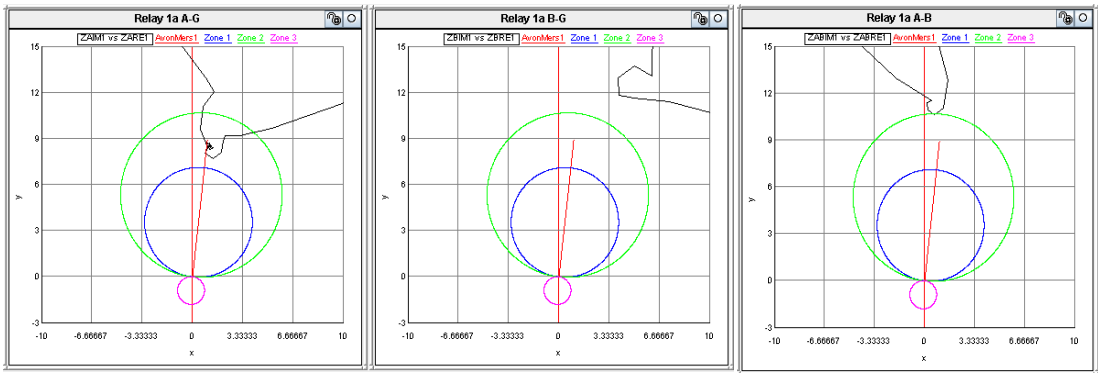

Figure 7.11: A-g, B-g and A-B impedance plots for relay 1a for a cross country fault at 95% of the line; ideally transposed lines with no mutual coupling, both transmission lines in service and no POTT scheme used

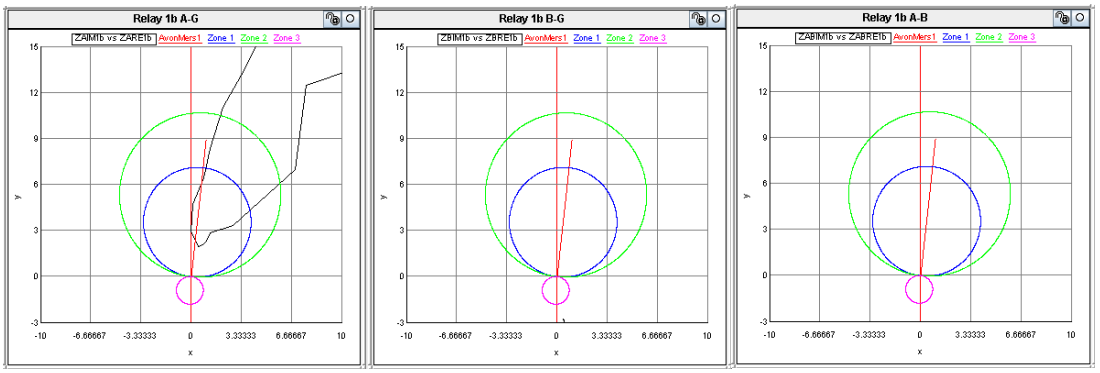

Figure 7.12: A-g, B-g and A-B impedance plots for relay 1b for a cross country fault at 95% of the line; ideally transposed lines with no mutual coupling, both transmission lines in service and no POTT scheme used

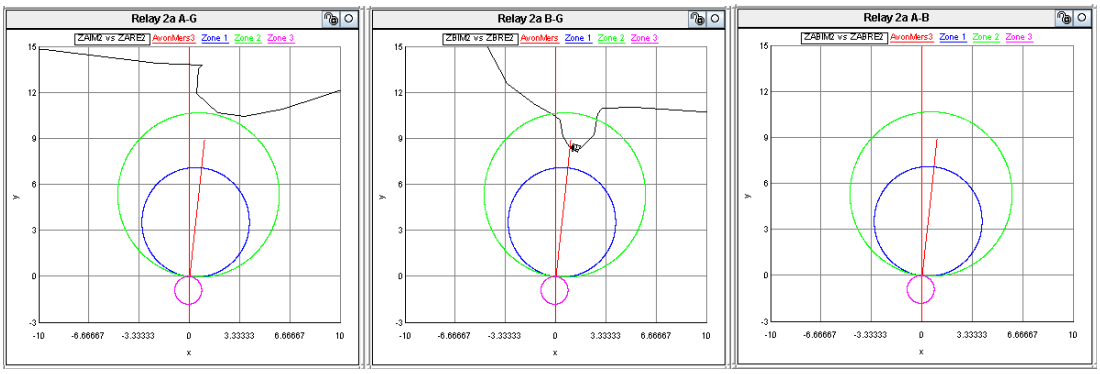

Figure 7.13: A-g, B-g and A-B impedance plots for relay 2a for a cross country fault at 95% of the line; ideally transposed lines with no mutual coupling, both transmission lines in service and no POTT scheme used

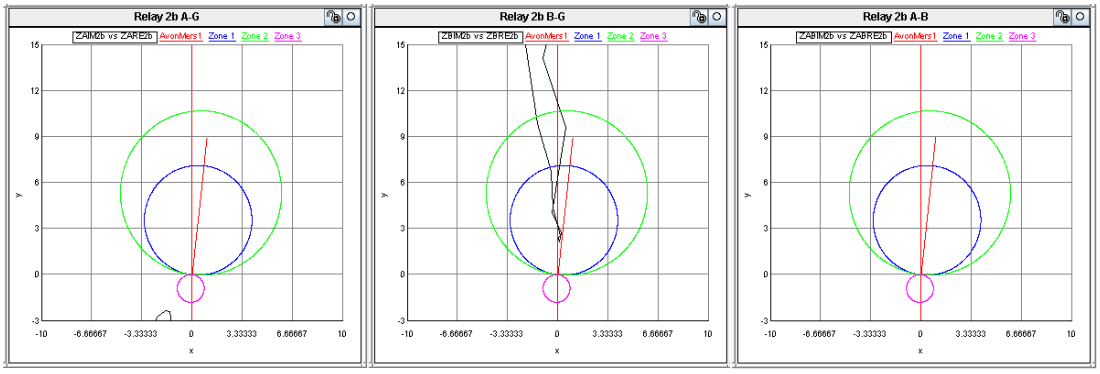

Figure 7.14: A-g, B-g and A-B impedance plots for relay 2b for a cross country fault at 95% of the line; ideally transposed lines with no mutual coupling, both transmission lines in service and no POTT scheme used

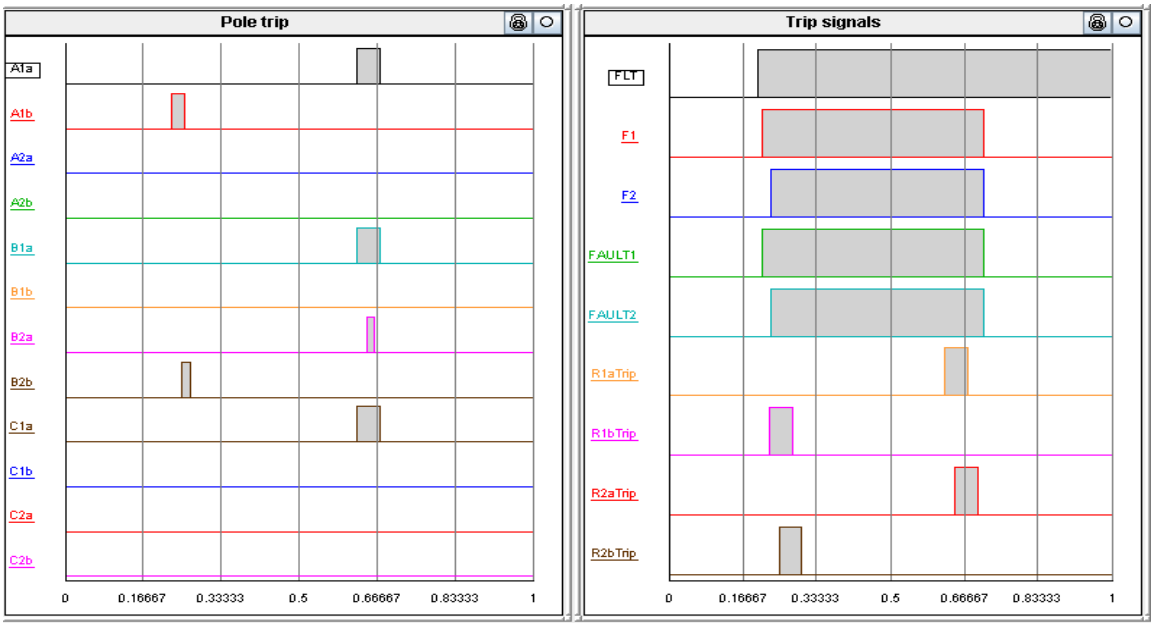

Figure 7.15: Relay single pole trip signal outputs (left) and real time model fault logic control inputs (right) for the cross country fault

For this fault scenario, the A-g fault on line 1 appears 1 cycle before the B-g fault appears on line 2. At the instant that the fault is placed on the system, relay 1b issues an instantaneous single pole trip and relay 1a picks up on A phase and starts to time 400ms. When the B-g fault appears on line 2, relay 2b issues an instantaneous single pole trip and relays 1a and 2a pick up on B phase and start to time 400ms. Since relay 1a has picked up on A phase and B phase, it issues a three pole trip, and relay 2a issues a single pole trip since it is isolated from the A-g fault on line 1 (breaker 1b opens first).

An additional case was then investigated in which the faults were placed on line 1 and line 2 at the same instant in time, again using only software relays, with the breakers allowed to operate, for the following faults placed on the system:

A-g fault at 95% on transmission line 1
B-g fault at 95% on transmission line 2

The results for this additional case are shown in Figures 7.16 to 7.20.

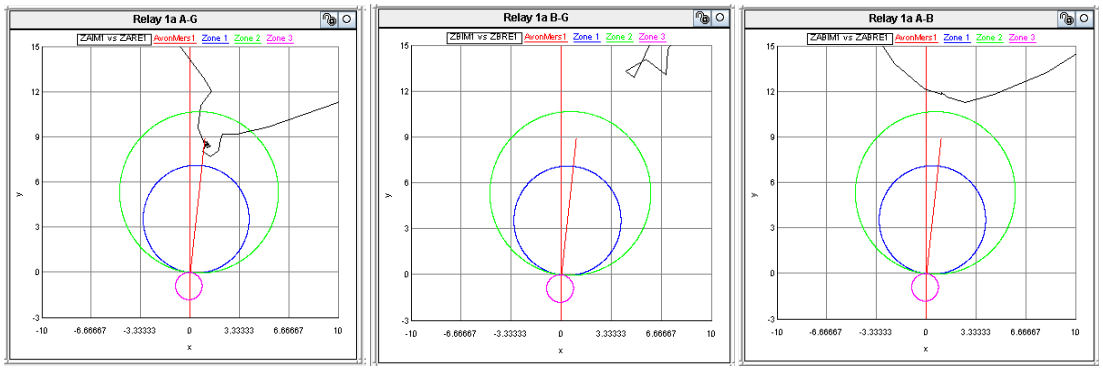

Figure 7.16: A-g, B-g and A-B impedance plots for relay 1a for a cross country fault at 95% of the line; ideally transposed lines, no mutual coupling, both transmission lines in service and no POTT scheme used

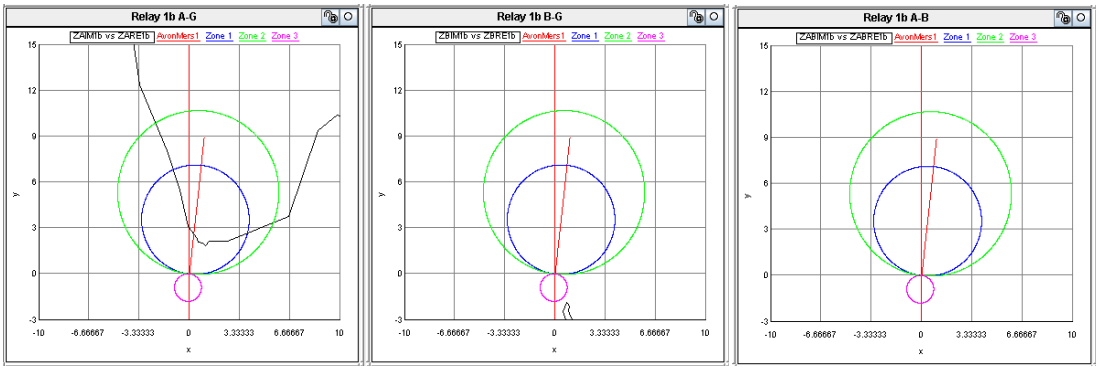

Figure 7.17: A-g, B-g and A-B impedance plots for relay 1b for a cross country fault at 95% of the line; ideally transposed lines, no mutual coupling present, both transmission lines in service and no POTT scheme used

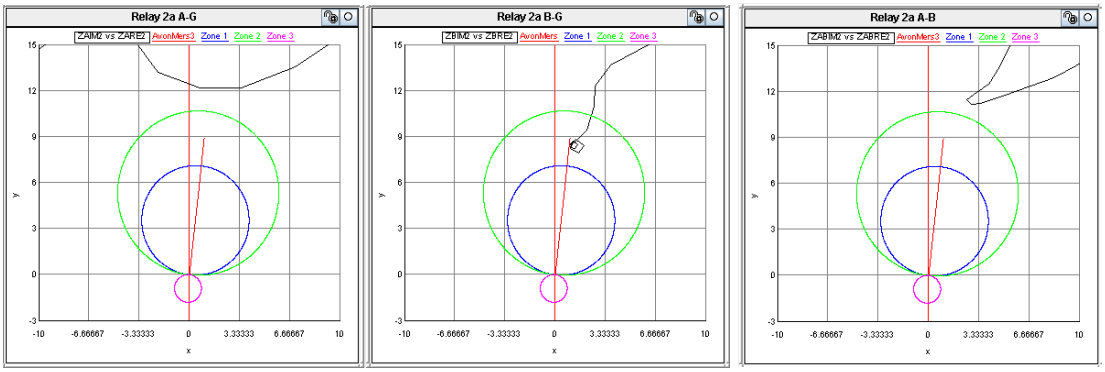

Figure 7.18: A-g, B-g and A-B impedance plots for relay 2a for a cross country fault at 95% of the line; ideally transposed lines, no mutual coupling present, both transmission lines in service and no POTT scheme used

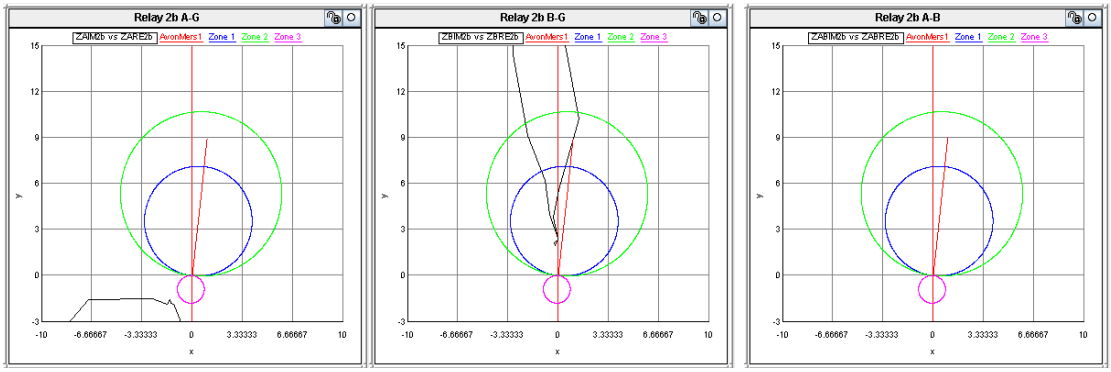

Figure 7.19: A-g, B-g and A-B impedance plots for relay 2b for a cross country fault at 95% of the line; ideally transposed lines, no mutual coupling present, both transmission lines in service and no POTT scheme used

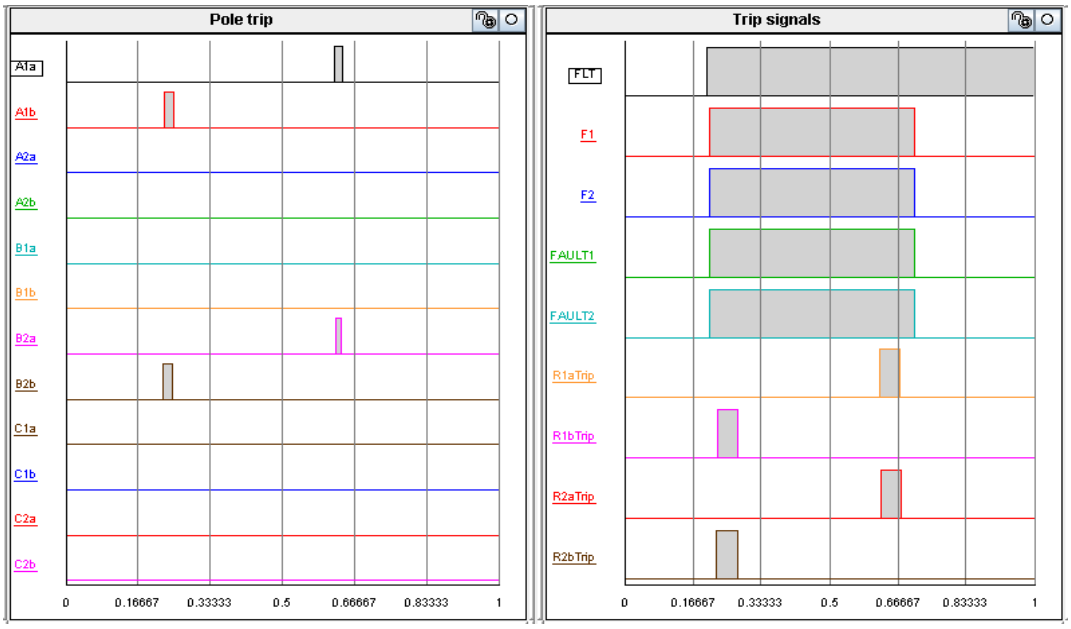

Figure 7.20: Relay single pole trip signal outputs (left) and real time model fault logic control inputs (right) for the cross country fault

For this fault, all relays issue a single pole trip since the relays at the receiving end (relays 1b and 2b) issue instantaneous single pole trips and the impedance trajectory of the A-B impedance loops of the sending end relays (relays 1a and 2a) do not have a chance to fall within any of the protection zones as seen in Figures 7.16 and 7.18. It is important to note that the closer the faults are to the remote end, the worse the effect of the cross country fault on the distance protection relay at the sending end. Although in the case considered above, all relays issue single pole trip signals, if for some reason the faults are cleared in a longer time due to slower breaker opening times, relay operating delays, breaker fail, etc., the relays at the sending end will operate incorrectly and issue three pole trip signals.

7.3. Investigating the effects of a cross country fault on the distance protection relay with a simple POTT scheme enabled

In many distance protection schemes used in South Africa, a simple POTT scheme as described in Chapter 2 is used to allow for fast tripping in response to faults on an overhead transmission line. The impact that a cross country fault has on a distance protection scheme where a POTT scheme is enabled was then investigated. Using only the RSCAD software relays, with the breakers allowed to operate, the following fault was placed on the system:

A-g fault at 95% on transmission line 1
B-g fault at 95% on transmission line 2

The fault on transmission line 2 was initiated 1 cycle after the fault appeared on transmission line 1, and the transmission lines were both ideally transposed with no mutual coupling between them. The results for this test are shown in Figures 7.21 to 7.25.

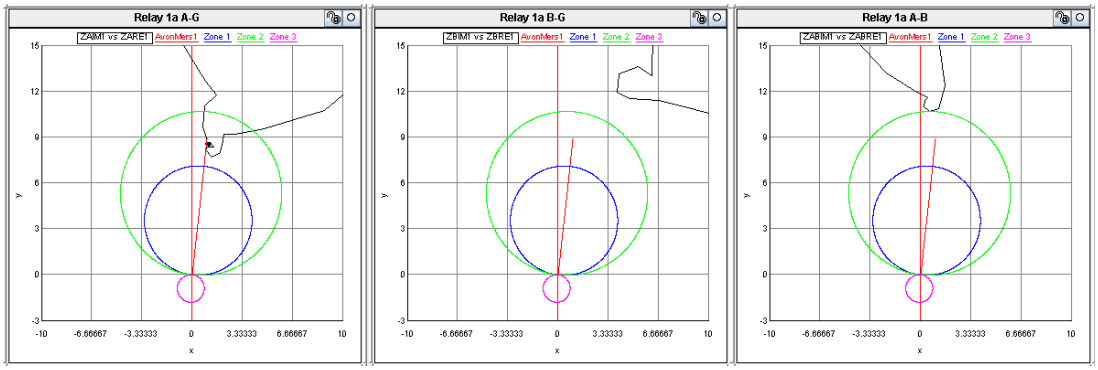

Figure 7.21: A-g, B-g and A-B impedance plots for relay 1a for a cross country fault at 95% of the line; ideally transposed lines, no mutual coupling present, both transmission lines in service and a simple POTT scheme used

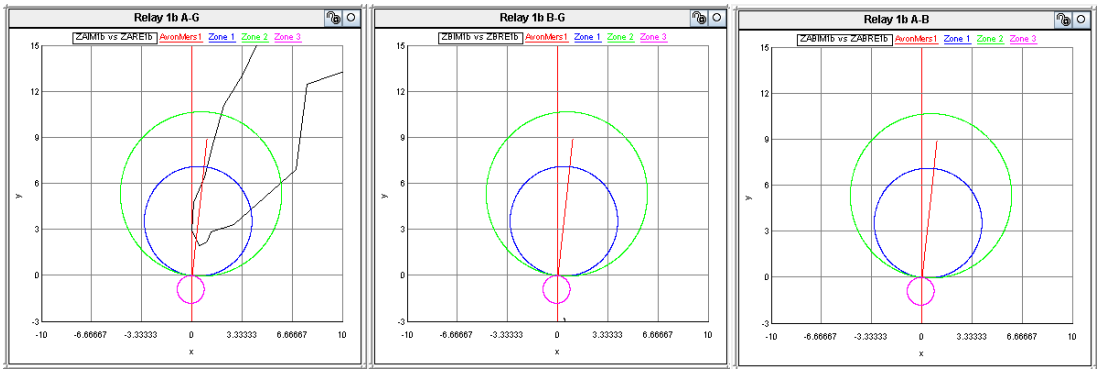

Figure 7.22: A-g, B-g and A-B impedance plots for relay 1b for a cross country fault at 95% of the line; ideally transposed lines, no mutual coupling present, both transmission lines in service and a simple POTT scheme used

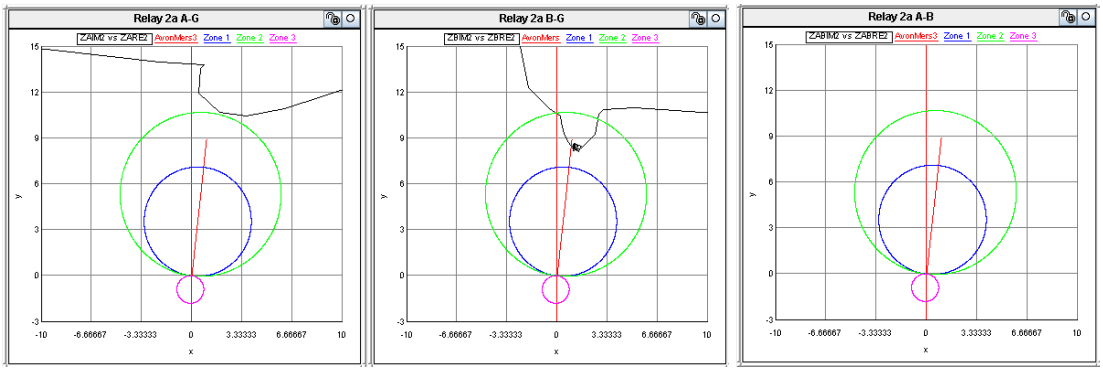

Figure 7.23: A-g, B-g and A-B impedance plots for relay 2a for a cross country fault at 95% of the line; ideally transposed lines, no mutual coupling present, both transmission lines in service and a simple POTT scheme used

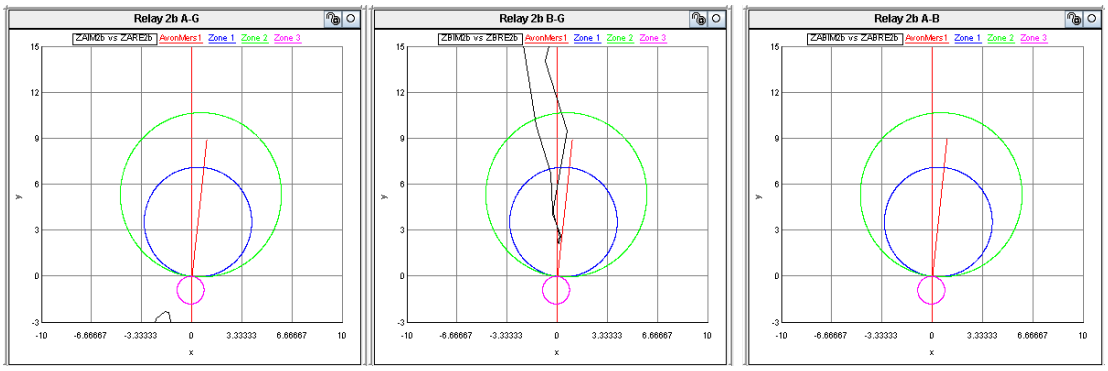

Figure 7.24: A-g, B-g and A-B impedance plots for relay 2b for a cross country fault at 95% of the line; ideally transposed lines, no mutual coupling present, both transmission lines in service and a simple POTT scheme used

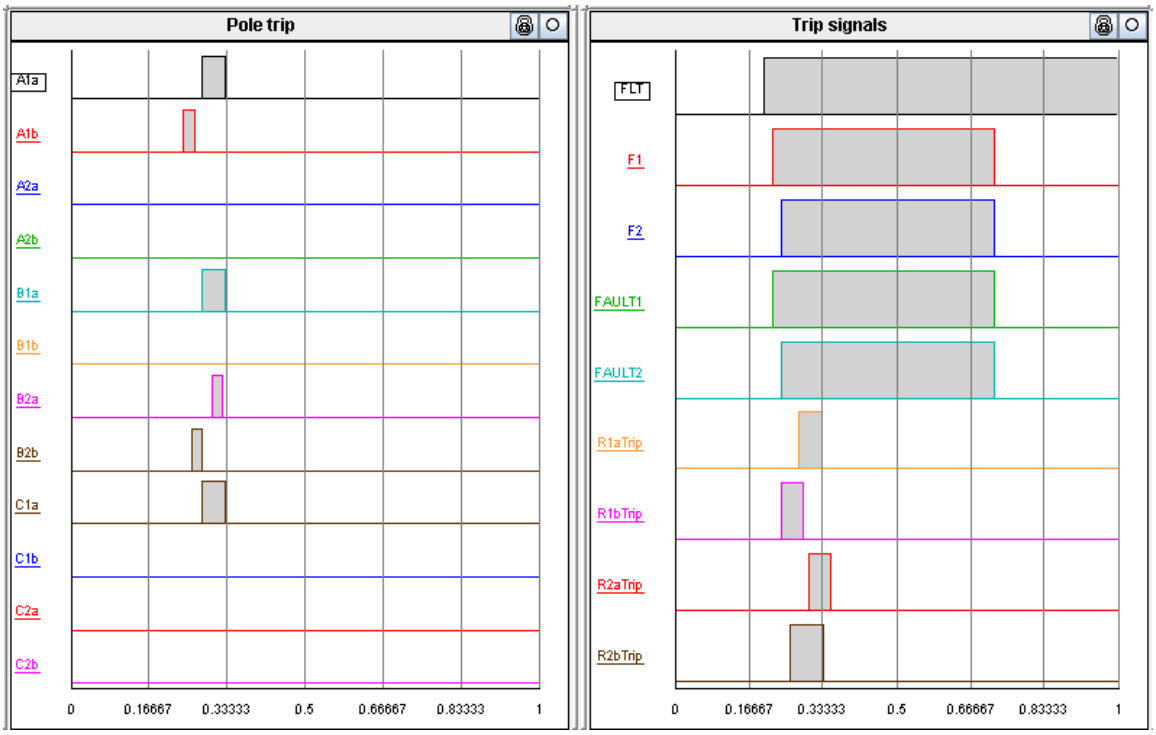

Figure 7.25: Relay single pole trip signal outputs (left) and real time model fault logic control inputs (right) for the cross country fault

For this fault scenario, the A-g fault on line 1 appears 1 cycle before the B-G fault appears on line 2. At the instant that the fault is placed on the system, relay 1b issues an instantaneous single pole trip and relay 1a picks up on A phase. When the B-g fault appears on line 2, relay 2b issues an instantaneous single pole trip and relays 1a and 2a pick up on B phase. Since relay 1a has picked up on A phase and B phase and receives permission to trip, it issues a near instantaneous three pole trip, and relay 2a issues a single pole trip since it is isolated from the A-g fault on line 1 (breaker 1b opens first) as noted from Figure 7.25.

From the analysis of the impedance trajectories, it can be seen that relays 1b and 2b, see A-g and B-g faults in zone 1 respectively, therefore only an instantaneous single pole trip is issued by these relays. The impedance trajectory for relay 1a shows that the relay sees fault impedance in the A-B fault loop at the edge of zone 2, therefore a three pole trip was issued. The impedance trajectory for relay 2a sits just outside the zone 2 boundary in the A-B impedance loop therefore a three pole trip was not issued for this particular fault. The relay 2a narrowly misses operating incorrectly and issuing a three pole trip. In the event of the cross country fault being further down the transmission line, the duration between the two faults being longer or any other factor that could contribute to the impedance trajectory of the A-B loop entering zone 2, the relay will issue an incorrect three pole trip.

7.4. Investigating the effects of a cross country fault on the distance protection relay with a simple POTT2 scheme enabled using the RSCAD distance protection relays only

Chapter 2 described a particular distance protection permissive tripping scheme that makes use of phase-segregated permissive signals from the remote end to provide selectivity at the sending end in order to eliminate the impact that a cross country fault has on the simple POTT scheme considered in the previous studies. This phase-segregated permissive scheme is more commonly known as a POTT2 scheme by most relay manufacturers. The POTT2 scheme needs to be operative on both parallel transmission lines in order to ensure single pole tripping.

The principles of the POTT2 distance protection scheme can be explained as follows.
For a cross country fault, the relays at the receiving end of the line will see a single phase to ground fault (P-g) and the sending end relays will see a phase to phase to ground (P-P-g) fault due to the current distributions discussed earlier. The relays at the receiving end will issue a single pole trip but the relays at the sending end will issue a three pole trip. For a standard POTT scheme, in the presence of a cross country fault, the sending end relay will receive permission to trip from the receiving end relay. However, because the fault is seen as a P-P-g fault by the sending end relay in its zone 2 and the sending end relay receives a permission to trip it will issue a three pole trip when the fault is actually a P-g fault. This problem will occur at the sending end relays of both parallel transmission lines, and is overcome by the introduction of a second POTT channel to distinguish between single phase to ground faults and faults involving more than one phase.
In this improved scheme, one signalling channel is used for transmitting a permission to trip for single phase faults (KEY1) and the second channel is used to transmit a permission to trip for multi-phase faults (KEY3). The POTT2 scheme works such that the internal logic of the

distance protection relay is set up to allow single pole tripping for the receipt of KEY1 only and the detection of a single phase to ground fault. A three pole trip is issued only when the relay receives a KEY1 signal, a KEY3 signal and the relay detects a multi-phase fault [61].

For example, if the sending end relay receives a KEY 1 permission to trip and identifies the fault as a single phase to ground fault, the relay will issue a single pole trip. If the sending end relay receives a KEY1 permission to trip, does not receive a KEY 3 permission to trip and identifies the fault as a phase to phase to ground fault the relay will not issue a trip. The tripping will be suspended until:

1) The sending end relay receives a KEY 3 permission to trip, or
2) The sending end relay fault identification changes to detect a single phase to ground fault.

The POTT2 scheme requires that both transmission lines have the POTT2 scheme enabled so that the sending end relay will change its fault identification from a multi-phase fault to a single phase fault once the receiving end breakers open to isolate the fault on the transmission line. The SEL 421 distance protection relay uses this principle to implement the POTT2 protection scheme. Before the SEL hardware relay can be used to test the POTT2 scheme, the RSCAD software relays must first be used to test the scheme as the impedance plots from the RSCAD software relays will provide the user with a clear understanding of:

- the current distribution,
- what the relay will see, and
- provide an insight into the relay's behaviour and response to the fault.

The generic RSCAD distance protection relay model does not have capabilities of a built in POTT2 scheme like the SEL 421 relay, therefore the logic for a POTT2 scheme had to be built using standard library components available in the RSCAD DRAFT user component library. The additional POTT2 scheme logic developed in RSCAD for this thesis is shown in Figures 7.26 to 7.29.

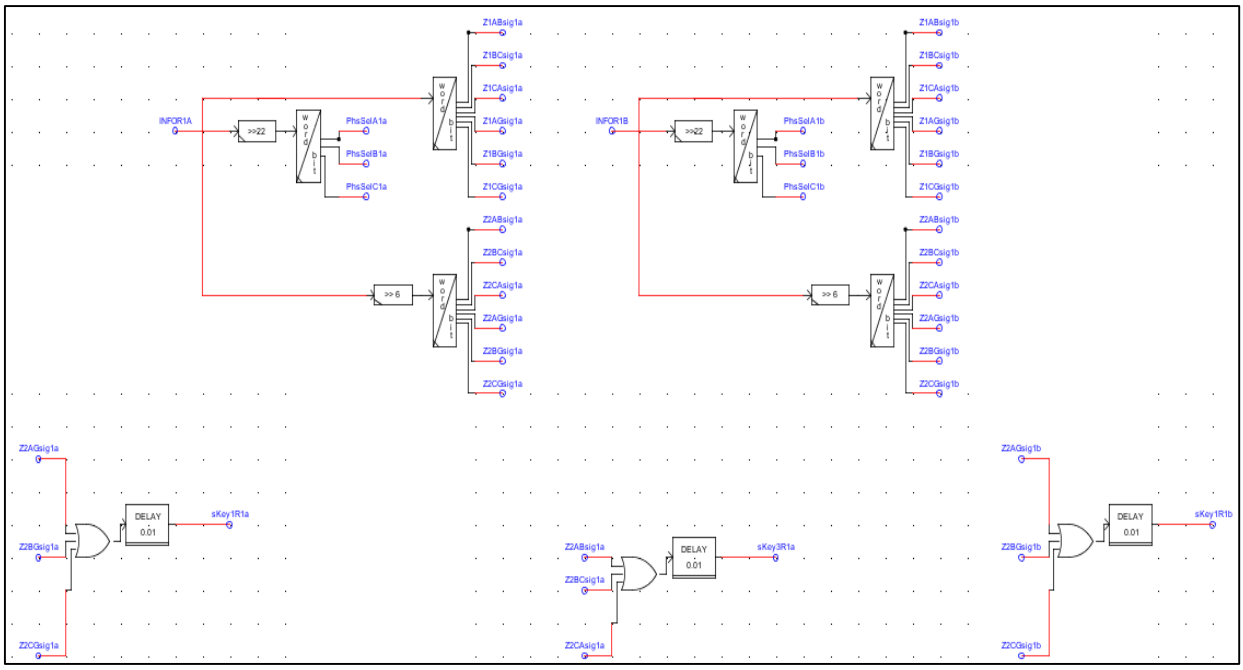

Figure 7.26: Additional POTT2 scheme logic designed using RSCAD library components

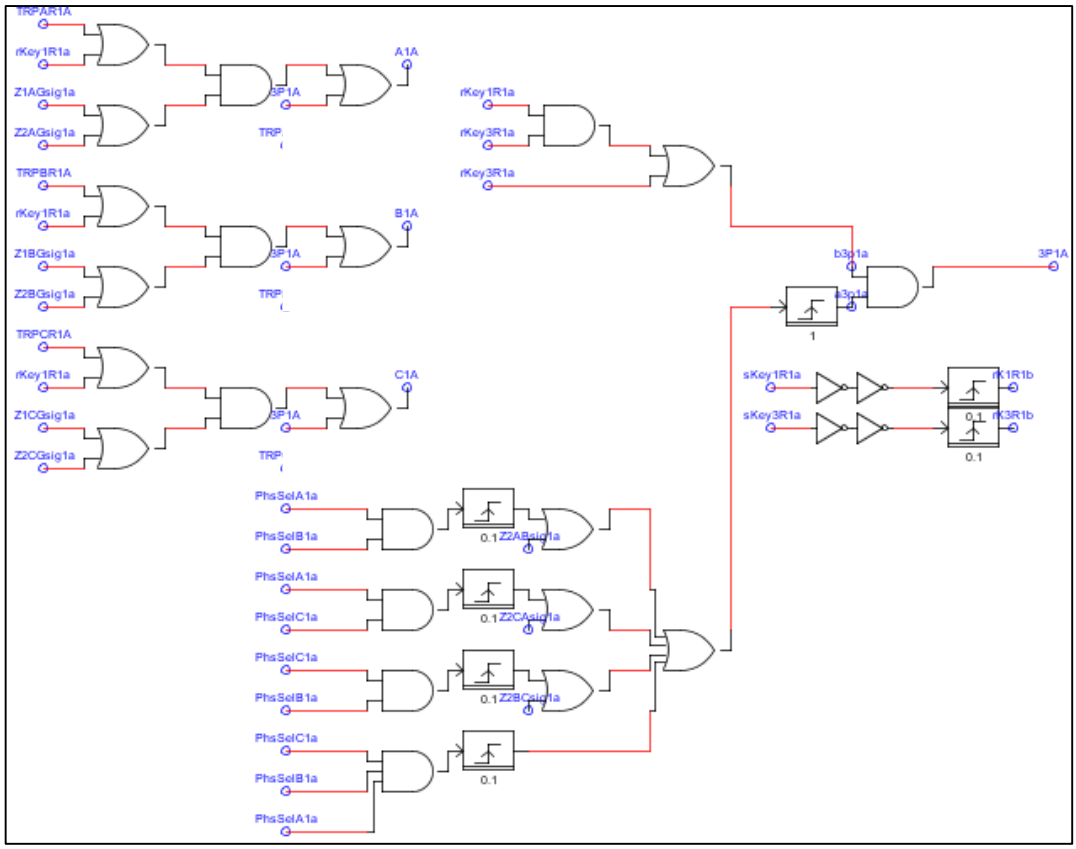

Figure 7.27: Additional POTT2 scheme logic designed using RSCAD library components

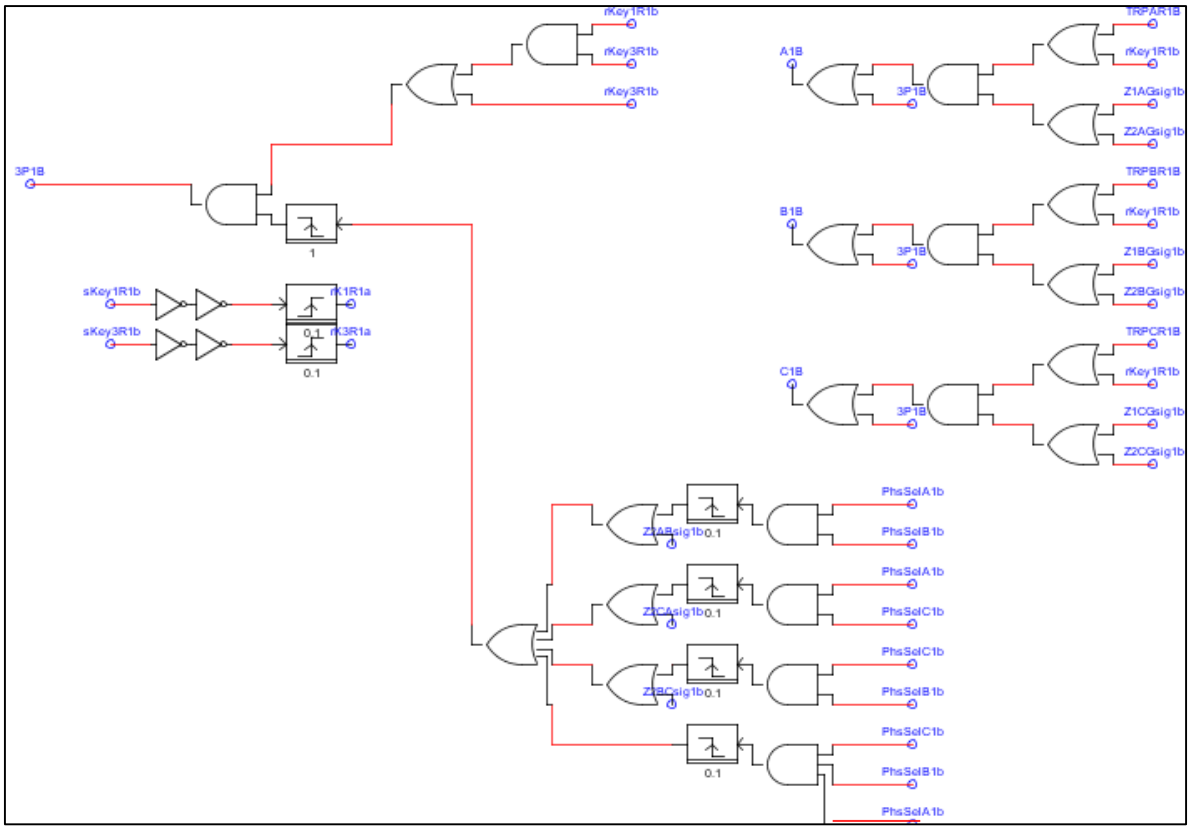

Figure 7.28: Additional POTT2 scheme logic designed using RSCAD library components

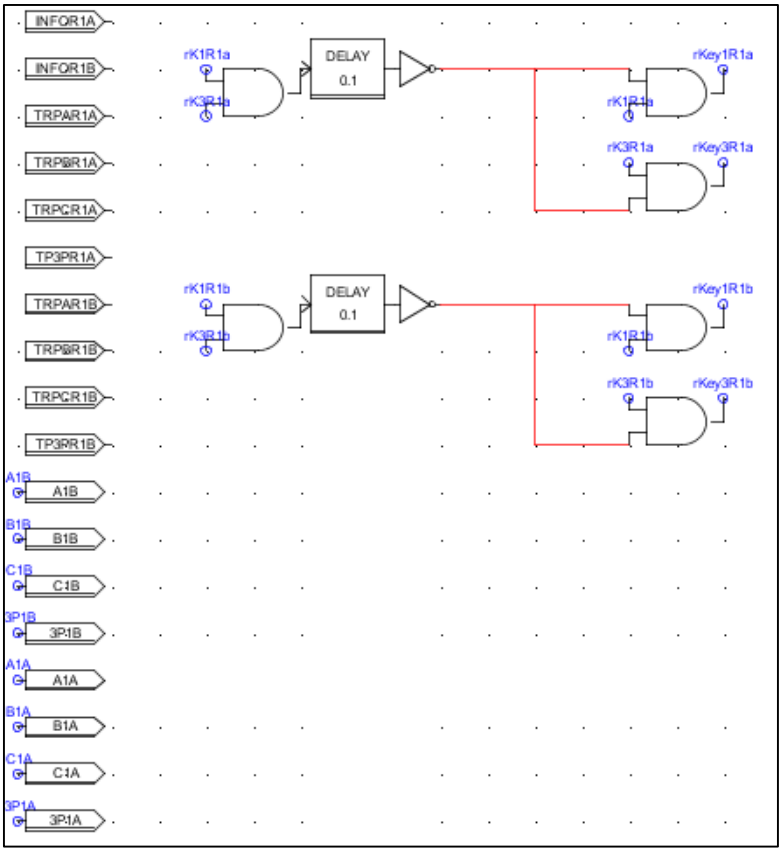

Figure 7.29: Additional POTT2 scheme logic designed using RSCAD library components

Figures 7.26 to 7.29 illustrate the POTT2 distance protection scheme that was designed to protect the parallel transmission lines for this study case replicating the performance of this type of protection scheme discussed earlier. Once the protection scheme was designed, it was tested for functionality. Using only software relays with the POTT2 scheme designed above enabled, and with the breakers allowed to operate, the following faults were placed on the system:

A-g fault at 95% on transmission line 1
B-g fault at 95% on transmission line 2

The fault on transmission line 2 was initiated 1 cycle after the fault appeared on transmission line 1, and the transmission lines were both ideally transposed with no mutual coupling between them. The results for this test are shown in Figures 7.30 to 7.35.

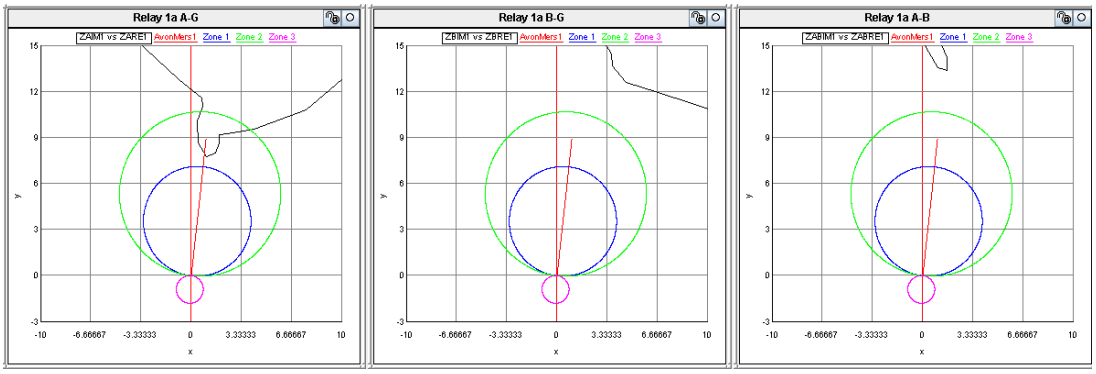

Figure 7.30: A-g, B-g and A-B impedance plots for relay 1a for a cross country fault at 95% of the line; ideally transposed lines, no mutual coupling present, both transmission lines in service and a POTT2 scheme used

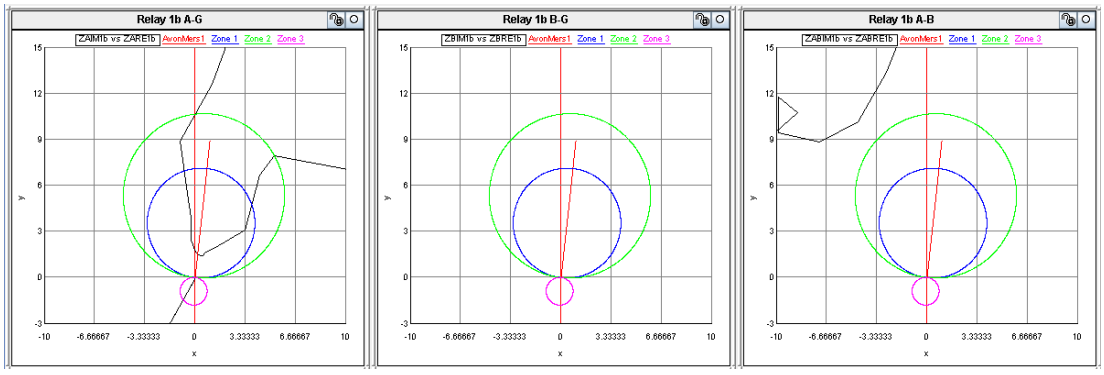

Figure 7.31: A-g, B-g and A-B impedance plots for relay 1b for a cross country fault at 95% of the line; ideally transposed lines, no mutual coupling present, both transmission lines in service and a POTT2 scheme used

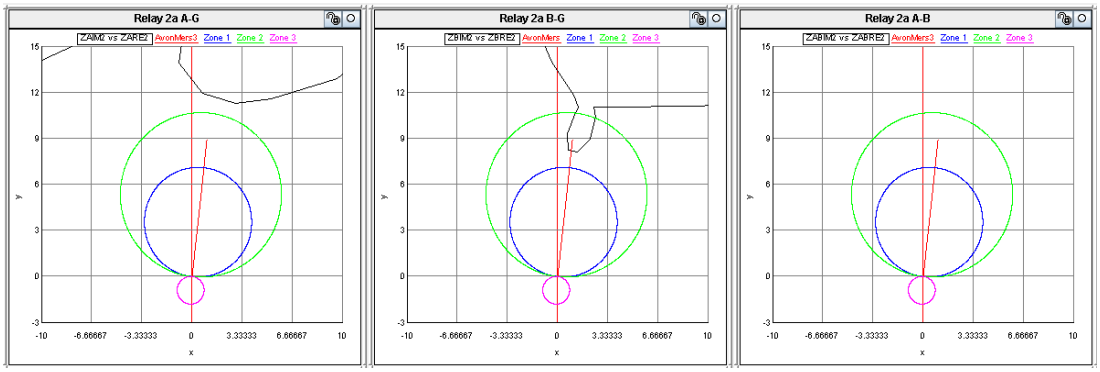

Figure 7.32: A-g, B-g and A-B impedance plots for relay 2a for a cross country fault at 95% of the line; ideally transposed lines, no mutual coupling present, both transmission lines in service and a POTT2 scheme used

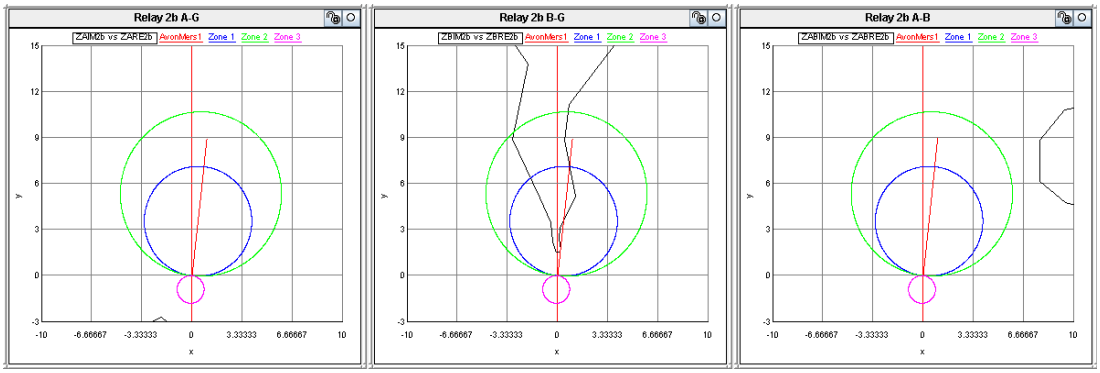

Figure 7.33: A-g, B-g and A-B impedance plots for relay 2b for a cross country fault at 95% of the line; ideally transposed lines, no mutual coupling present, both transmission lines in service and a POTT2 scheme used

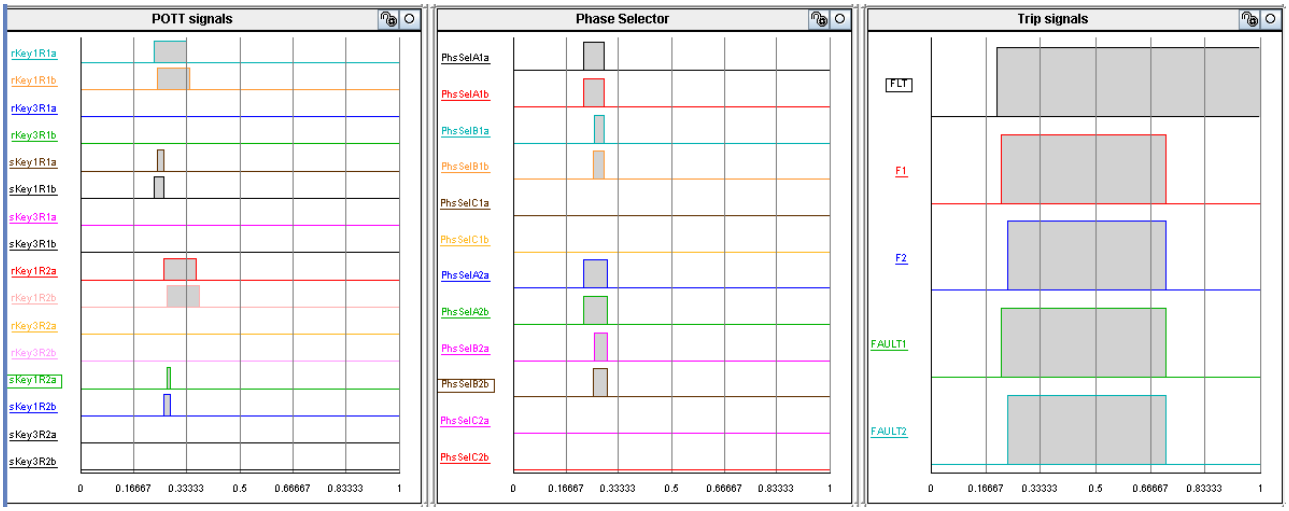

Figure 7.34: Relay POTT2 signal monitoring (left) relay phase selector signal monitoring (centre) and fault control logic monitoring (right) for a cross country fault.

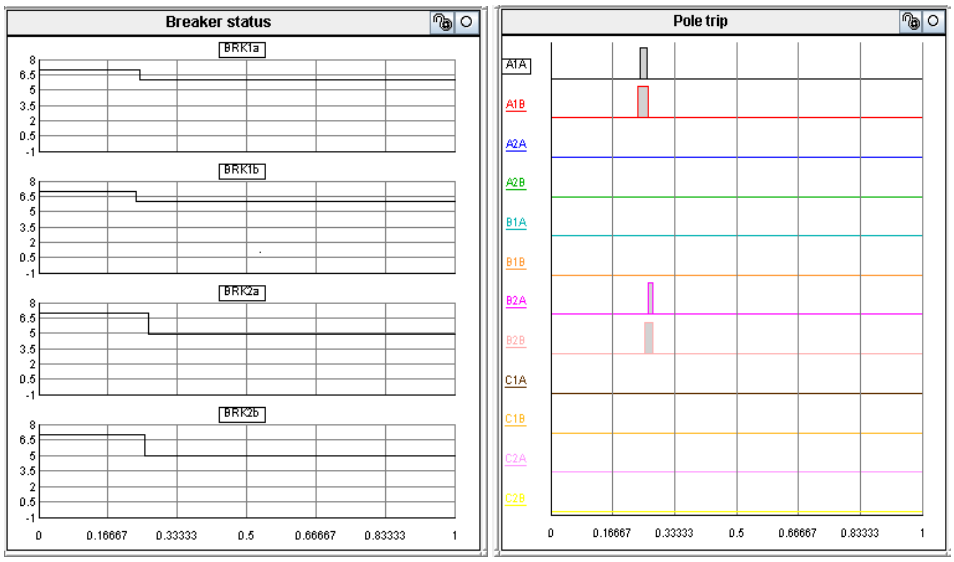

Figure 7.35: Breaker trip signal monitoring (left) and relay single pole trip signal monitoring (right) for a cross country fault

The signals in Figure 7.34 have the following meaning:
sKey1Rx – a KEY1 signal is sent from relay x (1a, 1b, 2a or 2b)
rKey1Rx – a KEY1 signal is received by relay x (1a, 1b, 2a or 2b)
sKey3Rx – a KEY3 signal is sent from relay x (1a, 1b, 2a or 2b)
rKey3Rx – a KEY3 signal is received by relay x (1a, 1b, 2a or 2b)
PhsSelAx – relay x (1a, 1b, 2a or 2b) detects a fault on phase A
PhsSelBx – relay x (1a, 1b, 2a or 2b) detects a fault on phase B
PhsSelCx – relay x (1a, 1b, 2a or 2b) detects a fault on phase C
Previously defined signals have the same meaning.

The signals in Figure 7.35 have the following meaning:
BRKx – The signal status for the breaker at point x (1a, 1b, 2a or 2b) showing the binary to decimal converted breaker status. E.g. 7 represents 111 in binary which means all poles of the breaker are closed. 6 represents 110 in binary which means pole A is open and all other poles are closed, etc.
Previously defined signals have the same meaning.

From the results in the figures above it can be seen that all relays now issue a single pole trip when the POTT2 scheme logic is used. The sending end relay receives a KEY1 permission to trip, does not receive a KEY 3 permission to trip and identifies the fault as a phase to phase to ground fault so that the relay will not issue a trip. Note that although the impedance trajectories for this fault and current distribution, combined with the POTT2 protection scheme implemented to protect this parallel transmission line, showed no impedance locus falling

within the A-B loop reach, the phase selectors for the RSCAD software relays indicate that the relay did see the cross country fault. The protection scheme for this fault type and operating scenario therefore did operate as required and no three pole trip was issued during this cross country fault.

7.5. Investigating the effects of a cross country fault on the distance protection relay with a POTT2 scheme enabled using the RSCAD distance protection relays and the SEL 421 hardware distance protection relays

The SEL 421 relay allows for the use of a manufacturer defined POTT 2 scheme as described earlier to rectify the problems associated with single pole tripping for cross county faults. This POTT2 scheme on the SEL 421 relays was studied, implemented and tested using the real time simulation model of the study system. The interface between the SEL 421 hardware relays and the RSCAD model for the tests of the POTT2 scheme is shown in Figure 7.36.

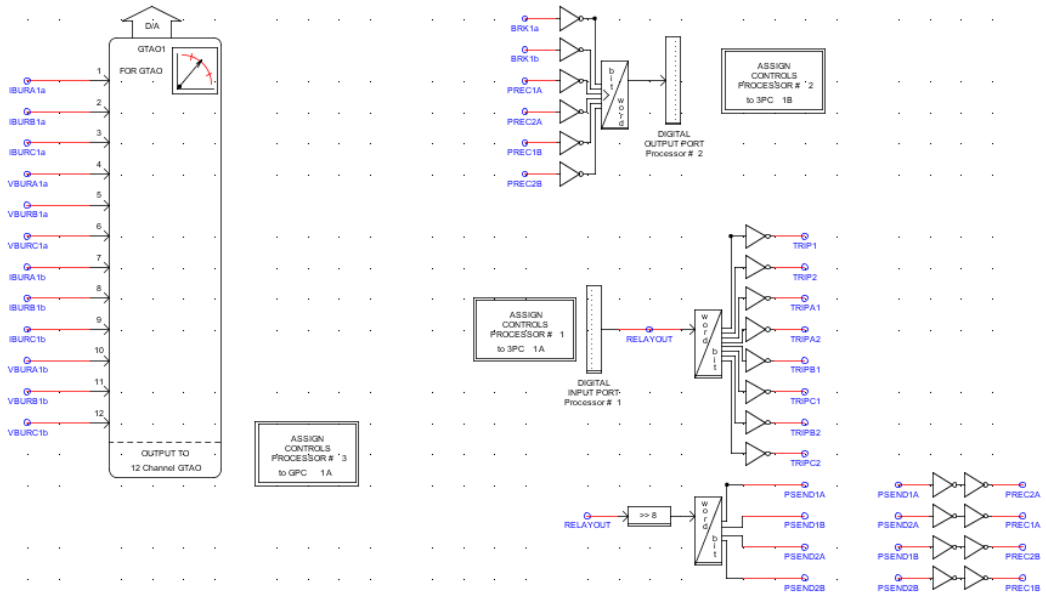

Figure 7.36: RSCAD DRAFT model components for the interface between the relay and the real time model for a closed loop hardware connection with a POTT2 scheme implemented on the hardware relays

Since only two SEL 421 distance protection relays were available for this stage of the study, the hardware relays were configured to protect line 1 and the RSCAD software relays were configured to protect line 2 with the POTT2 scheme implemented in all protection relays (both software and hardware). Using software relays on line 2 and hardware relays on line 1, with the breakers allowed to operate, the following fault was placed on the system:

A-g fault at 95% on transmission line 1

B-g fault at 95% on transmission line 2

The fault on transmission line 2 was initiated 1 cycle after the fault appeared on transmission line 1, and the transmission lines were both ideally transposed with no mutual coupling between them. The results for this test are shown in Figures 7.37 to 7.43.

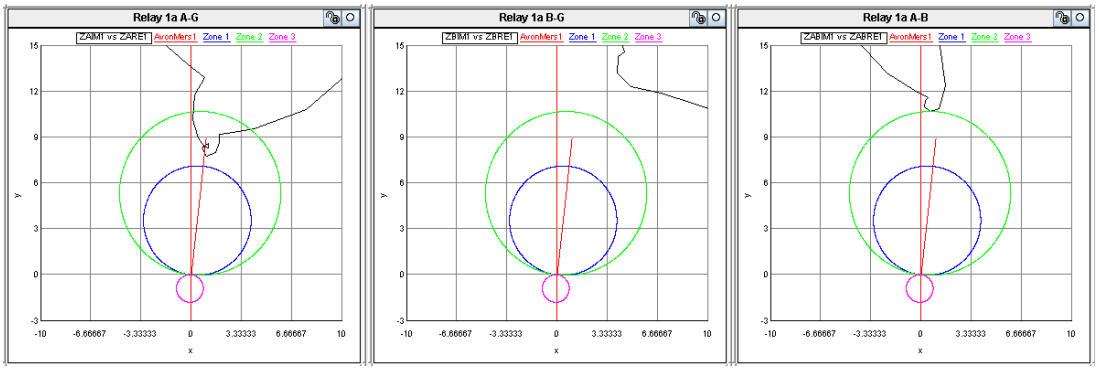

Figure 7.37: A-g, B-g and A-B impedance plots for relay 1a for a cross country fault at 95% of the line; ideally transposed lines, no mutual coupling present, both transmission lines in service and a POTT2 scheme used

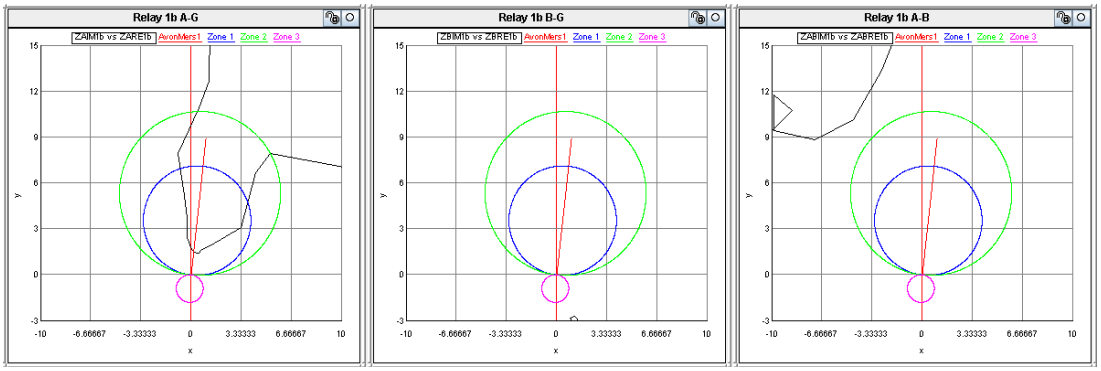

Figure 7.38: A-g, B-g and A-B impedance plots for relay 1b for a cross country fault at 95% of the line; ideally transposed lines, no mutual coupling present, both transmission lines in service and a POTT2 scheme used

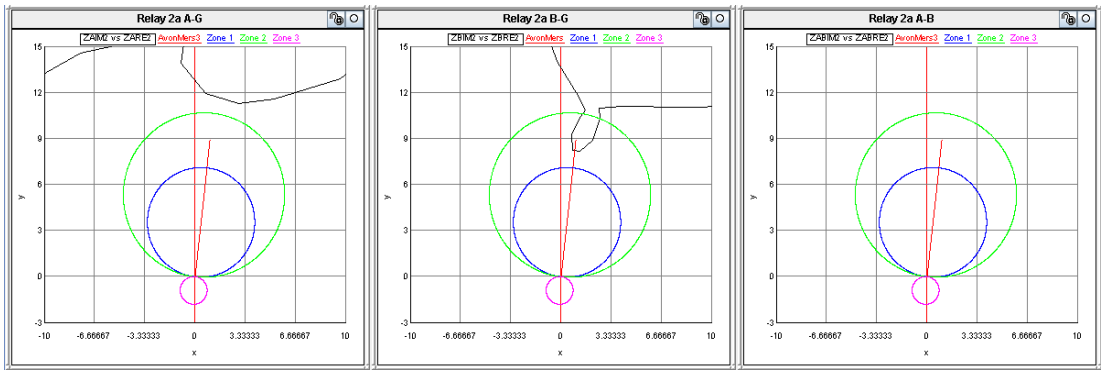

Figure 7.39: A-g, B-g and A-B impedance plots for relay 2a for a cross country fault at 95% of the line; ideally transposed lines, no mutual coupling present, both transmission lines in service and a POTT2 scheme used

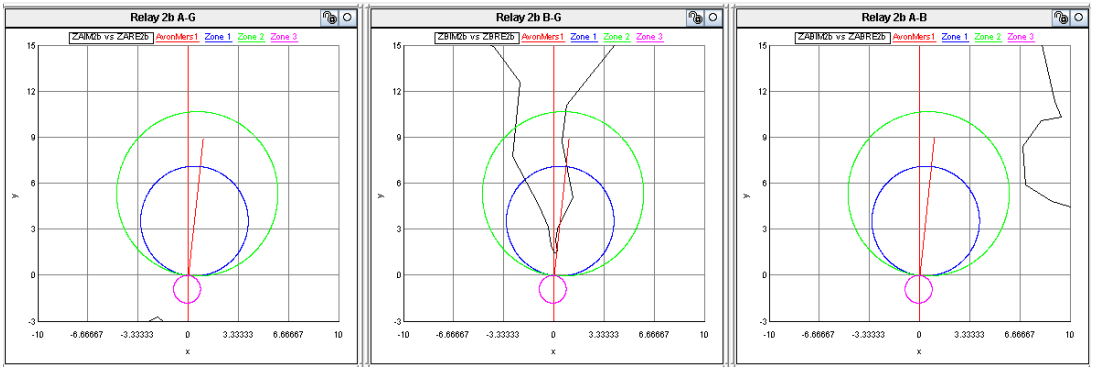

Figure 7.40: A-g, B-g and A-B impedance plots for relay 2b for a cross country fault at 95% of the line; ideally transposed lines, no mutual coupling present, both transmission lines in service and a POTT2 scheme used

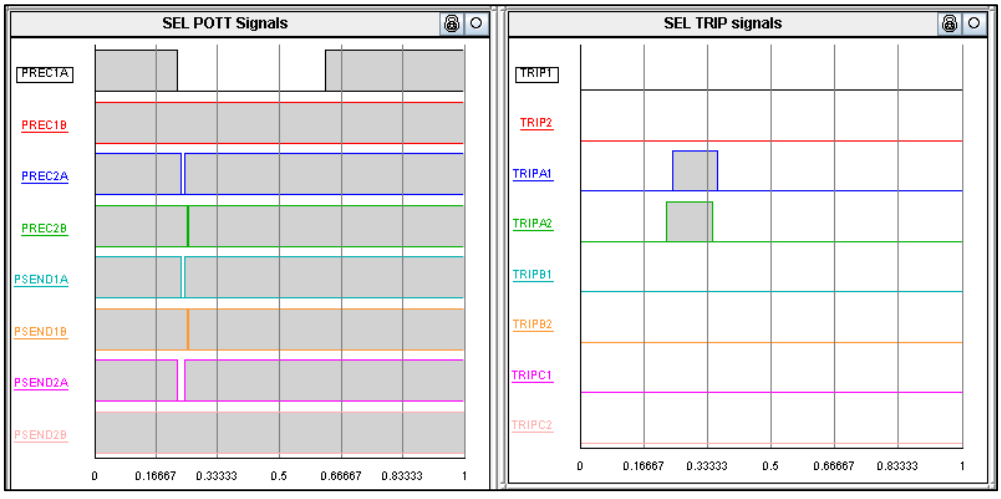

Figure 7.41: Hardware relay POTT2 signal monitoring on line 1 (left) and relay single pole trip signal monitoring on line 1 (right) for a cross country fault

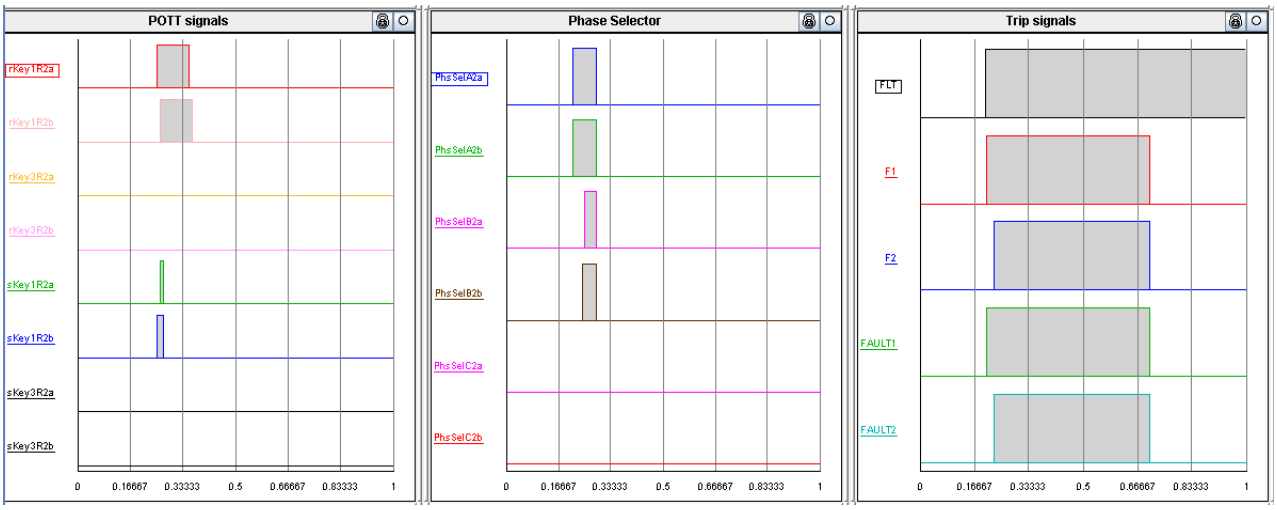

Figure 7.42: Software relay POTT2 signal monitoring (left) relay phase selector signal monitoring (centre) and fault control logic monitoring (right) for a cross country fault for the relays on line 2.

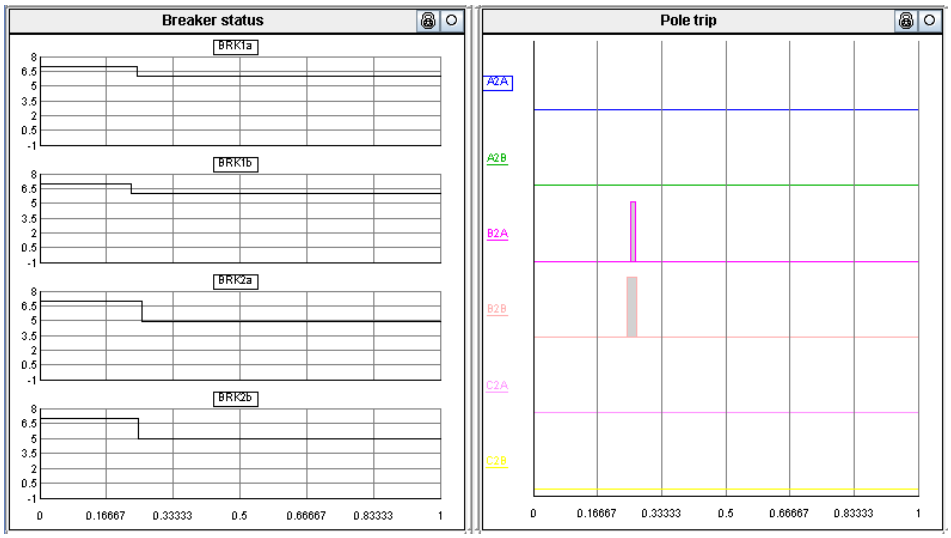

Figure 7.43: Breaker trip signal monitoring of all breakers (left) and relay single pole trip signal monitoring of the software relays on line 2 (right) for a cross country fault

The signals in the left plot in Figure 7.41 have the following meaning:

PSEND1A-Permission to trip sent on POTT channel 1 of the sending end relay

PREC1A-Permission to trip received on POTT channel 1 of the sending end relay

PSEND1B-Permission to trip sent on POTT channel 2 of the sending end relay

PREC1B-Permission to trip received on POTT channel 2 of the sending end relay

PSEND2A-Permission to trip sent on POTT channel 1 of the receiving end relay

PREC2A-Permission to trip received on POTT channel 1 of the receiving end relay

PSEND2B-Permission to trip sent on POTT channel 2 of the receiving end relay

PREC2B-Permission to trip received on POTT channel 2 of the receiving end relay

TRIP 1 – Indicates a three pole trip from relay 1a
TRIP 2 – Indicates a three pole trip from relay 1b
TRIPA1 – Indicates a single pole trip on phase A from relay 1a
TRIPB1 – Indicates a single pole trip on phase B from relay 1a
TRIPC1 – Indicates a single pole trip on phase C from relay 1a
TRIPA2 – Indicates a single pole trip on phase A from relay 1b
TRIPB2 – Indicates a single pole trip on phase B from relay 1b
TRIPC2 – Indicates a single pole trip on phase C from relay 1b

Where POTT channel 1 represents the KEY1 signal and POTT channel 2 represents the KEY3 signal used for the RSCAD software relay as described in section 7.4.

From the results in Figures 7.37 to 7.43 it can be seen that for this fault scenario the relay at the sending end of line 1 sees the fault as an A-B-g fault, as it can be noted that the impedance locus in the A-B impedance loop touched the edge of zone 2 relay characteristic. The relay at the receiving end of line 1 sees an A-g fault in zone 1 and issues an instantaneous trip command and a permission to trip to the remote end on channel 1 only, since it recognised the fault as a fault involving only one phase. The relay at the sending end clearly sees the fault as one involving more than one phase since a permission to trip to the remote end is sent on channel 1 and channel 2 of the POTT2 protection scheme. Note that even though the sending end relay sees a multiphase fault, since it receives a permission to trip from the remote end on channel 1 only it does not immediately issue a three pole trip command, since it has not received a permission to trip on channel 2 indicating that a fault involving only one phase has occurred in front of the relay at the remote end. Once the relay at the remote end (relay 1b) issues a trip and the breaker successfully opens to clear the fault from that end, the relay at the sending end then sees the fault as a phase to ground fault, and issues a single pole trip. The above operation confirms the functionality of the POTT2 scheme using the SEL 421 distance protection relay.

The results of the test above indicate that there exists a reliable way of resolving the problem of three pole tripping when a cross country fault is present on parallel transmission lines where a single pole trip scheme is implemented. The above test was then repeated for a variety of fault positions and faults involving different phases and in each case the tests showed similar results to those seen above (a POTT 2 scheme will prevent three pole tripping during a cross country fault where single pole tripping is implemented) but the detailed results from, these tests are not shown in order to avoid unnecessary repetition.

The next section considers the response of the POTT 2 scheme and the distance protection relays in the presence of cross country faults when the parallel transmission lines are both untransposed and mutually coupled.

7.6. Investigating the effects of a cross country fault with the addition of mutual coupling and the transmission line being untransposed

Now that the nature of a cross country fault is fully understood, and the design and testing of a distance protection scheme to protect parallel transmission lines in the presence of a cross country fault has been verified, under ideal conditions, this section considers the issue again but in the presence of more challenging practical conditions involving untransposed lines that are mutually coupled.

As in the previous studies in this chapter, the issue was tackled initially using only software relays, with the breakers forced to stay closed and the following fault was placed on the system with no POTT scheme enabled:

A-g fault at 95% on transmission line 1
B-g fault at 95% on transmission line 2

The fault on transmission line 2 was initiated 1 cycle after the fault appeared on transmission line 1, and the transmission lines were both untransposed and mutual coupling between them was represented. The results of this test are shown in Figures 7.44 to 7.47.

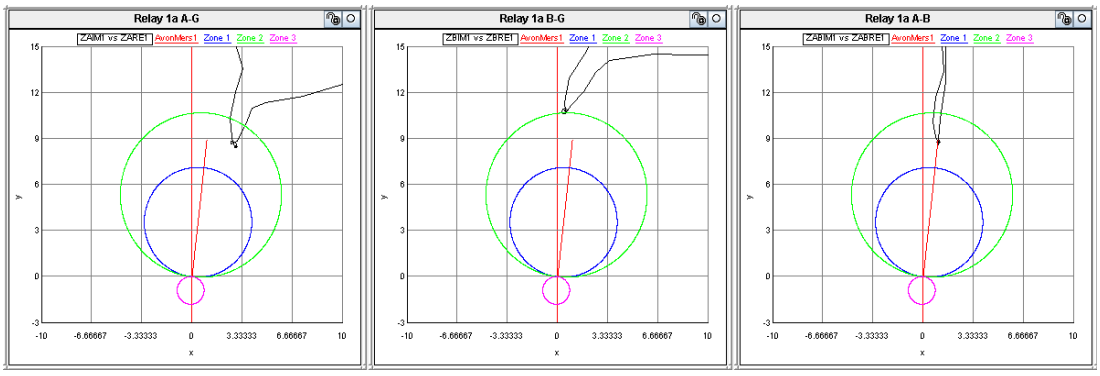

Figure 7.44: A-g, B-g and A-B impedance plots for relay 1a for a cross country fault at 95% of the line; untransposed lines with mutual coupling represented, both transmission lines in service, no POTT scheme used, and with the breakers held closed.

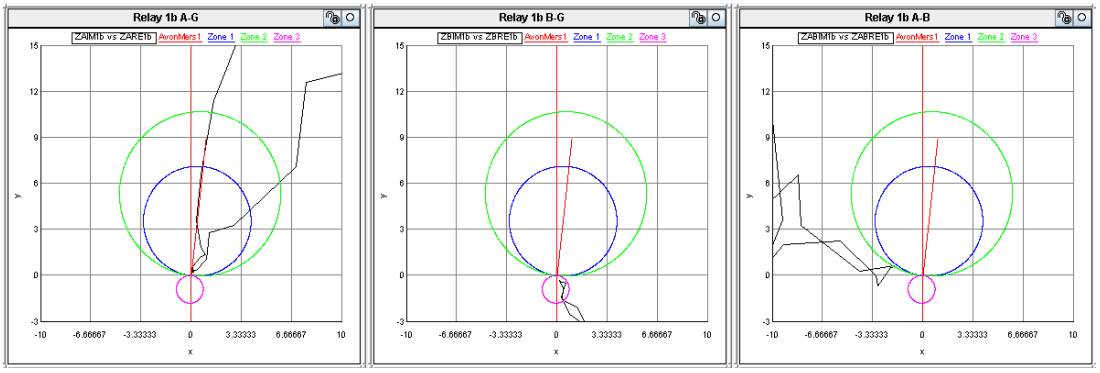

Figure 7.45: A-g, B-g and A-B impedance plots for relay 1b for a cross country fault at 95% of the line; untransposed lines with mutual coupling represented, both transmission lines in service, no POTT scheme used, and with the breakers held closed.

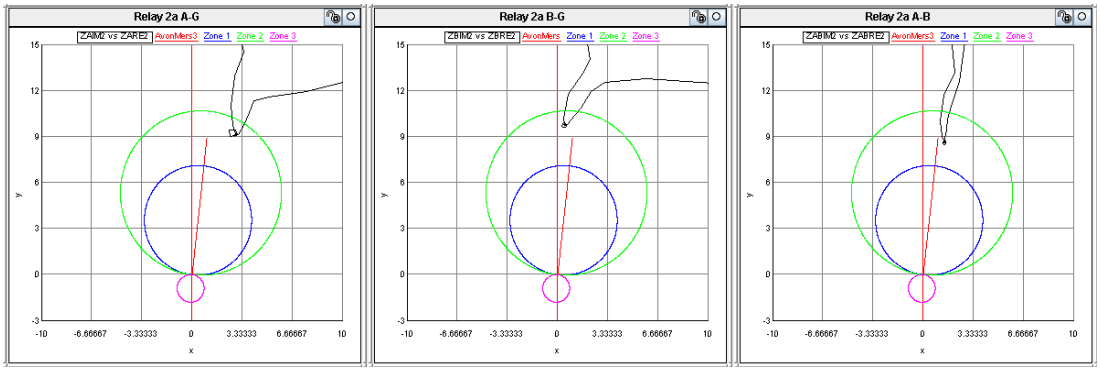

Figure 7.46: A-g, B-g and A-B impedance plots for relay 2a for a cross country fault at 95% of the line; untransposed lines with mutual coupling represented, both transmission lines in service, no POTT scheme used, and with the breakers held closed.

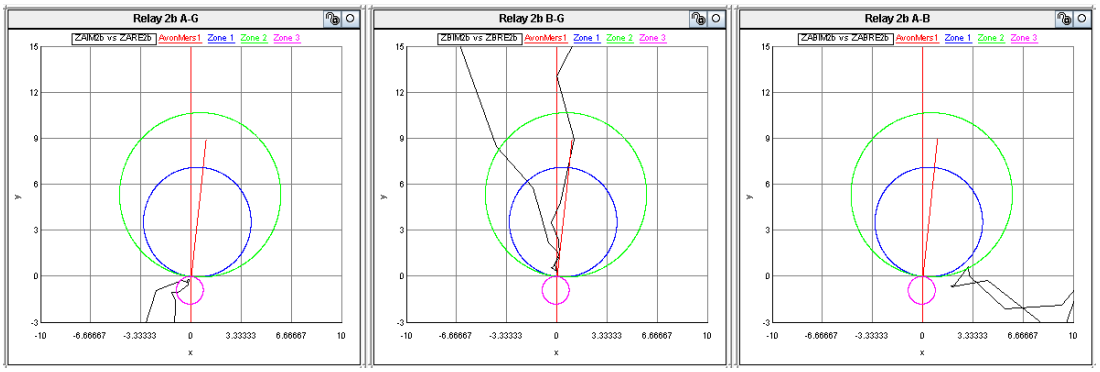

Figure 7.47: A-g, B-g and A-B impedance plots for relay 2b for a cross country fault at 95% of the line; untransposed lines with mutual coupling represented, both transmission lines in service, no POTT scheme used, and with the breakers held closed.

Comparison of the results in Figures 7.44 to 7.47 with those in Figures 7.5 to 7.8 illustrates the differences in the impedances seen by the relay when the lines are untransposed and mutual

coupling is represented. Mutual coupling, as shown previously, affects the phase to ground impedances and non-transposition affects the phase to phase impedances. Based on observations of the impedance plots the effects of the combination of both of these practical operating conditions are as follows:

Relay 1a: The A-g impedance is now shifted to the right of the line characteristic. Relay 1a sees a B-g fault within the boundary of its protected zone. The A-B impedance is pulled further into zone 2.
Relay 1b: Minimal difference.
Relay 2a: The A-g and B-g impedances are pushed further towards the boundary of zone 2. The A-B impedance is pulled further into zone 2.
Relay 2b: Minimal difference.

The effect of mutual coupling together with non-transposition of the transmission lines in the presence of a cross country fault, will have a more significant effect on the distance protection scheme, when compared to Figures 7.5-7.8. The effect of a cross country fault for this operating scenario will cause the A-B phase to phase impedance elements of both relays 1a and 2a to be pulled further into zone 2.

The study shown above was repeated once again, using only software relays, but now with the breakers allowed to operate in response to the relay trip signals. The following fault was placed on the system with no POTT scheme enabled:

A-g fault at 95% on transmission line 1
B-g fault at 95% on transmission line 2

The fault on transmission line 2 was initiated 1 cycle after the fault appeared on transmission line 1, and the transmission lines were both untransposed and mutual coupling between them was represented. The results of this test are shown in Figures 7.48 to 7.52.

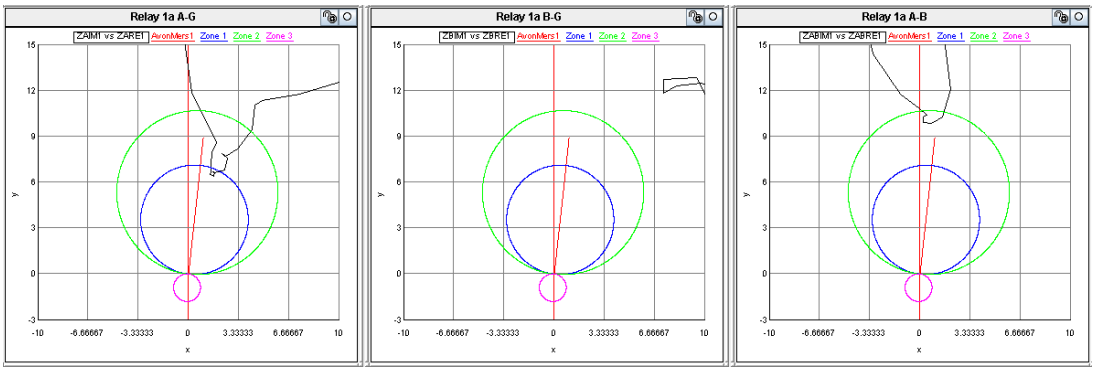

Figure 7.48: A-g, B-g and A-B impedance plots for relay 1a for a cross country fault at 95% of the line; untransposed lines with mutual coupling present, both transmission lines in service, no POTT scheme used, and with the breakers allowed to operate.

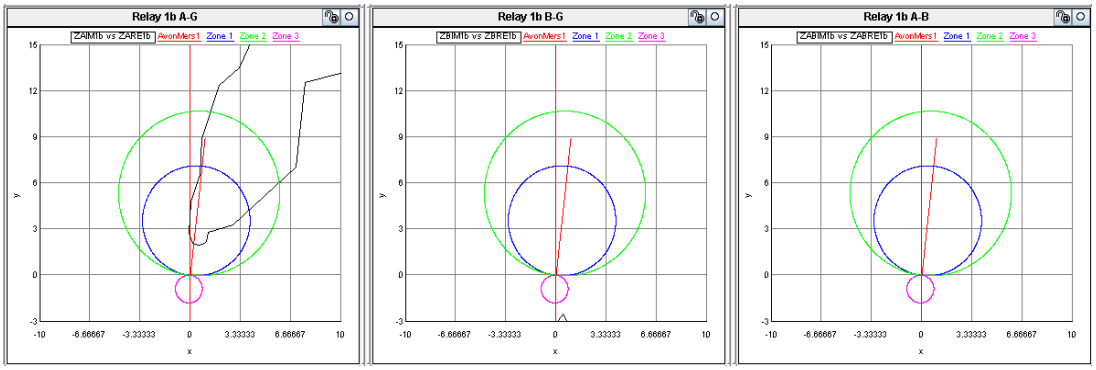

Figure 7.49: A-g, B-g and A-B impedance plots for relay 1b for a cross country fault at 95% of the line; untransposed lines with mutual coupling present, both transmission lines in service, no POTT scheme used, and with the breakers allowed to operate.

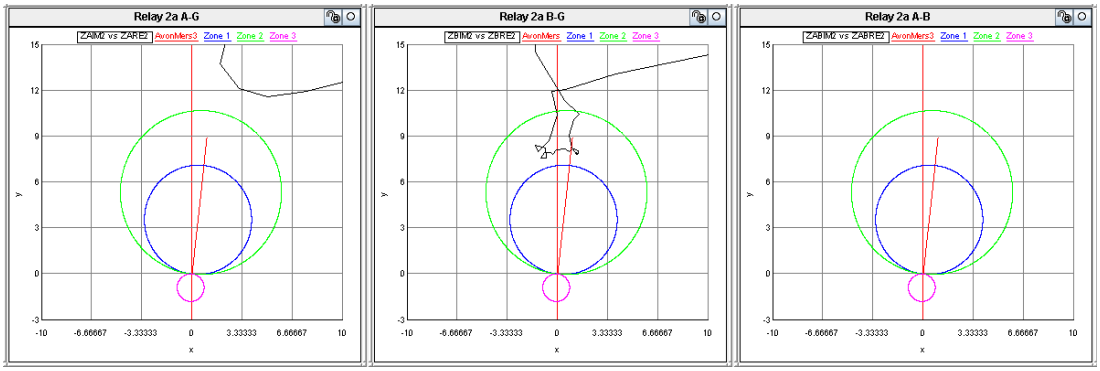

Figure 7.50: A-g, B-g and A-B impedance plots for relay 2a for a cross country fault at 95% of the line; untransposed lines with mutual coupling present, both transmission lines in service, no POTT scheme used, and with the breakers allowed to operate.

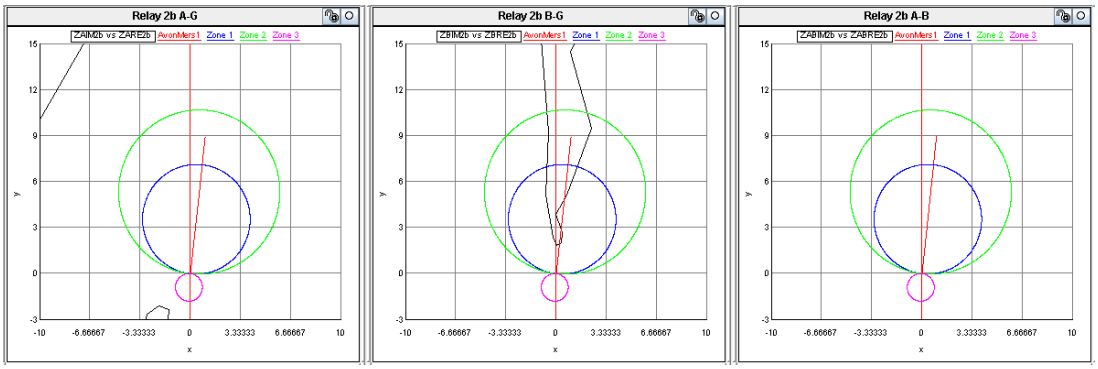

Figure 7.51: A-g, B-g and A-B impedance plots for relay 2b for a cross country fault at 95% of the line; untransposed lines with mutual coupling present, both transmission lines in service, no POTT scheme used, and with the breakers allowed to operate.

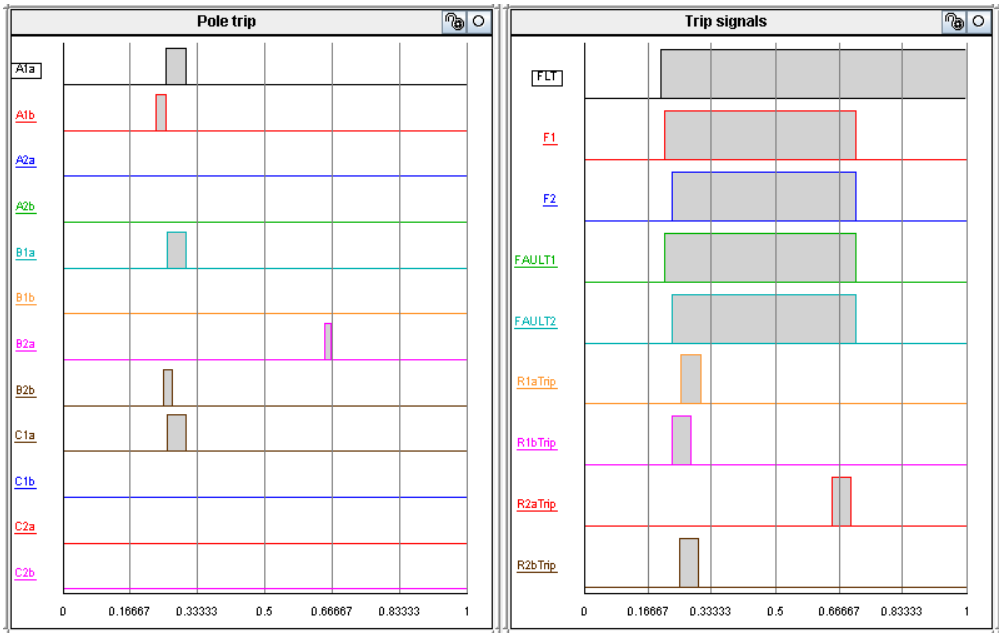

Figure 7.52: Relay single pole trip signal outputs (left) and real time model fault logic control inputs (right) for the cross country fault

In this test, the A-g fault on line 1 was initiated 1 cycle before the B-g fault appeared on line 2. At the instant that the fault is placed on the system, relay 1b issues an instantaneous single pole trip and relay 1a picks up on phase A in zone 1, and on the A-B phase in zone 2. Since the phase selectors are picked up on two phases and a zone 1 trip is initiated, a three pole instantaneous trip is issued. When the B-g fault appeared on line 2, relay 2b issues an instantaneous single pole trip and relay 2a picks up on B phase and trips after 400ms. Relay 2a issues a single pole trip since it is isolated from the A-g fault on line 1 (breaker 1b opens instantaneously).

The results in Figures 7.43 to 7.52 can be compared to the results of the same tests under ideal conditions (Figures 7.11 to 7.15). From this comparison it can be seen that the effect of mutual

coupling and non-transposition of transmission lines, together with a cross country fault, causes the relay 1a at the sending end to see the fault in zone 1 causing an instantaneous trip for a fault that is at 95% of the line length. If the fault was beyond the protected line, there could be a possibility of the relay 1a at the sending end issuing a three pole instantaneous trip if the transmission lines were situated closer together or if other measurement errors were present in the system affecting the impedance measurements of the distance protection relay.

An additional test was conducted to consider the case when the faults on both transmission lines appear at the same instant in time, again using only software relays, with the breakers allowed to operate for the following faults placed on the system:

A-g fault at 95% on transmission line 1
B-g fault at 95% on transmission line 2
The results for this additional test are shown in Figures 7.53 to 7.57.

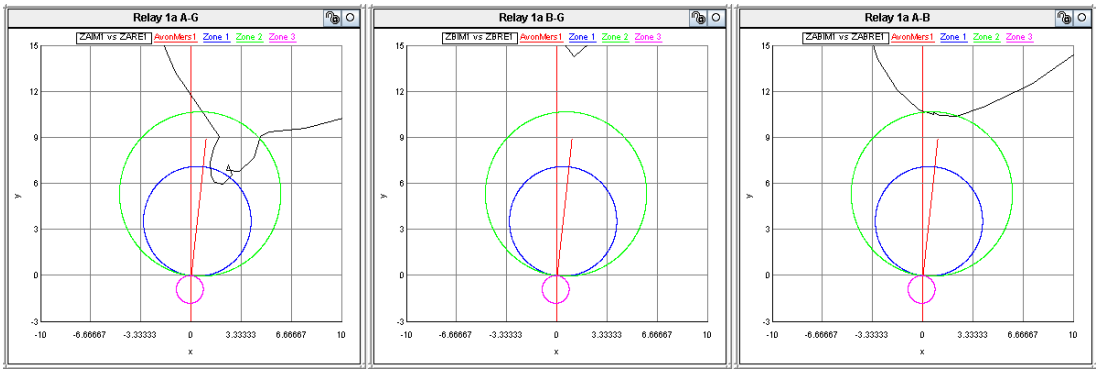

Figure 7.53: A-g, B-g and A-B impedance plots for relay 1a for a cross country fault at 95% of the line; untransposed lines with mutual coupling represented, both transmission lines in service, no POTT scheme used, and with the breakers allowed to operate

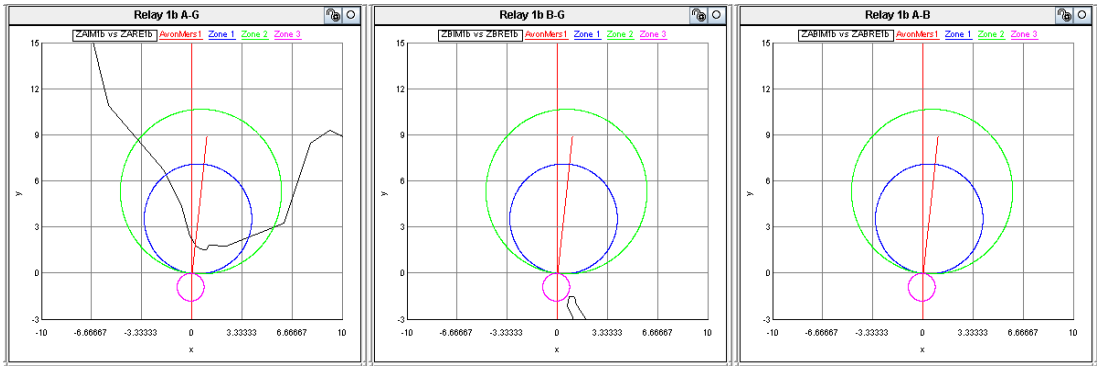

Figure 7.54: A-g, B-g and A-B impedance plots for relay 1b for a cross country fault at 95% of the line; untransposed lines with mutual coupling represented, both transmission lines in service, no POTT scheme used, and with the breakers allowed to operate

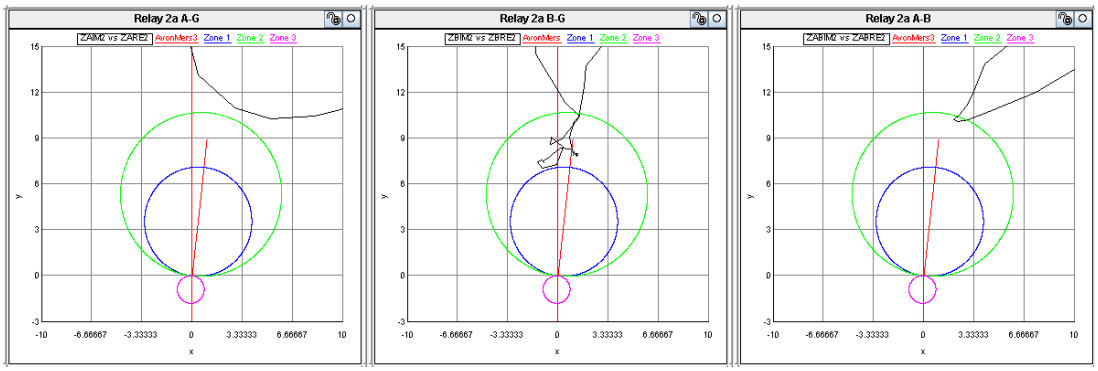

Figure 7.55: A-g, B-g and A-B impedance plots for relay 2a for a cross country fault at 95% of the lines; untransposed lines with mutual coupling represented, both transmission lines in service, no POTT scheme used, and with the breakers allowed to operate

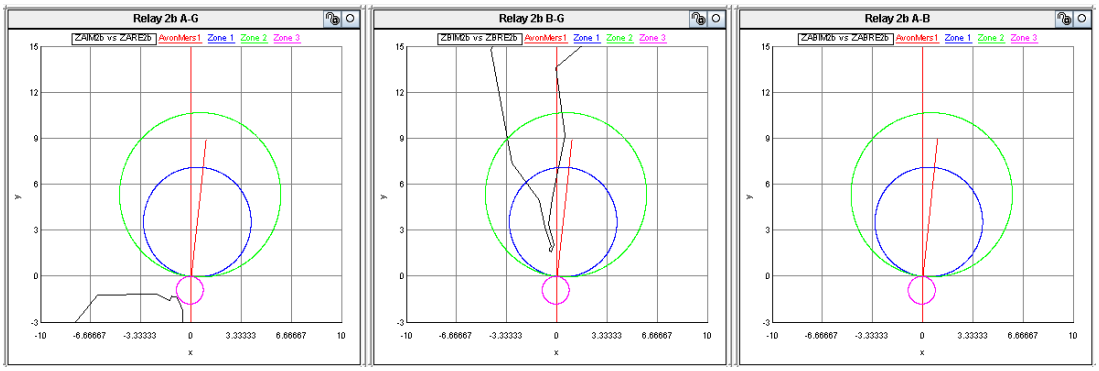

Figure 7.56: A-g, B-g and A-B impedance plots for relay 2b for a cross country fault at 95% of the line; untransposed lines with mutual coupling represented, both transmission lines in service, no POTT scheme used, and with the breakers allowed to operate

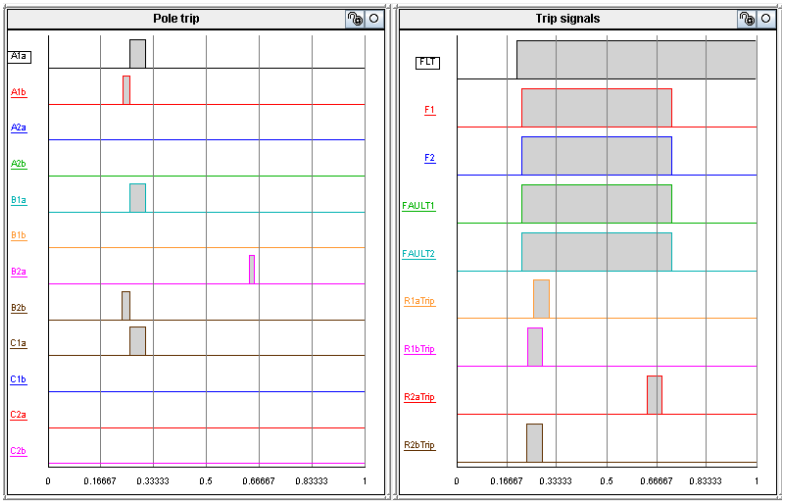

Figure 7.57: Relay single pole trip signal outputs (left) and real time model fault control inputs (right) for the cross country fault

The results in Figures 7.53 to 7.56 show that the relay 1a sees a single phase fault in zone 1 and a phase to phase fault in zone 2 and therefore issues a three pole instantaneous trip. All other

relays issue single pole trip commands as in the results shown in Figures 7.48 to 7.52 of the previous study.

The study was then repeated with a simple POTT scheme enabled to investigate the response of the distance protection scheme to a cross country fault when the transmission lines are both untransposed and mutually coupled. Using only software relays, with the breakers allowed to operate, the following faults were placed on the system with a simple POTT scheme enabled:

A-g fault at 95% on transmission line 1
B-g fault at 95% on transmission line 2

The fault on transmission line 2 was initiated 1 cycle after fault appeared on transmission line 1, and the transmission lines were both untransposed and mutual coupling between them was represented. The results of this test are shown in Figures 7.58 to 7.62.

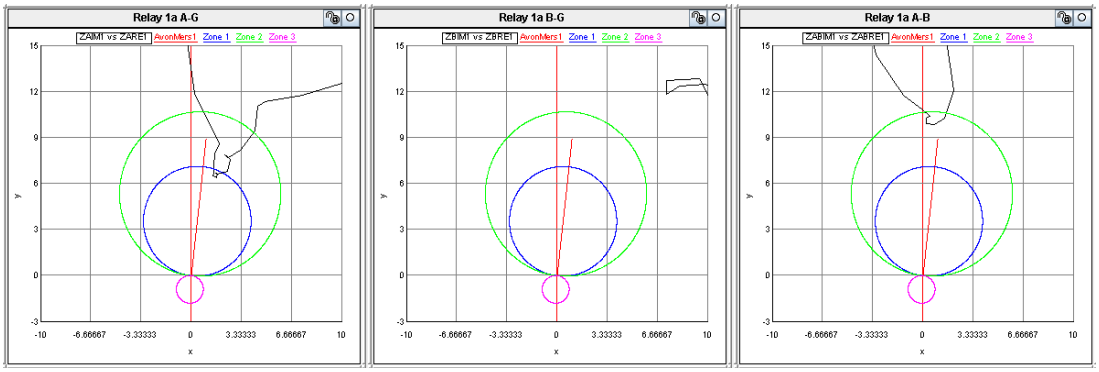

Figure 7.58: A-g, B-g and A-B impedance plots for relay 1a for a cross country fault at 95% of the line; untransposed lines and mutual coupling represented, both lines in service, a simple POTT scheme used, and with the breakers allowed to operate

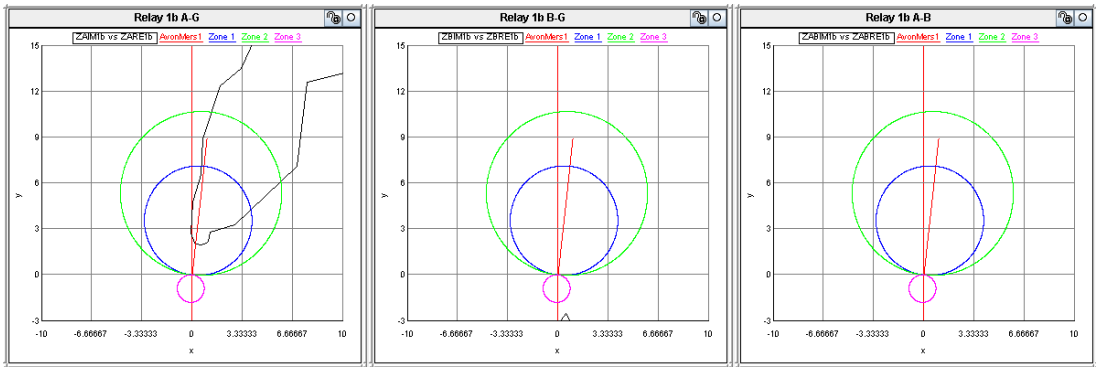

Figure 7.59: A-g, B-g and A-B impedance plots for relay 1b for a cross country fault at 95% of the line; untransposed lines and mutual coupling represented, both lines in service, a simple POTT scheme used, and with the breakers allowed to operate

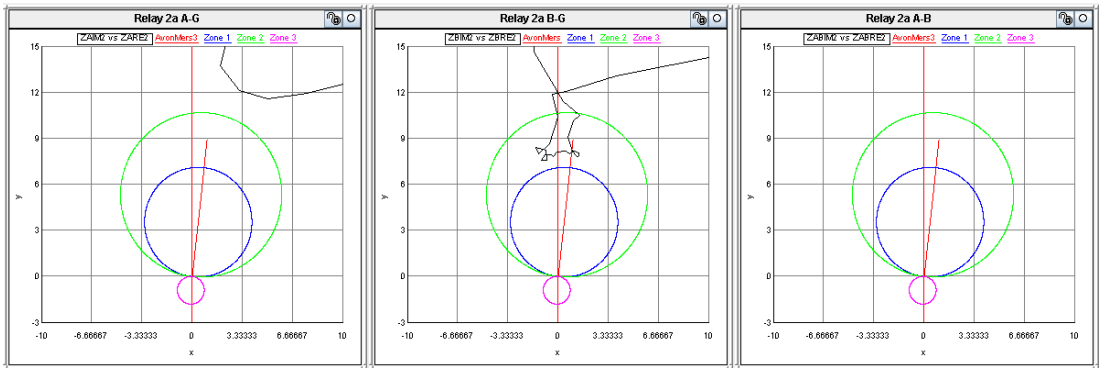

Figure 7.60: A-g, B-g and A-B impedance plots for relay 2a for a cross country fault at 95% of the line; untransposed lines and mutual coupling represented, both lines in service, a simple POTT scheme used, and with the breakers allowed to operate

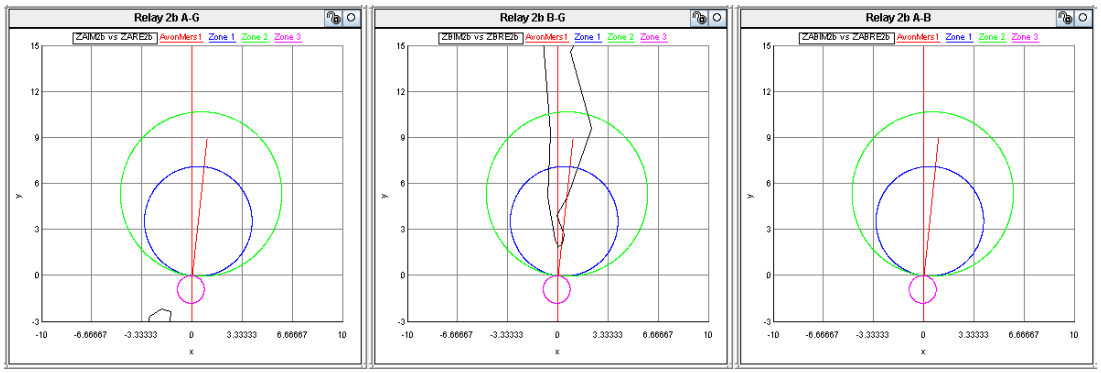

Figure 7.61: A-g, B-g and A-B impedance plots for relay 2b for a cross country fault at 95% of the line; untransposed lines and mutual coupling represented, both lines in service, a simple POTT scheme used, and with the breakers allowed to operate

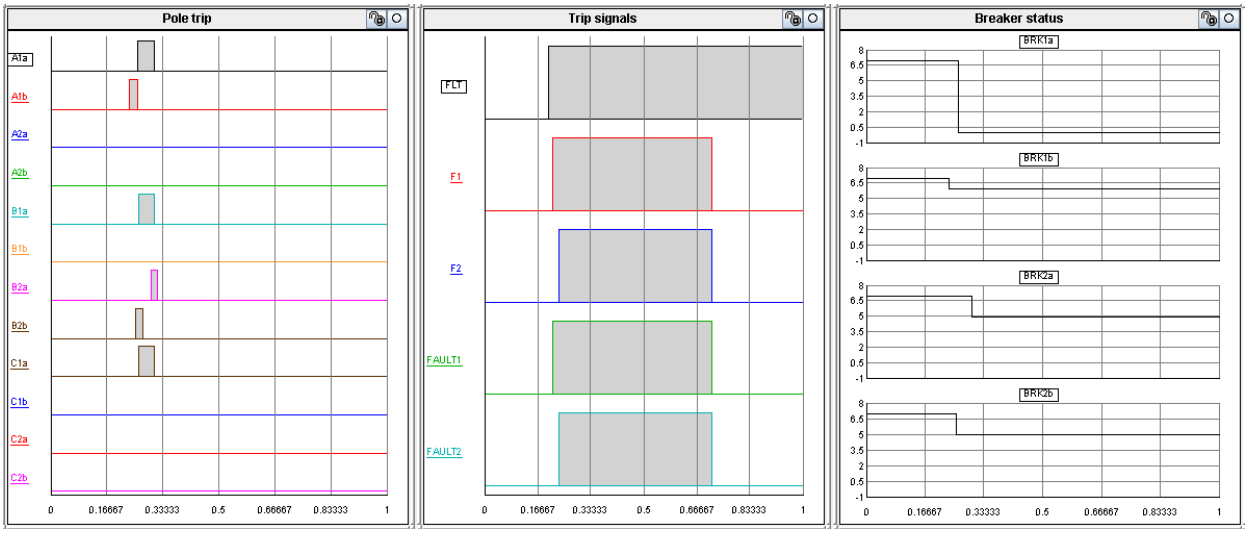

Figure 7.62: Relay single pole trip signal outputs (left), fault control signals (centre) and breaker trip signals (right) for a cross country fault

The results in Figures 7.58 to 7.61 show that the relay 1a sees a single phase fault in zone 1 and a phase to phase fault in zone 2, therefore a three pole instantaneous trip is issued by relay 1a. All other relays issue a single pole trip. The difference in this operation from those in Figures 7.48 to 7.51 is that relay 2a now issues a trip command instantaneously since it received permission to trip from relay 2b.

An additional test was conducted to consider the case when the faults on both transmission lines appear at the same instant in time, again using only software relays, with the breakers allowed to operate for the following faults placed on the system:

A-g fault at 95% on transmission line 1
B-g fault at 95% on transmission line 2

The results for this additional test are shown in Figures 7.63 to 7.67.

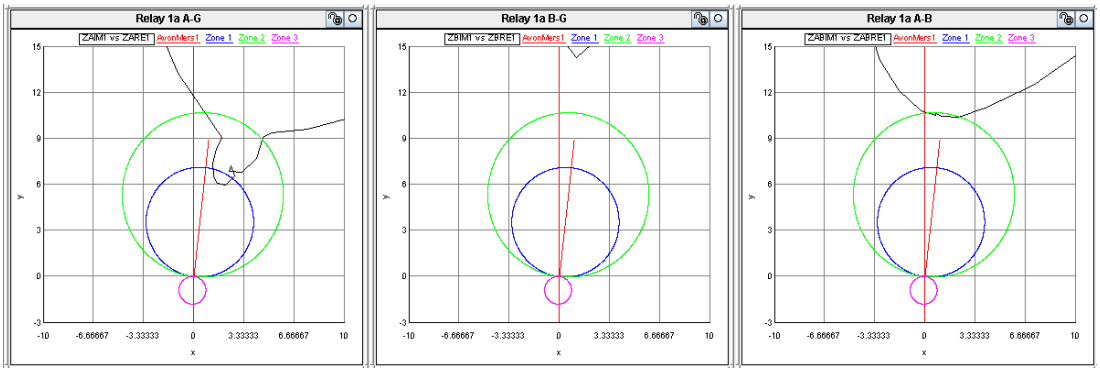

Figure 7.63: A-g, B-g and A-B impedance plots for relay 1a for a cross country fault at 95% of the line; untransposed lines and mutual coupling represented, both transmission lines in service, a simple POTT scheme used, and with the breakers allowed to operate

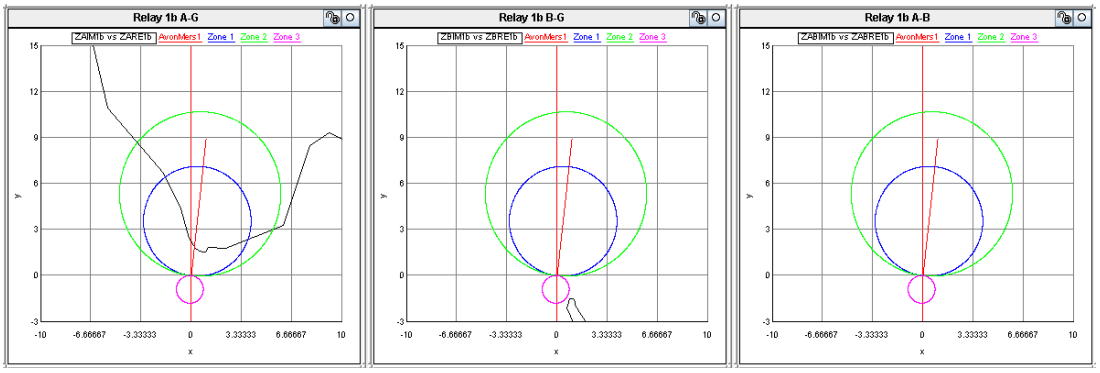

Figure 7.64: A-g, B-g and A-B impedance plots for relay 1b for a cross country fault at 95% of the line; untransposed lines and mutual coupling represented, both transmission lines in service, a simple POTT scheme used, and with the breakers allowed to operate

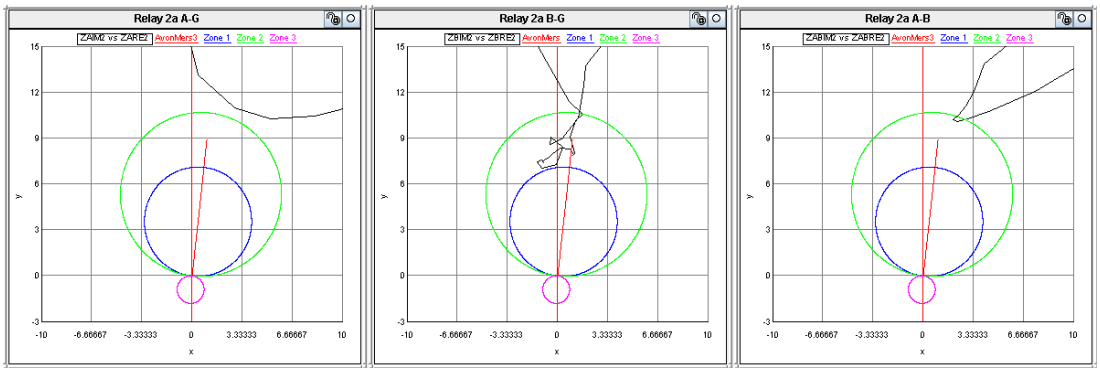

Figure 7.65: A-g, B-g and A-B impedance plots for relay 2a for a cross country fault at 95% of the line; untransposed lines and mutual coupling represented, both transmission lines in service, a simple POTT scheme used, and with the breakers allowed to operate

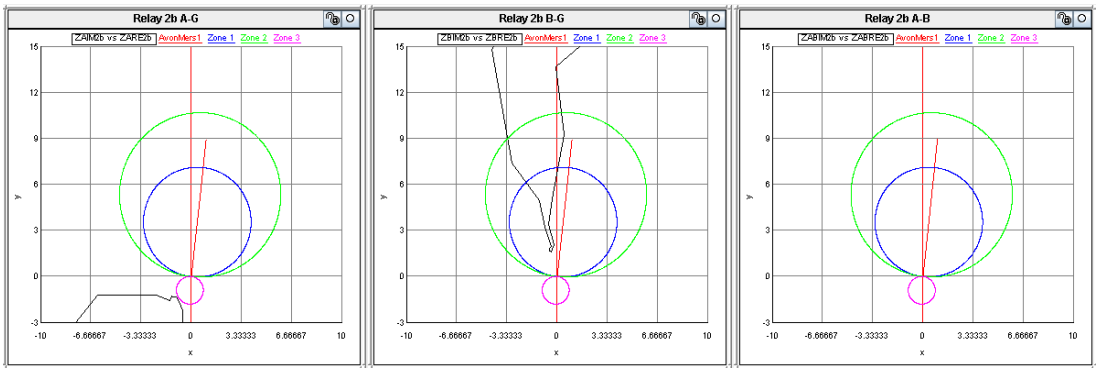

Figure 7.66: A-g, B-g and A-B impedance plots for relay 2b for a cross country fault at 95% of the line; untransposed lines and mutual coupling represented, both transmission lines in service, a simple POTT scheme used, and with the breakers allowed to operate

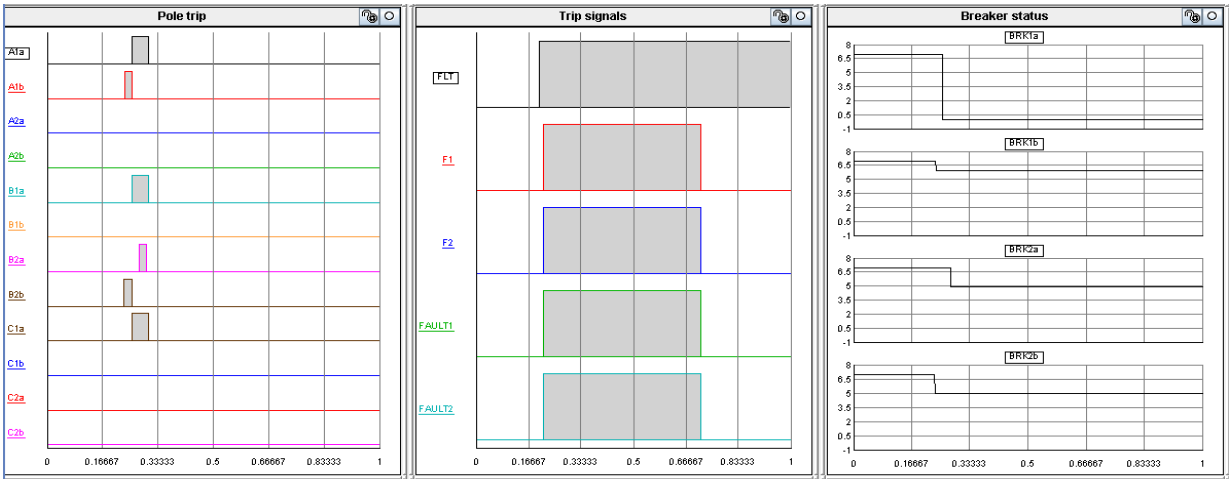

Figure 7.67: Relay single pole trip signal outputs (left), fault control signals (centre) and breaker trip signals (right) for the cross country fault

The results in Figures 7.63 to 7.66 show that the relay 1a sees a single phase fault in zone 1 and a phase to phase fault in zone 2, therefore a three pole instantaneous trip is issued by relay 1a. All other relays issue a single pole trip.

The response of the distance protection relay in the presence of a cross country fault on parallel untransposed transmission lines with mutual coupling represented is clearly noted in the test studies thus far. The POTT2 distance protection scheme designed for this power system (presented in Section 7.4) was then tested with this RSCAD model of the power system to investigate the use of such a distance protection scheme when the transmission lines are untransposed with mutual coupling represented.

Using only software relays with the POTT2 scheme enabled and with the breakers allowed to operate, the following faults were placed on the system:

A-g fault at 95% on transmission line 1
B-g fault at 95% on transmission line 2

The fault on transmission line 2 was initiated 1 cycle after the fault appeared on transmission line 1, and transmission lines were both untransposed with mutual coupling represented between them. The results of this study are presented in Figures 7.68 to 7.73.

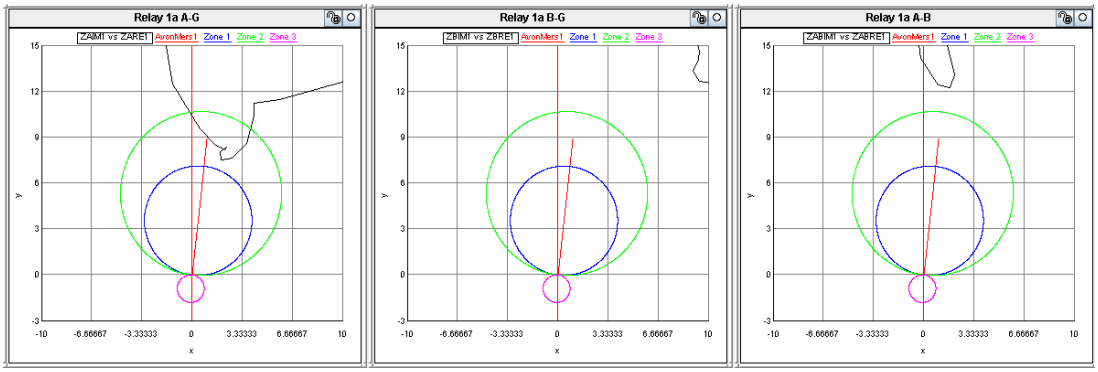

Figure 7.68: A-g, B-g and A-B impedance plots for relay 1a for a cross country fault at 95% of the line; untransposed lines with mutual coupling represented, both transmission lines in service, a POTT2 scheme used, and with the breakers allowed to operate

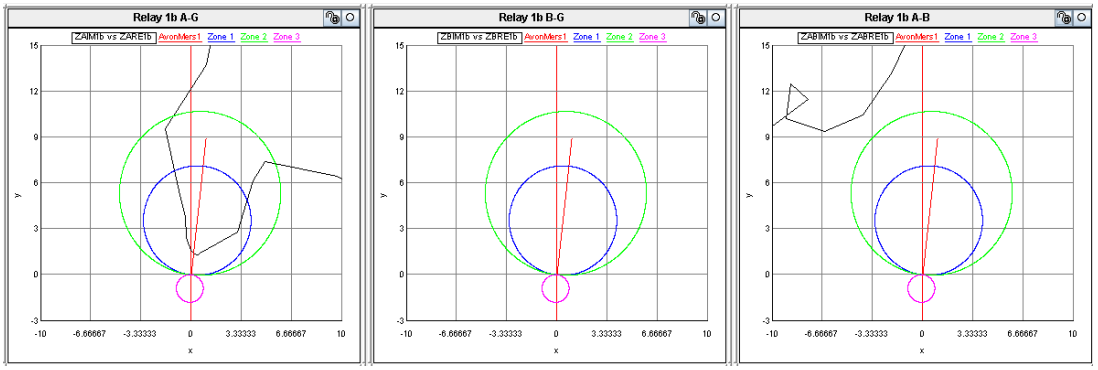

Figure 7.69: A-g, B-g and A-B impedance plots for relay 1b for a cross country fault at 95% of the line; untransposed lines with mutual coupling represented, both transmission lines in service, a POTT2 scheme used, and with the breakers allowed to operate

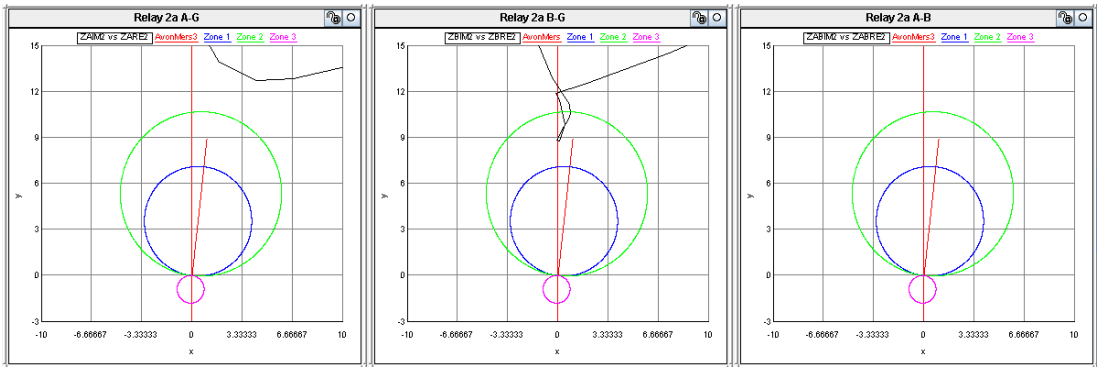

Figure 7.70: A-g, B-g and A-B impedance plots for relay 2a for a cross country fault at 95% of the line; untransposed lines with mutual coupling represented, both transmission lines in service, a POTT2 scheme used, and with the breakers allowed to operate

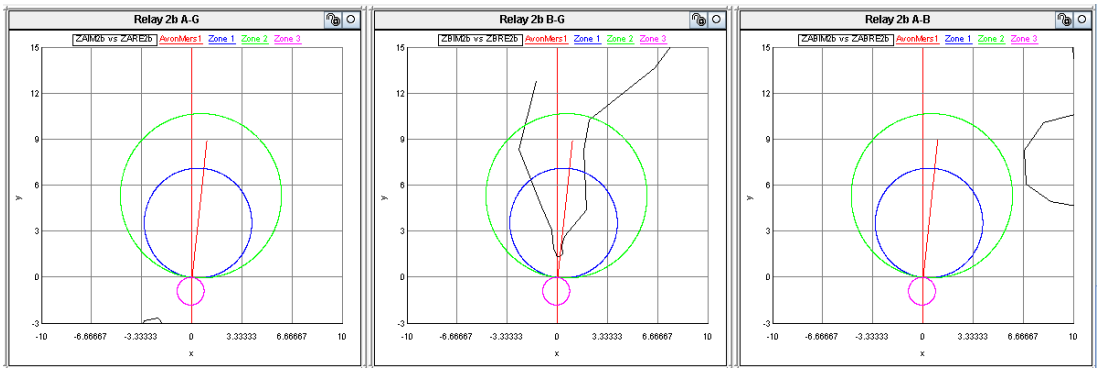

Figure 7.71: A-g, B-g and A-B impedance plots for relay 2b for a cross country fault at 95% of the line; untransposed lines with mutual coupling represented, both transmission lines in service, a POTT2 scheme used, and with the breakers allowed to operate

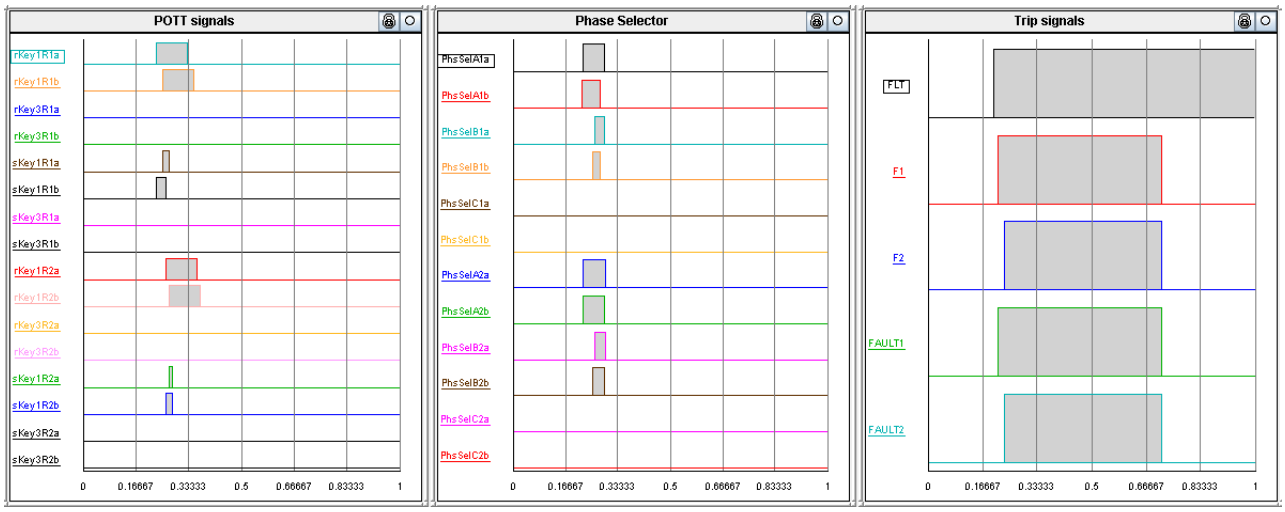

Figure 7.72: Relay POTT2 signal monitoring (left) relay phase selector signal monitoring (centre) and fault control monitoring (right) for the cross country fault

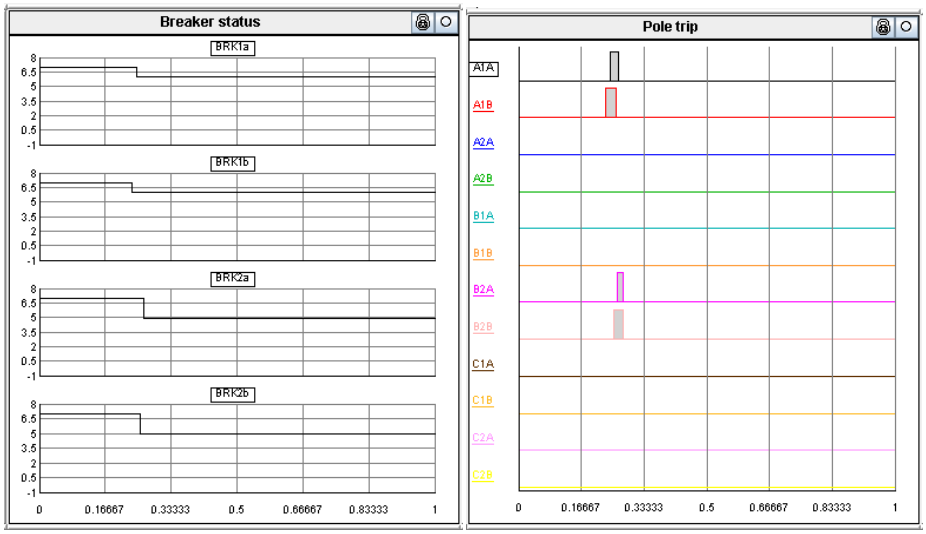

Figure 7.73: Breaker trip signal monitoring (left) and relay single pole trip signal monitoring (right) for the cross country fault

From the results in Figures 7.68 to 7.71, all relays issue a single pole trip when the POTT2 scheme logic is used, in the same manner as seen in the results presented in Figures 7.30 to 7.33 for the fault scenario in Section 7.4. The sending end relays receive a KEY1 permission to trip, and do not receive a KEY3 permission to trip, therefore single pole trip commands are issued to the respective breakers. Note that the impedance trajectories in Figures 7.68 to 7.71 for this fault and current distribution showed no impedance locus falling within the A-B loop reach when the POTT2 protection scheme logic is implemented. The phase selectors for the RSCAD software relays indicate that the relay did see the fault in phase A and B. The protection scheme for this fault type and operating scenario did operate as required and no three pole trip was issued during this cross country fault.

As in Section 7.5, the response of the POTT2 scheme under the same operating conditions was then investigated, using both hardware and software relays. Two SEL 421 hardware distance protection relays protected line 1 and two RSCAD software relays protected line 2, with the breakers allowed to operate, and the following fault was placed on the system:

A-g fault at 95% on transmission line 1
B-g fault at 95% on transmission line 2

The fault on transmission line 2 was initiated 1 cycle after the fault appeared on transmission line 1, and the transmission lines were both untransposed with mutual coupling represented between the transmission lines. The results for this test are shown in Figures 7.74 to 7.80.

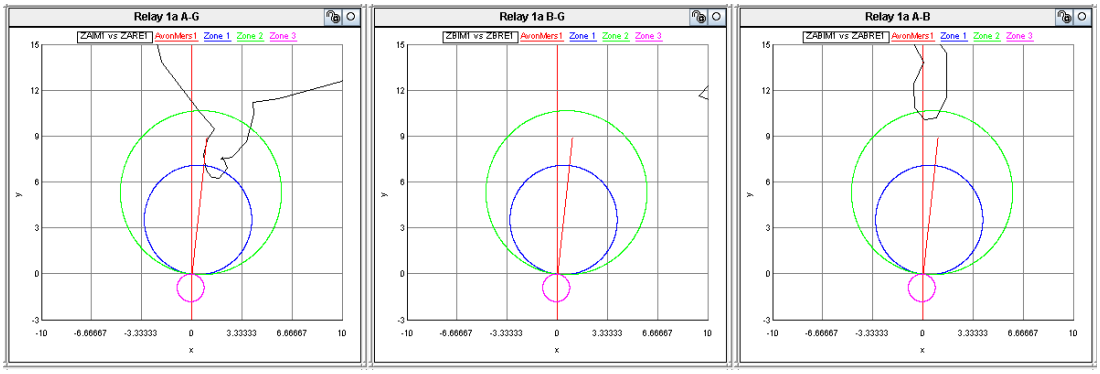

Figure 7.74: A-g, B-g and A-B impedance plots for relay 1a for a cross country fault at 95% of the line; untransposed lines with mutual coupling represented, both transmission lines in service, a POTT2 scheme used, and with the breakers allowed to operate

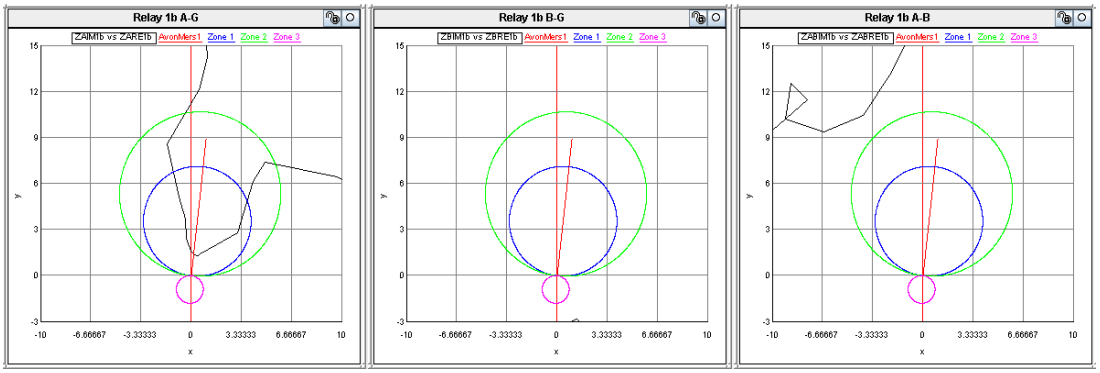

Figure 7.75: A-g, B-g and A-B impedance plots for relay 1b for a cross country fault at 95% of the line; untransposed lines with mutual coupling represented, both transmission lines in service, a POTT2 scheme used, and with the breakers allowed to operate

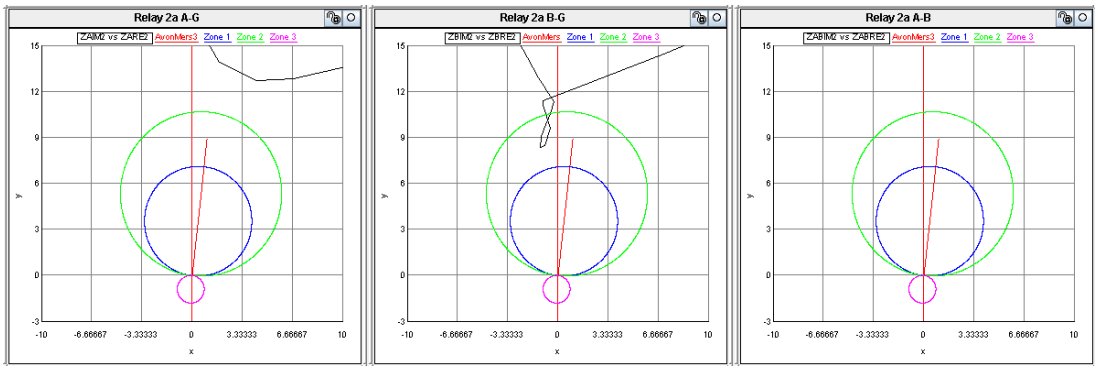

Figure 7.76: A-g, B-g and A-B impedance plots for relay 2a for a cross country fault at 95% of the line; untransposed lines with mutual coupling represented, both transmission lines in service, a POTT2 scheme used, and with the breakers allowed to operate

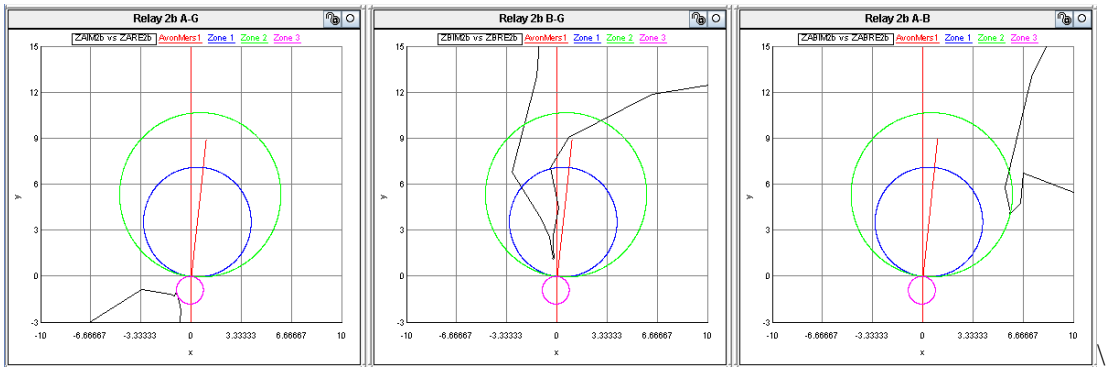

Figure 7.77: A-g, B-g and A-B impedance plots for relay 2b for a cross country fault at 95% of the line; untransposed lines with mutual coupling represented, both transmission lines in service, a POTT2 scheme used, and with the breakers allowed to operate

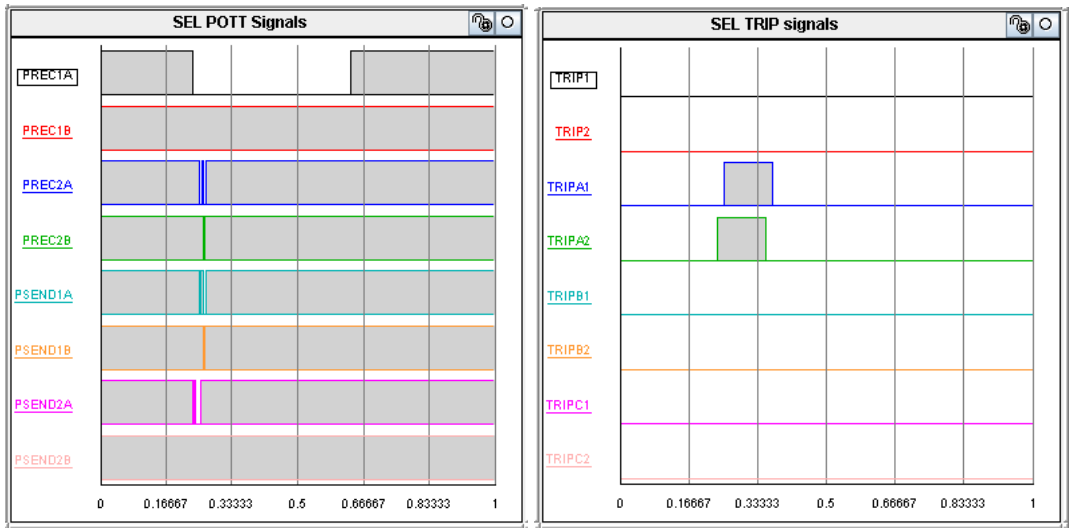

Figure 7.78: Hardware relay POTT2 signal monitoring on line 1 (left) and relay single pole trip signal monitoring on line 1 (right) for a cross country fault

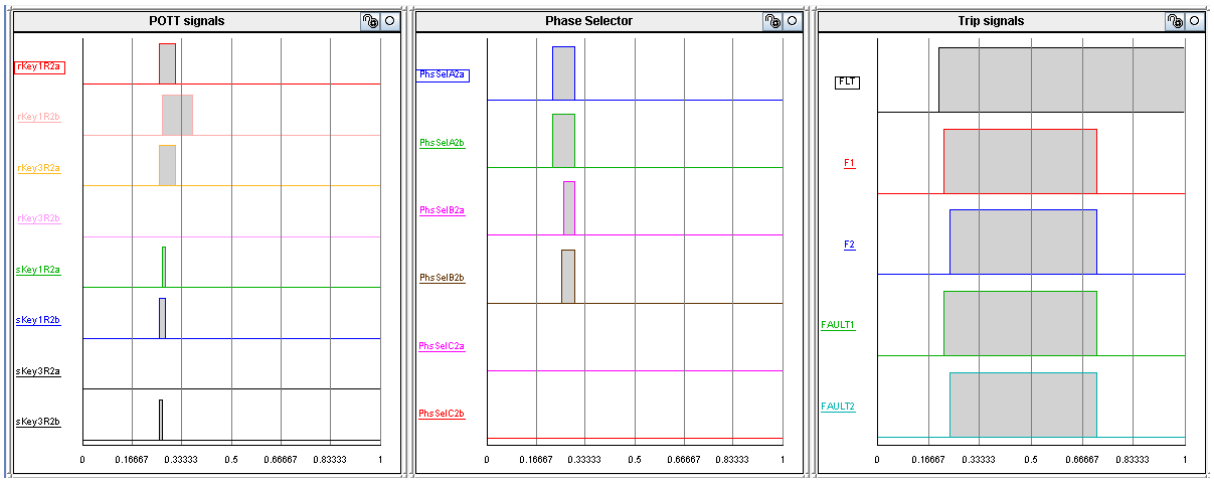

Figure 7.79: Software relay POTT2 signal monitoring (left) relay phase selector signal monitoring (centre) and fault control logic monitoring (right) for a cross country fault for the relays on line 2.

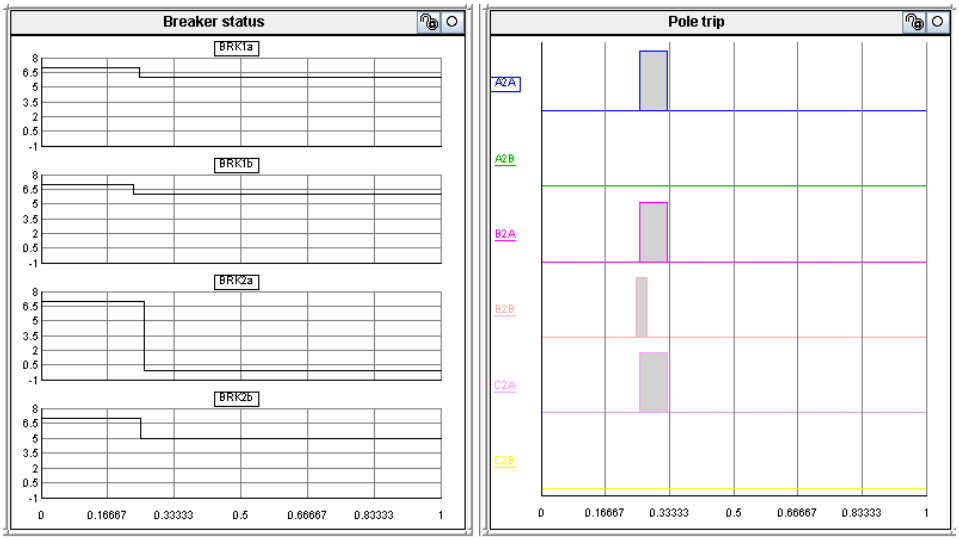

Figure 7.80: Breaker trip signal monitoring of all breakers (left) and relay single pole trip signal monitoring of the software relays on line 2 (right) for a cross country fault

From the results in Figures 7.74 to 7.80, all relays (with the exception of relay 2a) issue a single pole trip and operate correctly in line with the philosophy of a POTT2 protection scheme. The relay 2a still issues a three pole trip. Upon investigation of the impedance plots and signal plots it was uncovered that this was due to relay 2b issuing a KEY1 and KEY3 signal since relay 2b sees an A-B fault at the edge of its zone 2. Relay 2a therefore issues a three pole trip since the phase selectors picked up a fault in phase A and B and it received a KEY1 and KEY3 POTT signal.

The performance of the POTT2 protection scheme for a complex operating scenario where mutual coupling and non-transposition of the transmission line is represented in the real time model using the real time digital simulator has been shown. Again the use of such a tool and the

insight gained into the performance of a protection relay in the presence of various practical challenges has been presented here and the results obtained were analysed.

Thus far in this chapter, only A-g and B-g cross country faults have been considered. The next section considers the response of the distance protection to A-g and C-g cross country faults to see if the relay will respond differently to faults involving other phases.

7.7. Investigating the effects of a cross country fault involving phase A and C with mutual coupling and the transmission line being untransposed

Since the worst case fault scenario, from experience in previous chapters in this thesis, is an AC-g fault, the impact of a cross country fault involving phase A and C will now be presented.

Using only software relays without the POTT scheme enabled, with the breakers forced to stay closed, the following fault was placed on the system:

C-g fault at 95% on transmission line 1

A-g fault at 95% on transmission line 2

The fault on transmission line 2 was initiated 1 cycle after fault appeared on transmission line 1, and the transmission lines were both untransposed with mutual coupling represented between them. The results for this test are shown in Figures 7.81 to 7.84.

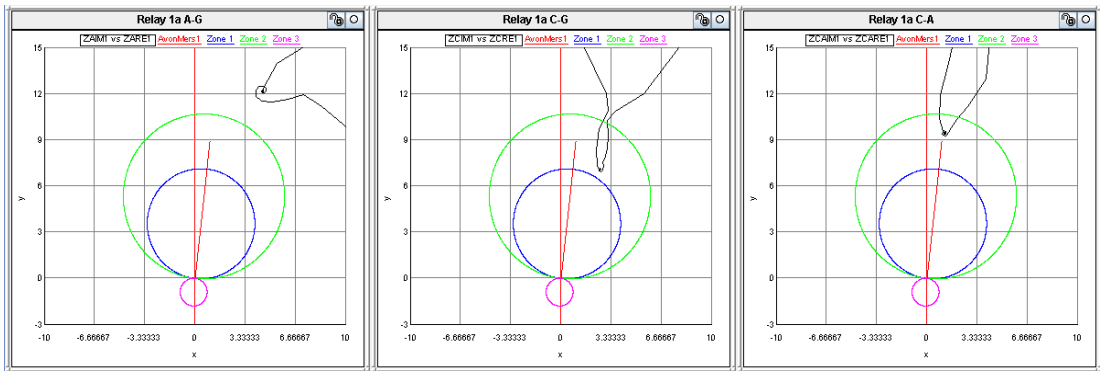

Figure 7.81: A-g, C-g and C-A impedance plots for relay 1a for a cross country fault at 95% of the line; untransposed lines with mutual coupling represented, both transmission lines in service, no POTT scheme used, and with the breakers held closed

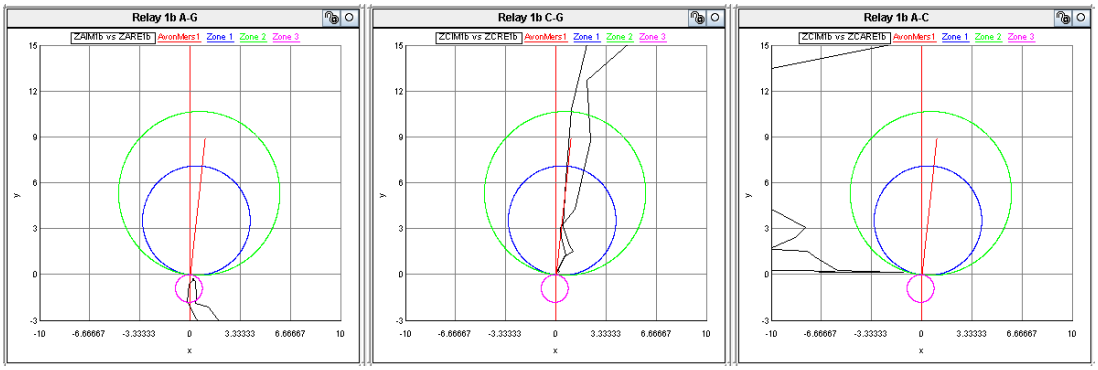

Figure 7.82: A-g, C-g and C-A impedance plots for relay 1b for a cross country fault at 95% of the line; untransposed lines with mutual coupling represented, both transmission lines in service, no POTT scheme used, and with the breakers held closed

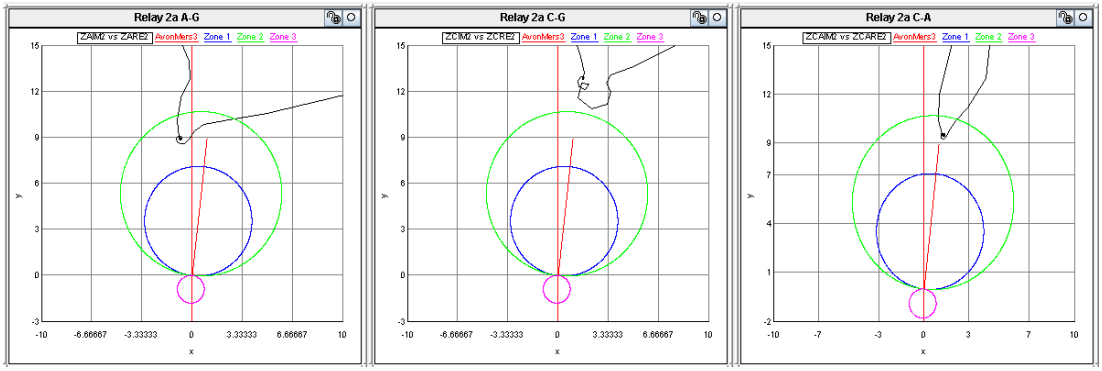

Figure 7.83: A-g, C-g and C-A impedance plots for relay 2a for a cross country fault at 95% of the line; untransposed lines with mutual coupling represented, both transmission lines in service, no POTT scheme used, and with the breakers held closed

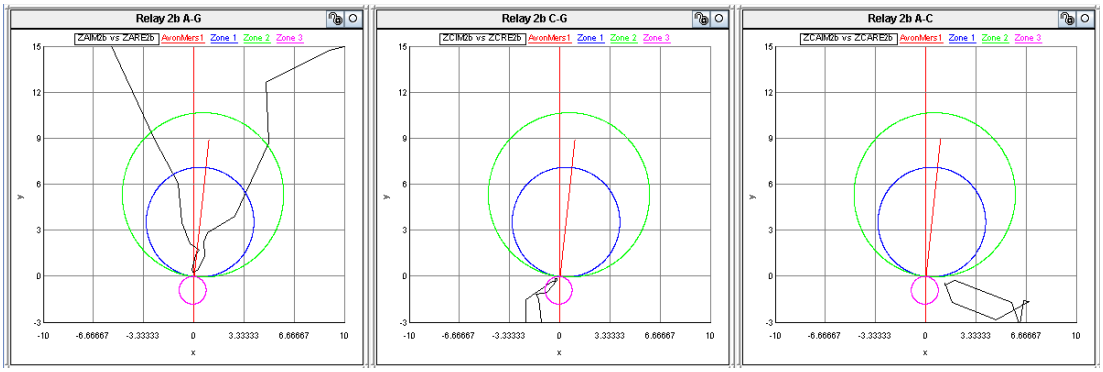

Figure 7.84: A-g, C-g and C-A impedance plots for relay 2b for a cross country fault at 95% of the line; untransposed lines with mutual coupling represented, both transmission lines in service, no POTT scheme used, and with the breakers held closed

From the impedance plots in Figures 7.81 to 7.84 when compared to the impedance plots in Figures 7.44 to 7.47, note that for this fault the relay 1a on line1 (with a fault on phase C) sees

the fault pulled further into zone 2 and it sees the fault on the parallel line (on phase A) pushed further out of zone 2. The C-A impedance plot shows the impedance pulled slightly further into zone 2. Although the results for this fault scenario differ slightly, the operation of the relays will still be the same. This was verified for a variety of operating conditions and compared to the results for the various fault sceanarios presented in Section 7.6. The results for these fault studies showed similar results to these seen in Section 7.6, particularly where the operation of distance protection relay is concerned. The detailed results from these tests are not shown in order to aviod unnecessary repetition.

The next section consideres fault scenarios in which the fault is placed closer to the zone 1 reach of the distance protection relays.

7.8. Investigating the effects of a cross country fault closer to the zone 1 reach where mutual coupling is present and the transmission lines are untransposed

The prior sections in this chapter have considers cross country faults in which the faults were placed close to the receiving end (at 95%) of the transmission line. This section considers a cross country fault in which the fault on one of the transmission lines is closer to the zone 1 reach. To investigate the response of the distance protection relay to this kind of cross country fault, using only the software relays, without the POTT scheme enabled, with the breakers forced to stay closed, the following fault was placed on the system:

A-g fault at 80% on transmission line 1
B-g fault at 95% on transmission line 2

The fault on transmission line 2 was initiated 1 cycle after the fault appeared on transmission line 1 and the transmission lines are untransposed with mutual coupling represented between them. The results of this test are shown in Figures 7.85 to 7.89.

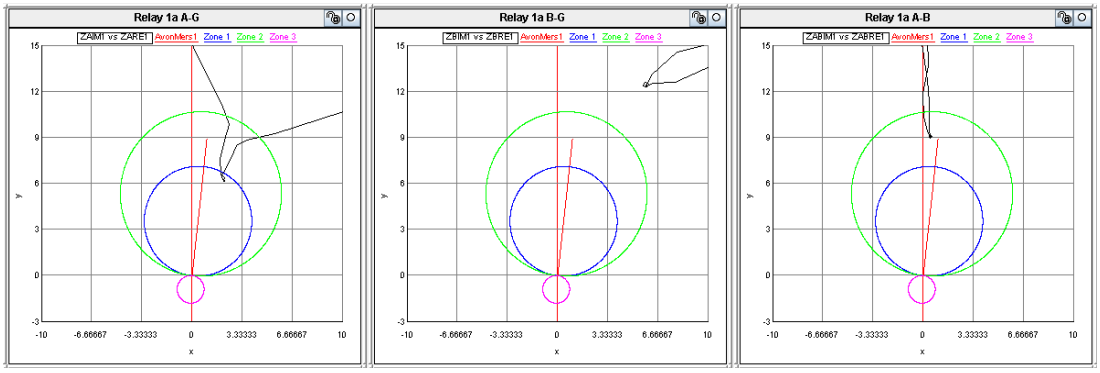

Figure 7.85: A-g, B-g and A-B impedance plots for relay 1a for a cross country fault at 80% and 95% of the parallel lines; untransposed lines with mutual coupling represented, both transmission lines in service, no POTT scheme used, and with the breakers held closed

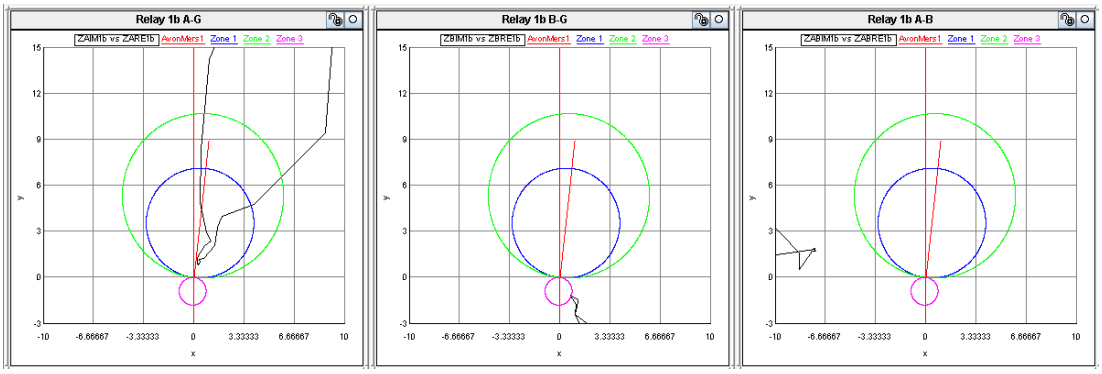

Figure 7.86: A-g, B-g and A-B impedance plots for relay 1b for a cross country fault at 80% and 95% of the parallel lines; untransposed lines with mutual coupling represented, both transmission lines in service, no POTT scheme used, and with the breakers held closed

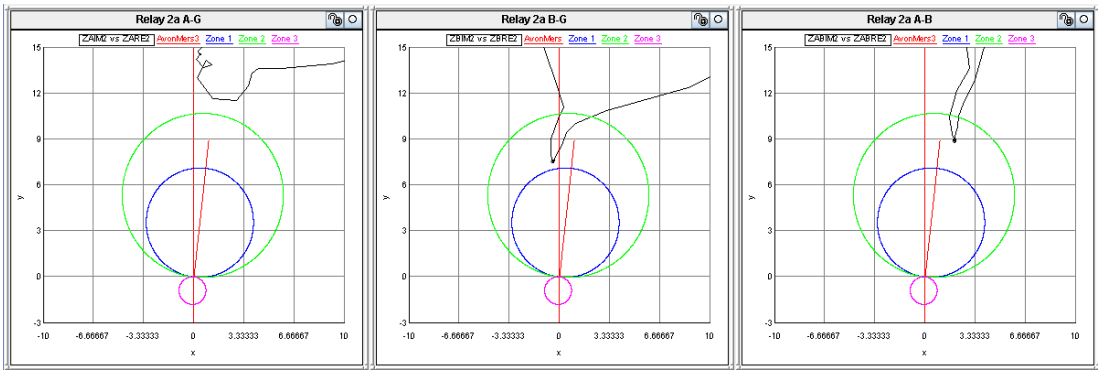

Figure 7.87: A-g, B-g and A-B impedance plots for relay 2a for a cross country fault at 80% and 95% of the parallel lines; untransposed lines with mutual coupling represented, both transmission lines in service, no POTT scheme used, and with the breakers held closed

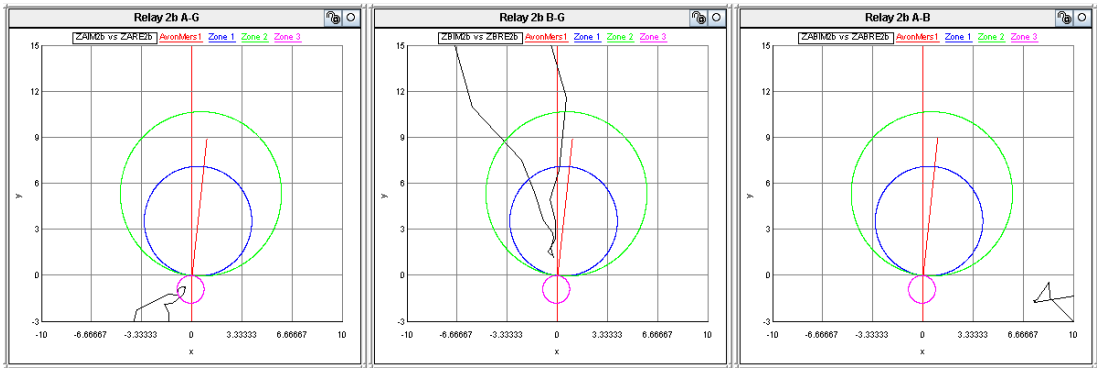

Figure 7.88: A-g, B-g and A-B impedance plots for relay 2b for a cross country fault at 80% and 95% of the parallel lines; untransposed lines with mutual coupling represented, both transmission lines in service, no POTT scheme used, and with the breakers held closed

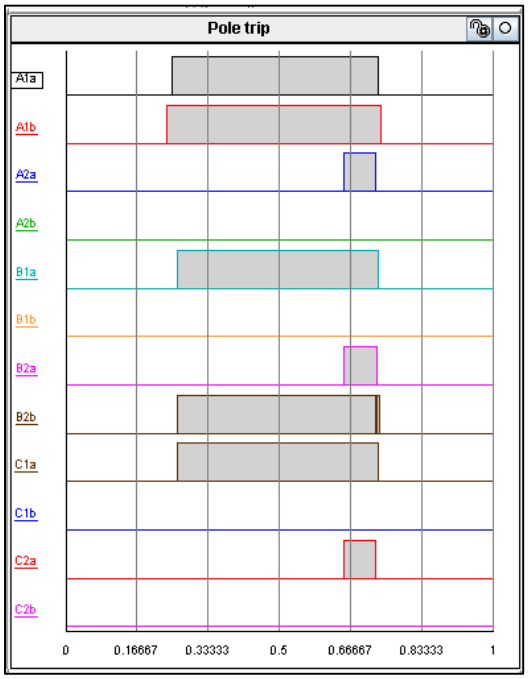

Figure 7.89: Single pole trip signal outputs of the relay

From the results in Figures 7.85 to 7.89, relays 1b and 2b see the fault in zone 1 and issue an instantaneous single pole trip. Relay 1a sees a single phase fault in zone 1 and a phase to phase fault in zone 2. Since the phase selectors are picked up on more than one phase, the relay 1a issues an instantaneous three pole trip. Relay 2a sees a single phase fault in zone 2 and a phase to phase fault in zone 2. This relay therefore issues a time delayed three pole trip since the fault is still on the system due to the breakers held closed.

The fault was investigated again, using only software relays with no POTT scheme enabled, but now with the breakers allowed to operate; the following fault was placed on the system:

A-g fault at 80% on transmission line 1

B-g fault at 95% on transmission line 2

The fault on transmission line 2 was initiated 1 cycle after the fault appeared on transmission line 1, and the transmission lines were untransposed with no mutual coupling between them. The results of this test are shown in Figures 7.90 to 7.94.

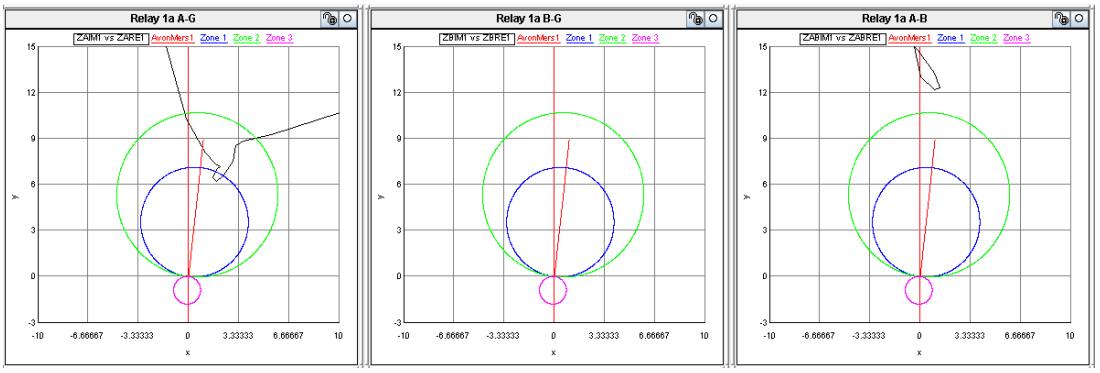

Figure 7.90: A-g, B-g and A-B impedance plots for relay 1a for a cross country fault at 80% and 95% of the parallel lines; untransposed lines with mutual coupling represented, both transmission lines in service, no POTT scheme enabled, and with the breakers allowed to operate

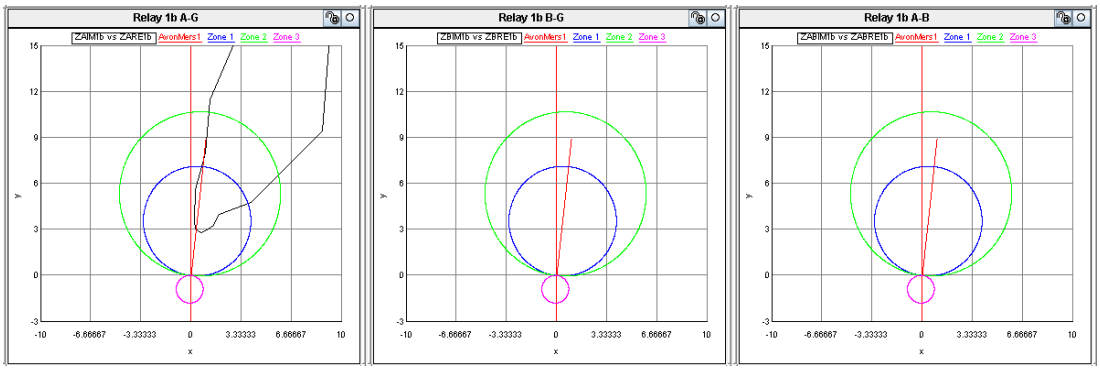

Figure 7.91: A-g, B-g and A-B impedance plots for relay 1b for a cross country fault at 80% and 95% of the parallel lines; untransposed lines with mutual coupling represented, both transmission lines in service, no POTT scheme enabled, and with the breakers allowed to operate

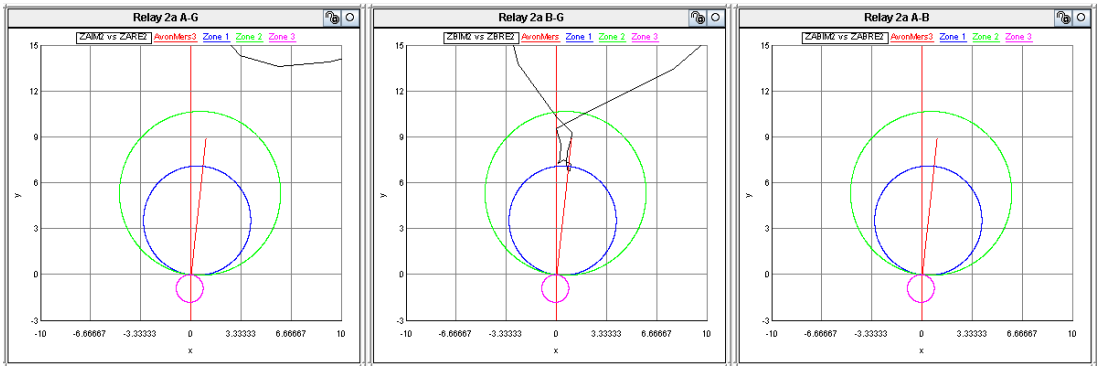

Figure 7.92: A-g, B-g and A-B impedance plots for relay 2a for a cross country fault at 80% and 95% of the parallel lines; untransposed lines with mutual coupling represented, both transmission lines in service, no POTT scheme enabled, and with the breakers allowed to operate

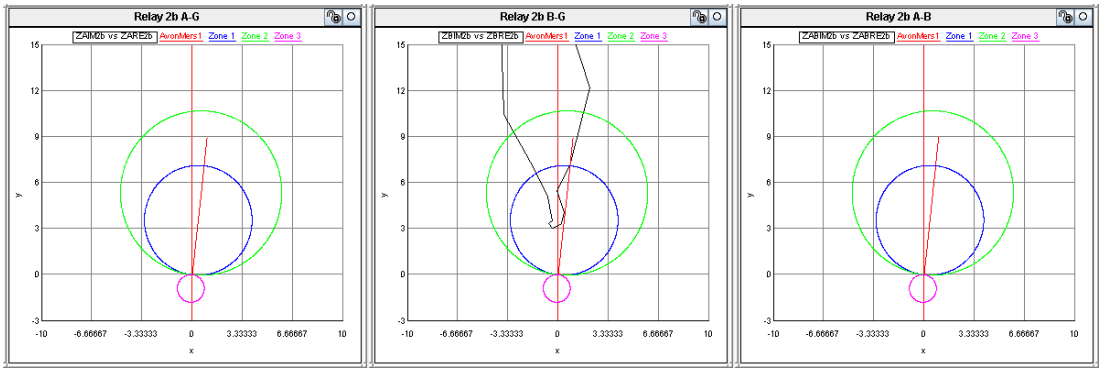

Figure 7.93: A-g, B-g and A-B impedance plots for relay 2b for a cross country fault at 80% and 95% of the parallel lines; untransposed lines with mutual coupling represented, both transmission lines in service, no POTT scheme enabled, and with the breakers allowed to operate

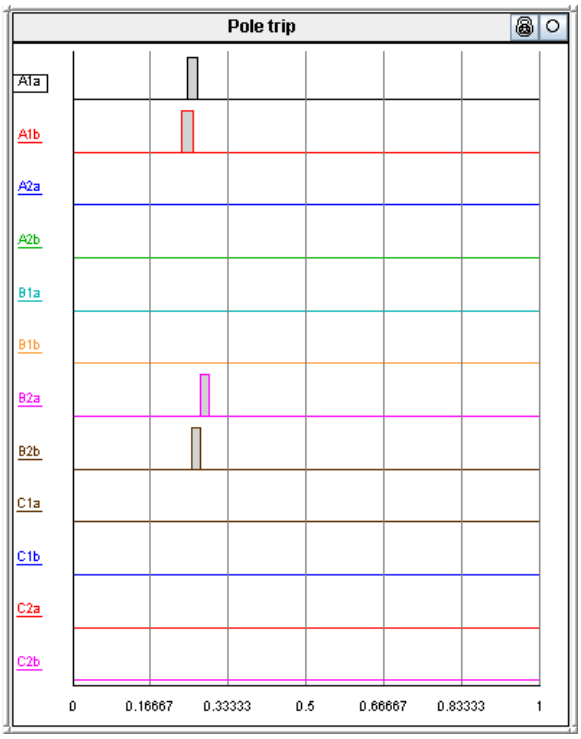

Figure 7.94: Single pole trip signal outputs of the relay

From the results in Figures 7.90 to 7.94, when the relays are allowed to issue trip signals to their respective breakers, the impedance plots reveal that no relay sees any phase to phase fault. Relays 1a and 1b see the A-g fault in zone 1 and instantaneously issue a single pole trip and the fault is cleared from the system. Thereafter the fault appears on the parallel line and relays 2a and 2b sees the B-g fault in zone 1 and instantaneously issue a single pole trip.

An additional case was then investigated in which the faults were placed on line 1 and line 2 at the same instant in time, again using only software relays, with the breakers allowed to operate for the following faults on the system:

A-g fault at 80% on transmission line 1
B-g fault at 95% on transmission line 2

The results for this test are shown in Figures 7.95 to 7.99.

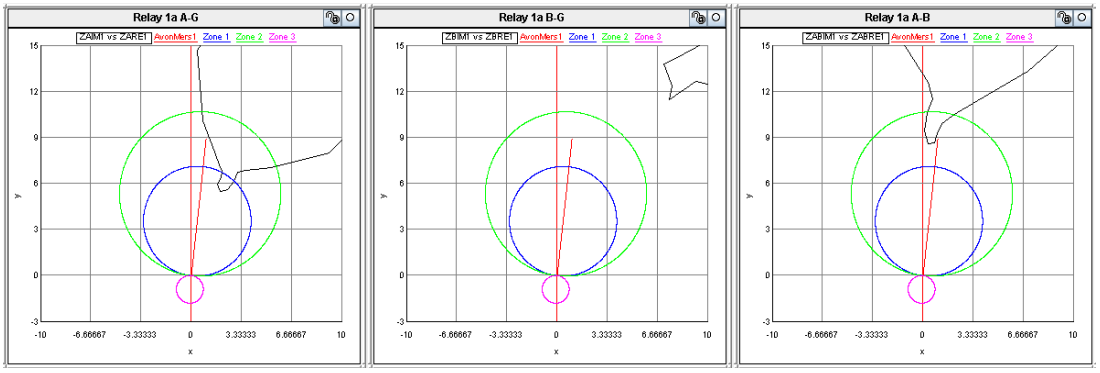

Figure 7.95: A-g, B-g and A-B impedance plots for relay 1a for a cross country fault at 80% and 95% of the parallel lines; untransposed lines with mutual coupling represented, both transmission lines in service, no POTT scheme used, and with the breakers allowed to operate

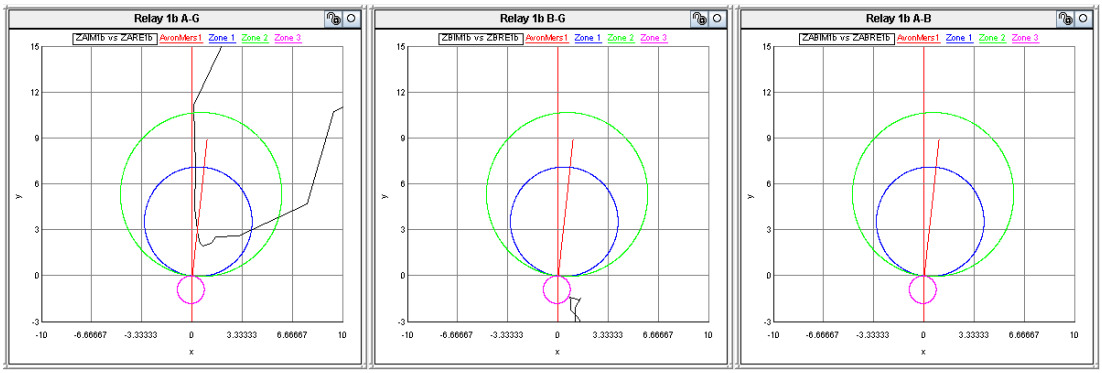

Figure 7.96: A-g, B-g and A-B impedance plots for relay 1b for a cross country fault at 80% and 95% of the parallel lines; untransposed lines with mutual coupling represented, both transmission lines in service, no POTT scheme used, and with the breakers allowed to operate

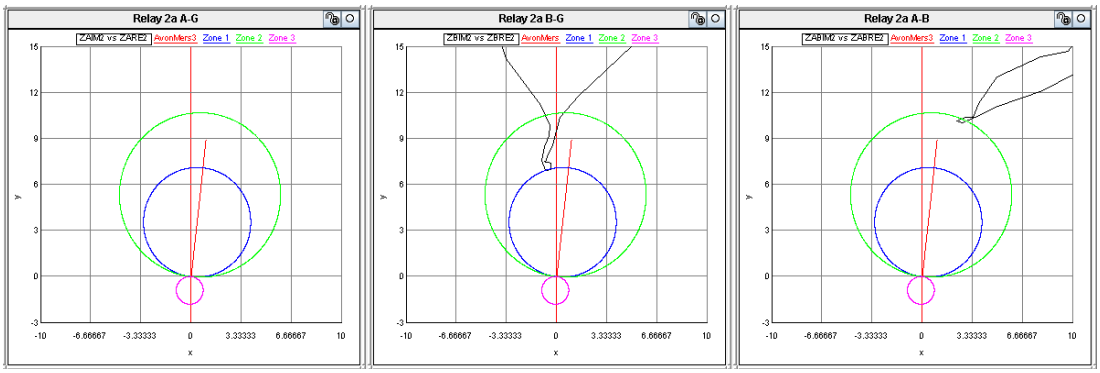

Figure 7.97: A-g, B-g and A-B impedance plots for relay 2a for a cross country fault at 80% and 95% of the parallel lines; untransposed lines with mutual coupling represented, both transmission lines in service, no POTT scheme used, and with the breakers allowed to operate

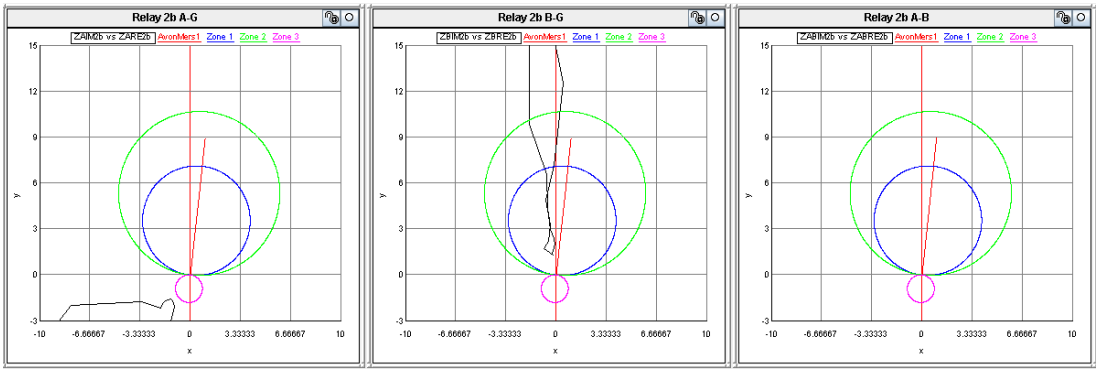

Figure 7.98: A-G, B-G and A-B impedance plots for relay 2b for a cross country fault at 80% and 95% of the parallel lines; untransposed lines with mutual coupling represented, both transmission lines in service, no POTT scheme used, and with the breakers allowed to operate

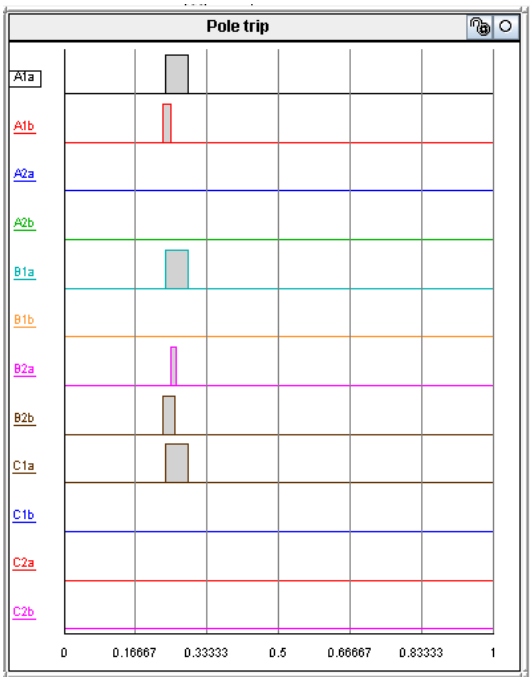

Figure 7.99: Single pole trip signal outputs of the relay

From the results shown in Figures 7.95 to 7.98, when the faults appear on the system at the same instant, relays 1a and 2a now see the cross country fault as a single phase fault in zone 1 and a phase to phase fault in zone 2 as shown in the impedance plots. Relays 1b and 2b issue single pole instantaneous trips since these relays see the cross country fault as single phase faults in zone 1. Relay 1a issues an instantaneous three pole trip since it sees an A-g fault in zone 1 but its phase selectors are also picked up for a fault involving phase B. Relay 2a thereafter issues a single pole instantaneous trip (2 cycles after relay 1a). The relay 2a saw the phase to phase fault at the very edge of its zone 2, and did not immediately take the decision to trip as noted from Figure 7.99. When relay 1a cleared the A-g fault from the system, relay 2a thereafter issued a near instantaneous single pole B phase trip.

The response of the distance protection relay to the above operating scenario was then investigated for the case when a simple POTT scheme was implemented. Again using only software relays, with the breakers allowed to operate, the following fault was placed on the system:

A-g fault at 80% on transmission line 1
B-g fault at 95% on transmission line 2

The fault on transmission line 1 was initiated at the same instant the fault appeared on transmission line 2 and the transmission lines were both untransposed with mutual coupling represented between them. The results for this test are shown in Figures 7.100 to 7.104.

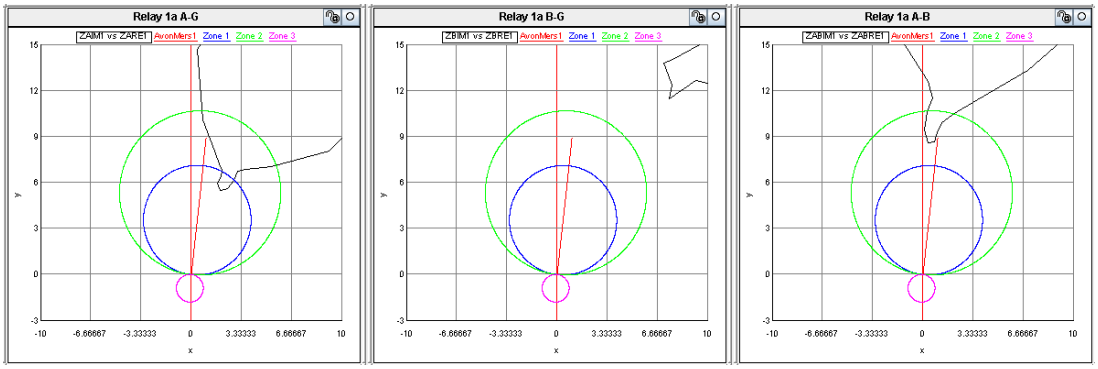

Figure 7.100: A-g, B-g and A-B impedance plots for relay 1a for a cross country fault at 80% and 95% of the parallel lines; untransposed lines with mutual coupling represented, both transmission lines in service, and a simple POTT scheme enabled

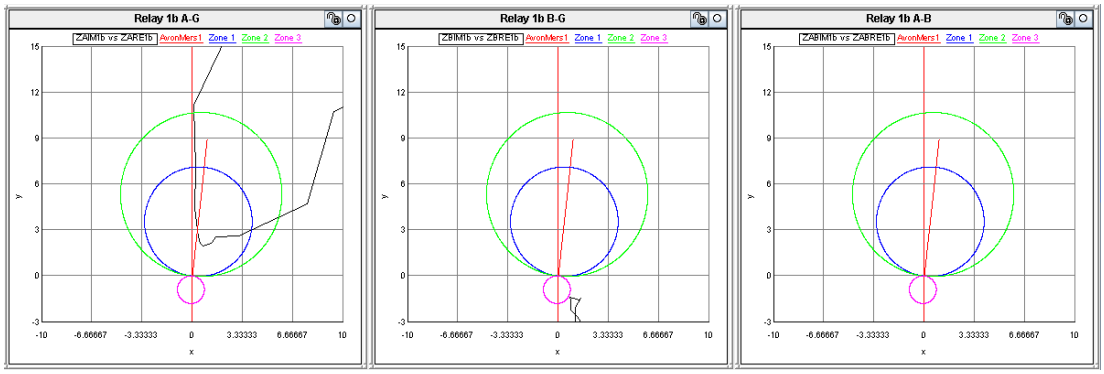

Figure 7.101: A-g, B-g and A-B impedance plots for relay 1b for a cross country fault at 80% and 95% of the parallel lines; untransposed lines with mutual coupling represented, both transmission lines in service, and a simple POTT scheme enabled

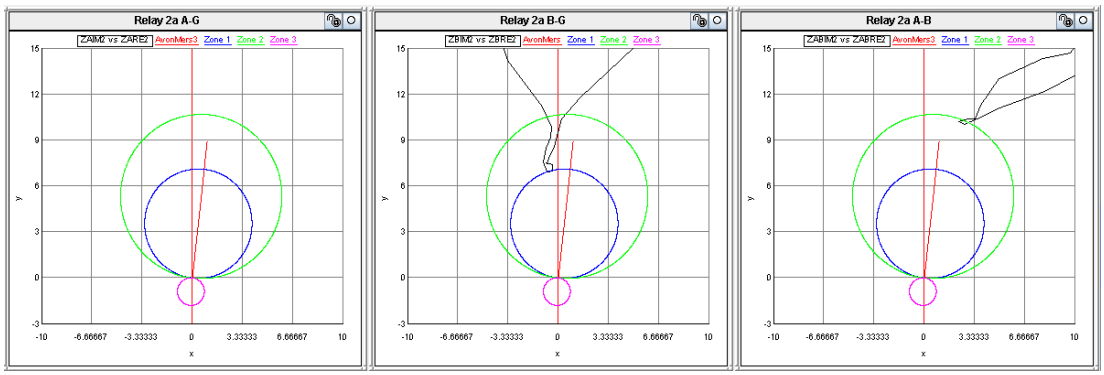

Figure 7.102: A-g, B-g and A-B impedance plots for relay 2a for a cross country fault at 80% and 95% of the parallel lines; untransposed lines with mutual coupling represented, both transmission lines in service, and a simple POTT scheme enabled

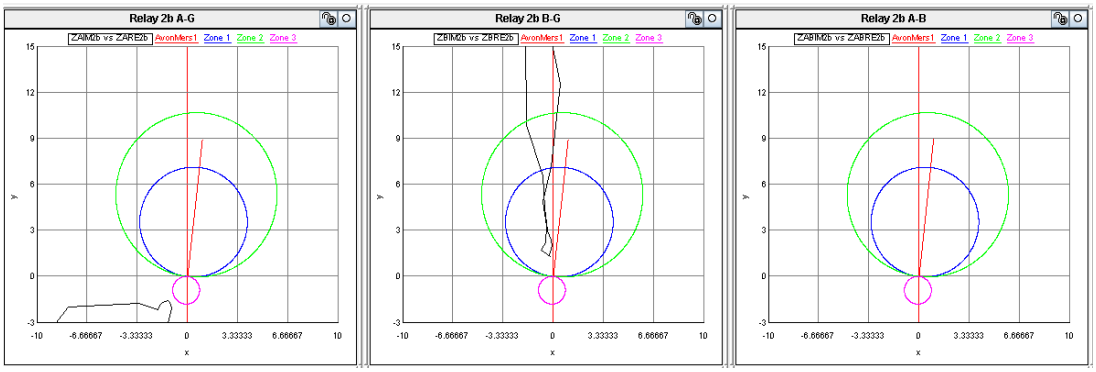

Figure 7.103: A-g, B-g and A-B impedance plots for relay 2b for a cross country fault at 80% and 95% of the parallel lines; untransposed lines with mutual coupling represented, both transmission lines in service, and a simple POTT scheme enabled

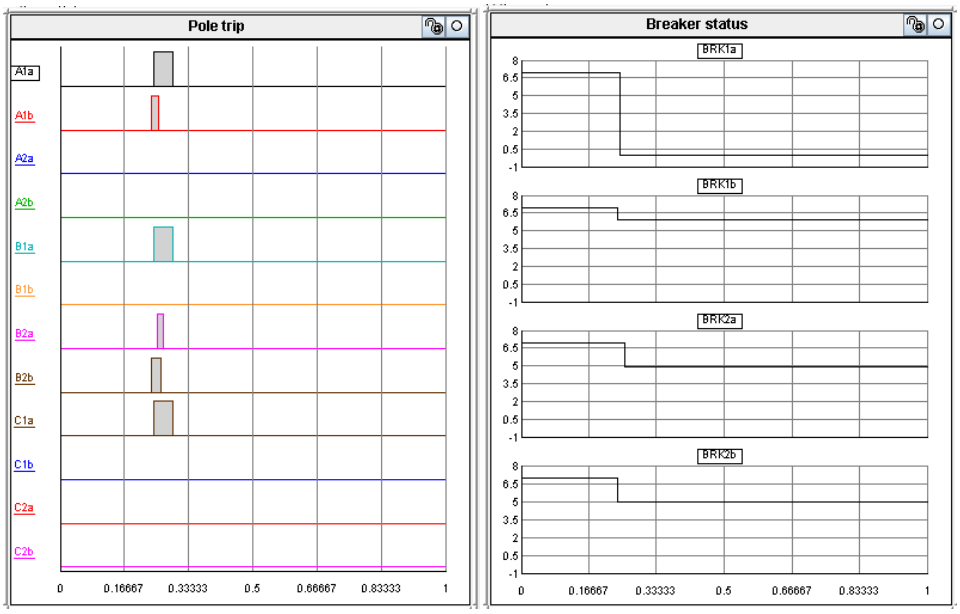

Figure 7.104: Single pole trip signal outputs of the relay (left) and breaker status (right)

From the results presented in Figures 7.100 to 7.104, the response of the relays to the operating condition considered in this case is similar to that seen in Figures 7.95 to 7.98. All relays issue an instantaneous trip command since all the relays see faults in zone 1. Relays 1b and 2b issue single pole instantaneous trips since they see single phase faults in zone 1 only. Relay 1a issues an instantaneous three pole trip since it sees an A-g fault in zone 1 and an A-B fault in zone 2. Relay 2a issues a single pole instantaneous trip command. The relay 2a saw a phase to phase fault at the edge of zone 2, and did not immediately take the decision to trip as noted from Figure 7.104. When relay 1a cleared the A-g fault from the system, relay 2a thereafter issued a near instantaneous single pole B phase trip.

The case study presented above was then repeated but with the POTT2 distance protection scheme protecting the transmission lines. For this case, both the software and hardware relays were used, with the breakers allowed to operate, and the following fault was placed on the system:

A-g fault at 80% on transmission line 1
B-g fault at 95% on transmission line 2

The fault on line 1 was initiated at the same time the fault appeared on line 2 and the transmission lines were both untransposed with mutual coupling represented between them. The results for this test are shown in Figures 7.105 to 7.111.

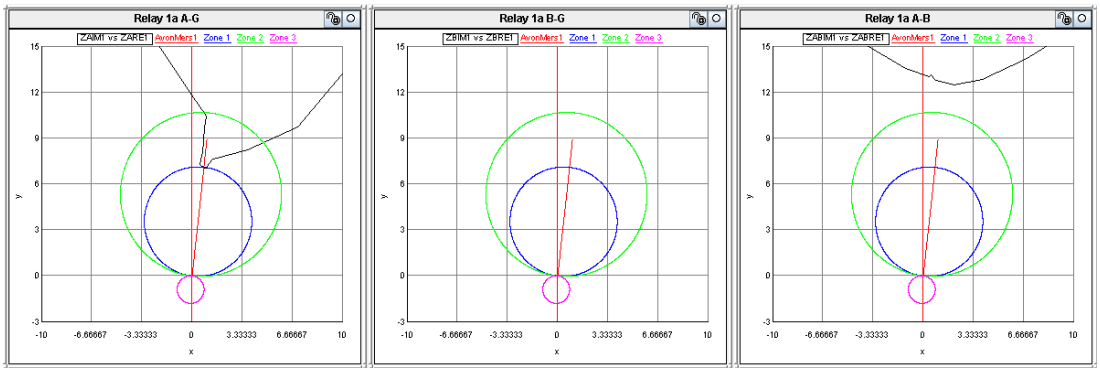

Figure 7.105: A-g, B-g and A-B impedance plots for relay 1a for a cross country fault at 80% and 95% of the parallel lines; untransposed lines with mutual coupling represented, both transmission lines in service, a POTT2 scheme enabled, and with the breakers allowed to operate

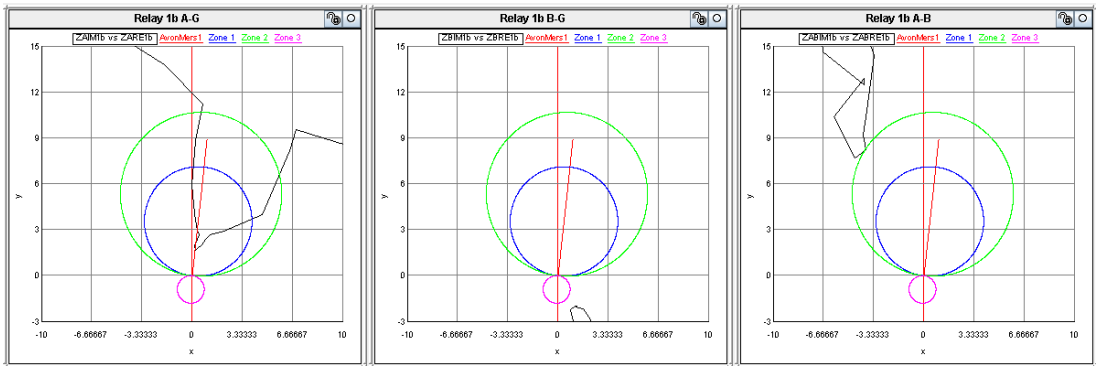

Figure 7.106: A-g, B-g and A-B impedance plots for relay 1b for a cross country fault at 80% and 95% of the parallel lines; untransposed lines with mutual coupling represented, both transmission lines in service, a POTT2 scheme enabled, and the breakers allowed to operate

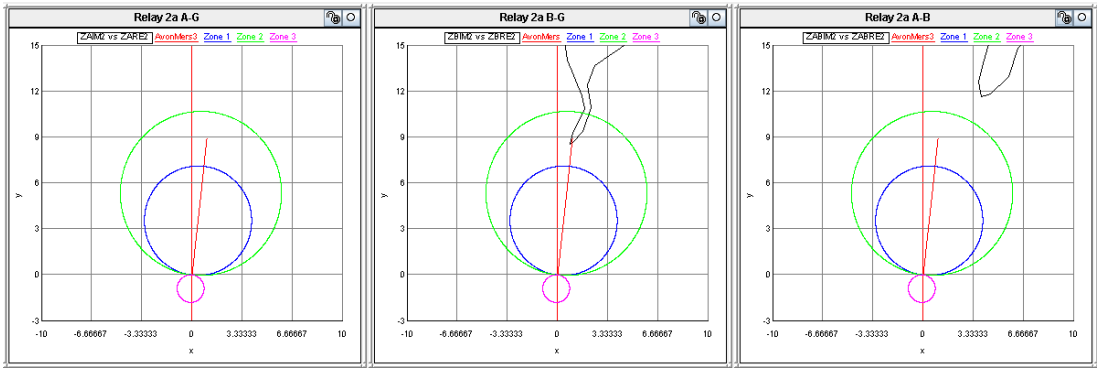

Figure 7.107: A-g, B-g and A-B impedance plots for relay 2a for a cross country fault at 80% and 95% of the parallel lines; untransposed lines with mutual coupling represented, both transmission lines in service, a POTT2 scheme enabled, and with the breakers allowed to operate

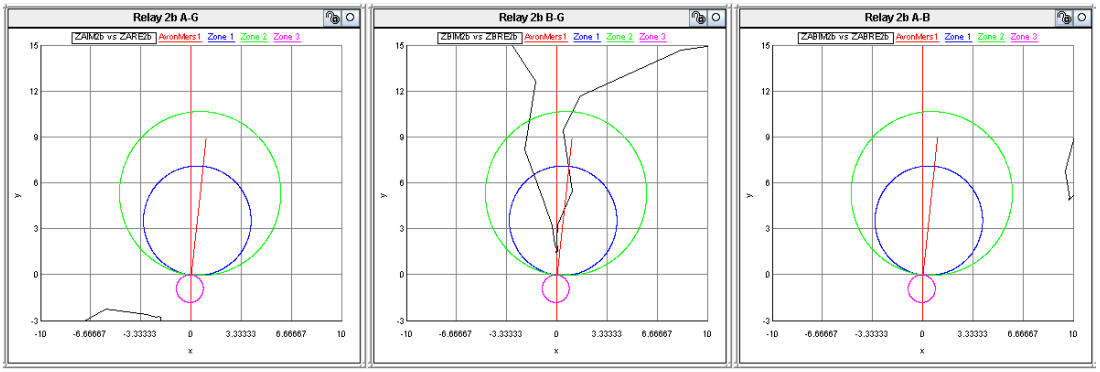

Figure 7.108: A-g, B-g and A-B impedance plots for relay 2b for a cross country fault at 80% and 95% of the parallel lines; untransposed lines with mutual coupling represented, both transmission lines in service, a POTT2 scheme enabled, and with the breakers allowed to operate

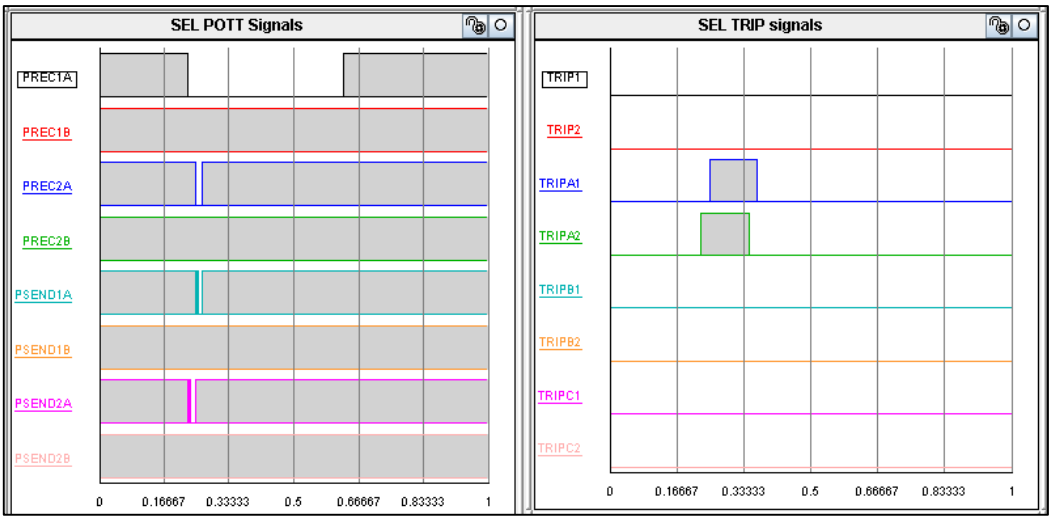

Figure 7.109: Hardware relay POTT2 signal monitoring on line 1 (left) and relay single pole trip signal monitoring on line 1 (right) for the cross country fault

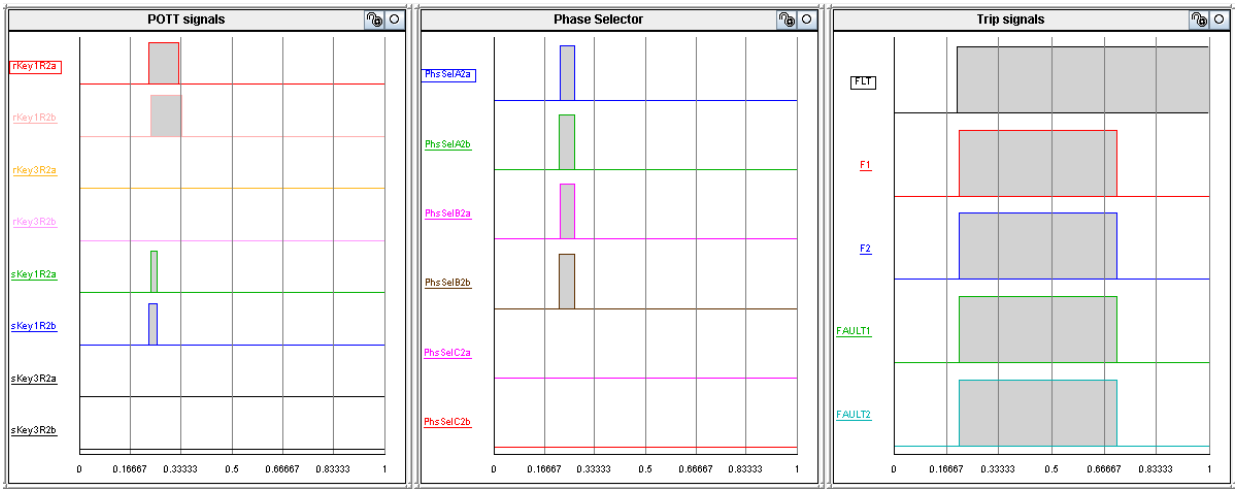

Figure 7.110: Software relay POTT2 signal monitoring (left) relay phase selector signal monitoring (centre) and fault control logic monitoring (right) for the cross country fault for the relays on line 2.

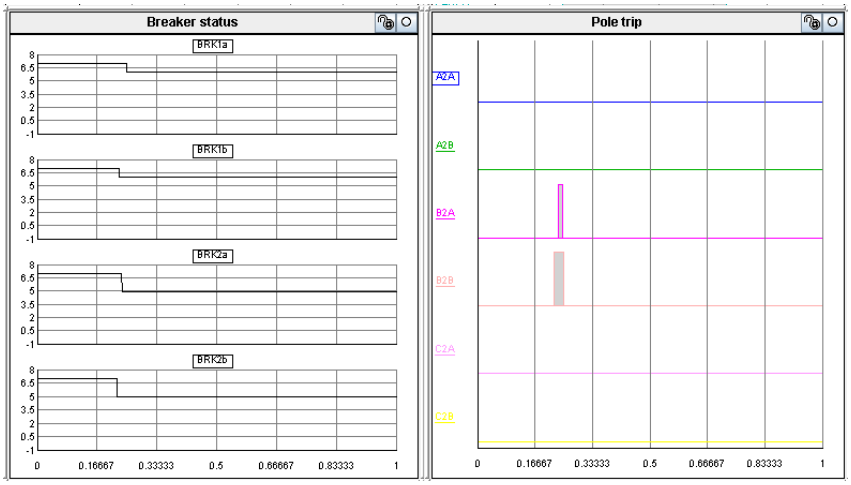

Figure 7.111: Breaker trip signal monitoring of all breakers (left) and relay single pole trip signal monitoring of the software relays on line 2 (right) for a cross country fault

From the results in Figures 7.105 to 7.111, all relays issue a single pole trip for this fault scenario. This is due to the sending end relays receiving a KEY1 permission to trip, and not receiving a KEY 3 permission to trip. Note that the impedance trajectories for this fault and current distribution, combined with the POTT2 protection scheme implemented to protect these parallel transmission lines, showed no impedance locus falling within the reach of the A-B measurement loop. The phase selectors for the RSCAD software relays indicate that the relays did see the fault in phase A and B. The protection scheme for this fault type and operating scenario did operate as required and no three pole trip was issued during this cross country fault. The POTT 2 scheme works as desired and all relays issue a single pole trip.

7.9. Conclusion

This chapter presented the definition of a cross country fault as found in the literature and this fault condition was replicated on the study system using the real time digital simulator. The results obtained from these studies with respect to the current distributions seen by the distance protection relays were found to agree with those presented in texts elsewhere.

The case studies presented in this chapter illustrate the compound effects of a cross country fault on parallel transmission lines, particularly where the transmission lines are untransposed and mutually coupled. From the studies included in this chapter, the severity of this complex operating scenario is clearly demonstrated with the use of the real time digital simulator. Such tools prove to give the user a better understanding of how the distance protection relay will respond to such complex operating conditions and how they would operate in service.

The following chapter presents the conclusions made throughout the chapters in the thesis and the main points regarding the research work will be summarised from the studies included in this thesis.

CHAPTER 8

CONCLUSION

The results of the studies presented in this thesis have shown that the Real Time Digital Simulator is a powerful research tool, allowing the user to gain greater insight during the design of protection settings, thereby increasing the protection scheme reliability. The thesis has presented a chapter by chapter study into the effects on a distance protection relay of mutual coupling between parallel transmission lines, non-transposition of transmission lines and cross country faults. This chapter now summarises the conclusions made in each of the prior chapters of the thesis and makes suggestions for further research work that could be carried out in this area of distance protection relay performance.

8.1 Chapter Conclusions

Chapter One presented a review of the known challenges that are experienced where the protection of double-circuit and parallel transmission lines is concerned, highlighting the importance of the research in the thesis and, in particular where utilities can gain from revisiting the topics presented. The aims and objectives of this study were presented as well as the methodical approach to achieving the desired outcomes of the study.

Chapter Two presented the background theory and literature review that was undertaken to provide the foundations for the fundamental, first-principles analyses to be conducted in subsequent chapters. This chapter also presented a review of the various challenges experienced in practice when protecting double-circuit and parallel transmission lines, so as to be able to replicate practical transmission line behaviour under complex operating conditions using the real time simulator in the studies to follow.

Chapter Three presented the mathematical derivation of the impedance matrix of a transmission line for the case where the line is mutually coupled to a parallel transmission line. Step by step hand calculations were carried out and compared to the impedance matrix output obtained from the modelling program used by the real-time simulator. The hand calculations were found to agree with the real time simulator's models.

Chapter Four presented a detailed, real-time simulator study to investigate the impact of mutual coupling on a distance protection relay. This chapter presented results which show that the error in the fault loop impedance measurement made by a distance protection relay, when two parallel

transmission lines are in service, can reach up to 6%, and where one line is taken out of service and grounded at both ends, this error could reach as high as 25%. The results in this chapter reinforce the notion that mutual coupling needs to be taken into account when designing distance protection settings for parallel transmission lines.

Chapter Five presented studies into the effect of non-transposition of transmission lines on a distance protection relay. Mathematical calculations of the symmetrical-component impedance matrix of the transmission line were made for the case when the transmission lines are untransposed, and the worst-case measurement error that will be made by the distance protection relay was found to be as high as 8.85% on the C-A impedance loop. This theoretical worst-case error was confirmed by means of real time simulation studies. The results in this chapter therefore underscore the need to also take into account non-transposition of transmission lines in the design of a distance protection scheme in cases where lines are not transposed in practice in the field.

Chapter Six presented a real-time simulator study of the combined effects of mutual coupling and non-transposition of parallel transmission lines on a distance protection relay. The studies in this chapter considered a variety of different complex operating conditions with varying results, showing that when the protection settings are designed for a distance protection scheme, all the different practical operating conditions likely to be encountered on the transmission lines should be taken into consideration, since the combined effects of complex interacting phenomena make distance protection relays respond in different ways under different conditions. This chapter clearly demonstrated how unreliable operation of a protection scheme could arise if such conditions are not considered during the design of the distance protection settings.

Chapter Seven presented a real-time simulator study of the effect on distance protection relays of cross country faults on parallel transmission lines. The results of these studies were shown to agree with those found in the literature. The studies in this chapter also considered the most complex combination of the different practical operating conditions studied earlier in the thesis (untransposed, mutually-coupled, parallel transmission lines) when analysing the impact of cross country faults. From the results presented in this chapter, the importance of representing such operating conditions in detail was again apparent when analysing the extent to which complex fault scenarios affect the performance of a distance protection relay, and showing that these issues should be considered carefully by protection settings engineers.

The results presented in this thesis have revisited some of the known problems associated with distance protection on parallel transmission lines. This research has demonstrated how modern

tools can be used to better understand the underlying nature of complex operating conditions, and how protection schemes respond to these conditions, thereby allowing engineers to enhance the performance of distance protection schemes. The realistic operating conditions presented in this thesis serve to remind protection engineers of the extent to which these phenomena can impact on the performance of distance protection relays, and that these issues should be considered carefully when settings are designed in order to ensure more reliable protection schemes.

8.2. Recommendations for further study

The studies in this thesis have focused on three of the most important aspects that affect the performance of distance protection schemes protecting parallel transmission lines. Further work can investigate other conditions and phenomena that such transmission lines are subjected to such as:

- mutual coupling on parallel transmission lines where the transmission lines are fed from a source on both ends,
- real time testing of mutual coupling compensation using protection relays from multiple vendors to investigate the advantages and disadvantages of the different relay algorithms used in various methods of mutual coupling compensation,
- the effects of pre-fault load transfer down the transmission line during such complex operating conditions,
- sequential tripping, and
- current reversal.

REFERENCES

[1] **Apostolov A, Tholomier D, Sambasivan S, Richards S, "**Protection of Double Circuit Transmission Lines"*, Proceedings of the 60th Annual Conference for Protective Relay Engineers*, College Station, TX, pp. 85-101, 2007.

[2] **Venayagamoorthy G K, "**Comparison of Power System Simulations Studies on Different Platforms-RSCAD, PSCAD/EMTDC, and SIMULINK SimPowerSystems", *Proceedings of the International Conference on Power Systems, Operation and Planning*, Missouri S and T Conference, pp 38-41, 2005.

[3] **Leoaneka M C, "**Dynamic Performance of Numerical Distance Protection Relays in Heavily Series Compensated Networks", *MSc Eng Thesis*, University of KwaZulu-Natal, 2009.

[4] **Pillay K R,** "Protection and Coordination Scheme for a Power Station Reticulation System*, BScEng Final Year Project Report*, University of KwaZulu-Natal, 2009.

[5] **Nofuya K, Bartylak A,** "Impact of Transmission Lines' Mutual Coupling on Protection Settings", *Report for Eskom System Operations and Planning*, Rev. 0, Dec 2010.

[6] **Rigby B S, "**Automated Real-Time Simulator Testing of Protection Relays", *Proceedings of the IEEE Power Africa 2007 Conference*, Johannesburg, July 16 – 20, 2007, ISBN 1-4244-1478-4.

[7] **Pillay K R, Rigby B S,** "A Real-Time Simulator Study to Investigate the Impact of Mutual Coupling on Distance Protection Relays", *Proceedings of the 20th South African Universities Power Engineering Conference* , Cape Town, 13-15 July 2011, ISBN 9780799224801.

[8] **Pillay K R, Rigby B S,** "Studying the Impact of Mutual Coupling on Distance Protection Relays Using a Real-Time Simulator", *Proceedings of the 10th IEEE AFRICON conference,* Livingstone, Zambia, 13-15 September 2011, ISBN 9781612849911.

[9] **Pillay K R, Rigby B S,** "An Investigation into the Performance of Distance Protection Relays During Cross Country faults On Closely-Coupled Parallel Transmission Lines" *Proceedings of the PAC World Africa Conference*, Cape Town, 30 July-2 August 2013.

[10] **Ziegler G,** "Numerical Distance Protection Principles and Applications", 2nd Edition, Publicis Cororate Publishing, Erlangen, Germany, 2006, ISBN 3-89578-266-1.

[11] **Alstom T&D Energy Automation and Information,** "Network Protection and Automation Guide", 1st Edition, France, July 2002, ISBN 2-9518589-0-6.

[12] **Anderson E M,** "Electric Transmission Line Fundamental", Virginia, USA : Reston Publishing Company (Prentice-Hall), 1985, ISBN O-8359-1597-2.

[13] **RTDS,** "Transmission Line Models", *Real Time Digital Simulator Power System Users Manual,* RTDS Canada, Nov 2006.

[14] **Introduction to Transmission Lines and Waveguides**, *TechLearner,* [Accessed Online] Available at: http://www.techlearner.com/library.htm. [Cited: 14 April 2011]

[15] **Roberts J, Guzman A, Schweitzer E O,** "Z=V/I does not make a distance relay", *Proceeding of the 20th Annual Western Protective Relay Conference*, Spokane, Washington, October 1993.

[16] **Zocholl S E,** "Three Phase Circuit Analysis and the Mysterious k_0 Factor", *Proceedings of the 22nd Annual Western Protective Relay Conference"*, Spokane, Washington, 24-26 October 1995.

[17] **Andrichak J G, Alexander G E,** "Distance Relay Fundamentals", *General Electric Co.*, Technical Papers, Malvern PA, 1998.

[18] **SEL,** "SEL 421 Relay Instruction Manual", *SEL 421 Relay Reference Manual,* Schweitzer Engineering Labratories Inc, 2010.

[19] **ABB Substation Automation and Protection Division,** "The Effect of Zero Sequence Infeed on Ground Distance Measurement", *ABB Application Note*, Allentown , PA, Rev. 09/23/99.

[20] **GE Industrial Systems,** "D60 Line Distance Relay", *Relay Instruction Manual*, Rev. 4.9x, GE Multilin, 2006.

[21] **Klapper U, Krueger M, Wurzer W,** "Measurement of line impedances and mutual coupling of parallel lines", *Proceedings of the Relay Protection and Substation Automation of Modern Power Systems Conference,* Cheboksary, September 2007.

[22] **Quintin V Jr, "**Ground Distance Relays-Understanding the Various Methods of Residual Compensation, Setting the Resistive Reach of Polygon Characteristics and Ways of Modelling and Testing the Relay", *32nd Annual Western Protective Relay Conference,* Spokane, WA, 25-27 October 2005

[23] **Bartylak A, "**Evaluation of weak infeed tripping technique on the Eskom transmission network*" Proceedings of the 3rd International Conference on Power System Protection and Automation*, New Delhi, India, Nov 2004.

[24] **Matshidza R D, "**Improved Transmission Line Protection Performance Concerning High Resistance Faults", *A postgraduate thesis submitted to the Disipline of Electrical Engineering in partial fulfilment for the requirements for the degree of Master of Science in Power and Energy*, Durban, Dec 2006.

[25] **Yang S,** "The Effect of Soil Resistivity on the LV Surge Environment", *Master of Science in Engineering Thesis,* University of Witwatersrand, Johannesburg, April 2006.

[26] **Jain A, Thoke A S, Patel R N,** "Classification of Single Line to Ground Faults on Double Circuit Transmission Line using ANN", *Proceedings of the International Journal of Computer and Electrical Engineering",* Vol 1, No. 2, June 2009.

[27] **Hu Y, Novosel D, Saha M M, Leitloff V**, "An Adaptive Scheme for Parallel-Line Distance Protection", *Proceedings of the IEEE Transactions on Power Delivery*", Vol 17, No. 1, Pages 105-110, January 2002.

[28] **Gustavsen B**, "Transmission Line Models for the Simulation of Interaction Phenomena Between Parallel AC and DC Overhead Lines", *Proceedings of the International Conference on Power System Transients*, Budapest, Hungary, 1999.

[29] **Gallego C, Urresty J, Gers J**, "Analysis of Phenomena, that Affect the Distance Protection", *Proceeding of the Transmission and Distribution Conference and Exposition,* Latin America, Vol. 8, 13-15 August 2008.

[30] **Calero F**, "Mutual Impedance in Parallel Lines – Protective Relaying and Fault Location Considerations", *Proceedings of the 27th Annual Western Protective Relay Conference,* Spokane WA, October 2000.

[31] **Lee J**, "Protection of Complex Transmission Lines-parallel feeders, multi-ended feeders, series-compensated lines", *M.Eng Thesis,* Western University, Faculty of Engineering, Canada, 2005.

[32] **Jacome Y,** "An Example Distance Protection Application with Complicating Factors", *Proceedings of the Western Protective Relay Conference,* Spokane, Washington, USA, 2009.

[33] **Srivani S G, Vittal P K, Atla C R,** "Development of Three Zone Quadrilateral Adaptive Distance Relay for the Protection of Parallel Transmission Line", *Proceedings of the 2009 IEEE International Conference on Industrial Technology,* Gippsland, 2009.

[34] **Spoor D, Zhu J,** "Selection of Distance Relaying Schemes when Protecting Dual Circuit Lines", *Publication of the School of Electrical Engineering University of Technology,* Sydney, 2003.

[35] **Roberts J, Turner S,** "Setting the Zero-Sequence Compensation Factors in SEL 321 Relays to Avoid Over-reach in Mutual Coupled Lines", *SEL Application Guide AG98-03*, [Online] Available at: http://www.selinc.com/aglist.htm, [Cited: 14 April 2011].

[36] **Gashimov A M, Babayeva A R, Nayir A,** "Transmission Line Transposition", *Proceedings of the ELECO International Conference,* Bursa, 18 December 2009.

[37] **Johnson W C, "**Transmission Lines and Networks", *McGraw-Hill,* USA, 1950, ISSN: 20212223-MNMM-76.

[38] **Neamt L, Petrean L E, Chiver O, Erdei Z, "**The Influence on Phase Transposing on Double Circuit Overhead Power Line Magnetic Field"*, Proceedings of the International Conference on Energy and Environment Technologies and Equipment*, Romania, Page 35-39, 20-22 April 2010, ISBN 978-960-474-181-6.

[39] **Fehr R E,** "Sequence Impedance of Transmission Lines", May 2004, Accessed online from: http://helios.acomp.usf.edu/~fehr/carson.pdf, [Accessed: 21 April 2012].

[40] **Fortescue C L,** "Method of Symmetrical Coordinates Applied to the Solution of Polyphase Networks", *Transactions of the AIEE,* Vol. 37, Pages 1027-1140, 1918.

[41] **Zocholl S E,** "Sequence Components and Untransposed Transmission Lines", Document 6090, Schweitzer Engineering Laboratories, Inc, Pullman, WA.

[42] **Roberts J, Schweitzer E O, Arora R, Poggi E,** "Limits to the Sensitivity of Ground Directional and Distance Protection", *Proceedings of the 1997 Spring Meeting of the Pennsylvania Electric Association Relay Committee,* Allentown, Pennsylvania, 15-16 May 1997.

[43] **Hesse M H, Gross E T B,** "Electromagnetic Unbalance of Untransposed Transmission Lines", *Transactions of the American Institute of Electrical Engineers Power Apparatus and Systems,* Part III, Pages 1323-1336, Jan 1953.

[44] **Hesse H E,** "Circulating Currents in Parallel Untransposed Multicircuit Lines: I-Numerical Evaluations", *IEEE Transactions on Power Apparatus and Systems*, Vol. 85, No. 7, July 1966.

[45] **Hesse H E,** "Circulating Currents in Parallel Untransposed Multicircuit Lines: II-Methods for Investigating Current Unbalance", *IEEE Transactions on Power Apparatus and Systems*, Vol. 85, No. 7, July 1966.

[46] **Alexander G E, Mooney J and Tyska W,** "Advances Application Guidelines for Ground Fault Protection", *Proceedings of the 28th Western Protective Relaying Conference,* Washington, October 2001.

[47] **Jackson B W, Best M, "**Application of a Single Pole Protection Scheme to a Double-Circuit 230 kV Transmission Line*", Proceedings of the 52nd Annual Georgia Tech Protective Relaying Conference,* Atlanta, 1998.

[48] **SEL,** "SEL-421 Protection and Automation System", *SEL-421 Flyer,* Acessed online from: www.selinc.com, Schweitzer Engineering Labratories Inc, [Accessed: 1 July 2009].

[49] **SEL,** SEL 421 Relay Instruction Manual. *SEL 421 Relay Application Handbook,* Schweitzer Engineering Labratories Inc, 2010.

[50] **Rigby B S,** "Introductory Training Course on Real-Time Simulation Techniques for Hardware-In-Loop Testing of Protective Relays", Durban , Rev 1.1, 2009.

[51] **McLaren P G, Kuffel R, Wierckx R, Giesbrecht J, Arendt L, "**A Real Time Digital Simulator For Testing Relays*", IEEE Transactions on Power Delivery*, Vol. 7, Jan 1992.

[52] **RTDS Technologies,** "Real Time Digital Simulation for the Power Industry", *RTDS Technologies,* Accessed online from: www.rtds.com, RTDS, [Accessed: 28 July 2009].

[53] **Nagoorsamy N C, Rigby B S**, "Investigation of High-Resistance Faults and the Weak-End Infeed Phenomenon in Distance Protection", Proceedings SAUPEC 2007, Cape Town, South Africa, 25 – 26 January 2007, ISBN 978-0-7992-2367-5, pg. 155 – 160.

[54] **Leoaneka M C, Rigby B S,** "Investigation Into Under-Reaching Of Distance Relays In Heavily Series Compensated Transmission Networks", Proceedings SAUPEC 2008, Durban, South Africa, 24 – 25 January 2008, ISBN 978-1-86840-6593, pg. 115 – 121.

[55] **Oullette D S, Geisbrecht W J, Wierckx R P, Forsyth P A**, "Modeling an Impedance Relay Using a Real Time Digital Simulator", *Proceedings of the 8th IEE International*

Conference on Developments in Power System Protection , Amsterdam, 5-8 April 2004, ISBN 0-86341-385-4, pg 665-668.

[56] **Oullette D S, Wierckx R P, McLaren P G**, "Using a Multi-Threaded Time-Step to Model a Multi-Function Relay in a Real-Time Digital Simulator", *Proceedings of the IET 9th International Conference on Developments in Power System Protection,* Glasgow, March 2008, ISBN 978-0-86341-902-7, pg. 162 – 167.

[57] **RTDS,** "Relaying: Multi-function Distance", *Real Time Digital Simulator Power System Users Help File,* RTDS Canada, Nov 2006, pg 8.3-8.25.

[58] **Glover J D, Sarma M S, Overbye T J,** "Power System, Analysis and Design", 5th edition, Cenage Learning, Stamford, USA, 2008, ISBN-10: 1-111-42573-5.

[59] **Carson J R,** "Wave Propagation in Overhead Wires with Ground Return", *Bell System Technical Journal*, Vol 5, New York, 19263.

[60] **eThekwini Electricity,** "Klaarwater Setting Sheet", *eThekwini Electricity Protection and Test Settings Records,* Accessed: 1 February 2013.

[61] **McDaniel R,** "Applying the SEL 421 Relay to Permissive Overreaching Transfer Trip Scheme", *SEL Application Guide*, Volume 1, AG2010-01, 02 September 2010.